TONI SIMOLIN

Electric Vehicle Charging Load Management

Algorithm and Modelling Perspectives

TONI SIMOLIN

Electric Vehicle Charging Load Management
Algorithm and Modelling Perspectives

ACADEMIC DISSERTATION
To be presented, with the permission of
the Faculty of Information Technology and Communication Sciences
of Tampere University,
for public discussion in the Auditorium TB109
of the Tietotalo Building, Korkeakoulunkatu 1, Tampere,
on 2 September 2022, at 12 o'clock.

ACADEMIC DISSERTATION
Tampere University, Faculty of Information Technology and Communication Sciences
Finland

Responsible supervisor and Custos	Professor Pertti Järventausta Tampere University Finland	
Supervisor	Docent Antti Rautiainen Tampere University Finland	
Pre-examiners	Associate Professor Mattia Marinelli Technical University of Denmark Denmark	Professor Wilfried van Sark Utrecht University Netherlands
Opponent	Professor Hannu Laaksonen University of Vaasa Finland	

The originality of this thesis has been checked using the Turnitin OriginalityCheck service.

Cover design: Roihu Inc.

Preface

The work presented in this thesis was carried out during the years 2018–2022 in the Electrical Engineering unit of Tampere University. This thesis has been supervised by Professor Pertti Järventausta and Docent Antti Rautiainen to whom I would like to express my deepest gratitude. Their insights and participation in the publications have been invaluable. Additionally, this thesis work would not have been possible without the work of Professor Pertti Järventausta to secure funding. The funding from Emil Aaltonen Foundation is also greatly appreciated.

I would also like to thank all other coauthors contributing to my research: M.Sc. Juha Koskela, Pasi Santikko, Hannu Järvensivu, Dr. Kalle Rauma, Professor Christian Rehtanz, M.Sc. Riku Viri, and M.Sc. Johanna Mäkinen. I would like to express special gratitude to Dr. Kalle Rauma who not only helped me to understand the laboratory implementation of the developed charging control algorithms but also worked hard to carry out the countless laboratory experiments required to test and evaluate the developed algorithms. I am also grateful for the electric vehicle charging data provided by IGL Technologies.

Finally, I would like to thank my family and friends for their support.

Tampere, February 2022

Toni Simolin

Abstract

Electric vehicles are seen as the key solution for emission-free private transportation. The share of electric vehicles is small at the time of writing this thesis, but their share is increasing rapidly. The charging demand is consequently also increasing at a fast pace. Uncontrolled charging has been seen as an inefficient solution in a large-scale implementation; thus, there is more pressure to develop intelligent and efficient charging infrastructure solutions.

This thesis assesses electric vehicle charging from two perspectives: charging load modelling and control algorithm development. It is necessary to ensure that tests are carried out reliably in order to develop and evaluate the operation of different charging algorithms. Electric vehicle charging, especially a large-scale implementation, often must be examined using simulations; thus, emphasis must be given to the simulation details. Different solutions may be necessary in different scenarios in charging algorithm development. The focus in this thesis is on charging mode 3 of the international charging standard IEC 61851. This thesis divides control algorithms into three components to advance the algorithm development: *Capacity determination*, *Capacity allocation*, and *Capacity usage rate correction*. Each component corresponds to managing a certain objective in a charging control algorithm.

One of the key findings of this thesis relates to a phenomenon called "non-ideal charging characteristics": how to take them into account in charging load modelling and in charging control algorithms. The non-ideal charging characteristics have often been neglected in charging load modelling-related studies in the scientific literature, yet it is shown that they can notably influence the results. A charging current measurement-based simulation model is developed to take the non-idealities into account in the charging load modelling, and its accuracy is validated using hardware-in-the-loop simulations. Additionally, an algorithm feature called "charging characteristics expectation" is developed to take the non-idealities into account in the charging control algorithms. The feature allows a control algorithm to track the potential mismatches between the charging current limits set by the charging stations and the actual charging currents to overcome the related issues. Additionally, this thesis assesses peak load limitation-based charging control solutions. It is concluded that home charging demand can likely be fulfilled in most cases in Finnish households without a need to increase peak loads of the whole real estate. Furthermore, to consider varying charging demands of electric vehicle users,

different charging control prioritization principles, such as mobility requirement, battery energy status, or price-based, are investigated.

Table of contents

Abbreviations

AC	Alternating Current
BESS	Battery Energy Storage System
BEV	Battery Electric Vehicle
CC	Constant Current
CCE	Charging Characteristics Expectation (a developed algorithm functionality)
CP	Constant Power
CV	Constant Voltage
CSO	Charging System Operator
DC	Direct Current
DR	Demand Response
DSO	Distribution System Operator
EDF	Earliest Deadline First
EV	Electric Vehicle
EVSE	Electric Vehicle Supply Equipment
FCFS	First-Come-First-Served
FEV	Full Electric Vehicle (synonym for BEV)
G2V	Grid-to-Vehicle
HIL	Hardware-in-the-loop
ICEV	Internal Combustion Engine Vehicle
LLF	Least Laxity First
OBC	On-Board Charger
PHEV	Plug-in Hybrid Electric Vehicle
PV	Photovoltaic
RES	Renewable Energy Sources
RMSE	Root Mean Square Error
SoC	State of Charge
TOU	Time-of-Use
TSO	Transmission System Operator
V2B	Vehicle-to-Building
V2G	Vehicle-to-Grid
V2H	Vehicle-to-Home
V2V	Vehicle-to-Vehicle

V2X   Vehicle-to-X (i.e., Vehicle-to-anything)

List of publications

This thesis is based on the 12 following original publications, which are referred to in the text as [P1]–[P12].

[P1] **T. Simolin**, A. Rautiainen, J. Koskela, P. Järventausta, "Control of EV charging and BESS to reduce peak powers in domestic real estate", *International Review of Electrical Engineering (IREE)*, vol. 14, no. 1, Feb. 2019, pp. 1–7.

[P2] **T. Simolin**, A. Rautiainen, P. Järventausta, "Control of EV charging to reduce peak powers in domestic real estate", *proceedings of the 25th international conference and exhibition on electricity distribution (CIRED)*, June 2019, Madrid, Spain, 5 p.

[P3] **T. Simolin**, A. Rautiainen, P. Järventausta, "Assessment of prediction uncertainties in EV charging management", *International Review of Electrical Engineering (IREE)*, vol. 15, no. 4, Aug. 2020, pp. 262–271.

[P4] **T. Simolin**, A. Rautiainen, P. Järventausta, P. Santikko, H. Järvensivu, "Load control of residential real estate to improve circumstances for EV charging", *in 17th International Conference on the European Energy Market (EEM20)*, Sep. 2020, Stockholm, Sweden, 6 p.

[P5] **T. Simolin**, K. Rauma, A. Rautiainen, P. Järventausta, "Optimized controlled charging of electric vehicles under peak power-based electricity pricing", *IET Smart Grid*, vol. 3, no. 6, Dec. 2020, pp. 751–759.

[P6] K. Rauma, **T. Simolin**, A. Rautiainen, P. Järventausta, C. Rehtanz, "Overcoming non-idealities in electric vehicle charging management", *IET Electrical Systems in Transportation*, vol 11, no. 4, Dec. 2021, pp. 310–321.

[P7] **T. Simolin**, K. Rauma, A. Rautiainen, P. Järventausta, C. Rehtanz, "Foundation for Smart Charging Solutions: Optimizing Capacity Usage Rate of Electric Vehicle Charging", *IET Smart Grid*, vol 4, no. 6, Dec. 2021, pp. 599–611.

[P8] **T. Simolin**, K. Rauma, A. Rautiainen, P. Järventausta, "Realistic QoS optimization potential in commercial EV charging sites through pricing-based prioritization", *proceedings of the 26th international conference and exhibition on electricity distribution (CIRED)*, Sep. 2021, Geneva, Switzerland, p. 5.

[P9] **T. Simolin**, K. Rauma, R. Viri, J. Mäkinen, A. Rautiainen, P. Järventausta, "Charging powers of the electric vehicle fleet: Evolution and implications at commercial charging sites", *Applied Energy*, vol. 303, Dec. 2021, p. 117651.

[P10] K. Rauma, **T. Simolin**, P. Järventausta, A. Rautiainen, C. Rehtanz, "Network-adaptive and capacity-efficient electric vehicle charging site", *IET Generation Transmission Distribution*, vol. 16, no. 3, Feb. 2021, pp. 548–560.

[P11] **T. Simolin**, K. Rauma, A. Rautiainen, P. Järventausta, "Assessing the influence of the temporal resolution on the electric vehicle charging load modeling accuracy", *Electric Power Systems Research*, vol. 208, July 2022, p. 107913.

[P12] **T. Simolin**, K. Rauma, A. Rautiainen, P. Järventausta, C. Rehtanz, "Assessing the influence of electric vehicle charging profile modelling methods", *IET Generation, Transmission Distribution*, Early View, April 2022.

1   Introduction

There is an increasing need to develop sustainable transportation solutions as global warming causes pressure to reduce greenhouse gas emissions and oil dependency. Electric vehicles (EVs) are often seen as the key solution for personal transportation. However, a wide adoption of EVs poses both challenges and opportunities from the electricity grid viewpoint as the EVs are charged. EV charging can be controlled to minimize negative impacts and improve the operation of the electricity grid and electricity markets. This controlled charging is sometimes known as "smart charging" (Rautiainen, 2015).

According to a global survey (Mäki *et al.*, 2021), EV charging is expected to be one of the largest untapped sources for demand response (DR) potential. DR means the change of power consumption in response to, e.g., market-based signals or grid states. to balance the electricity supply and demand. Further assessment of different aspects and applications of DR is excluded from this thesis but can be found, e.g., in (Rautiainen, 2015).

1.1   The motivation of the thesis

It is commonly known that uncontrolled EV charging is likely to cause negative influences on the grid, such as transformer overloading (Lacey *et al.*, 2017), notable load peaks at the distribution network level (Qian *et al.*, 2011), or voltage violations (Shafiq *et al.*, 2021). EV charging has been studied extensively over the past two decades to overcome these issues. Significant contributions related to EV charging control and charging load modelling have been made, yet gaps still remain in the scientific literature. The goal of this thesis is to make a further advancement to the knowledge around the topic and enable a smoother transition to EVs from the charging solutions perspective.

1.2   The scope and objectives of the thesis

This thesis deals with EV charging. Its initial focus was on the development and evaluation of charging control algorithms. However, it became clear during the work that more attention must be given to the methods used to model or test the algorithms' operation in order to reliably evaluate the operation of different charging control algorithms. Therefore, the thesis was extended to include the charging load modelling perspective in addition to the original control algorithm perspective.

Additionally, this thesis gives a special emphasis to "non-ideal charging characteristics," which have notable influences on the modelling of EV charging loads and on optimized control algorithms. Fig. 1.1 illustrates the research areas of the publications of the thesis.
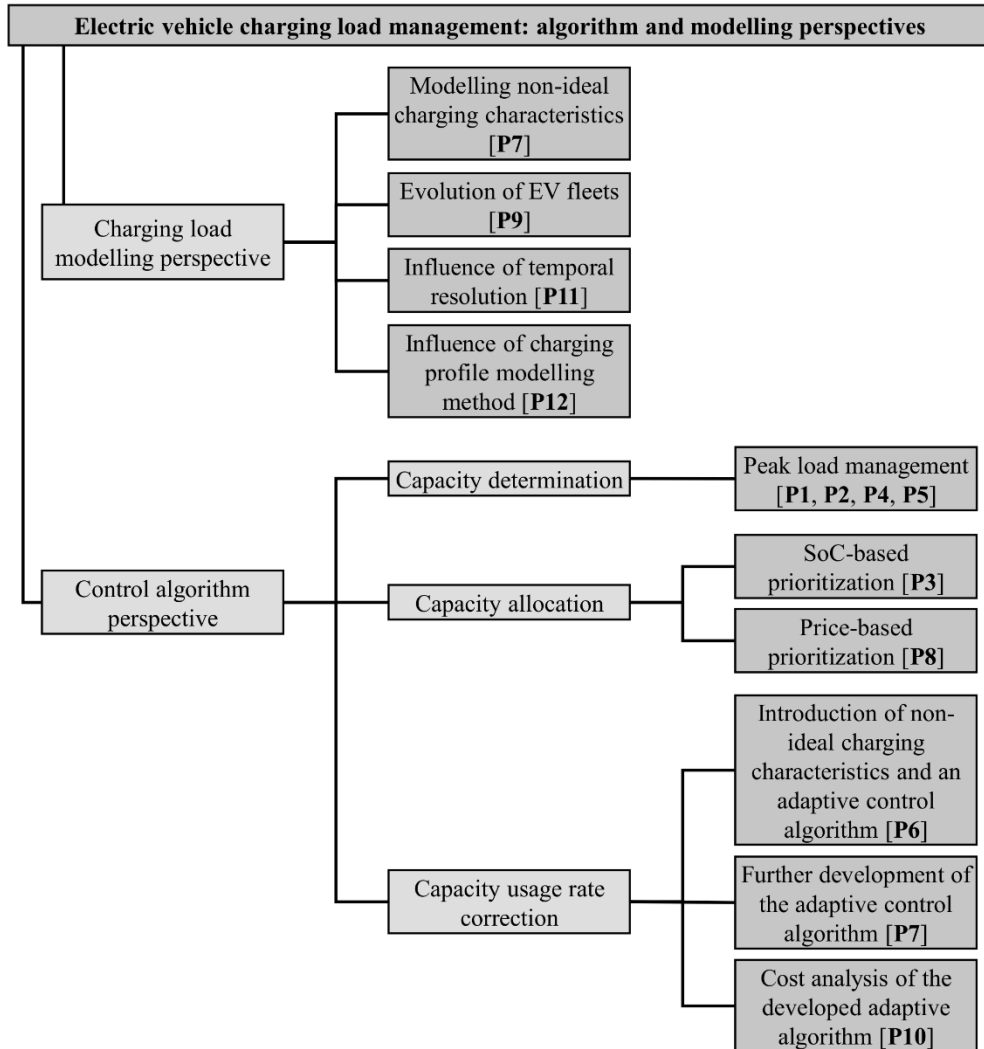
Figure 1.1 Content of this thesis, where P with a number refers to a related original publication.

This thesis focuses on charging mode 3 (IEC 61851), which is intended for the basic EV charging and includes extended control possibilities. Additionally, this thesis focuses on decentralized charging solutions in which a charging site can optimize its operation based on control signals, but no data from the charging site are transferred to any centralized control unit. Section 2.1.3 presents further

explanations of charging mode 3, along with a brief introduction to other charging modes. Section 2.2.4 discusses the main differences between centralized and decentralized charging control methods. The thesis covers different charging locations and their properties, but home charging and commercial charging are studied more thoroughly than the other locations. Additionally, the thesis focuses only on private EVs. However, some of the developed control algorithms and especially the developed modelling methods may also be applicable to other charging locations, such as work charging, or to other types of EV fleets, such as buses or trucks. Furthermore, this thesis focuses on the more traditional grid-to-vehicle (G2V) operation. However, Subsection 2.2.3. discusses a general outlook of the potential benefits and issues of the vehicle-to-grid (V2G) operation.

1.3   Research methods

The results of this thesis were mostly achieved by conducting different simulations. Different initial data, laboratory equipment, and hardware-in-the-loop simulations were used to improve the accuracy of the simulations. The average driving distance in publications [P1] and [P2] was based on driving statistics provided by Statistics Finland (Lahtinen, 2018). A national household travel survey was used in [P3] and [P5] as a basis to determine the EVs' driving distance. Travel survey-based modelling have been shown to be relatively accurate to model EV charging as long as various input parameters, such as battery sizes and charging powers, are accurately chosen (Pareschi *et al.*, 2020). Real charging session data was used in [P7]–[P12] to give a more accurate basis for values such as the charging timings, the energy requirements, and the charging powers. The electricity consumption of a household was used in [P4], [P5], [P11] and the electricity consumption of an apartment building was used in [P1]–[P3] to evaluate home charging. Furthermore, Photovoltaic (PV) data was used in [P1] to investigate solar power-based charging control.

Commercial EVs were used to carry out hardware-in-the-loop (HIL) simulations to ensure realistic charging characteristics and compliance with the related charging standard (namely IEC 61851) in publications [P5], [P6], [P8], [P10], [P11], [P12]. The HIL simulations were carried out at the Smart Grid Technology Lab (Spina *et al.*, 2018) at TU Dortmund University. The laboratory equipment included, e.g., the four EVs mentioned in Table 1, two charging stations (i.e., Wirelane Doppelstele and RWE eStation, which both include two 22 kW sockets), and a controllable load up to 45 kW used as a fast-charging station emulator. Fig. 1.2 presents a picture of the laboratory setup. Experimental laboratory measurements of multiple EVs were used in [P7]–[P12] to form more realistic charging profile models for simulation purposes.

Table 1. Key properties of the used EVs

Model	Max charging current	Max charging power
Nissan Leaf 2012	1×16 A	3.7 kW
Nissan Leaf 2019	1×32 A	7.4 kW
BMW i3 2016	3×16 A	11.0 kW
Smart EQ ForFour 2020	3×32 A	22.1 kW
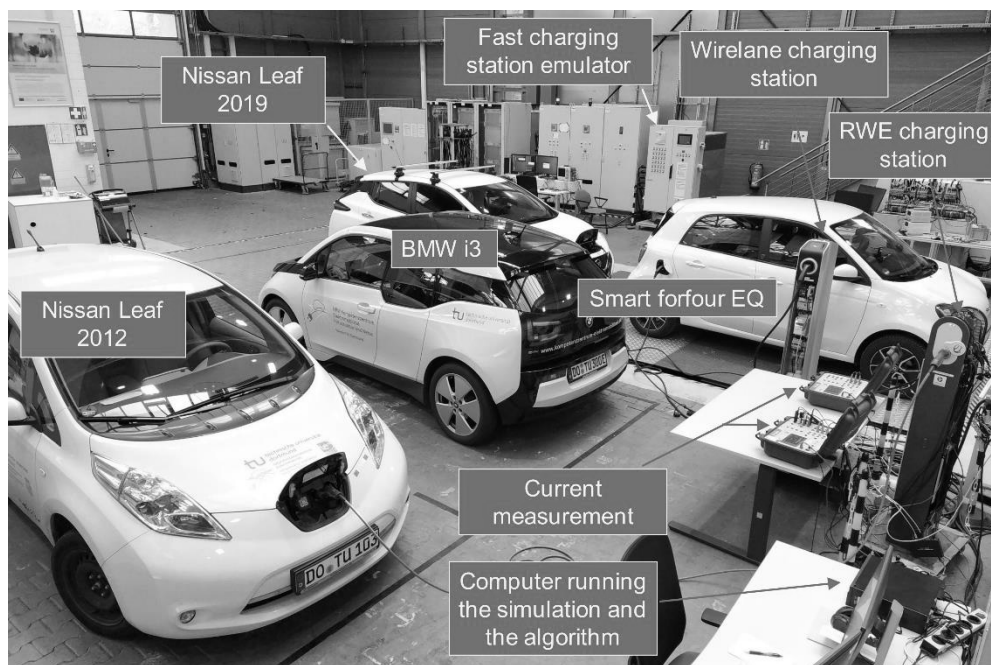
Figure 1.2 Laboratory equipment at Smart Grid Technology Lab at TU Dortmund University [P10].

The electricity consumption of a detached house located in Satakunta, Finland, was measured in December 2018 in ten-second resolution for [P4]. The electricity consumption data of a detached house located in Pirkanmaa, Finland, was measured in December 2018 in one-second resolution for studies [P5] and [P11]. The data for [P5] and [P11] were provided by Tampere University of Applied Sciences (TAMK). The charging session data used in [P7]–[P12] were provided by IGL technologies. The data were measured during 2018–2020 in REDI and Tripla and included arrival time, departure time, active charging time, charged energy and charging peak power of the charging sessions. REDI and Tripla are both shopping centers located in

Helsinki, Finland, and include over 200 charging points (REDI, 2021; Mall of Tripla, 2021).

1.4 Author's contributions in publications

The thesis is mainly based on the 12 original publications in which the author of this thesis has been an essential contributor. Publications [P1]–[P8] and [P10] assess EV charging management from the control algorithm perspective, whereas publications [P9],[P11],[P12] focus on the charging load modelling viewpoint. Apart from publications [P6] and [P10], the author of this thesis has been the corresponding author and has been responsible for writing and editing most of the publications' content. Prof. **Pertti Järventausta** and Docent **Antti Rautiainen** have been the supervisors of this thesis and have also contributed to all publications through guidance and providing comments prior to publishing. Dr. **Kalle Rauma** has contributed to publications [P5], [P7]–[P9], [P11], [P12] by providing ideas and comments prior to publishing and has been the corresponding author for publications [P6], [P10].

The author of this thesis is responsible for developing the control algorithms and the charging load simulation models in each publication. M.Sc. **Juha Koskela** provided insights on the considered PV system, BESS, and apartment building in [P1]. **Pasi Santikko** and **Hannu Järvensivu** were the creators of the original control system that is examined in [P4]. The HIL simulations were carried out by Dr. **Kalle Rauma** in publications considering the use of commercial EVs [P5], [P6], [P8], [P10]. Additionally, the experimental measurements used as initial data in [P7]–[P12] were carried out by Dr. **Kalle Rauma**. Furthermore, Dr. **Kalle Rauma** helped with the laboratory implementations of the charging control algorithms in [P5], [P6], [P8], [P10]. M.Sc. **Riku Viri** and M.Sc. **Johanna Mäkinen** provided the viewpoints in publication [P9] related to the parking policy and the model to predict the number of EVs in the future. All data curation and analysis were done by the author of this thesis with the exceptions of [P6] and [P10].

1.5 The structure of the thesis

The rest of the thesis is organized as follows. Chapter 2 introduces the main properties of EVs and smart charging solutions. Additionally, the chapter briefly introduces the three main components in a smart charging algorithm (namely *Capacity determination*, *Capacity allocation*, and *Capacity usage rate correction*). Chapter 3 discusses the EV charging load modelling and presents the modelling method

developed in [P7]. Chapter 4 explains the meaning of *Capacity determination* and discusses different capacity determination principles. Chapter 5 discusses *Capacity allocation* along with related issues and solution proposals. Chapter 6 discusses the need for *Capacity usage rate correction* along with the developed solution. Chapter 7 finalizes the thesis with its main contributions, a discussion of the results, and future work proposals. The structure of the thesis was chosen so that the original publications would be cited in a semi-chronological order, illustrated in Fig. 1.1. The developed modelling method plays a crucial role in the control algorithm-related studies [P7], [P8], [P10], so it is necessary to assess the modelling perspective before the algorithm perspective.

2 Background to EV charging management

This chapter introduces the background of EVs and smart charging. First, it briefly discusses EVs in terms of the drivers and barriers to wide adoption, different charging modes, potential charging locations, and a general outlook on the charging loads. It then discusses the general properties of smart charging. This includes topics such as the key players in EV charging management, controllability of EV charging, objectives of smart charging control methods, and structural perspectives of smart charging algorithms.

2.1 Introduction to electric vehicles

This thesis defines the term EV similar to (Rautiainen, 2015) as being a road vehicle that utilizes on-board electrical energy storage that can be charged from an energy source outside the vehicle. EVs include plug-in hybrid electric vehicles (PHEVs) and battery electric vehicles (BEVs). PHEVs can utilize both electrical energy and a more traditional liquid fuel, i.e., gasoline or diesel. BEVs, sometimes also referred to as full electric vehicles (FEVs), utilize only electrical energy and, thus, often have a larger battery capacity compared to PHEVs. At the time of writing this thesis, new commercial PHEVs and BEVs have battery capacities mostly around 8–18 kWh and 40–100 kWh, respectively (Kane, 2021). The efficiencies vary between the models, so the rough estimations of the all-electric ranges are mostly around 25–50 km and 250–500 km, respectively (Kane, 2021).

2.1.1 Drivers for EV adoption and the current state

There is a need to reduce greenhouse gas emissions to combat climate change, and this reduction extends to the transportation sector in which EVs are seen as the key solution. This also requires that carbon neutral energy resources will be used to charge EVs. Different reduction goals have been set between countries. The goal in Finland is to reduce domestic transportation emissions by half by 2030 from the 2005 level and completely by 2045 (Ministry of Transport and Communications, 2020). The target is to have 700,000 EVs by 2030, most of which should be BEVs (Ministry of Transport and Communications, 2020). Various incentives are used to promote EV adoption to achieve the national targets. In Finland, these incentives include lower taxation for EVs compared to traditional internal combustion engine vehicles (ICEVs) (Andersson *et al.*, 2020) and procurement support for buying a new electric car or signing a long-term lease agreement for an EV (Finnish Transport and Communications Agency Traficom, 2018). Besides reducing greenhouse gas

emissions, the use of EVs could help improve the local air quality (International Energy Agency, 2021) and reduce the noise level (Cao *et al.*, 2012).

The number of EVs at the time of writing this thesis is relatively small from a national perspective and represents only a few percent of all road vehicles, yet it is increasing at a fast pace. According to E-mobility (Sähköinen liikenne ry, 2020), the number of EVs in Finland after the second quartal in 2021 was 77,468. That amount increased from 40,315 by 37,153 (+92%) in a year. Most of these EVs are PHEVs, but the share of BEVs increased from 16% to 19% during the year. Around 28% of the newly registered road vehicles were EVs during the first half of 2021. The total number of EVs was over 10 million at the end of 2020, which globally represents 1% stock share (International Energy Agency, 2021). The amount increased by 43% during the year.

2.1.2   Barriers for EV adoption

Five, more or less intertwined, fundamental barriers to a wide adoption of EVs have been identified: high EV prices, "range anxiety", battery lifetime, lack of sufficient charging infrastructure, and uncertainty of the availability of raw materials to produce enough battery packs for all EVs. High EV prices are mostly due to high battery prices, which can account for up to around one-third of the total costs of the vehicle (Ruffo, 2020). However, EV prices have decreased over the past few years, and there are indications that their prices will decrease further. For example, according to (Miller, 2020; Ruffo, 2020), the gap between the production costs of emission-free EVs and the ICEV is estimated to decrease from 45% to 9% in the ten years from 2020 to 2030. Car manufacturers such as Volkswagen (Halvorson, 2021) and Toyota (Agence France-Presse, 2021) have set plans to reduce EV battery costs by half in a similar timeframe.

The phenomenon called range anxiety refers to a concern that a BEV might not have enough driving range to reach a desired destination (Pevec *et al.*, 2020). The concern may also affect potential buyers and thus slow the BEV adoption rate. PHEVs can utilize traditional fuels to extend their driving range, so range anxiety mostly affects BEV users. However, (Pevec *et al.*, 2020) mentioned that modern BEVs have enough battery capacity to meet an average driving demand of one week. Additionally, according to the National Travel Survey 2010–2011, around 51% of all kilometers are driven as trips with a length of ≤ 50 km in Finland (Rautiainen, 2015), which can be driven with modern PHEVs by using electrical energy only. Furthermore, around 90% of all kilometers are driven as trips with a length of ≤ 300 km (Rautiainen, 2015), which are suitable for modern BEVs. The remaining

kilometers are driven as trips that are likely to require a charging stop. Besides the initial effective range, there have been concerns about the battery lifetime. Batteries slowly degrade and lose their effective capacity as they are used, and the battery is often considered unsuitable for an EV if the remaining capacity falls below 60–70 % of the original level (Ceyhan, 2019). However, according to (Ceyhan, 2019), manufacturers already give warranties from 8 years (or ~ 160,000 km) up to lifetime coverage for EV batteries, which should ease the concerns of potential EV buyers.

At the time of writing this thesis, the number of public charging locations in Finland is 1,392 (Sähköinen liikenne ry, 2020), whereas the number of gas stations is 1,900 (Öljy- ja biopolttoaineala ry, 2016). The numbers are not that different, but the difference is more impactful when considering the driving ranges and fueling times. In turn, there may be an opportunity to charge EVs at a destination location such as home, workplace, or shopping center. As mentioned earlier, the driving ranges of modern EVs are mostly less than 500 km, whereas the driving range of ICEVs can be over 1,000 km. Additionally, the fueling time of an ICEV is roughly around 300 km/min, whereas the charging time of EVs vary more notably. For example, a 350 kW high power charger could provide almost 30 km/min, whereas 3.7 kW charging power would mean 0.3 km/min (Sähköinen liikenne ry, 2020). This causes pressure to add new charging sites and to improve the charging power to provide faster charging. However, it should be noted that the actual charging speed is also dependent on the EV. Additionally, the charging speed may be affected if a charging control strategy is used. Section 2.2 discusses the general details of charging control.

The millions of EVs must first be manufactured to make a wide adoption of EVs possible, and the material to make their batteries have not yet been mined (Castelvecchi, 2021). Lithium-ion batteries are expected to be the dominant energy storage solution for EVs in the foreseeable future, and a common lithium-ion battery pack can contain several kilos of lithium, nickel, manganese, and cobalt (Castelvecchi, 2021). According to (BloombergNEF, 2021), the supply of these metals is assumed to be sufficient till 2030. The goal is to cut down the usage of scarce metals and improve battery recycling to solve potential issues of the supply in the future (Castelvecchi, 2021). The challenges are generally seen as solvable, even though a very large amount of material will be needed to manufacture the EVs, and temporal supply hiccups may be seen (Castelvecchi, 2021).

2.1.3 Charging of EVs

There are essentially two options for charging an EV: a charging station or a socket-outlet. Charging stations can be divided into regular alternating current (AC)

charging and fast direct current (DC) charging. AC charging is when an on-board charger (OBC) located inside the EV is used to convert the AC into DC to charge the battery. DC charging is when an off-board charger located in the charging station is used to feed DC into the EV to charge its battery.

Four charging modes are defined in the international charging standard IEC 61851-1: mode 1, mode 2, mode 3 and mode 4. Modes 2–4 are intended for charging EVs, whereas mode 1 is mostly intended for charging mopeds and other light vehicles. Modes 1–3 utilize AC charging, whereas mode 4 utilizes DC. An EV can be charged from a regular "Schuko" socket outlet using a charging cable that includes an in-cable control and a protection device in mode 2 charging. The device includes protection functionalities, e.g., residual current detection. An EV can be charged using such sockets, although it should be used with caution if the socket is not intended to withstand continuous high currents such as 16 A, if the socket is old, or if there is uncertainty regarding the condition of the socket (SESKO ry, 2019).

A specific charging connector or socket outlet is used in mode 3 charging. "Type 2," as defined in IEC 62196-2, is used as the *de facto* socket outlet for mode 3 charging in Europe. Besides safety-related functionalities, the mode 3 charging method enables the EV supply equipment (EVSE) to control the maximum current drawn by the connected vehicle. It should be emphasized that the EVSE cannot force a certain charging current but instead can only set an upper limit for it, and the EV itself chooses the actual current to ensure safe and efficient charging of the EV's battery. Mode 3 charging can utilize 1–3 phases and currents of 6–80 A. However, public mode 3 charging stations in Europe provide currents mostly up to 32 A, which equals a charging power of 22 kW. An EVSE can also set a current limit of 0 A in mode 3 charging, which effectively equals temporarily disabling the charging session.

Much higher currents can often be used in mode 4 charging, because the method utilizes an off-board charger and bypasses the EV's OBC and its potential limitations. The supported charging powers in mode 4 charging stations are generally between 22 kW and 150 kW, but there are already a few charging stations in Finland that provide charging powers up to 350 kW (Sähköinen liikenne ry, 2020). The charging powers of mode 4 charging stations have increased over the past years, and the powers are anticipated to increase much more (Halvorson, 2021). Similar to mode 3 charging, the maximum charging current can be controlled by the EVSE.

Additionally, an EV could potentially be charged wirelessly, for which there are standards such as IEC 61980-1. Wireless charging could be a more convenient solution from the EV users' perspective because they are not required to plug in their EV (Rautiainen, 2015) if the technology evolves enough to enable practical,

safe, energy efficient and cost-effective wireless charging. However, this thesis focuses on conductive mode 3 charging because it is robust, it enables a charging current limitation from the EVSE side, and the charging point costs are much lower compared to mode 4 charging point costs.

Furthermore, EVs could be re-energized by using battery swapping in which an EV's depleted battery is replaced with a charged one. However, because battery swapping is seen more promising for, e.g., taxis and buses rather than for passenger vehicles (Zhang, Chen, *et al.*, 2018), a further discussion of battery swapping is excluded from this thesis.

2.1.4   EV charging locations

EVs can be charged at destination locations such as homes, workplaces, or shopping centers if suitable charging infrastructures exist, unlike traditional ICEVs. According to a charging behavior survey (The Finnish Information Centre of Automobile Sector, 2020), 93% of EV users in Finland have the opportunity for home charging. (Thingvad *et al.*, 2021) mentions that the probability for private home charging is around 60–80% in the United States and in Germany. The higher probability is in rural areas, whereas the lower probability is in metropolitan areas. Charging infrastructure exists to a much lesser extent for other charging locations besides the home. Therefore, adoption of EVs may be especially problematic for people living in cities because they may not have a home charging option (Thingvad *et al.*, 2021). This also highlights the importance of a public charging opportunity.

As mentioned earlier (subsection 2.1.2), most of the charging demand could be fulfilled by having a charging opportunity at every destination. However, there is still a need for public charging stations on the road to ease the range anxiety and to enable convenient long trips with BEVs. According to E-mobility (Sähköinen liikenne ry, 2020), the number of public charging locations in Finland after the second quartal in 2021 was 1,392. That amount increased by 283 (+26%) in one year. Out of all public charging locations, 301 have a fast-charging option. In total, the locations include 4853 mode 3 and 417 mode 4 charging points.

2.1.5   EV charging load

EVs are charged in most cases using the electrical energy from the power grid. According to the Finnish National Travel Survey (Finnish Transport and Communications Agency Traficom, 2016), passenger cars were driven 42.1 km/day in Finland in 2016. According to (Kane, 2021), a new BEV consumes roughly 215 Wh/km, which would lead to an average energy demand of around 9.1 kWh per EV

per day. The total energy demand of EVs also increases as the number of EVs increases. According to the average domestic travel distance of passenger vehicles (including vans) and the number of people in Finland (Finnish Transport and Communications Agency Traficom, 2016), a total of 119 million kilometers are driven per day. Assuming 215 Wh/km, this would lead to an energy consumption of around 9.4 TWh per year. According to the open data of Fingrid (Fingrid, 2021), this represented around 12% of the total electricity consumption in 2020. Thus, the required charging energy is not seen as a threat from the transmission system and energy generation viewpoints.

Conversely, because the charging demand varies in terms of time and location, it may pose a challenge to the local distribution system and electricity consumer level. (Belonogova *et al.*, 2020) estimated that a wide-scale workplace charging would not cause overloading problems in the Helsinki, Finland, distribution network. However, the results are very case specific; thus, the results may not apply to other distribution networks. The charging load at a household level will be even more notable compared to its other electricity usage. [P5] mentioned that a household using a geothermal heat pump as the main heating system can consume 30–60 kWh of electrical energy in a day, which means that an average charging demand could increase consumption by 15–30%. More notably, even a relatively slow charging of an EV with a power of 3.7 kW (230 V, 1×16 A) can be over 50% of the peak load of the household itself. It is also seen as significant when considering the fact that a fuse size of 3×25 (three phases with maximum current of 25 A) is common in Finnish households.

There are increasing opportunities to charge elsewhere, although a home is the most common charging location. The increased possibilities to charge at different locations may result in more even distribution of the charging load throughout the day. Vehicles were on the road a total of 2.5 million hours per day, according to the average time spent as drivers of passenger vehicles (including vans) in the case of domestic travelling and the number of people in Finland (Finnish Transport and Communications Agency Traficom, 2016). Furthermore, according to the Finnish Transport and Communication Agency, there were 2.9 million passenger cars (including vans) in Finland in 2016. Based on these values, the vehicles were on the road only 3.6% of the time, while they were parked at different locations the rest of the time. A very similar value, 4%, was also mentioned by (Kempton and Tomić, 2005). This means that there is plenty of time available for charging. A charging data analysis (Rauma *et al.*, 2021) showed that the charging load is divided throughout the day because EV users mostly charge at work from 06:00–13:00, at commercial

locations from 09:00–20:00, and at home from 14:00–05:00. Even though the load is not equally distributed over the day, it is likely to enable charging control options at different times.

2.2 Introduction to smart charging

In this thesis, "smart charging" or "controlled charging" refer to a situation in which the charging of an EV is influenced to achieve a secondary goal while still trying to meet the EV's energy need. A similar definition was used before in, e.g., (Rautiainen, 2015). Smart charging is essentially the opposite of uncontrolled charging in which EV's charging begins as soon as it is plugged in to an EVSE, and the charging current is only limited by the maximum current supported by the OBC of the EV and the EVSE. This also means that any smart charging control action can only reduce the charging current or retain it as the same compared to uncontrolled charging. Thus, compared to uncontrolled charging, smart charging can only prolong the required charging time or limit the energy that is charged into the EV in a certain time period. However, the fact that a smart charging solution can be used to improve the cost-effectiveness of the charging from different perspectives makes it very interesting. Despite the name, "smart charging" may not always be smart. A poorly chosen control method may have even more severe negative influences than uncontrolled charging.

The following subsections present different properties of a typical smart charging solution. The topics include the key actors in a smart charging scheme, the controllability of EV charging, bidirectional charging, smart charging control objectives and approaches, available data and related standards in charging control, challenges in charging control, and, finally, the three components of a typical smart charging control algorithm. Each topic is discussed in a separate subsection.

2.2.1 Key actors in smart charging scheme

The charging loads of electrified car fleets are notable and pose both challenges and opportunities for multiple actors related to the electricity grid. These actors could benefit from the use of smart charging. However, each actor may have different needs and goals, which can complicate the situation and cause conflicts of interest. The solution may pose notable challenges for another actor when smart charging is optimized from a single actor perspective. Furthermore, charging schemes include objects, namely EV and EVSE, which may pose certain limitations.

Perhaps the most obvious object and actor in a smart charging scheme are the EV and its user. The EV user naturally wants to be able to drive the next trip without

any unnecessary inconveniences, which means there should be enough energy in the EV's battery for the next trip before the intended departure time. The energy demand could be "flexible," depending on the driving demand, EV and charging infrastructure. In this thesis, "flexible" charging load or charging session means that it is unnecessary to start charging right away to meet the charging demand. However, the opposite, "non-flexible" charging load or charging session, means that the charging should be started right away to fulfill the demand as much as possible. Besides the user's needs, the EV's properties also play an important role because the battery capacity impacts the driving range, and the OBC's properties define the supported charging rates.

As mentioned earlier, EVs can be charged in different locations that may have different charging infrastructures. The infrastructure can directly influence the charging power. For example, if the EVSE supports only a single-phase charging of 32 A (230 V), the EV cannot charge with a power greater than 7.4 kW even if the OBC of the EV could support it. Furthermore, the charging system operator (CSO) who is responsible for the functioning of the charging site may want to control the charging to achieve safety- or cost-effectiveness-related objectives that may temporally limit the available charging power even further.

Similar to the CSO, distribution system operators (DSOs) and transmission system operators (TSOs) may also want to influence EV charging to achieve safety- or cost-effectiveness-related objectives. Additionally, energy providers could utilize the controllability of EVs to ensure certain energy usage at certain times. One EV or even one EV charging site may be too small to have a clear impact on the distribution system level, transmission system level, or energy provider level; thus, there may be an aggregator that gathers the flexibility of multiple smaller units together.

2.2.2 Controllability of EV charging

Mode 3 charging is controllable, yet there are some limitations to be considered. As mentioned earlier, only the maximum current limit can be adjusted, and the EV itself chooses the actual current. This also means that the charging control system does not know the actual charging current without feedback. The standard IEC 61851-1 states that the available charging currents in mode 3 charging are 6–80 A. Additionally, the same current limit indicated by the EVSE is applied for each phase. However, the maximum and minimum charging currents may be limited by the OBC of the EV or by the supported currents of the EVSE, and either the EVSE or the OBC may support only one-phase charging. For example, using a 11 kW (3×16 A,

230 V) EVSE to charge a Nissan Leaf 2019 that supports 7.4 kW charging (1×32 A, 230 V) leads to a maximum charging power of 3.7 kW (1×16 A, 230 V).

Besides the maximum current, the charging currents supported by the EVSE or by the EV may be limited to only a discrete set, and the minimum non-zero current may not always be 6 A. For example, the EVSEs used in the publications of this thesis support only current limit integers {0, 6, 7, …, 32}. According to (Lee *et al.*, 2021), some EVSEs may support only charging current limits of {0, 8, 16, 24, 32}, {0, 16, 32, 48, 64}, or {0.0, 6.0, 6.1, 6.2, …, 79.9, 80.0}. Similar properties may also be in EVs. For example, Smart EQ ForFour 2020 only supports charging current limits between 8–32 A, whereas BMW i3 2016 in "low" mode charges with around 7.5 A when the current limit is 15 A. Fig. 2.1 illustrates the charging currents under different current limits set by the EVSE. According to the BMW i3 user manual (BMW AG, 2015), BMW i3 has three different modes ("low", "reduced", and "maximum") that influence its charging properties. The BMW is in "low" mode in Fig. 2.1.
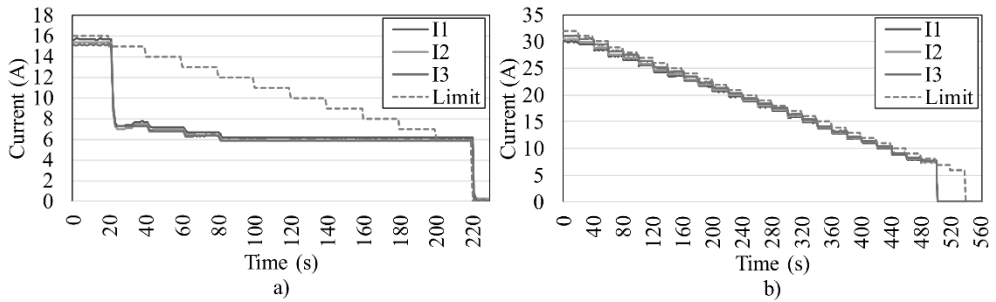

Figure 2.1 Charging currents under different current limits set by the EVSE for a) BMW i3 2016 and b) Smart EQ ForFour 2020. The BMW in this example is in "low" mode. The charging current limit decreases by 1 A every 20 seconds until at 6 A it goes to zero.

A lower charging current than the current limit can also occur if, e.g., the OBC of the EV chooses to charge more slowly to protect the EV's battery from overheating or the EV's battery is at a high state of charge (SoC) and requires a slower charging rate (Lee, Chang, *et al.*, 2019). It is common that the charging profile of a lithium-ion battery consists of constant current (CC) and constant voltage (CV) stages (Li *et al.*, 2020). The battery voltage level increases in the CC stage as the battery SoC increases. However, the charging current decreases in the CV stage before the battery is fully charged. These stages are used to ensure safe charging and prolonged battery lifetime. Further examination of the electronics inside the EV was excluded from this thesis because the focus is on the EV charging loads from the electricity grid perspective. Measurements of charging loads have shown that two

stages are usually seen from the grid perspective: constant power (CP) and CV. The charging currents are often very steady in the CP stage with a variation of less than 0.5 A [P7]; however, minor temporal deviances may occur. The charging currents often decrease before the charging is finished in the CV stage. However, during the CV stage, the charging currents are not likely to decrease linearly, and differences between the three phases may be seen. Fig. 2.2 illustrates this, where the charging currents of BMW i3 2016 in "low" mode and Nissan Leaf 2019 are presented. Both charging sessions are uncontrolled, and the energy consumptions are 3.1 kWh and 11.3 kWh, respectively. Fig. 2.2a shows that the OBC of the BMW chooses to switch from three-phase charging into single-phase charging because the battery is becoming nearly fully charged and thus requires slower charging. In Fig. 2.2b, the charging current is around 0.3 A for about 4 min three times before the charging session finishes.
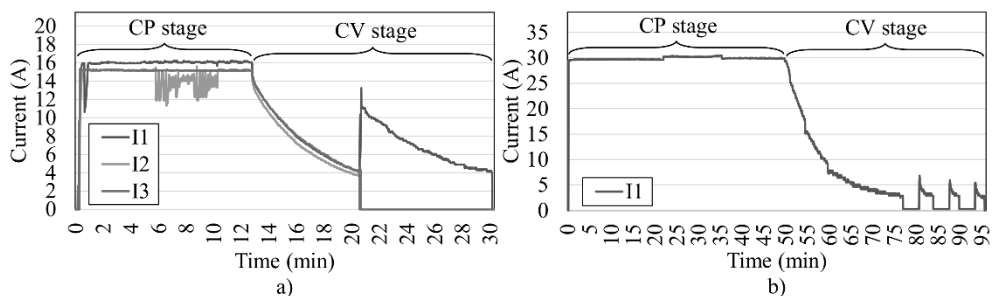

Figure 2.2 Charging currents in CP and CV stages for a) BMW i3 2016 and b) Nissan Leaf 2019.

As just mentioned, there are various reasons why an EV may choose a lower charging current than indicated by the EVSE or why an EV may not utilize three-phase charging even if the EVSE would support it. This means that even though the EV charging is considered a controllable load, the charging currents are likely to deviate from the "ideal" level indicated by the EVSE; thus, feedback is required to track the actual charging currents. This thesis uses the term "non-ideal charging characteristics" to define the situation in which the realized charging currents deviate from the current limit indicated by the EVSE. Additionally, the term "non-linear charging profile" is commonly used to define a situation in which the charging currents decrease before the battery is fully charged, which is often the case.

2.2.3   Bidirectional EV charging

The EV acts only as an energy consumer in traditional grid-to-vehicle (G2V) charging. However, the energy in an EV's battery could also be discharged back to the grid, which is called vehicle-to-grid (V2G). This allows an EV to act as energy

storage instead of only as an energy consumer. Both the EV and the EVSE must support this operation to enable a V2G operation. Related international standards, such as ISO 15118, are being developed to enable a wide adoption of V2G support.

V2G is generally seen as very valuable from the grid perspective (van Triel and Lipman, 2020) and doable from the EV-usage perspective. As mentioned earlier, EVs are parked most of the time, and their average daily energy requirement is quite moderate (Section 2.1.5). This means that the EVs' batteries are not likely to be under constant usage; thus, there is a notable potential to use the batteries for DR. For example, studies have shown that V2G can be used to reduce peak loads (Wang and Liang, 2017), reduce charging costs (Mouli *et al.*, 2019), and improve the balance between energy generation and consumption (Zhou and Sun, 2020). There are also a few variations of V2G. Instead of injecting the discharged power to the grid as in V2G, the discharged power can be consumed by a household as in vehicle-to-home (V2H), by a building as in vehicle-to-building (V2B), or by other vehicles as in vehicle-to-vehicle (V2V). The term vehicle-to-X (V2X) has generally been used to include all these use cases of bidirectional EV charging. Use case examples in (Datta *et al.*, 2019) showed that V2H could be used to decrease household electricity costs by around 11.6% compared with the G2V operation mode. In (Dagdougui *et al.*, 2019), V2B is used to limit peak loads in a smart building, and in (Koufakis *et al.*, 2020), V2V is used to reduce charging costs.

However, despite the V2X potential, there are concerns related to user willingness and the operation's technicalities. According to a user survey (Geske and Schumann, 2018), battery degradation and range anxiety are the most notable concerns. It is commonly considered that batteries degrade as they are charged and discharged; thus, utilizing V2X may lead to faster battery degradation because the batteries are charged and discharged more frequently. This is an especially important factor from the EV user perspective, because the battery can be the most expensive EV component and determines its driving range. Additionally, if the battery is being discharged by a CSO and the EV is needed by the user before the expected departure time, the remaining energy may not be enough for the next trip. This kind of situation or the concern that this might happen can cause range anxiety and thus reduce the willingness of EV users to participate in V2X. Furthermore, the survey responders were concerned about the usage of their data and giving away such access for their vehicle that they cannot control (Geske and Schumann, 2018). However, the results also show that the responders are willing to participate in V2G if they receive monetary benefits. Therefore, the benefits should outweigh the concerns and

the potential extra effort required from the EV users to encourage them to participate in V2G operation.

Besides user willingness, the potential benefits of V2G depend on various technical factors such as battery degradation costs and the efficiency of charging and discharging. However, multiple studies have not considered battery degradation, as mentioned in (Ahmadian, Sedghi, Elkamel, *et al.*, 2018; Ahmadian, Sedghi, Mohammadi-Ivatloo, *et al.*, 2018; Gschwendtner *et al.*, 2021). Nevertheless, if the battery degradation is considered, different costs or degradation models have been considered. For example, (Mouli *et al.*, 2019) considered a fixed value of 4.2 ¢/kWh (~3.7 c/kWh) for cycling degradation, whereas (Ahmadian, Sedghi, Elkamel, *et al.*, 2018) considered a total battery degradation that includes calendar degradation in addition to the cycling degradation. (Gschwendtner *et al.*, 2021) mentioned that the impact of V2X on battery degradation varies from negative to positive depending on the parameters and assumptions used in the study. V2G usage leads to higher energy losses in addition to its influence on battery degradation. According to (Apostolaki-Iosifidou *et al.*, 2017), total charging and discharging losses vary between 12–17% and 30–36%, respectively, and are mostly caused by the power electronics used for AC-DC conversion. The values mentioned in (Apostolaki-Iosifidou *et al.*, 2017) lead to a roundtrip efficiency between 53% and 62%. Notably better roundtrip efficiencies of 79–88% were measured in (Schram *et al.*, 2020). The losses seem to be higher for a low power transfer (~10 A) compared to a higher power transfer (~16–50 A) (Apostolaki-Iosifidou *et al.*, 2017; Schram *et al.*, 2020). These values are seen as significant, because V2G-related studies have assumed widely different roundtrip efficiencies or neglected the losses completely (Shirazi and Sachs, 2018; Schram *et al.*, 2020). These assumptions, especially both extremes, may lead to either unrealistically optimistic or pessimistic results from a V2G perspective.

V2X solutions proposed in the literature, such as (Kempton and Tomić, 2005; Wang and Liang, 2017; Ahmadian, Sedghi, Mohammadi-Ivatloo, *et al.*, 2018; Mouli *et al.*, 2019; Datta *et al.*, 2019; Koufakis *et al.*, 2020), depend on user behavior input to ensure fulfilment of the mobility needs. However, this may pose issues regarding the required effort from the user and the data's accuracy (Subsection 5.2.1 discusses the issues further) and thus complicate the solutions' implementation. The results in (Venegas *et al.*, 2021) indicate that V2G would more likely be viable in workplace charging where the plug-in duration and charging patterns are relatively consistent versus commercial or home charging. However, a behind-the-meter usage of V2H or V2B may still be viable for private users (Venegas *et al.*, 2021).

According to a review study (Ahmadian, Sedghi, Elkamel, *et al.*, 2018), the benefits of V2X have been assessed using different modeling methods and scenarios, and some studies have seen V2X as economically beneficial, whereas some studies have not. Thus, some uncertainties seem to remain regarding the actual benefits of V2X. Additionally, the discharging in V2X may work similarly to the charging in charging mode 3 (IEC 61851), meaning that an EVSE can potentially set only the maximum discharging current limit and the EV itself chooses the actual discharging current. As in G2V operation, there may be several reasons why an EV chooses a lower current than the EVSE indicates. This may complicate the practical and efficient implementation of V2X control algorithms even further.

2.2.4   Smart charging control objectives and approaches

A smart charging solution can be designed from the perspective of any of the key actors included in the scheme, and more complex solutions may be designed to consider the benefits of multiple actors. There may be a conflict of interests in the case of multiple objectives when two or more objectives may not be achieved simultaneously. This can be taken into account by prioritizing the most important objective first, such as a grid safety-related objective, over the secondary objective, such as the charging cost optimization. There are different objectives, such as minimizing the costs of the used electricity, minimizing load peaks, improving renewable energy resource (RES) utilization, providing frequency or voltage regulation, and improving the quality of charging service from the EV user perspective.

Depending on the charging site location (e.g., home, work, commercial), there may be different charging behaviors that might make certain objectives more beneficial than others. For example, it may be difficult to utilize home charging to improve PV generation usage if the EV is not plugged into the charging point at the time of available PV generation. Different charging sites may also have different limitations to be taken into account, such as the available total charging capacity.

Smart charging solutions are generally divided into two approaches: centralized and decentralized. All EVs in a certain area are directly controlled by a centralized unit in the centralized control approach. The centralized unit gathers data from the grid and the EVs to optimize the charging control. EV charging in a single charging site is optimized in a decentralized control approach by considering only simple control signals, such as electrical energy pricing, distribution tariffs, local load, and other EVs in the same charging site. Both approaches have their own advantages and disadvantages.

The centralized approach utilizes the power grid and the EV data; thus, it can be used to achieve the global optimum in objectives such as minimizing the peak loads in distribution networks while considering different limitations and satisfying the EV users' charging demand. However, the required data can also become a problem. For example, the implementation requires the existence of certain communication links to gather the power grid and EV data. Furthermore, collecting confidential data of vehicles and their usages in one location may increase the threat of exposure to malicious cyber-attacks, and a large-scale implementation might result in an exponentially high computational burden (Al-Ogaili *et al.*, 2019).

Due to the limited information available in a decentralized approach, the goal is to achieve only a local optimum, which may differ from the global optimum. The charging is optimized using only the locally available control signals, so the importance of the control signals' designs, such as distribution tariffs, is emphasized. However, the approach neither needs very complex communication links nor utilizes enormous amount of data, so it can be implemented much easier compared to centralized approaches. Subsection 2.1.5 mentioned that the required total charging energy at a national level is unlikely to be an issue from the transmission system and energy generation viewpoints. This also indicates that a reliable operation of a transmission system may not require charging control that achieves the global optimum solution. Unevenly distributed charging demands may pose more challenges at the distribution system level, yet achieving the global optimum at the load control might not be necessary. Due to these reasons, this thesis focuses on decentralized approaches.

2.2.5　Available information for charging control and related standards

According to charging mode 3 of the international charging standard IEC 61851-1, an EV shall indicate its charging status by adjusting the pilot signal voltage. The four statuses under normal operation (excluding errors and faults) are (A) EV not connected, (B) EV connected but not ready to receive energy, (C) EV connected and ready to charge or already charging, and (D) EV connected and ready to charge or already charging but requires charging area ventilation. This status is known by the charging controller in the EVSE, and the information can be forwarded to the charging control system. Within this thesis, EVs with a status of (C) or (D) are referred to as "active EVs" because they are actively charging or ready to be charged.

At the time of writing this thesis, the information regarding the status is often the only data available for the charging control system from the charge controller. Especially newer EVSEs include energy meters, so data such as charging currents

are often also available. However, charging mode 3 of the standard IEC 61851-1 also supports digital communication between the EVSE and the EV. General parts of the digital communication are defined in standard ISO 15118-1. The standard also defines communication between the EV and EVSE whereby data such as battery status and EV user mobility needs can be transferred to a charging control system through the EVSE. The EV user is expected to input the needs into the EV first. This standard is especially interesting from a smart charging solution viewpoint, because the aforementioned data could be used to implement different charging control optimization principles.

2.2.6   Challenges in EV charging control

There are generally many uncertainties regarding the EV charging management. The uncertain factors may include EV-related information such as arrival and departure times, energy requirements, and the willingness of the users to plug in their EVs. The uncertainties may also be extended to include other factors such as electricity consumption and production profiles or electricity pricing. These factors may have an influence especially on an optimized charging control with a certain objective, such as cost minimization. These factors are not always known beforehand, so EV charging control often has to deal with predictions or assumption. However, this thesis excludes a more thorough assessment of different forecasting methods and their accuracies.

2.2.7   Main components in a smart charging algorithm

There are several aspects to be considered to achieve the desired and optimized operation in a smart charging algorithm. This thesis divides charging control algorithms into three components. These components may be intertwined or unnecessary in some cases, yet each one represents a key function that is often needed in efficient and optimized control algorithms. The three components are:

- *Capacity determination*,
- *Capacity allocation*, and
- *Capacity usage rate correction*.

Out of the three components, the charging capacity determination is likely the most studied in the scientific literature. *Capacity determination* describes the logic behind the determination of the available charging capacity of a charging site. *Capacity allocation* describes the logic behind the distribution of the available charging capacity. Last, *capacity usage rate correction* describes the logic behind overcoming the negative impacts of the non-ideal charging characteristics to achieve the desired

capacity usage. This is perhaps the least-studied component in the literature. However, over the past few years, the non-ideal charging characteristics (discussed in Section 2.2.2) have gained more attention [P7], and the need for *capacity usage rate correction* is becoming more widely known. These three components are discussed separately in Chapters 4–6 to further elaborate them.

3   EV charging load modelling

Accurate modelling of EV charging loads is important to ensure safe and optimal operation of the power grid in a case of a notable EV penetration (Ge *et al.*, 2020). A more accurate modelling generally requires more complex methods and a higher computational capacity that, in turn, leads to more reliable results. Furthermore, the influences of certain phenomena, such as the non-ideal charging characteristics or phase unbalance, may not be properly assessed by using simulation parameters, methods or assumptions that oversimplify the situation. The developed algorithms may consequently not be applicable or work as intended in real-life charging systems (Lee *et al.*, 2021). Multiple studies have been carried out in the scientific literature to improve the accuracy of the charging load modelling and give more strengthened scientific background for the results.

For example, (Pareschi *et al.*, 2020) showed that national travel surveys can be used relatively accurately to model EV charging loads. However, the study underlines the importance of several modeling parameters such as charging powers and battery sizes. (Sadeghianpourhamami *et al.*, 2018) and (Wolbertus *et al.*, 2018) analyzed charging sessions in terms of arrival, sojourn and idle times using data of 1.5 million and 2.6 million charging sessions, respectively. These studies give insight into the plug-in behavior of EVs and their charging energy requirements, which can be used to, e.g., assess the flexibility potential of the EVs. Additionally, (Venegas *et al.*, 2021), for example, assessed the probability of EV users plugging in their EVs. The results of the study show that EV fleets with large battery sizes may have decreased their flexibility potential compared to EV fleets with low battery sizes. This is because the plug-in frequency decreases and the energy requirement increases for EVs with a larger battery size. (Zhang *et al.*, 2020) and (Yi *et al.*, 2020) established spatial-temporal models of EV charging loads. (Zhang *et al.*, 2020) showed that the demographics of the EV users have an effect on the daily charging loads. (Yi *et al.*, 2020), based on the results, gave different recommendations for charging infrastructure deployments for different charging locations.

Four gaps were found and assessed despite the numerous studies related to EV charging modelling. The following subsections discuss these modelling aspects and present the related advancements made in the original publications. The data and the laboratory equipment, including the commercial EVs described in Section 1.3, played an important role in ensuring that the developed methods and obtained results were realistic.

3.1　Modelling non-ideal charging characteristics

Section 2.2.2 mentioned that an EVSE can only set the maximum charging current limit and the EV itself chooses the actual charging current. The charging current will likely decrease, especially when the EV's battery is nearly fully charged. Additionally, an EV may not always use all three phases even if the EVSE supports it. Commercial EVs can be used in, e.g., a laboratory environment as in [P6] to study the influences of realistic non-ideal charging characteristics on a small scale. It is necessary, however, to model them in a reasonable manner to assess the influences caused by the non-ideal charging characteristics on a large scale. So far, according to the author's knowledge, there have been no reasonably accurate models proposed in the scientific literature. (Lee *et al.*, 2021) acknowledged the importance of modeling the unbalanced three-phase electrical network and incorporating non-ideal charging characteristics. However, the study does not propose a method to model non-ideal three-phase charging sessions.

[P7]'s aim was to develop a charging control algorithm (the algorithm is described in Section 6.2) to overcome the negative influences of the non-ideal charging characteristics. It was necessary to model the non-ideal charging characteristics in a realistic manner to do so. Extended laboratory measurements of the charging profiles of the Nissan Leaf 2012 and BMW i3 2016 were carried out to this end. The analysis of the measurements confirmed that the charging currents were steady in the CP stage with a variation of less than 0.5 A. At around 97.5–99.7% SoC, the CP stage changed to the CV stage, and the current began to decrease. The analysis also showed that the exact SoC depends on the charging current limit set by the EVSE. Fig. 3.1 illustrates the charging currents in the CV stage for a Nissan Leaf 2012 and BMW i3 2016 for four different current limits set by the EVSE: 16, 12, 9, and 6 A. The BMW is on "maximum" mode in the figure.
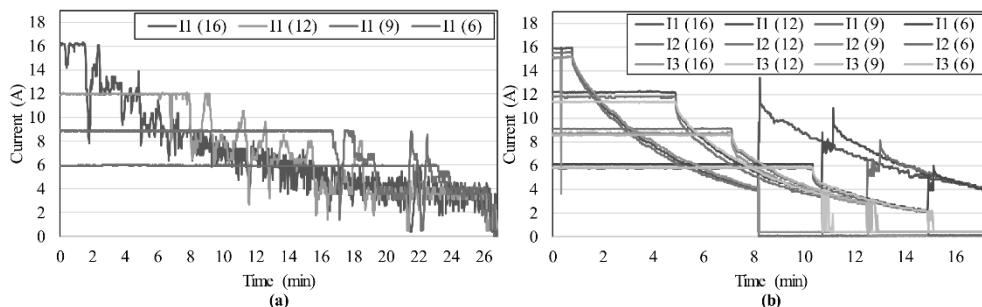

Figure 3.1 Charging currents for (a) Nissan Leaf 2012 and (b) BMW i3, where I1–I3 represents phases and the number in the parentheses represents the current limit set by the EVSE [P7].

Based on the analysis, it seems reasonable to assume a linear charging profile during the CP stage. The CV stages of the two charging profiles shown in Fig. 2.2 are clearly non-linear and dissimilar; thus, their modelling in [P7] was done using separate lookup tables for both EVs. The energy that is missing from the EV's battery is calculated at each one second time step of the measurements to form a lookup table. The energy that is missing from the EV's battery is referred to as the energy requirement. The calculations begin from the end of the charging sessions where the missing energy is zero, i.e., the EV is fully charged. The energy requirements are calculated up to the point that separates the CP and CV stages. After the energy requirements of each time step are calculated, the lookup table is formed to link the energy requirements to the realized charging currents. A separate lookup table is formed for all possible current limit integers supported by the EVs (6, 7, 8, …, 32 A). Only integers are considered here because the used EVSEs (described in Section 1.3) do not allow floating point current limits. As a result, the simulation model can determine realistic charging currents based on the following parameters: EV model, energy requirement (Wh), and current limit set by the EVSE (A). Fig. 3.2 shows an illustration of the process. The EV is a BMW i3 in "low" mode in the figure, and the current limit is 6 A. The CP stage changes to the CV stage in the figure when the energy requirement is 199 Wh.
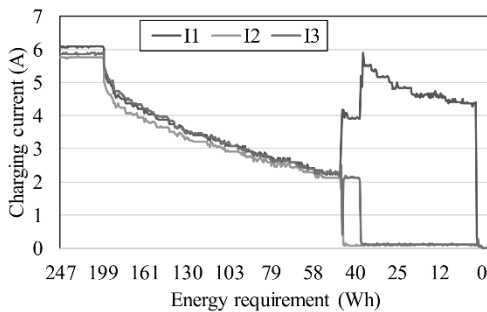

Figure 3.2 Illustration of the lookup table for the charging profile of BMW i3 2016 with 6 A charging current limit set by the EVSE. I1–I3 represent phases.

This modelling method is used in [P7] and [P8]. The modelling is extended for [P9]–[P12] to include charging profiles of a Nissan Leaf 2019 and a Smart EQ ForFour 2020 using the same method. These four EVs have different charging characteristics in terms of the maximum charging current and the number of used phases; thus, they have notably different charging profiles. Therefore, the formed charging profile models can be used to incorporate widely different charging current behaviors into the simulation.

3.2　Evolution of EV fleets

It has been a common practice in EV charging-related studies to assume that all EVs are similar or that they can utilize the full power supported by the EVSEs. Charging powers of up to 22 kW are typical for EVSEs in Europe at commercial charging locations. However, not all EVs can presently utilize such powers due to the limitations of their OBCs. However, it is reasonable to assume that a higher share of EVs will adopt more powerful OBCs as the technology evolves. This may naturally impact the charging loads of the charging site as the EVs become able to draw higher powers and, perhaps, become fully charged faster. Furthermore, this would impact long-term decisions such as the optimal sizing of charging infrastructures and parking policies.

[P9]'s objective was to analyze the current state of the EV fleet, model its evolution over the next 20 years, and then assess its implications to overcome the gap in the literature. The main focus was on commercial charging at the Finnish capital region. The current state of the EV fleet was analyzed using charging data of Tripla and REDI over a 4-month period (Nov. 2019 – Feb. 2020), including over 8,600 charging sessions in total. The analysis focused on attributes such as charging powers, energy requirements, arrival times, stay duration, and idle time. The idle time refers to a duration in which an EV is plugged into the charging point but is not charging. After the analysis, the development of the EV fleet in terms of the number of EVs was estimated. The EVs were categorized based on the highest supported power of their OBCs. The model used data from the Finnish vehicle register and the socio-demographic data of the vehicle owner to estimate the average speed of car renewals within different user and area groups. The results of the analysis and the estimated number of EVs were then used to generate different scenarios, which were then simulated considering the non-ideal charging characteristics (described in Section 3.1) to achieve realistic results for the future charging loads.

According to the analysis, most EVs (79.4%) utilize a charging power of 0–4.5 kW. The share of EVs with a maximum power of 4.5–10 kW is 8.1%, 10–15 kW is 9.0%, and 15–25 kW is 3.5%. Fig. 3.3 illustrates the shares of different charging powers. Another key finding is that most of the charging sessions that have a plug-in time ≤5 hours are non-flexible. Around 77% of these charging sessions have an idle time of less than 5 min, and only around 8% have an idle time of ≥1 hour. Importantly, the idle time does not seem to have a correlation to the charging powers. This indicates that the evolution of the OBCs of the EV fleet will likely increase their charging loads instead of their flexibility at commercial charging sites. The evolution may cause the load peak to occur 1–2 hours earlier in the case of

uncontrolled charging (Dixon and Bell, 2020) at other charging locations such as workplaces or homes. In contrast, if the charging is controlled, the evolution could increase the flexibility of the charging control because the available charging time is presumably long enough to allow EVs to be fully charged. However, the flexibility may remain the same if the EVSEs' supported powers or the available charging capacity at such locations become the limiting factor.
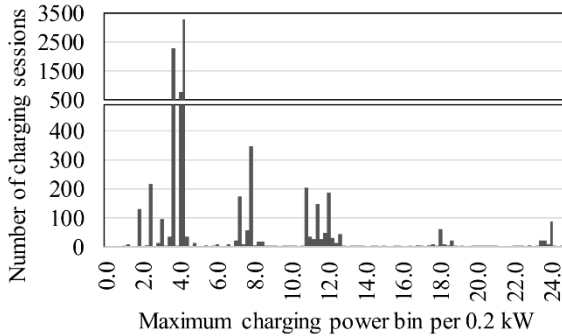

Figure 3.3 Distribution of charging peak powers in Tripla and REDI between Nov. 2019 – Feb. 2020 [P9].

The simulation results show that the charged energy and the highest peak load will increase at a faster pace than the number of EVs. The number of EVs are estimated to increase by a factor of around 21 between 2020 to 2040, whereas the daily charged energy and the highest daily peak load will increase by a factor of 39–72 and 29–48, respectively. The average charging energy per EV will increase from 5.6 to 8.7 kWh to 13.0–19.6 kWh. These values emphasize the importance of considering the evolution of the EV fleet when evaluating the long-term benefits or optimal sizing of charging-related infrastructure, such as the total charging capacity (Dong *et al.*, 2021), PV system (Deshmukh and Pearce, 2021), or energy storage system (Haupt *et al.*, 2020). The results also indicate that a larger charging site could utilize the available total charging capacity more efficiently. This further means that a centralized charging location would be more cost-efficient compared to multiple smaller charging sites.

3.3   Influence of temporal resolution

EV charging-related studies use a wide range of temporal resolutions from 10 s (Kikusato *et al.*, 2020) to 2 h (Sadeghianpourhamami *et al.*, 2020) for model charging, and 15–60 min resolutions generally seem to be the most commonly used [P11]. However, the use of a certain resolution is rarely justified, or very little effort has

been made to analyze the influence of the temporal resolution on the charging load modelling accuracy [P11]. (Shepero and Munkhammar, 2018) assessed the peak of the normalized power of uncontrolled charging using six temporal resolutions 1, 5, 10, 15, 30, 60 min. The study shows that the 60 min resolution is relatively accurate when considering charging powers of 3.7 kW. In contrast, the 1 min resolution is notably more accurate than the others when considering 22 kW charging powers. More thorough assessments of the temporal resolution's influence have been carried out in (Beck *et al.*, 2016) and (Jaszczur *et al.*, 2021) from a PV self-consumption viewpoint. The studies indicate that the 15 min temporal resolution is reasonable for assessing the self-consumption of a PV system. However, when simulating EV charging, especially controlled charging, a complex control signal and the non-ideal charging characteristics may complicate the modelling; thus, a finer resolution may be necessary [P11].

[P11]'s objective was to assess the temporal resolution's influence on different scenarios. The electricity consumption data of a five-day period of a detached house located in Pirkanmaa, Finland, was used to investigate EV charging in a household. The household data was measured in a one second resolution in December 2018 and provided by Tampere University of Applied Sciences. In addition to home charging, the influence of temporal resolution was assessed at a small and at a large charging site. Real charging session data were used for the large charging site to ensure a more realistic evaluation, and three subscenarios were considered to further compare controlled and uncontrolled charging. The REDI charging data (described in Section 1.3) over a three-month period (Jan. – Mar. 2020) were used. The same method developed in [P7] to pair charging profiles with charging sessions was used. The study was carried out using numerous simulations, and HIL simulations were conducted at the Smart Grid Technology Lab of TU Dortmund (described in Section 1.3).

[P11]'s assessment was carried out by comparing baseline results with simulation results obtained by using different temporal resolutions. Depending on the scenario, a baseline is either the results of the actual laboratory measurements or the results obtained using the finest temporal resolution. Simulations with different resolutions were carried out using the same charging characteristics modelling method developed in [P7], which linked the EVs' energy requirement to charging currents, and, thus, allowed the simulation model to consider realistic, non-ideal charging characteristics. After simulating with all temporal resolutions, the results were compared to the baselines to calculate root mean square errors (RMSE). RMSEs were calculated for the highest peak load of a single time step in a day, the highest

hourly peak load in a day, and the hourly charging energies, because these were seen as the key values that define, e.g., the charging costs.

To summarize [P11]'s results, it was shown that a temporal resolution of one hour may lead to significant modelling errors, whereas a resolution of 60 seconds is reasonably accurate in most cases. These results are in line with the study of (Shepero and Munkhammar, 2018). However, the results also show that a very fine resolution of one second may be necessary if there is a volatile charging control signal (e.g., a household's electricity consumption-based control). In contrast, the uncontrolled charging of a single EV could be modelled sufficiently accurately with a resolution of up to 15 min. The results indicate that even though the battery temperature is an important factor in battery charging, it does not necessarily have to be taken into account to achieve accurate modelling results. This further means that the non-ideal charging characteristics modelling method (developed in [P7] and described in Section 3.1) used in [P7]–[P10] and the used 10 second resolution provide reasonably accurate results.

3.4   Influence of charging profile modelling method

It has been a common practice to assume linear charging profiles to model EV charging, i.e., EVs draw constant current over the whole charging session. However, Section 2.2.2 mentioned that the actual charging current may be below the limit set by the EVSE, especially when the EV's battery is becoming fully charged. This naturally impacts the charging loads; thus, the charging load modelling may be inaccurate if the non-idealities are not considered. Bilinear charging profiles were considered in fast charging in (Wei *et al.*, 2018) and (Mouli *et al.*, 2019) to overcome the inaccuracies. The charging current was assumed to be constant over the CP stage in the bilinear charging profiles and to then decrease linearly to zero over the CV stage. The stage transition was assumed to occur at 60% SoC (Wei *et al.*, 2018) or at 80% SoC (Mouli *et al.*, 2019), but these assumptions' accuracies were not assessed. (Sun *et al.*, 2020) classified different charging profiles using an iterative clustering framework. The study showed that the number of different charging profiles is significant, yet they could be classified into a small number of types. These few charging profile types could then be used to model EV charging profiles with good accuracy. (Frendo *et al.*, 2020) modelled charging profiles using machine learning. A sensitivity analysis was also carried out to demonstrate that the EV charging loads could be accurately modelled without knowledge of the exact EV model. Instead, it showed that the maximum charging current and the number of used phases were much more important attributes. However, the aforementioned studies did not

assess the influence of different charging profile modelling methods. Therefore, it remains unknown whether certain simplifications can be made while ensuring reasonable modelling accuracy.

[P12]'s objective was to assess the influence of different charging profile modelling methods and the method developed [P7] (described in Section 3.1). The influence of the modelling methods was assessed in the case of a small and a large charging site. Real charging session data were used to ensure a more realistic evaluation for the large charging site. Three subscenarios were considered for the large charging site to further compare the modelling methods in the case of controlled or uncontrolled charging. [P11], [P12] similarly utilized the REDI charging data (described in Section 1.3) over a three-month period (Jan. – Mar. 2020) and the same method developed in [P7] to pair charging profiles with charging sessions. Additionally, the study was carried out using numerous simulations and HIL simulations conducted at the Smart Grid Technology Lab (described in Section 1.3).

[P12]'s assessment was carried out by comparing baseline results with the simulation results obtained by using different charging profile modelling methods. Depending on the scenario, the baseline was either the results of the actual laboratory measurements or the results obtained using the method to model the non-ideal charging characteristics (developed [P7] and described in Section 3.1) because it was shown to be the most accurate according to the small charging site' results. After simulating using each charging profile modelling method, the results were compared to the baselines to calculate RMSEs. RMSEs were calculated for the highest peak load of a single time step in a day, the highest hourly peak load in a day, and the hourly charging energies, similar to [P11].

[P12]'s results show that the modelling method incorporating the non-ideal charging characteristics yields accurate results, whereas the linear charging profile modelling method leads to significant inaccuracies. The results also demonstrate that a bilinear charging profile modelling method may be sufficiently accurate in most cases as long as the slope of the current in the CV stage is justified, even though the modelling method incorporating the non-ideal charging characteristics yields more accurate results. This result is in line with the studies by (Sun *et al.*, 2020) and (Frendo *et al.*, 2020), because they mention that it is not necessary to know the EV type or the exact charging profile in order to model charging loads with reasonable accuracy.

4 Capacity determination

This thesis uses *capacity determination* to describe the logic of determining a charging site's available capacity or intended capacity usage. There are several reasons that either directly limit or encourage a CSO to limit a charging site's available charging capacity. It is generally important to provide enough energy for each EV for their next trip. However, this may not always be possible due to certain bottlenecks limiting the available charging capacity. Additionally, there may also be bottlenecks on the EV side, such as limited plug-in time or limited power supported by the EV's OBC.

The factors that directly limit the charging capacity include all of the charging infrastructure's and electricity grid's bottlenecks, such as charging point sizing, feeder fuse, feeding cable size, transformer, etc. These limits should have the highest priority and must be considered at the charging site to ensure safe and continuous operation. There may be enough capacity to allow uncontrolled charging in some cases, especially if there are only a few EVSEs. Additionally, if the electricity prices are static and there are no other incentives to control the charging, uncontrolled charging is a common solution (Lee *et al.*, 2021). However, uncontrolled charging at a larger charging site often leads to unnecessarily high investment costs and a lower return on investment for the charging site because the cables and grid connection point, etc., must be sized accordingly (Brinkel *et al.*, 2020). A notable share of new charging sites will likely be retrofitted into an old electricity grid as the number of EVs increases, which may set more tight limitations for the available EV charging capacity [P10]. Additionally, (Brinkel *et al.*, 2020) mentioned that the benefits of a higher charging capacity limit often do not outweigh the costs of upgrading the infrastructure.

There may be economical incentives that encourage the charging site to temporally limit the charging capacity even further besides the directly limiting factors that set an upper limit for the available charging capacity. (Lee *et al.*, 2021) mentioned that certain objectives do not lead to a unique solution; thus, multiple objectives with different priorities can be considered to optimize charging. The following sections discuss different objectives that lead to different *capacity determination* principles. The focus is on the charging site perspective and the decentralized control approach.

4.1 Minimizing charging costs under variable electricity pricing

Minimization of the electrical energy costs of EV charging has been one of the most studied objectives. For example, charging costs have been minimized under time-of-use (TOU) pricing in (Cao *et al.*, 2012) and real-time electricity pricing in (Wan *et al.*, 2018). These kinds of solutions may be feasible in small-scale implementations in which the EV charging loads do not significantly influence the total loading at a distribution or transmission system level. However, this could lead to a situation in a large-scale implementation in which a notable share of EVs charge at the same time, creating a high peak demand. Optimizing charging with only TOU prices have been shown to do as poorly as or even worse than uncontrolled charging because it reduces the diversity in charging times and thus leads to very high load peaks at the distribution system level (Kutt *et al.*, 2015; Powell *et al.*, 2020). This is also seen as problematic in other demand response applications (Repo *et al.*, 2021), and similar results are expected when real-time pricing is used as the only control signal.

4.2 Peak load management

A DSO can utilize a demand charge to incentivize peak load limitation in the decentralized control approach so that the electricity distribution costs increase based on the highest peak consumption in a certain timeframe. This is also likely to improve the cost reflectivity of the network tariff structure (Lummi *et al.*, 2019; Repo *et al.*, 2021). There were already a few DSOs in Finland, such as (Helen Electricity Network Ltd, 2021; Kuopion Sähköverkko Oy, 2021; Lahti Energia Sähköverkko Oy, 2021), that utilized demand charges for small-scale customers during the work on this thesis. This can make peak load management in EV charging a beneficial strategy. The use of a demand charge can also be combined with the TOU electricity pricing as in (Helen Electricity Network Ltd, 2021).

4.2.1 Potential benefits of peak load management

Potential benefits in home charging in detached house

[P5] studied home charging in a detached house. The household under investigation included two EVs (Nissan Leaf 2012 and BMW i3 2016, shown in Table 1) that should be charged in the evening or at night so they would be ready for use in the morning. Both EVs were charged using EVSEs that support only single-phase charging. The driving distances and the departure and arrival times of the EVs in the experiment were chosen according to the average values of the national passenger traffic survey (National Travel Survey, 2016). Therefore, the setup represented an

average household with two cars in which the ICEVs were simply replaced with EVs. The study considered a tariff structure that included a demand charge component and a TOU pricing component and compared three scenarios: uncontrolled charging, uncontrolled night-time charging, and the proposed peak power limiting control algorithm.

According to [P5]'s results, the proposed algorithm can mitigate the peak load increment completely and reduce the charging costs almost 60% when compared with uncontrolled charging. Uncontrolled night-time charging mostly reduces the volumetric electricity costs instead of the demand charges; thus, it reduces charging costs around 40% when compared to uncontrolled charging.

Potential benefits in home charging in an apartment building energy community

[P1] investigated the peak loads in an apartment building energy community that were under 15% EV penetration. An apartment building energy community model is one in which the apartments form a community that makes only one contract with the energy retailer and another with a DSO and divides the electricity costs between the apartment owners. This model essentially aggregates the total charging load of all EVs on the apartment building's premises; thus, a charging control system could benefit the whole energy community.

The results show that the peak power of the whole real estate would rise around 24% and 13% in the case of uncontrolled charging, even with charging powers of 3.7 kW (1×16 A, 230 V) and 1.8 kW (1×8 A, 230 V). The peak power increments could lead to extra electricity costs of 20.2 €/month and 10.6 €/month, respectively, in the case of a demand charge of 1.59 €/kW/month as in (Helen Electricity Network Ltd, 2021). Conversely, the peak load increment could be avoided completely while still satisfying the charging demand with the use of a simple peak load management.

Potential benefits in home charging in the case of distributed energy resources

[P1] also studied the use of a battery energy storage system (BESS) and a PV system in the apartment building energy community. According to the [P1] results, a moderately sized PV system (30 kW) and a BESS with 35 kWh energy capacity and 10 kW charging/discharging power can be used to decrease monthly peak powers of around 22% on average in an apartment building energy community. Interestingly, the combined use of BESS and PV systems seems to be slightly more beneficial than

the sum of the benefits of using the BESS and PV systems separately. A simple peak load management can be used to completely avoid the peak load increment while still satisfying the charging demand in the case of the considered 15% EV penetration.

4.2.2   Home charging potential under peak load management

Home charging in a detached house

The power drawn by an EV may be significant, especially in home charging. For example, in [P4] and [P5], the highest average power consumption of the households over a one-hour time interval varied between 8.8–12.5 kW (electric heating) and 3.1–6.9 kW (geothermal heating), respectively. When considering charging powers such as 3.7 kW (1×16 A, 230 V) or 11.0 kW (3×16 A, 230 V) that are typical charging power for EVs, it can be seen that an EV can be one of the highest power-consuming units in a household.

[P5]'s analysis of the household's electricity consumption showed that there is, on average, around 50 kWh charging capacity available during the night time (22:00–7:00) without the need to increase peak demand. The available charging capacity (50 kWh) equals around 274 km when assuming the average driving efficiency of 182 Wh/km seen in the [P5] experiments. Therefore, home charging can likely be carried out satisfyingly under peak power-based tariffs without increased demand charges if a proper charging control algorithm is used.

Home charging in an apartment building energy community

[P2] studied home charging in an apartment building energy community. The study investigated the charging load potential in a situation in which the charging load should not increase the peak loads of the whole real estate. According to [P2]'s results, charging demand in the case of up to around 30–50% EV penetration could be fulfilled in an apartment building energy community without increasing the whole real estate's peak loads. Conversely, it is estimated that around 65–75% of the total energy demand could be fulfilled at home without increasing the peak loads if the EV penetration is 100%.

Improving home charging potential using heating load control

[P4] studied the use of heating load control in an electrically heated household to improve circumstances for EV charging. The available charging capacity is notable on average as seen in [P5]'s results, but it is not always guaranteed. Different

households' electricity consumption profiles, a shorter available charging time at home, or an increased charging demand may still cause range anxiety. Heating loads, such as space heating and a hot water heater, can often be controlled without a notable negative impact on the comfort of living, which opens up an opportunity for improved charging load potential. Unbalanced household electricity consumption may cause issues, especially in the case of three-phase charging. Charging mode 3 (IEC 61851) does not allow each phase to be controlled separately, so three-phase charging is limited according to the phase with the lowest available capacity. Therefore, controlling a household's electricity consumption may significantly influence the available charging capacity. [P4] developed a pilot system that scheduled heating loads and tested them in an electrically heated household and measured the available charging capacity.

According to [P4]'s results, the heating load control enabled up to a 30% higher amount of energy to be charged into an EV. That improvement correlated with the peak load limitation: The lower the available charging capacity, the more effective the heating load control will be to improve circumstances for EV charging. Results also showed that the pilot system is able to reduce peak currents up to 15% compared with the original situation without heating load control or EV charging. Additionally, indoor temperatures were measured during the experiment, which confirmed that the comfort of living did not degrade due to heating load control.

Conclusions of the home charging potential under peak load management

The [P2], [P4] and [P5] results generally indicated that there is likely to be enough available charging capacity in Finnish households to fulfill most of the charging demand without needing to increase the whole real estate's peak loads. Heating load control can also be used to improve the charging load potential even further or reduce the peak loads from the original level. Additionally, as mentioned earlier, home will not likely be the only charging location available; thus, it may not be necessary to always fully charge EVs at home. Therefore, the use of demand charge can likely prevent the peak loads from increasing notably for residential customers even though EVs are becoming more popular and the total energy demand of the whole real state is increasing due to the charging loads.

4.2.3   Potential issues in peak load management

There is often uncertainty regarding the load level when minimizing peak loads, which leads to optimal results. There is a risk if a load management system tries to limit peak loading too much that the charged energy will also be limited too much

and that EV user satisfaction will consequently suffer. However, not limiting the peak loads enough may cause unnecessary costs if there is a demand charge in use; thus, it may provide less value for the charging site operator. Historical data can be used to estimate the upcoming peak load of a real estate. For example, it was seen in [P2] that the month-to-month variations of the peak loads were -30–+10% for the apartment building under consideration. Additionally, in (Lee *et al.*, 2021), the historic month-to-month variability in the peak loads of an office building was -16–+11%. However, this thesis excluded a detailed analysis of the estimation of the optimal peak load level.

It is also worth noting that even though the tariff that includes a demand charge is seen as more cost-reflective than the ones using only a constant basic fee and a volumetric electricity charge, the tariff may have negative influences on the grid's available flexibility (Repo *et al.*, 2021). If the loads are controlled for the benefit of the charging site, less flexibility may be available for the market, or the required compensation for the flexibility may increase (Repo *et al.*, 2021). A wide adoption of demand charge and peak load limitation-based control systems may become non-optimal from the DSO viewpoint, especially in the case of high penetration of centralized RES production.

4.3   Utilization of RES in EV charging

RES, such as production of a local PV system, could be used to charge EVs in a simple decentralized behind-the-meter control approach where the charging power is adjusted based on the availability of the RES production. Different load balancing methods have been proposed using a decentralized control approach in the case of centralized RES production. (Gong *et al.*, 2020) proposed the dynamic electricity price control approach to guide EV charging patterns to alleviate the negative impacts of volatile RES output. This is a relatively simple decentralized control approach, yet it can be beneficial in small-scale implementations similar to (Spencer *et al.*, 2021). However, in a large-scale implementation, it is likely to face challenges identical to other charging cost minimization principles (Kühnbach *et al.*, 2021) (discussed in Section 4.1). The charging load can be more directly controlled to match the volatile production of RES in a centralized control approach. For example, (Schuller *et al.*, 2015) showed that an aggregator controlling the charging loads increases RES usage notably compared to a case of uncontrolled charging. However, due to the centralized control approach issues (mentioned in Subsection 2.2.4), this thesis excludes their further examination. It is generally problematic to control EV charging to effectively utilize centralized RES production in the case of

the decentralized control approach. However, to some extent, the load balancing can be done indirectly through participating in DR markets.

5   Capacity allocation

Capacity allocation means the principle that is used to divide the available total charging capacity for the EVs that are plugged in. As mentioned earlier, the main focus in EV charging is to enable users to drive their vehicle to the next location, preferably without unnecessary stops or inconveniences. This charging demand varies in terms of due time (departure time) and energy requirement (intended driving distance and driving efficiency). Capacity allocation principles can influence EV user satisfaction and even the benefits of the charging site in the case of limited available charging capacity. Naturally, if the available capacity is large enough, the maximum capacity supported by the EVSE and the EV can be given to each charging session; thus, the capacity allocation principle is not needed. However, Chapter 4 mentioned that more situations are expected in the future in which the available charging capacity is limited; thus, capacity allocation principles will have an increased importance. This chapter presents and discusses different capacity allocation principles.

5.1   Basic allocation principles

The simplest capacity allocation principles include first-come-first-served (FCFS)-based, round robin, and fair sharing charging. The EVs that have arrived first are prioritized in FCFS-based charging and can often charge as fast as possible within the limits of their OBC, the EVSE, and the available charging capacity. There may be one or more EVs charging with their maximum power while the charging of the other EVs has been temporally disabled until it is their turn, depending on the available charging capacity. The FCFS principle can be naturally suitable for some situations. However, it can often lead to poor EV user convenience in EV charging, because some EVs do not have to be fully charged and some EVs may experience very long waiting times. The round robin principle is similar to FCFS, because the full charging capacity is always given to some EVs, while the others wait for their turn. However, instead of serving only the ones that arrived first, the EVs that get charged are cycled, e.g., randomly or based on the amount of time that the charging current has been supplied (Lee *et al.*, 2021).

Fair sharing is when the available total charging capacity is divided evenly for all EVs that are actively requesting charging (Zhang, Pota, *et al.*, 2018). This benchmark solution allows all EVs to be simultaneously charging as long as the available charging capacity is at least $n_{EVSE} \times 6$ A, where n_{EVSE} is the number of EVSEs. This limitation is based on the standard IEC 61851 that states that the minimum charging current in mode 3 charging is 6 A. Fair sharing is a reasonable and simple principle

that does not require any additional data or communication connections, although it may not be optimal due to the EVs' unbalanced charging demands. For example, a prioritization is used to improve RES usage in (Zhang, Pota, *et al.*, 2018) and total capacity usage rate in [P3], [P8], and, in (Lee *et al.*, 2021).

5.2   EV usage-based allocation

EV usage-based capacity allocation could ideally be used to minimize the electricity costs (Chen *et al.*, 2017; Datta *et al.*, 2019; Khaki *et al.*, 2019; Mouli *et al.*, 2019; Wei *et al.*, 2018) and peak loads (Chen *et al.*, 2017; Datta *et al.*, 2019; Khaki *et al.*, 2019; Wang and Liang, 2017) while ensuring that the EVs will always be fully charged or at least have enough energy for the next trip before departure time. The following subsection discusses different EV usage-based capacity allocation principles. However, before that it discusses the acquisition of the EV usage-related data, which might be problematic and include uncertainties.

5.2.1   Data acquisition

Two solutions have been proposed to acquire the charging requirements of the EVs: request user inputs or utilize historical data-based estimations (Dogan and Alci, 2018). However, both solutions to acquire the necessary information have drawbacks. Requesting inputs such as departure times and energy requirements may feel burdensome from an EV user perspective. This may become an issue and cause response fatigue such that customers may be unwilling to see a continuous extra effort for cost savings. This is a known issue in DR applications (Kim and Shcherbakova, 2011). The solution developed in (Lee *et al.*, 2021) disables the charging after 15 min from the start if the input is not received to ensure that EV users input the necessary data. However, this kind of solution may not be attractive from the EV user perspective. The input data may also not be very accurate, because it can sometimes be difficult or burdensome to accurately estimate such values (Lee *et al.*, 2021). Participants significantly underestimated the number of trips in a day in a mobility prediction survey (Hahnel *et al.*, 2013). The analysis also shows that work-related traveling was predicted most accurately, whereas shopping and leisure trips were predicted less accurately. Therefore, it seems that the EV usage-based charging control can be more reliable in work charging or overnight home charging when the next departure is work related because the mobility behavior in these cases can be relatively consistent. It is also worth noting that the user input-based principles are vulnerable to users exaggerating their needs to improve their own convenience. It

may be required to provide an incentive for the EV users to increase the accuracy of the input data (Lee *et al.*, 2021).

Historical data-based allocation, however, may not require any extra effort from the EV user. (Lee, Li, *et al.*, 2019) showed that EV user inputs can be more inaccurate than a historical data-based prediction. Gaussian mixture models and data over an 8-month period were used in the study, and the charging sites under consideration were mostly used for work charging. However, much data is required to provide accurate estimations in all cases. For example, data from multiple years would be required using machine learning to predict EV usage behavior reasonably accurately in the case of different holidays (Unterluggauer *et al.*, 2021). The approach might become unfeasible if the necessary data are unavailable.

5.2.2   EV usage-based charging control principles

(Lee *et al.*, 2021) investigated and compared two basic benchmark solutions to schedule EV charging: earliest deadline first (EDF) and least laxity first (LLF) to round robin. Both EDF and LLF are based on the round robin method in which some of the EVs receive full charging capacity and some have to wait for their turn. In EDF, the priority is given to the charging sessions based on the earliest departure time; in LLF, the priority is given based on the necessary charging starting time needed to meet the charging demand. According to (Xu *et al.*, 2016), both of these principles are seen as optimal if there is enough charging capacity to fulfil all energy requirements before departures. However, these principles may not be optimal if the available charging capacity is insufficient to fulfil the charging requirements. As indicated in (Xu *et al.*, 2016), these kinds of prioritizations can lead to a situation in which the charging capacity allocation is significantly unbalanced, and some EVs may not receive practically any capacity.

[P3] modified the least laxity first algorithm to take advantage of the flexible charging current control included in IEC 61851 mode 3 charging. Instead of disabling the charging of the non-prioritized charging sessions, the developed method simply allocated a lower charging capacity. This reduced the risk that some EVs did not receive any charging capacity. In the developed method, the available total charging capacity (P_{tc}) was divided based on the energy requirement (E_r) and the remaining time before departure (Δt_d) to determine the individual charging capacities (P_c) according to Eq. 5.1. In the equation, *n* is an index for an active EV and *N* is the total number of active EVs.

$$P_c(n) = P_{tc} \times \frac{E_r(n)}{\Delta t_d(n)} \Big/ \sum_{k=1}^{N} \frac{E_r(k)}{\Delta t_d(k)} \qquad (5.1)$$

[P3] analyzed the charging control operation in an apartment building in the case of perfect knowledge of the energy requirements and departure times and of some uncertainties. The results showed that the total energy that is charged into the EVs can be improved by 2–3% compared to the fair sharing principle when using the developed method and assuming perfect knowledge of the input data. Additionally, the amount of energy charged into the EVs is essentially unaffected (change is less than 0.5%), even if there are prediction errors of $\pm30\%$ in the energy requirements or ±2 h in the departure times. This is because the prediction uncertainties do not influence the available total charging capacity (P_{tc}), and thus, the control system tries to allocate the same total capacity for the EVs. However, the prediction errors can have notable impacts on the EVs whose energy requirement or departure time has been wrongly predicted. Both errors, expecting 30% lower energy requirement or 2 hours later departure, lead to around 0.5–1 kWh reduced charging energy on average, which equals around a 3–6 km reduced all-electric range. Even if the reduction is seen as quite modest on average, the magnitude can vary from day-to-day and cause inconveniences for the EV users.

5.3   SoC-based allocation

Subsection 2.2.5 mentioned that standard ISO 15118 enables more advanced communication between EVs and the charging system; thus, parameters such as battery status could be used in the charging control. Battery status-related information could be transferred automatically without the need for any predictions as opposed to departure times and energy requirements. The logic behind the charging control could also be more transparent and secure from the EV user perspective, because it does not utilize the estimated or direct data of user behavior. This makes it an interesting alternative for the EV usage-based principles.

[P3] developed and compared four different battery status-based principles to the fair sharing principle and to the principle presented in Eq. 5.1 in the previous subsection. The principles are based on absolute energy in the battery (Eq. 5.2a), based on percentual SoC (Eq. 5.2b), based on missing absolute energy of the battery (Eq. 5.2c), or based on missing percentual SoC (Eq. 5.2d). In the equations, E_{EV} is the absolute energy in the battery in kWh, SoC is the battery SoC as a percentage, and $E_{EV,max}$ is the maximum battery capacity in kWh. E_{EV} is rounded up to 0.001 kWh if it is less than that to avoid division with zero in Eq. 5.2a. This also means that the divider in 5.2b, the percentual SoC, is never zero. In the equations, a higher priority is given to the EVs that have a lower amount of energy in the battery (Eq.

5.2a), a lower SoC of the battery (Eq. 5.2b), a higher amount of missing energy in the battery (Eq. 5.2c), or a higher missing SoC of the battery (Eq. 5.2d).

$$P_c(n) = P_{tc} \times \frac{1}{E_{EV}(n)} / \sum_{k=1}^{N} \frac{1}{E_{EV}(k)} \tag{5.2a}$$

$$P_c(n) = P_{tc} \times \frac{1}{SoC(n)} / \sum_{k=1}^{N} \frac{1}{SoC(k)} \tag{5.2b}$$

$$P_c(n) = P_{tc} \times (E_{EV,max}(n) - E_{EV}(n)) / \sum_{k=1}^{N} (E_{EV,max}(k) - E_{EV}(k)) \tag{5.2c}$$

$$P_c(n) = P_{tc} \times (100\% - SoC(n)) / \sum_{k=1}^{N} (100\% - SoC(k)) \tag{5.2d}$$

According to [P3]'s results, each of these four principles perform better than the fair sharing principle but worse than the principle presented in Eq. 5.1 using the EV usage-based information with perfect predictions. The principles shown in Eq. 5.2a, 5.2b, and 5.2d perform almost as well as the EV usage-based principle (Eq. 5.1) in the case of perfect predictions, whereas the principle shown in Eq. 5.2c is less efficient. However, if the EV usage-related information is inaccurate, the principles shown in Eq. 5.2a, 5.2b, and 5.2d might become more efficient. The lower performance of the principle shown in 5.2c is most likely due to the fact that the missing energy in a BEV can be notable even though the BEV already has enough energy for the next trip. Additionally, the absolute value of the missing energy in a PHEV can be relatively small even though the battery is nearly empty. Therefore, the principle shown in Eq. 5.2c may heavily prioritize BEVs over PHEVs. The principle shown in Eq. 5.2d is the most efficient, even though the performance of the principles shown in Eq. 5.2a, 5.2b, and 5.2d are almost equally good. The results also indicate that the fair sharing principle is especially inefficient for utilizing the total charging capacity when the charging demand of the EVs is notably unbalanced. This kind of situation can occur in a home charging scheme, especially if some of the EVs are charged at work while the others are charged only at home.

5.4   Price-based prioritization

Another option for allocating charging capacity in a public charging site such as shopping centers could be based on a price-based prioritization in which the charging under a higher prioritization costs more than a low priority charging. This

kind of solution could guide EV users to choose the higher prioritization only when necessary. The charging price in a fast-charging station (powers usually 50–350 kW) can generally be notably higher than in a mode 3 charging station (powers usually up to 22 kW). Conversely, smart home charging can be cheaper than most public charging stations. Assuming a scenario where an EV user stops at a shopping center that has a charging option (up to 22 kW) before going home (and home charging is available), it is likely that the user will decide not to pay for the charging if the available electric range of the vehicle is clearly enough for the trip home. However, an EV user might want to charge with a low priority if the available electric range is not quite enough or the user experiences range anxiety. If there is a very potential need for fast-charging in order to drive home, the user might be willing to pay extra for the prioritized charging at the shopping center to avoid even more expensive fast-charging costs.

[P8] developed a charging control algorithm that considers different prioritization levels when allocating the available charging capacity between the active EVs and assessed its operation at a shopping center's charging site. In the examined scenario, it was assumed that there was enough charging capacity to enable all charging sessions with the minimum charging current (3×6 A). After allocating the minimum capacity for each charging session, the algorithm allocated one more ampere for a charging session as long as possible, considering the available charging capacity. The one ampere increment was given to the charging session with the highest priority index (p_i) which was calculated using the currently allocated capacity (p_c) and priority level (p_l) according to Eq. 5.3. The control system applied the determined charging current limits by sending them to the corresponding EVSEs after the capacity allocation was finished. The algorithm was tested using HIL simulations with commercial EVs and real charging data, which validated its compatibility with real EVs and IEC 61851 standard as described in [P8].

$$p_i(n) = \frac{p_c(n)}{p_l(n)} \qquad (5.3)$$

[P8] considered two prioritization levels (low and high) and investigated different penetrations of EV users requesting prioritization. The EV users were assumed to request prioritization based on laxity: The lower the laxity (i.e., the more acute charging demand), the more likely they request prioritization. The solution operates essentially the same as the fair sharing principle if all or none of the EV users request prioritization. According to the results, the total charging capacity usage was improved by up to 2% compared to the fair sharing principle. This result was

achieved when 20% of the EVs with the lowest laxity were requesting prioritization. The prioritization improved the charged energy up to 16% from a single EV perspective.

It is worth noting that a higher prioritization may not always lead to a higher charging power due to the different limitations in the charging characteristics of EVs. For example, a Nissan Leaf 2012 has a maximum charging current of 16 A; therefore, if the EVSE increases the allowed charging current from 16 A to > 16 A, the charging will be unaffected. This might lead to a situation in which EV users are uncertain whether they benefit from the higher prioritization or not, which might discourage them from choosing it. The charging system could calculate the realized prioritization value, and the potential price increment could be based on that to alleviate the issue. This kind of solution ensures that EVs users do not pay extra for nothing.

5.5   Charging with low currents

(Apostolaki-Iosifidou *et al.*, 2017) mentioned that, due to the lower efficiency of power electronics in the case of low charging currents, the charging efficiency of EVs correlates with the charging current when the currents are ≤ 40 A: Higher charging currents tend to lead to a higher efficiency. Therefore, limiting the charging currents of EVs might also decrease the general energy efficiency. The measurement results of (Kutt *et al.*, 2013) also indicate that the total harmonic distortion percentage might be higher with lower charging currents. Furthermore, a lower charging power may also be inefficient in low ambient temperatures. Some EVs are equipped with battery heaters, so a lower charging power in a cold ambient temperature might lead to a more notable share of the power being used for the battery heating instead of actual charging (Tikka *et al.*, 2021).

It might be more energy efficient to allow maximum charging current for some EVs while disabling the charging of other EVs to avoid overloading in the case of a limited available charging current. The charging mode 3 (IEC 61851-1) allows 0 A current limit, which effectively disables the charging temporally, so this kind of control solution is easy to implement. However, this can also be problematic, because the laboratory measurements have shown that at least the BMW i3 2016 may not start charging again after a few minutes of being disabled. Additionally, most EVs notify their user if the charging stops (Lee *et al.*, 2021). This could lead to a bad user experience in a public charging site if the EV users experience range anxiety due to this, or if they assume that the charging site is malfunctioning. Therefore, in the

case of limited charging capacity, it may often be advisable to keep charging sessions ongoing with reduced charging currents despite a slightly reduced energy efficiency.

5.6   Capacity allocation intertwined with capacity determination

It is common in the scientific literature that the charging capacity determination and allocation are intertwined. This is especially true when they are based on user mobility demand. It is possible to find the optimum level for, e.g., peak shaving or charging cost reduction while ensuring customer satisfaction by utilizing EV usage-based information. However, Subsection 5.2.1 mentioned that uncertainties remain regarding EV usage-based information.

According to [P3]'s results (discussed in Subsection 5.2.2), the prediction uncertainties of individual EVs can have a notable impact on the charging of these specific EVs if the control algorithm utilizes the said data. Conversely, prediction of the total charging demand of multiple EVs can be quite accurate, because the prediction uncertainties of individual EVs may partly nullify each other. This indicates that EV usage-based information could be suitable for determining the total available capacity needed to achieve certain objectives in EV charging. However, even if the EV usage-based data are used to determine the total available capacity, it is worth considering using a separate principle to allocate the available capacity that is not susceptible to significant prediction errors. This could increase the robustness against the influences cause by the data uncertainties in real-life implementations.

6 Capacity usage rate correction

This chapter discusses *capacity usage rate correction*. It first discusses the background and related research. It then introduces a developed adaptive solution that can efficiently take non-ideal charging characteristics into account and improve the capacity usage rate. Subsection 2.2.2 mentioned that an EVSE can only set the maximum charging current limit for EV charging in mode 3 charging according to IEC 61851 and that the EV itself chooses the actual charging current. There are many different reasons why all or some of the phase currents in three-phase charging are below the limit set by the EVSE (discussed in Subsection 2.2.2). The charging current limit set by an EVSE is often the ideal charging current wanted by the control system in EV charging management; hence, the real charging current behaviors, in which the actual charging currents might deviate from the current limit, are referred to as non-ideal charging characteristics.

6.1 Background

The realized charging currents may vary notably from the limit indicated by the EVSE due to the EVs' non-ideal charging characteristics. This also means that the charging control system does not know the realized current consumption without a charging current measurement feedback. The upper limit for the charging currents is controllable and known by the control system, so this issue is unlikely to pose safety-related risks such as overloading. However, the issue may lead to a suboptimal operation of the charging site in the case of controlled charging if it is not addressed in the charging control algorithm.

Unknown charging currents can have two especially notable consequences. First, in the case of limited available charging capacity for multiple EVs, the issue can lead to a situation in which a part of the available charging capacity is being unused. Second, the issue may compromise the efficiency of other potential DR objectives. Two toy examples are given and discussed below to illustrate the problems.

Toy example of an EVSE with two charging sockets

Let us assume that we have a charging station that has two 1×32 A (230 V) charging sockets but only supports a total charging capacity of 1×32 A. Now, if there are two EVs simultaneously that can both draw up to 1×32 A, the fair sharing principle would allocate 1×16 A for both EVs. Then, if the other EV becomes nearly fully charged and draws a lower current than 1×16 A, there will be more capacity available

for the other EV. The available capacity goes to waste if it is not reallocated for the other EV. There should be a mechanism in the control system that recognizes the non-idealities (i.e., the mismatch between the current limit set by the EVSE and the realized current) and reallocates the capacity to the other EV to reclaim the otherwise unused capacity. According to the measurements conducted for [P9], the CV stage lasts around 36 min for the Nissan Leaf 2019 when the current limit is 16 A. The average current is only 3 A during the CV stage. This means that around 13 A charging current on average could be reallocated in this example for the other EV, which equals around 1.8 kWh in terms of energy or 10 km in terms of driving distance (assuming 180 Wh/km). This capacity reallocation could increase the charging rate of the other EV without causing any negative impacts to the EV with a lower charging current.

Toy example of a charging site participating in DR market

It may be difficult to participate in DR markets if the charging system is able to adjust only the upper limit for the charging control and the actual charging currents are unknown. Let us assume that a BMW i3 2016 with SoC of < 80% is charging at a charging station that allows 3×32 A (230 V) charging and the charging current limit is set to 32 A to allow charging as fast as possible. The BMW only supports charging currents up to 3×16 A, so it charges with a power of 11 kW instead of the available 22 kW assumed by the charging system if the non-idealities are not considered. Now, if the non-idealities are not considered and there is a DR signal that requests a load reduction of 10 kW, the charging control system would try to reduce the charging load from 22 kW (3×32 A, 230 V) to 12 kW (3×~17 A, 230 V). In this case, the charging of the BMW would continue with the previous charging current of 3×16 A because the internal limitations of the EV are still tighter than the limit set by the EVSE. Therefore, the realized power consumption has not changed, and the DR signal has no impact.

Discussion of the background

A better utilization of the charging capacity, from the EV user perspective, leads either to a faster charging time or a higher SoC if the EV departs before being fully charged. This improves the quality of the charging service and can make the charging site more attractive. Chapter 4 mentioned that there may be very limited charging capacity available per EV as the number of EVs increases rapidly and the grid is upgraded relatively slowly. Therefore, the available charging capacity should be used as effectively as possible. An improved capacity usage rate, from the CSO viewpoint,

leads to higher income if energy-based (€/kWh) charging pricing is used. Additionally, participating in DR markets can increase the CSO's income even further. However, effective participation to the DR markets may not be possible if the non-idealities are not considered properly.

Both of the aforementioned toy examples are very simplified to illustrate the issue as clearly as possible. There may be a variety of different, simultaneous non-ideal charging characteristics in a larger charging site with three-phase charging stations; thus, an efficient and scalable solution is required.

6.2   Related research

It has been common in the scientific literature to assume "ideal" charging characteristics in which the realized charging current will always be exactly the same as the current limit set by the EVSE. However, the non-idealities have been gaining more attention during the past few years. Section 3.1 mentioned that a charging profile classification was done in (Sun *et al.*, 2020) and bilinear charging profiles are considered in the modelling in (Mouli *et al.*, 2019) and (Wei *et al.*, 2018). (Frendo *et al.*, 2020) took a machine learning approach to form a lookup table consisting of SoC and power draw for each EV. This method can be used to consider realistic non-idealities in the charging modelling, although it may not be suitable for real-time charging control due to each EV's significant data requirements.

(Lee, Chang, *et al.*, 2019) described an adaptive charging network and recognized the non-idealities. The used charging control utilizes EV user inputs, such as expected departure time and energy demand, in the charging control. The study recognizes the non-idealities, although they are not considered in the capacity allocation. The control system instead uses only the measurements to track the actual energy delivered, which may deviate from the expected value due to non-ideal charging characteristics.

[P5] considered home charging of two EVs and recognized the non-idealities. Charging current measurements are used to calculate the EVs' unused charging capacity in real time and reallocate the capacity if possible to improve the capacity usage rate. A condition shown in Eq. 6.1 was used in the study to determine whether the charging current is limited by the EV's OBC instead of the current limit set by the EVSE. In the condition, θ is a threshold of 1 A, l is the current limit, and m is the measured charging current. The charging current was assumed to remain the same even if the current limit was increased if the charging current was limited by the OBC. This information can be used to determine the amount of unused charging capacity of one EV and allocate this capacity to the other EV and thus improve the

capacity usage rate. The study considered home charging with a peak load limitation, so the available total charging capacity was constantly changing based on the electricity consumption of the household.

$$\begin{cases} \textbf{\textit{if }} l - m > \theta, \textbf{\textit{then }} charging\ current\ is\ limited\ by\ the\ OBC \\ \quad \textbf{\textit{else }} charging\ current\ is\ limited\ by\ the\ current\ limit \end{cases}$$

(6.1)

(Lee *et al.*, 2021) described an upgraded version of the adaptive charging network. The study also recognized that the non-ideal charging characteristics can lead to a wasted capacity if it is not taken into account. An algorithm was developed slightly similar to that in [P5] to reclaim the otherwise unused capacity. The algorithm used two thresholds, θ_d and θ_u, to determine whether there is unused capacity by an EV or more capacity could be used by the EV. If the measured current (m) is more than θ_d lower than the current limit (l), the current limit is lowered to 1 A higher than the measured current. The current limit is increased by 1 A if the measured current is less than θ_u lower than the current limit, because it is possible that the charging current is only temporarily lowered by the OBC of the EV. Eq. 6.2 illustrates the capacity reclamation, where $\theta_d \geq \theta_u$. Compared to the algorithm developed in [P5], the advantage of the capacity reclamation algorithm developed in (Lee *et al.*, 2021) is that it can be scaled for a charging site with multiple EVSEs instead of just two as in [P5].

$$\textbf{\textit{if }} l - m > \theta_d, \textbf{\textit{then }} m + 1 \rightarrow l \qquad (6.2a)$$
$$\textbf{\textit{if }} l - m < \theta_u, \textbf{\textit{then }} l + 1 \rightarrow l \qquad (6.2b)$$

The algorithms presented in [P5] and (Lee *et al.*, 2021) allowed a reclamation of the unused capacity and were able to recognize if the capacity reclamation was premature. However, the solutions considered only a single-phase charging; thus, they do not work efficiently in the case of unbalanced three-phase charging. Furthermore, the algorithm developed in (Lee *et al.*, 2021) was unable to recognize certain charging characteristics, such as that the Smart EQ ForFour charges only with current limits between 8–32 A. In the case of the Smart and a current limit of 7 A, the charging current would be 0 A and the algorithm developed in (Lee *et al.*, 2021) would likely assume that the EV is not requesting charging anymore and try to reallocate its capacity to other EVs. This would leave the Smart uncharged.

The algorithms developed in (Lee *et al.*, 2021) and [P5] utilized real-time measurements, so they can likely adapt quite well to most situations in single-phase

charging systems. However, the solutions do not include any further memory features regarding the charging characteristics of the active EVs. Therefore, in case the total capacity or the number of active EVs change, it may take multiple adjustments before the algorithms reach the optimal capacity allocations. The standard IEC 61851 does not allow the current limit to be adjusted more frequently than once per 5 seconds, so the adaptation to new situations might take a while (up to a few minutes). The capacity usage might not be as efficient as possible during this delay. Additionally, long delays in the adaptation might have negative influences, for example, in situations where the charging site participates in DR markets.

6.3   Adaptive charging characteristics expectation

In a case with only a couple of EVs, as in [P5], or in case of single-phase charging, as in [P5] or (Lee *et al.*, 2021), it was possible to use simpler algorithms to determine potentially unused charging capacity and reallocate it. However, in a larger charging site with multiple three-phase EVSEs, it is crucial that the solution is computationally efficient and can take into account all kinds of non-ideal charging characteristics. Furthermore, from the convenience perspective, it is necessary that the solution is easily scalable and can be applied to charging sites with different amount of charging points up to several hundred charging points, as in REDI (REDI, 2021) or Mall of Tripla (Mall of Tripla, 2021).

    An adaptive charging characteristics expectation (CCE) feature was developed to fill this demand. This feature allows the control algorithm to estimate the charging currents before the current limit is applied. The following two subsections discuss the operation principle and potential benefits.

6.3.1   Operation principle

In [P6], the first version of the CCE feature is developed and introduced. The fundamental principle of the developed feature is to separately measure the realized charging currents of each EV and use the measurements to update the charging characteristics models of the EVs. The charging characteristics model links current limits to the realized charging currents, and thus, the model can be used to estimate the charging currents before the current limit is applied. Section 3.1 showed that the correlation between different current limits and realized currents may be difficult to model analytically. Therefore, the CCE feature uses a matrix that includes all possible current limit integers and the corresponding charging currents. This enables an easy way for the charging control algorithm to calculate the expected charging currents for each EV depending on the considered current limits. The CCE feature initially

assumed that each EV has 'ideal' charging characteristics, i.e., each phase's current will be exactly as indicated by the current limit set by the EVSE. As the charging sessions continue, the feature keeps updating the matrix based on the measurements and thus improving the prediction accuracy. The basic measurement-based updating is called *direct memorization* function. Fig. 6.1 illustrates the initial charging characteristics model (a matrix) along with the *direct memorization* function. In the figure, I_L represents the current limit set by the EVSE, I_M represents the measured value, and notation *1–3* denotes different phases in the three-phase system.

New measurement:
$I_L = 6$ A,

$$
\begin{array}{cccc}
I_L & I_{M,1} & I_{M,2} & I_{M,3} \\
\end{array}
\quad
\begin{array}{l}
I_{M,1} = 6.2 \text{ A}, \\
I_{M,2} = 6.1 \text{ A}, \\
I_{M,3} = 5.9 \text{ A}
\end{array}
\quad
\begin{array}{cccc}
I_L & I_{M,1} & I_{M,2} & I_{M,3} \\
\end{array}
$$

$$
\begin{bmatrix}
6 & 6.0 & 6.0 & 6.0 \\
7 & 7.0 & 7.0 & 7.0 \\
8 & 8.0 & 8.0 & 8.0 \\
\vdots & \vdots & \vdots & \vdots \\
32 & 32.0 & 32.0 & 32.0
\end{bmatrix}
\longrightarrow
\begin{bmatrix}
6 & 6.2 & 6.1 & 5.9 \\
7 & 7.0 & 7.0 & 7.0 \\
8 & 8.0 & 8.0 & 8.0 \\
\vdots & \vdots & \vdots & \vdots \\
32 & 32.0 & 32.0 & 32.0
\end{bmatrix}
$$
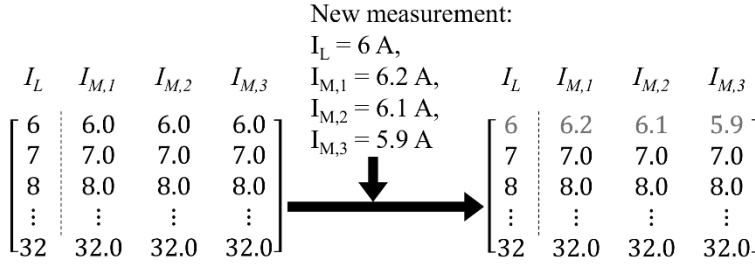
Figure 6.1 Illustration of the initial charging characteristics model (on the left) and *Direct Deduction* function which updates the model with a current measurement where the current limit was 6 A.

Additionally, the feature evaluates the phase usage of each charging sessions using the so-called *phase detection* function. If a phase current is zero while another phase current in non-zero, the feature recognizes the unused phase and adjusts the matrix so that the expected currents of that phase are zero for all current limits. Fig. 6.2 illustrates this. The illustrations of the functions related to CCE feature (Figs. 6.1 – 6.4) are independent in order to demonstrate the operation of each function as clearly as possible. It is worth noting that there may be some delays before the charging currents ramp up at the beginning of a charging session. Additionally, the phase currents might have different delays. Therefore, it seems reasonable to activate the *phase detection* function, for example, 1 minute after the charging session has begun, to reduce the risk of incorrectly identifying the used phases of a charging session.

$$
\begin{array}{cccc}
I_L & I_{M,1} & I_{M,2} & I_{M,3} \\
\end{array}
\begin{bmatrix}
6 & 6.0 & 6.0 & 6.0 \\
7 & 7.0 & 7.0 & 7.0 \\
8 & 8.0 & 8.0 & 8.0 \\
\vdots & \vdots & \vdots & \vdots \\
32 & 32.0 & 32.0 & 32.0
\end{bmatrix}
$$

New measurement:
$I_L = 6$ A,
$I_{M,1} = 6.1$ A,
$I_{M,2} = 0$ A,
$I_{M,3} = 0$ A

$$
\begin{array}{cccc}
I_L & I_{M,1} & I_{M,2} & I_{M,3} \\
\end{array}
\begin{bmatrix}
6 & 6.1 & 0.0 & 0.0 \\
7 & 7.0 & 0.0 & 0.0 \\
8 & 8.0 & 0.0 & 0.0 \\
\vdots & \vdots & \vdots & \vdots \\
32 & 32.0 & 0.0 & 0.0
\end{bmatrix}
$$
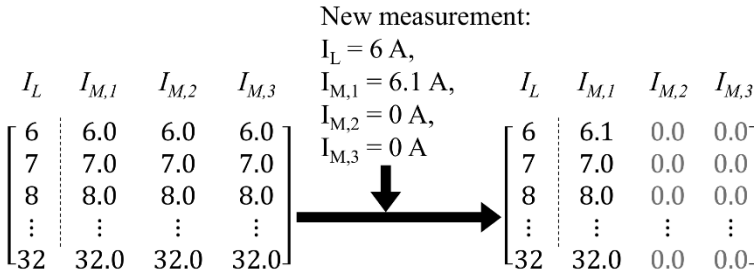
Figure 6.2 Illustration of *Phase Deduction* function. In the illustration, the function recognizes that phases 2 and 3 are unused and thus updates the model so that the phases are assumed to have zero charging currents regardless of the current limit.

[P7] developed the CCE feature further to achieve more accurate predictions of the charging currents. The feature was essentially improved with two additional functions: *Maximum Current Deduction* and *Indirect Deduction*. *Maximum Current Deduction* function determines the highest current that the EV can use. Public charging points may very well support charging currents up to 32 A in mode 3. However, EVs whose OBCs support charging currents only up to 16 A are very common. Therefore, deducting the maximum charging current can notably improve the charging current prediction. The function evaluates if the realized charging current is notably below the set current limit to determine the maximum charging current. In the function, a threshold of 5 A was assumed to be suitable to determine whether the charging sessions had reached its maximum current or not. The prediction model includes the maximum current variable *Imax* in addition to the matrix.

Indirect Deduction function aims to improve the estimation accuracy of those current limits that are yet not measured but that are between two directly measured current limits. The initial assumption is 'ideal' charging characteristics, so the estimated currents of the unmeasured current limits may be significantly inaccurate. The function estimates that the charging currents of the non-measured current limits are interpolated linearly between the two measured values to enhance the estimation accuracy. The matrix is extended to include Boolean variables to describe whether or not the charging currents of certain current limits are measured to accomplish this. Figs. 6.3 and 6.4 illustrate the operation of *Maximum Current Deduction* and *Indirect Deduction* functions.

New measurement:
$I_L = 32$ A,
$I_{M,1} = 16.1$ A,
$I_{M,2} = 16.3$ A,
$I_{M,3} = 15.8$ A

I_L	$I_{M,1}$	$I_{M,2}$	$I_{M,3}$	Boolean
⋮	⋮	⋮	⋮	⋮
29	29.0	29.0	29.0	False
30	30.0	30.0	30.0	False
31	31.0	31.0	31.0	False
32	32.0	32.0	32.0	False

I_{max} [32.0] →

I_L	$I_{M,1}$	$I_{M,2}$	$I_{M,3}$	Boolean
⋮	⋮	⋮	⋮	⋮
29	29.0	29.0	29.0	False
30	30.0	30.0	30.0	False
31	31.0	31.0	31.0	False
32	16.1	16.3	15.8	True

I_{max} [16.3]
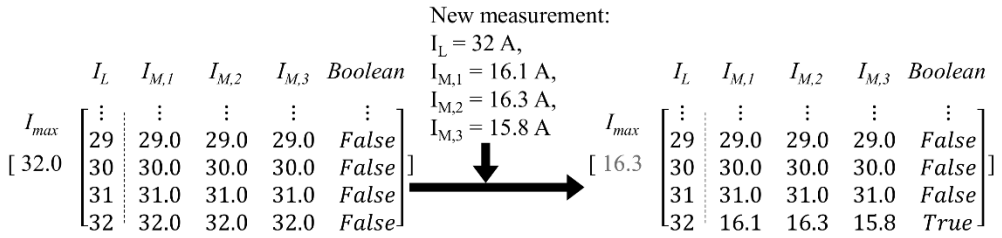
Figure 6.3 Illustration of *Maximum Current Deduction* function. In the illustration, the function recognizes that charging sessions does not draw a higher current than 16.3 A and thus updates the model so that it is remembered in the future.

New measurement:
$I_L = 14$ A,
$I_{M,1} = 14.1$ A,
$I_{M,2} = 13.8$ A,
$I_{M,3} = 13.7$ A

I_L	$I_{M,1}$	$I_{M,2}$	$I_{M,3}$	Boolean
⋮	⋮	⋮	⋮	⋮
14	14.0	14.0	14.0	False
15	15.0	15.0	15.0	False
16	15.7	15.8	15.3	True
⋮	⋮	⋮	⋮	⋮

I_{max} [32.0] →

I_L	$I_{M,1}$	$I_{M,2}$	$I_{M,3}$	Boolean
⋮	⋮	⋮	⋮	⋮
14	14.1	13.8	13.7	True
15	14.9	14.8	14.5	False
16	15.7	15.8	15.3	True
⋮	⋮	⋮	⋮	⋮

I_{max} [32.0]
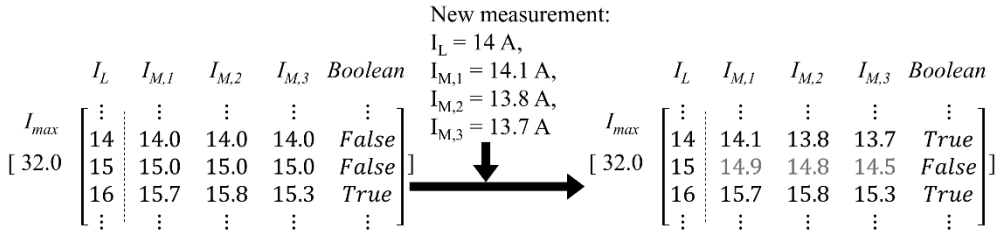
Figure 6.4 Illustration of *Indirect Deduction* function. In the illustration, the function indirectly deducts new estimated charging currents for the current limit of 15 which is not measured but lies between measured current limits of 14 and 16.

The charging characteristics model is updated continuously as the charging sessions goes on. Eq. 6.3 was used to estimate the charging currents. In the equation, I_E represents the expected current, p denotes a phase, and L represents the current limit index. The developed algorithm in [P7] used an iterative approach to allocate the total charging capacity while considering the built charging characteristics models. The algorithm started by allocating a minimum 6 A current limit for each active charging session at the beginning of each iterative loop. Afterwards, in each iteration, the algorithm evaluated whether a certain current limit could be increased by 1 A (i.e., the minimum increment with the used EVSEs) without violating the peak load limitation. The increment was made if the current limit increment was not estimated to violate the peak limit. In the case of peak load violation, the charging session was removed from the consideration in the following iterations within the loop. The process continued as long as there were available capacity and suitable charging sessions to allocate more capacity. [P7] considered the fair sharing principle. Therefore, the algorithm tried to increase the EVs' capacity with even prioritization. However, by modifying the order in which the capacity increment was considered for the charging sessions, the algorithm could accomplish different prioritizations. The price-based prioritization developed in [P8] is an example of this.

$$I_{E,p}(L) = \min(I_{M,p}(L), I_{max}) \qquad (6.3)$$

Each EV was modelled and measured separately, so a separate current measurement was required for each EVSE. However, it seems that modern IEC 61851 charging mode 3 EVSEs tend to include inbuilt current measurement devices; thus, this requirement is not likely an issue. The solution does not require any preliminary information of the EVs, so it does not include a similar data requirement issue like the machine learning approach presented in (Frendo *et al.*, 2020). Furthermore, as mentioned earlier, an EVSE should not adjust charging currents more frequently than every 5 seconds, and the run time of the algorithms, including the CCE feature developed in [P6] and [P7], is a fraction of a second. Therefore, the proposed algorithm is not likely constrained by the computational capacity requirements.

6.3.2 Benefits

By improving the capacity usage rate, both the EV users and charging system operator will benefit. [P7] analyzed the capacity usage rate in the case of a peak load limitation algorithm and the fair sharing principle with and without the CCE feature. The solution was essentially the benchmark solution presented in (Zhang, Pota, *et al.*, 2018) without the CCE feature. [P7]'s results demonstrate that the CCE feature does not have an impact in case the charging load is minimal compared to the available charging capacity. This is because the charging load does not have to be controlled in these cases. Therefore, the charging is only limited by the internal limitations of the EVs, and any kind of capacity reallocation is not needed. However, in the case of a significant charging congestion, it was seen that the CCE feature significantly increases capacity usage rate [P7].

[P10] considered the charging current estimation accuracy and the charging site profits. The study's goal was to estimate the charging currents of the next 10 seconds before the considered current limits were applied. According to the results, the developed CCE feature can increase the charging energy output of the charging site by 5.8% on average compared to a solution that does not include the capacity usage rate correction. The examined case included a peak load limitation algorithm with the fair sharing principle similar to [P7], in which the solution without the CCE feature was essentially the same as the benchmark presented in (Zhang, Pota, *et al.*, 2018). The CCE feature also leads to faster charging times and increased customer satisfaction by improving the charging energy output. The gross profit of the CSO increases by the same proportion as the energy output if a volumetric energy price

(€/kWh) is used. Additionally, the CCE feature enables the algorithm to estimate the current consumption of the charging site before the current limits are applied, which can be necessary in the case of participating in DR markets. This also means that the CCE feature enables the charging control algorithm to achieve a certain total charging power usage more accurately. According to the results, the average prediction error of the total power consumption was ±1% with the CCE feature, while the benchmark solution without the CCE feature would have a prediction error of ±123%. The results also emphasized that the realized charging currents did not match the current limits set by the EVSE very well. It is necessary in most smart charging solutions for the control system to be able to accurately control the charging powers. The control actions might not have the intended effects, otherwise; thus, the desired results may not be achieved.

6.4   Capacity usage rate potential

[P7] analyzed the capacity usage rate in the case of perfect knowledge of the charging characteristics. The results showed that even the algorithm with perfect knowledge of individual EVs may not reach a 100% capacity usage rate in the case of a fuse-based limitation. The study considered alternating phase order connections for the charging points, which is a common practice to mitigate unnecessary phase unbalance at installation stage. The ideal algorithm instead reached up to an 89% capacity usage rate over a 70 min congestion period. This was caused by the unevenly balanced load in the three-phases network. It may not be possible to fully balance the charging load on the three phases because all EVs are not likely to support three-phase charging, EVSEs cannot set phase-specific current limits, and single-phase EVs are unlikely to be evenly distributed on each phase. It is also worth noting that the ideal situation leads to only one percentage unit higher capacity usage rate than the algorithm with the proposed CCE feature (89% versus 88%). Therefore, the CCE feature is seen as relatively optimal.

However, if the charging load is limited according to a certain peak power instead of a fuse-based limitation, the charging capacity allocation is much simpler because the charging load does not have to be perfectly balanced over the three phases. In this case, a 100% capacity usage rate is possible if an adaptive algorithm including, e.g., the proposed CCE feature, is used [P7].

6.5 Non-ideal charging characteristics and standardization

It would be possible, in theory, for an EV to communicate the charging characteristics to the EVSE using, e.g., ISO 15118 and the digital communication supported by the IEC 61851. However, this solution can be problematic from two perspectives. First, the charging characteristics are not constant but instead depend on, e.g., the temperature of the battery and the SoC of the battery. Thus, there would be a need to update the charging characteristics continuously during the charging session, which would significantly increase the necessary data transfer between the EV, EVSE, and the control system. Second, it may not be likely that all EVs would begin to support the said communication within a short amount of time. Thus, even if the non-idealities were included in the standardization, there will most likely be at least a transition period when an adaptive charging solution, such as the CCE feature, can remarkably improve the charging capacity usage rate [P7].

7   Conclusions

This thesis assesses electric vehicle charging from a charging control algorithm perspective as well as from a charging load modelling perspective. Although the topics are somewhat independent from each other, the modelling methods play an important role in designing and validating the charging control algorithms.

The charging demand increases as EVs become more popular. The lack of sufficient charging infrastructure is one of the key challenges that hinders EV adoption; thus, it is necessary to increase the charging opportunities. However, the reinforcements of the electricity network are usually very expensive, so the EV charging infrastructure often has to be retrofitted into an existing electricity grid. A charging control is needed to ensure the grid's safe and efficient operation, especially in these kinds of cases. This thesis refers to any situation in which the charging of one or more EVs is controlled as "smart charging," even though it may not always be optimal. The focus is on mode 3 charging of the IEC 61851 standard.

The main focus in this thesis is on individual charging sites, although it also discusses distribution system operator and EV user viewpoints. It gives a special emphasis to so-called "non-ideal charging characteristics," which poses challenges both from the algorithm development and the charging load modelling perspectives. The following section presents and discusses separately the main contributions of the thesis, the potential limitations of the key findings, and the proposed future work.

7.1   Main contributions

The contributions of this thesis are divided into two categories: scientifically oriented research results, which could aid future research, and practical implementation-oriented algorithm development, which can promote smart charging solution implementations. The contributions are presented within the two categories in the order of the related publication numbering when possible.

The scientifically oriented research contributions:
- ✓ A phenomenon called "non-ideal charging characteristics" is recognized, and different charging characteristics in which the realized charging current deviates from the maximum current limit set by the EVSE are examined and illustrated in the case of three-phase charging [P6].
- ✓ A simulation model that considers non-ideal charging characteristics is developed [P7]. The non-ideal charging characteristics are modelled based on comprehensive measurements of commercial EVs. The accuracy of the

simulation model is validated by comparing the simulation results to laboratory measurements of the EVs [P11], [P12].

✓ The influence of temporal resolution in EV charging load modelling is investigated [P11]. A temporal resolution of one minute is seen as sufficiently accurate in most cases. However, a finer resolution may be necessary in the case of a complex charging control system. Conversely, a resolution of 15 minutes can give relatively accurate results in the case of uncontrolled charging.

✓ Different charging profile modelling methods are compared [P12]. It is shown that the use of linear charging profile models will likely oversimplify the simulations and lead to notable inaccuracies. It is also shown that the use of bilinear charging profile models can be quite accurate; thus, more complex models may not be needed in most cases.

✓ A novel way to divide algorithms into three key components is introduced (presented for the first time in this introductory part). The components are *Capacity determination*, *Capacity allocation*, and *Capacity usage rate correction*. Each component is responsible for achieving a certain objective, and optimized smart charging solutions are likely to include each of them. This division can help to clarify the objectives of future research, because there may be a need to improve the optimality of these components separately.

The practical implementation-oriented contributions:

✓ Home charging is analyzed using Finnish National Travel Survey data and real household electricity consumption data. It seems that the home charging demand can often be fulfilled in Finland without increasing the peak loads of the whole real estate [P1], [P2], [P4], [P5]. Therefore, a charging control can be used to mitigate demand charges in case peak power-based tariffs become more popular.

✓ Alternative approaches are developed to avoid issues regarding the implementation and the uncertainties of EV usage-based control algorithms. Battery state-based [P3] or charging price-based [P8] control algorithms could be used to allocate available charging capacity for EVs with higher charging demands. It is also shown that these principles can improve the total energy dispatch of the charging site.

✓ In home charging, controlling of household's electric heating loads could be used to improve circumstances for EV charging and reduce the peak currents of the whole real estate [P4].

- ✓ It is shown that a peak load mitigation-based algorithm can completely mitigate the peak load increment and significantly reduce home charging costs when compared with uncontrolled charging [P5].
- ✓ The Charging Characteristics Expectation (CCE) algorithm feature is developed [P6], [P7] to mitigate the negative influences of the non-ideal charging characteristics. This feature allows a control algorithm to track the charging characteristics of the EVs, which further allows the algorithm to control the actual charging load more precisely despite the non-idealities. This is also a key functionality needed by the charging control system in the case of a DR market participation. According to the results, the use of the CCE feature can notably improve the capacity usage rate [P7] and the charging site operator profits [P10].
- ✓ Average charging loads in some public charging sites are estimated to notably increase [P9]. Most EVs currently support charging powers only up to around 4 kW. EVs are expected to draw more energy within the limited amount of parking time in public charging locations such as shopping centers as EV technology evolves and EVs begin to support higher charging powers. It also shown that a centralized charging location could be more cost efficient from the charging infrastructure viewpoint compared to multiple smaller charging sites.

7.2   Discussion

Many assumptions and uncertainties still remain, even though most of the key findings and results of the thesis are either obtained using simulations with real data or validated using HIL simulations with commercial EVs. The accuracy of the results could generally be improved by using more detailed data and complex simulation methods. However, this could also lead to an increased computational capacity requirement or increased effort required to gather or prepare the necessary data. Therefore, some compromises often have to be made in simulations.

The charging demand and the buildings' energy consumption play important roles when assessing home charging with peak load management, as in [P1]–[P5]. Besides the driving distance, the charging demand is influenced by many factors, such as driving behavior and ambient temperature, which may vary between every trip, yet the impact of these factors is not assessed in the publications. Additionally, the simulations focus on the average driving behavior in Finland; thus, the results may not be applicable in the case of notably different charging behaviors. The simulations consider real electricity consumption data of the buildings under study, so the available charging capacity is realistic. However, these few cases represent Finnish households; thus, the results may not be applicable in, e.g., other countries

with dissimilar space heating requirement. Nonetheless, the used simulation models and methodologies can be used to carry out similar case studies in other environments.

This thesis acknowledges that EV users do not always plug in their EVs even if it would be possible, yet, due to a lack of the necessary data, it has not been considered in the original publications. The results are likely to be affected by the EV users' tendency to plug-in when estimating the charging loads of multiple years into the future. On the one hand, public charging could be more expensive than home charging; thus, some EV users might choose not to charge unless it is needed to drive home. On the other hand, RES-powered public charging could occasionally be cheap in the case of surplus PV of wind power generation; thus, it could encourage EV users to take advantage of it. However, this is not considered in the analysis of public charging loads of the future in [P9].

[P11] and [P12] compared the results of the developed simulation model to the actual EV charging measurements. The modelling errors are minimal in the case of one second temporal resolution and non-ideal charging characteristics models, so the simulation model can be considered to be very accurate. However, since the simulation model considers only the four EV models mentioned in Table 1, it may not be suitable for modelling other EV models as accurately.

The CCE feature is developed in [P6] and improved in [P7] to overcome non-ideal charging characteristics in EV charging control. HIL tests have shown that the feature is able to track the charging characteristics of the considered EVs and allows the charging control algorithm to estimate the upcoming charging currents with certain current limits before applying the current limits. It is not possible to know how well the feature works with other EV models with different charging characteristics without further testing. However, as the feature does not use any kind of EV model-specific assumptions or preliminary data, it is assumed to work reliably with all kinds of EVs.

[P3] and [P8] considered different charging capacity allocation principles. It has not been possible to test the developed solutions in a large charging site in real life, so some issues may remain to be solved to make them feasible. The EV user perspective or experience are especially heavily influenced by the capacity allocation principle in the case of limited available charging capacity. A profitable charging site should operate efficiently and be attractive from its customers' perspective. The EV user experience and perspective are not thoroughly assessed in this thesis, so it remains uncertain which types of charging sites or control systems will be most beneficial.

7.3 Future work

This thesis focuses on decentralized charging solutions in which grid or market operators have no direct way to control the controllable loads. These solutions are likely to be easier to implement, but they pose risks and challenges from the grid operators' perspective. Therefore, in the case of a wide implementation of the decentralized solutions, the grid operators', energy retailers' and the flexibility aggregators' perspectives should also be investigated to determine whether the centralized solutions are necessary or not. This thesis also acknowledges the existence of non-ideal charging characteristics and studies them from algorithm development and modelling viewpoints. However, the extent to which these non-idealities influence certain topics is yet to be thoroughly determined. These topics include, for example, V2G operation, charging flexibility and optimized charging infrastructure design. Therefore, more work regarding the non-idealities is required. Furthermore, the EV users' perspective can be a key factor that influences a charging site's profitability; thus, it could be valuable to investigate it more thoroughly.

References

Agence France-Presse (2021) '*Toyota Targets Halving Battery Costs for Electric Vehicles by 2030, to Invest $13.6 Billion in Battery R&D*', [Online], Available at: https://www.firstpost.com/tech/auto-tech/toyota-targets-halving-battery-costs-for-electric-vehicles-by-2030-to-invest-13-6-billion-in-battery-rd-9946081.html, (Accessed 24.11.2021).

Ahmadian, A., Sedghi, M., Mohammadi-Ivatloo, B., *et al.* (2018) 'Cost-Benefit Analysis of V2G Implementation in Distribution Networks Considering PEVs Battery Degradation', *IEEE Transactions on Sustainable Energy*, 9(2), pp. 961–970, DOI: 10.1109/TSTE.2017.2768437.

Ahmadian, A., Sedghi, M., Elkamel, A., *et al.* (2018) 'Plug-in Electric Vehicle Batteries Degradation Modeling for Smart Grid Studies: Review, Assessment and Conceptual Framework', *Renewable and Sustainable Energy Reviews*, 81(2), pp. 2609–2624, DOI: 10.1016/j.rser.2017.06.067.

Al-Ogaili, A.S., Tengku, H., Tengku, J., *et al.* (2019) 'Review on Scheduling, Clustering, and Forecasting Strategies for Controlling Electric Vehicle Charging: Challenges and Recommendations', *IEEE Access*, 7, pp. 128353–128371, DOI: 10.1109/ACCESS.2019.2939595.

Andersson, A., Jääskeläinen, S., Saarinen, N., *et al.* (2020) '*Fossiilittoman Liikenteen Tiekartta -Työryhmän Loppuraportti (Final Report of Fossil Free Traffic Roadmap)*', Ministry of Transport and Communications, Report number: 2020:17. (In Finnish)

Apostolaki-Iosifidou, E., Codani, P. and Kempton, W. (2017) 'Measurement of Power Loss during Electric Vehicle Charging and Discharging', *Energy*, 127, pp. 730–742, DOI: 10.1016/j.energy.2017.03.015.

Beck, T., Kondziella, H. and Bruckner, T. (2016) 'Assessing the Influence of the Temporal Resolution of Electrical Load and PV Generation Profiles on Self-Consumption and Sizing of PV-Battery Systems', *Applied Energy*, 173, pp. 331–342, DOI: 10.1016/j.apenergy.2016.04.050.

Belonogova, N., Honkapuro, S., Partanen, J., Simolin, T., *et al.* (2020) 'Assessment of Ev Hosting Capacity in a Workplace Environment in Different', *CIRED 2020 Berlin Workshop*, Berlin, Germany, pp. 1–4.

BloombergNEF (2021) '*Electric Vehicle Outlook 2021*', [Online], Available at: https://about.bnef.com/electric-vehicle-outlook/, (Accessed 24.11.2021).

BMW AG (2015) '*The BMW i3. Owner's Manual.*', Online edition for part no. 01 40 2 960 865 - II/15.

Brinkel, N.B.G., Schram, W.L., AlSkaif, T.A., *et al.* (2020) 'Should We Reinforce the Grid? Cost and Emission Optimization of Electric Vehicle Charging under Different Transformer Limits', *Applied Energy*, 276, p. 115285, DOI: 10.1016/j.apenergy.2020.115285.

Cao, Y., Tand, S., Li, C., *et al.* (2012) 'An Optimized EV Charging Model Considering TOU Price and SOC Curve', *IEEE Transactions on Smart Grid*, 3(1), pp. 388–393, DOI: 10.1109/TSG.2011.2159630.

Castelvecchi, D. (2021) 'Electric Cars: The Battery Challenge', *Nature*, 596, pp. 336–339.

Ceyhan, C. (2019) '*How Long Should an Electric Car's Battery Last?*', [Online], Available at: https://www.myev.com/research/ev-101/how-long-should-an-electric-cars-battery-last, (Accessed 24.11.2021).

Chen, Q., Wang, F., Bri-Mathias, H., *et al.* (2017) 'Dynamic Price Vector Formation Model-Based Automatic Demand Response Strategy for PV-Assisted EV Charging Stations', *IEEE Transactions on Smart Grid*, 8(6), pp. 2903–2915, DOI: 10.1109/TSG.2017.2693121.

Dagdougui, H., Ouammi, A. and Dessaint, L.A. (2019) 'Peak Load Reduction in a Smart Building Integrating Microgrid and V2B-Based Demand Response Scheme', *IEEE Systems Journal*, 13(3), pp. 3274–3282, DOI: 10.1109/JSYST.2018.2880864.

Datta, U., Saiprasad, N., Kalam, A., *et al.* (2019) 'A Price-Regulated Electric Vehicle Charge-Discharge Strategy for G2V, V2H, and V2G', *International Journal of Energy Research*, 43(2), pp. 1032–1042, DOI: 10.1002/er.4330.

Deshmukh, S.S. and Pearce, J.M. (2021) 'Electric Vehicle Charging Potential from Retail Parking Lot Solar Photovoltaic Awnings', *Renewable Energy*, 169, pp. 608–617, DOI: 10.1016/j.renene.2021.01.068.

Dixon, J. and Bell, K. (2020) 'Electric Vehicles: Battery Capacity, Charger Power,

Access to Charging and the Impacts on Distribution Networks', *ETransportation*, 4, p. 100059, DOI: 10.1016/j.etran.2020.100059.

Dogan, A. and Alci, M. (2018) 'Heuristic Optimization of EV Charging Schedule Considering Battery Degradation Cost', *Elektronika Ir Elektrotechnika*, 24(6), pp. 15–20, DOI: 10.5755/j01.eie.24.6.22283.

Dong, H., Wang, L., Wei, X., *et al.* (2021) 'Capacity Planning and Pricing Design of Charging Station Considering the Uncertainty of User Behavior', *International Journal of Electrical Power and Energy Systems*, 125, p. 106521, DOI: 10.1016/j.ijepes.2020.106521.

Fingrid (2021) '*Electricity Consumption in Finland*', [Online], Available at: https://data.fingrid.fi/en/dataset/electricity-consumption-in-finland, (Accessed 24.11.2021).

The Finnish Information Centre of Automobile Sector (2020) 'User Survey of Electric Vehicles - User Habits of Plug-in Hybrid and Battery Electric Vehicles in Finland', Report number: 20.1.2020.

Finnish Transport and Communications Agency Traficom (2016) '*National Passenger Traffic Survey*'.

Finnish Transport and Communications Agency Traficom (2018) '*Purchase Subsidy for Electric Cars*', [Online], Available at: https://www.traficom.fi/en/services/purchase-subsidy-electric-cars, (Accessed 24.11.2021).

Frendo, O., Graf, J., Gaertner, N. and Stuckenschmidt, H. (2020) 'Data-Driven Smart Charging for Heterogeneous Electric Vehicle Fleets', *Energy and AI*, 1, p. 100007, DOI: 10.1016/j.egyai.2020.100007.

Ge, X., Shi, L., Fu, Y., *et al.* (2020) 'Data-Driven Spatial-Temporal Prediction of Electric Vehicle Load Profile Considering Charging Behavior', *Electric Power Systems Research*, 187, p. 106469, DOI: 10.1016/j.epsr.2020.106469.

Geske, J. and Schumann, D. (2018) 'Willing to Participate in Vehicle-to-Grid (V2G)? Why Not!', *Energy Policy*, 120, pp. 392–401, DOI: 10.1016/j.enpol.2018.05.004.

Gong, L., Cao, W., Liu, K., *et al.* (2020) 'Demand Responsive Charging Strategy

of Electric Vehicles to Mitigate the Volatility of Renewable Energy Sources', *Renewable Energy*, 156, pp. 665–676, DOI: 10.1016/j.renene.2020.04.061.

Gschwendtner, C., Sinsel, S.R. and Stephan, A. (2021) 'Vehicle-to-X (V2X) Implementation: An Overview of Predominate Trial Configurations and Technical, Social and Regulatory Challenges', *Renewable and Sustainable Energy Reviews*, 145, DOI: 10.1016/j.rser.2021.110977.

Hahnel, U.J.J., Gölz, S. and Spada, H. (2013) 'How Accurate Are Drivers' Predictions of Their Own Mobility? Accounting for Psychological Factors in the Development of Intelligent Charging Technology for Electric Vehicles', *Transportation Research Part A: Policy and Practice*, 48, pp. 123–131, DOI: 10.1016/j.tra.2012.10.011.

Halvorson, B. (2021) '*VW Targets 50% Cut in Battery Costs by 2030, Transition to Solid-State Tech*'. [Online], Available at: https://www.greencarreports.com/news/1131589_vw-targets-50-cut-in-battery-costs-by-2030-transition-to-solid-state-tech, (Accessed 24.11.2021).

Haupt, L., Schöpf, M., Wederhake, L. and Weibelzahl, M. (2020) 'The Influence of Electric Vehicle Charging Strategies on the Sizing of Electrical Energy Storage Systems in Charging Hub Microgrids', *Applied Energy*, 273, p. 115231, DOI: 10.1016/j.apenergy.2020.115231.

Helen Electricity Network Ltd. (2021) '*Electricity Distribution Tariffs*', [Online], Available at: https://www.helensahkoverkko.fi/globalassets/hinnastot-ja-sopimusehdot/hsv---enkku/distribution_tariffs.pdf, (Accessed 24.11.2021).

International Energy Agency (2021) 'Global EV Outlook 2021', Report number: April 2021.

Jaszczur, M., Hassan, Q., Abdulateef, A.M. and Abdulateef, J. (2021) 'Assessing the Temporal Load Resolution Effect on the Photovoltaic Energy Flows and Self-Consumption', *Renewable Energy*, 169, pp. 1077–1090, DOI: 10.1016/j.renene.2021.01.076.

Kane, M. (2021) '*Compare Electric Cars: EV Range, Specs, Pricing & More*', [Online], Available at: https://insideevs.com/reviews/344001/compare-evs/, (Accessed 24.11.2021).

Kempton, W. and Tomić, J. (2005) 'Vehicle-to-Grid Power Fundamentals:

Calculating Capacity and Net Revenue', *Journal of Power Sources*, 144(1), pp. 268–279, DOI: 10.1016/j.jpowsour.2004.12.025.

Khaki, B., Chu, C. and Gadh, R. (2019) 'Hierarchical Distributed Framework for EV Charging Scheduling Using Exchange Problem', *Applied Energy*, 241, pp. 461–471, DOI: 10.1016/j.apenergy.2019.03.008.

Kikusato, H., Fujimoto, Y., Hanada, S., *et al.* (2020) 'Electric Vehicle Charging Management Using Auction Mechanism for Reducing PV Curtailment in Distribution Systems', *IEEE Transactions on Sustainable Energy*, 11(3), pp. 1394–1403, DOI: 10.1109/TSTE.2019.2926998.

Kim, J.H. and Shcherbakova, A. (2011) 'Common Failures of Demand Response', *Energy*, 36(2), pp. 873–880, DOI: 10.1016/j.energy.2010.12.027.

Koufakis, A.M., Rigas, E., Bassiliades, N. and Ramchurn, S. D. (2020) 'Offline and Online Electric Vehicle Charging Scheduling with V2V Energy Transfer', *IEEE Transactions on Intelligent Transportation Systems*, 21(5), pp. 2128–2138, DOI: 10.1109/TITS.2019.2914087.

Kühnbach, M., Stute, J. and Klingler, A.L. (2021) 'Impacts of Avalanche Effects of Price-Optimized Electric Vehicle Charging - Does Demand Response Make It Worse?', *Energy Strategy Reviews*, 34, p. 100608, DOI: 10.1016/j.esr.2020.100608.

Kuopion Sähköverkko Oy (2021) '*Hinnasto, Verkkopalvelu (Price list, grid service)*', [Online], Available at: https://www.kuopionenergia.fi/wp-content/uploads/2021/07/Verkkopalvelumaksut-150721-010121.pdf, (Accessed 24.11.2021). (In Finnish)

Kutt, L., Saarijärvi, E., Lehtonen, M, *et al.* (2013) 'Current Harmonics of EV Chargers and Effects of Diversity to Charging Load Current Distortions in Distribution Networks', *2013 International Conference on Connected Vehicles and Expo, ICCVE 2013 - Proceedings*, pp. 726–731, DOI: 10.1109/ICCVE.2013.6799884.

Kutt, L., Saarijärvi, E., Lehtonen, M, *et al.* (2015) 'Load Shifting in the Existing Distribution Network and Perspectives for EV Charging-Case Study', *IEEE PES Innovative Smart Grid Technologies Conference Europe*, Istanbul, Turkey, pp. 1–6, DOI: 10.1109/ISGTEurope.2014.7028938.

Lacey, G., Putrus, G. and Bentley, E. (2017) 'Smart EV Charging Schedules:

Supporting the Grid and Protecting Battery Life', *IET Electrical Systems in Transportation*, 7(1), pp. 84–91, DOI: 10.1049/iet-est.2016.0032.

Lahti Energia Sähköverkko Oy (2021) '*Verkkopalveluhinnasto 1.8.2019 Alkaen (Grid service price list from 1.8.2019 onwards)*', [Online], Available at: https://www.lahtienergia.fi/wp-content/uploads/2021/06/verkkopalveluhinnasto_01082019.pdf, (Accessed 24.11.2021). (In Finnish)

Lahtinen, S. (2018) 'Henkilöautoilla Ajettiin Edellisvuosien Lailla – Maanteiden Tavarankuljetukset Tehostuivat (*Passenger Cars Were Driven as in Previous Years - Efficiency of Road Freight Transportation Improved*'), [Online], Available at: http://www.stat.fi/tietotrendit/artikkelit/2018/henkiloautoilla-ajettiin-edellisvuosien-lailla-maanteiden-tavarankuljetukset-tehostuivat/, (Accessed 24.11.2021). (In Finnish)

Lee, Z.J., Lee, G., Lee, T., *et al.* (2021) 'Adaptive Charging Networks: A Framework for Smart Electric Vehicle Charging', *IEEE Transactions on Smart Grid*, 12(5), pp. 4339–4350, DOI: 10.1109/TSG.2021.3074437.

Lee, Z.J., Chang, D., Jun. C., *et al.* (2019) 'Large-Scale Adaptive Electric Vehicle Charging', *2018 IEEE Global Conference on Signal and Information Processing, GlobalSIP 2018 - Proceedings*, pp. 863–864, DOI: 10.1109/GlobalSIP.2018.8646472.

Lee, Z.J., Li, T. and Low, S.H. (2019) 'ACN-Data: Analysis and Applications of an Open EV Charging Dataset', *E-Energy 2019 - Proceedings of the 10th ACM International Conference on Future Energy Systems*, pp. 139–149, DOI: 10.1145/3307772.3328313.

Li, Y., Li, K., Xie, Y., *et al.* (2020) 'Optimized Charging of Lithium-Ion Battery for Electric Vehicles: Adaptive Multistage Constant Current–Constant Voltage Charging Strategy', *Renewable Energy*, 146, pp. 2688–2699, DOI: 10.1016/j.renene.2019.08.077.

Lummi, K., Mutanen, A. and Järventausta, P. (2019) 'Upcoming Changes in Distribution Network Tariffs - Potential Harmonization Needs for Demand Charges', *25th International Conference on Electricity Distribution (CIRED)*, Madrid, Spain, pp. 1–5, DOI: 10.34890/741.

Mäki, K., Aro, M. and Bindner, H. (2021) 'Global Analysis on Demand Response

Status and Further Needs for Joint Research', *26th International Conference on Electricity Distribution (CIRED)*, Geneva, Switzerland, pp. 1–4.

Mall of Tripla (2021) '*How to Get There*' [Online], Available at: https://malloftripla.fi/en/saapuminen, (Accessed 24.11.2021).

Miller, J. (2020) '*Electric Car Costs to Remain Higher than Traditional Engines*', [Online], Available at: https://www.ft.com/content/a7e58ce7-4fab-424a-b1fa-f833ce948cb7, (Accessed 24.11.2021).

Ministry of Transport and Communications. (2020) '*Transport Emissions Halved by 2030 – Requires an Extensive Range of Options*', [Online], Available at: https://valtioneuvosto.fi/en/-/transport-emissions-halved-by-2030-requires-an-extensive-range-of-options, (Accessed 24.11.2021).

Mouli, G.R.C., Kefayati, M., Baldick, R. and Bauer, P. (2019) 'Integrated PV Charging of EV Fleet Based on Energy Prices, V2G, and Offer of Reserves', *IEEE Transactions on Smart Grid*, 10(2), pp. 1313–1325, DOI: 10.1109/TSG.2017.2763683.

Finnish Transport Infrastructure Agency (2016) '*Henkilöliikennetutkimus 2016 Suomalaisten liikkuminen (Finnish Passenger Traffic Survey 2016)*', Report number: 1/2018. (In Finnish)

Öljy- ja biopolttoaineala ry. (2016) '*Suomessa Lähes 1 900 Huoltoasemaa (Almost 1 900 Gas stations in Finland)*', [Online], Available at: https://www.sttinfo.fi/tiedote/suomessa-lahes-1-900-huoltoasemaa?publisherId=4020&releaseId=45229273, (Accessed 24.11.2021). (In Finnish)

Pareschi, G., Küng, L., Georges, G. and Boulouchos, K. (2020) 'Are Travel Surveys a Good Basis for EV Models? Validation of Simulated Charging Profiles against Empirical Data', *Applied Energy*, 275, p. 115318, DOI: 10.1016/j.apenergy.2020.115318.

Pevec, D., Babic, J., Carvalho, A., *et al.* (2020) 'A Survey-Based Assessment of How Existing and Potential Electric Vehicle Owners Perceive Range Anxiety', *Journal of Cleaner Production*, 276, p. 122779, DOI: 10.1016/j.jclepro.2020.122779.

Powell, S., Kara, E.C., Sevlian, R., *et al.* (2020) 'Controlled Workplace Charging of Electric Vehicles: The Impact of Rate Schedules on Transformer Aging',

Applied Energy, 276, p. 115352, DOI: 10.1016/j.apenergy.2020.115352.

Qian, K., Zhou, C., Allan, M., Yuan, Y., (2011) 'Modeling of Load Demand Due to EV Battery Charging in Distribution Systems', *IEEE Transactions on Power Systems*, 26(2), pp. 802–810, DOI: 10.1109/TPWRS.2010.2057456.

Rauma, K., Funke, A., Simolin, T., *et al.* (2021) 'Electric Vehicles as a Flexibility Provider: Optimal Charging Schedules to Improve the Quality of Charging Service', *Electricity*, 2(3), pp. 225–243, DOI: 10.3390/electricity2030014.

Rautiainen, A. (2015) '*Aspects of Electric Vehicles and Demand Response in Electricity Grids*', Tampere University, Publication 1327.

REDI (2021) '*Parking*', [Online], Available at: https://www.redi.fi/parking/?lang=en, (Accessed 24.11.2021).

Repo, S., Attar, M., Supponen, A., *et al.* (2021) 'Coordination Concepts for Interactions between Energy Communities , Markets , and Distribution Grids', *26th International Conference on Electricity Distribution (CIRED)*, Geneva, Switzerland, pp. 1–5.

Ruffo, G.H. (2020) '*EVs Are Still 45% More Expensive To Make Than Combustion-Engined Cars*', [Online], Available at: https://insideevs.com/news/444542/evs-45-percent-more-expensive-make-ice/, (Accessed 24.11.2021).

Sadeghianpourhamami, N., Refa, N., Strobbe, M. and Develder, C. (2018) 'Quantitive Analysis of Electric Vehicle Flexibility: A Data-Driven Approach', *International Journal of Electrical Power and Energy Systems*, 95, pp. 451–462, DOI: 10.1016/j.ijepes.2017.09.007.

Sadeghianpourhamami, N., Deleu, J. and Develder, C. (2020) 'Definition and Evaluation of Model-Free Coordination of Electrical Vehicle Charging with Reinforcement Learning', *IEEE Transactions on Smart Grid*, 11(1), pp. 203–214, DOI: 10.1109/TSG.2019.2920320.

Sähköinen liikenne ry (2020) '*Sähköisen Liikenteen Tilannekatsaus Q2 / 2020 (E-mobility status report)*', Report number: 30.8.2021. (In Finnish)

Schram, W., Brinkel, N., Smink, G., *et al.* (2020) 'Empirical Evaluation of V2G Round-Trip Efficiency', *3rd International Conference on Smart Energy Systems and Technologies*, Istanbul, Turkey, pp. 1–6, DOI: 10.1109/SEST48500.2020.9203459.

Schuller, A., Flath, C.M. and Gottwalt, S. (2015) 'Quantifying Load Flexibility of Electric Vehicles for Renewable Energy Integration', *Applied Energy*, 151, pp. 335–344, DOI: 10.1016/j.apenergy.2015.04.004.

SESKO ry (2019) '*Sähköajoneuvojen Lataussuositus (Recommendations for Electric Vehicle Charging)*', Report number: 2019-05-27.

Shafiq, S., Khan, B., Raussi, P. and Al-Awami, A.T. (2021) 'A Novel Communication-Free Charge Controller for Electric Vehicles Using Machine Learning', *IET Smart Grid*, 4(3), pp. 334–345, DOI: 10.1049/stg2.12032.

Shepero, M. and Munkhammar, J. (2018) 'Spatial Markov Chain Model for Electric Vehicle Charging in Cities Using Geographical Information System (GIS) Data', *Applied Energy*, 231, pp. 1089–1099, DOI: 10.1016/j.apenergy.2018.09.175.

Shirazi, Y.A. and Sachs, D.L. (2018) 'Comments on "Measurement of Power Loss during Electric Vehicle Charging and Discharging" – Notable Findings for V2G Economics', *Energy*, 142, pp. 1139–1141, DOI: 10.1016/j.energy.2017.10.081.

Spencer, S.I., Fu, Z., Apostolaki-Iosifidou, E. and Lipman, T.E. (2021) 'Evaluating Smart Charging Strategies Using Real-World Data from Optimized Plugin Electric Vehicles', *Transportation Research Part D: Transport and Environment*, 100, p. 103023, DOI: 10.1016/j.trd.2021.103023.

Spina, A., Rauma, K., Aldejohann, C., *et al.* (2018) 'Smart Grid Technology Lab - A Full-Scale Low Voltage Research Facility at TU Dortmund University', *110th AEIT International Annual Conference*, Bari, Italy, pp. 1–6, DOI: 10.23919/AEIT.2018.8577378.

Sun, C., Li, T., Low, S. and Li, V.O.K., (2020) 'Classification of Electric Vehicle Charging Time Series with Selective Clustering'. *Electric Power Systems Research*, 189, p. 106695, DOI: 10.1016/j.epsr.2020.106695.

Thingvad, A., Andersen, P.B., Unterluggauer, T., *et al.* (2021) 'Electrification of Personal Vehicle Travels in Cities - Quantifying the Public Charging Demand', *ETransportation*, 9, p. 100125, DOI: 10.1016/j.etran.2021.100125.

Tikka, V., Lassila, J. and Laine, T. (2021) '*Technical Report: Measurements of Cold Climate EV Charging*', Report number: 130.

van Triel, F. and Lipman, T.E. (2020) 'Modeling the Future California Electricity Grid and Renewable Energy Integration with Electric Vehicles', *Energies*, 13(20), pp. 1–20, DOI: 10.3390/en13205277.

Unterluggauer, T., Rauma, K., Järventausta, P., and Rehtanz, C. (2021) 'Short-term Load Forecasting at Electric Vehicle Charging Sites Using a Multivariate Multi-step Long Short-term Memory: A Case Study from Finland', *IET Electrical Systems in Transportation*, in press, DOI: 10.1049/els2.12028.

Venegas, F.G., Petit, M. and Perez, Y. (2021) 'Plug-in Behavior of Electric Vehicles Users: Insights from a Large-Scale Trial and Impacts for Grid Integration Studies', *ETransportation*, 10, p. 100131, DOI: 10.1016/j.etran.2021.100131.

Wan, Z., Li, H., He, H. and Prokhorov, D. (2018) 'A Data-Driven Approach for Real-Time Residential EV Charging Management', *IEEE Power and Energy Society General Meeting*, Portland, Oregon, USA, pp. 1–5, DOI: 10.1109/PESGM.2018.8585945.

Wang, X. and Liang, Q. (2017) 'Energy Management Strategy for Plug-in Hybrid Electric Vehicles via Bidirectional Vehicle-to-Grid', *IEEE Systems Journal*, 11(3), pp. 1789–1798, DOI: 10.1109/JSYST.2015.2391284.

Wei, Z., Li, Y., Zhang, Y. and Cai, L. (2018) 'Intelligent Parking Garage EV Charging Scheduling Considering Battery Charging Characteristic', *IEEE Transactions on Industrial Electronics*, 65(3), pp. 2806–2816, DOI: 10.1109/TIE.2017.2740834.

Wolbertus, R., Kroesen, M., van den Hoed, R. and Chorus, C. (2018) 'Fully Charged: An Empirical Study into the Factors That Influence Connection Times at EV-Charging Stations', *Energy Policy*, 123, pp. 1–7, DOI: 10.1016/j.enpol.2018.08.030.

Xu, Y., Pan, F. and Tong, L. (2016) 'Dynamic Scheduling for Charging Electric Vehicles: A Priority Rule', *IEEE Transactions on Automatic Control*, 61(12), pp. 4094–4099, DOI: 10.1109/TAC.2016.2541305.

Yi, T., Zhang, C., Lin, T. and Liu, J. (2020) 'Research on the Spatial-Temporal Distribution of Electric Vehicle Charging Load Demand: A Case Study in China', *Journal of Cleaner Production*, 242, p. 118457, DOI: 10.1016/j.jclepro.2019.118457.

Zhang, J., Yan, J., Liu, Y., *et al.* (2020) 'Daily Electric Vehicle Charging Load Profiles Considering Demographics of Vehicle Users', *Applied Energy*, 274, p. 115063, DOI: 10.1016/j.apenergy.2020.115063.

Zhang, T., Chen, X., Yu, Z., et al. (2018) 'A Monte Carlo Simulation Approach to Evaluate Service Capacities of EV Charging and Battery Swapping Stations', *IEEE Transactions on Industrial Informatics*, 14(9), pp. 3914–3923, DOI: 10.1109/TII.2018.2796498.

Zhang, T., Pota, H., Chu, C. and Gadh, R. (2018) 'Real-Time Renewable Energy Incentive System for Electric Vehicles Using Prioritization and Cryptocurrency', *Applied Energy*, 226, pp. 582–594, DOI: 10.1016/j.apenergy.2018.06.025.

Zhou, T. and Sun, W. (2020) 'Research on Multi-Objective Optimisation Coordination for Large-Scale V2G', *IET Renewable Power Generation*, 14(3), pp. 445–453, DOI: 10.1049/iet-rpg.2019.0173.

PUBLICATIONS

PUBLICATION
1

Control of EV charging and BESS to reduce peak powers in domestic real estate

T. Simolin, A. Rautiainen, J. Koskela, P. Järventausta

Control of EV Charging and BESS to Reduce Peak Powers in Domestic Real Estate

T. Simolin, A. Rautiainen, J. Koskela, P. Järventausta

Abstract – *The paper discusses the effects of electric vehicle (EV) charging and battery energy storage systems (BESS) on monthly peak powers in domestic apartment buildings. The introduced control method for both EV charging and BESS utilizes real-time measurements and memorized peak power consumptions to determine the available power before exceeding the previous peak power. This kind of control method could lead to cost savings if the power-based distribution tariff of distribution system operators (DSO) includes a price component based on monthly peak power. Some Finnish DSOs have also launched this kind of power-based distribution tariff for small-scale customers. Simulations indicate that EVs can likely be charged without increasing the monthly peak powers of real estate when EV penetration is relatively small. Higher EV penetration would lead to a higher risk of some EVs to not fully charge. There are also indications that BESS can be effective in limiting monthly peak powers when utilizing the peak saving control method.* **Copyright © 2009 Praise Worthy Prize S.r.l. - All rights reserved.**

Nomenclature

$\eta_{B,C}$	BESS charging efficiency
$\eta_{B,D}$	BESS discharging efficiency
η_{CP}	Charging point efficiency
η_I	Inverter efficiency
$E_{B,max}$	Maximum state of charge of BESS
$E_{B,SOC}$	State of charge of the BESS
$E_{EV,miss}$	Missing energy of EV before becoming fully charged
$P_{B,C}$	BESS charging power
$P_{B,C,max}$	Maximum BESS charging power
$P_{B,C,max,p}$	Maximum BESS charging power which has already taken battery SOC into account
$P_{B,D}$	Battery discharging power
$P_{B,D,max}$	Maximum BESS discharging power
$P_{B,D,max,p}$	Maximum BESS discharging power which has already taken battery SOC into account
$P_{CP,max}$	Maximum power of a charging point
P_{EV}	Charging power of a single EV
$P_{EV,C,max}$	Maximum charging power of EV
$P_{Grid,f}$	Power taken from the grid
$P_{Grid,max,f}$	Limit for the power taken from the grid due to the main fuse
$P_{Grid,f,mm}$	Maximum measured peak power of the ongoing month
$P_{Grid,t}$	Power injected to the grid
$P_{Grid,max,t}$	Limit for the power injected to the grid due to the main fuse
$P_{I,max}$	Maximum output power from inverter
$P_{I,out}$	Power from PV system after inverter losses
P_{Load}	Total load of the building and EV charging
$P_{Load,ab}$	Power consumption of the apartment building
$P_{Load,EV}$	Total EV charging power
$P_{Local,out}$	Total power output from PV system and BESS
P_{PV}	Power from PV system

I. Introduction

The interest in EVs has increased globally. For example, the Finnish government has set a target for Finland to acquire 250 000 EVs by 2030 [1]. With the current relative growth of EVs, this target might be achieved much sooner. Although the target EV count is equivalent to an EV penetration of less than 10%, the importance of smart charging should not be overlooked. Over the last few years, a lot of research has centered on controlling EV charging. Some work has been made, e.g., in [2] and [3], where the EV charging power is limited based on the limits of the feeder. EV charging peak load–related studies are presented, e.g., in [4], [5], [6], and [7], in which the principle for mitigating the increase of peak load is based on scheduling the EV charging. In [8], a valley-filling control method has been introduced, making the increase of peak powers negligible. However, the research lacks studies of peak power–related problems and their solutions in the internal networks of domestic real estate with charging station groups.

In recent years, there has been ongoing discussion in Europe on shifting DSOs' distribution tariffs in a power-based direction. This means that in addition to or instead of traditional basic (€/month) and volumetric charges

(€/kWh), there would be a tariff component (€/kW) based on peak power of some time period, i.e., the latest year or month. It is worth noting that as peak power is the highest average power taken from the grid in any 1-hour time period, momentary power consumption can be higher. Power-based distribution tariffs are enabled by a rollout of smart meters. In Finland, the electricity consumption of >99% of network customers including households is measured by smart meters [9]. As some distribution system operators in Finland have already started using power-based distribution tariffs for small-scale customers, suboptimal control of EV charging could cause an unnecessary increase in operational costs for EV owners or their apartment buildings. Therefore, it is reasonable to investigate options to reduce peak powers.

BESS and photovoltaic (PV) system could be utilized for the whole building's load if the energy community model is used; the apartments form an energy community, which makes only common contracts with the energy retailer and DSO when all electricity purchased by the building from the grid or grid feed is measured with one meter. The problem is that the law requires that every customer have the possibility to tender out energy retailers. The energy community model is possible if all apartment owners accept and they have the possibility to resign from the community. This also requires each apartment to have its own electricity meters in addition to the common meter so the customers can divide the cost.

This paper investigates a simple peak-shaving control method in which the free power capacity of the feeder before exceeding the current peak power of the ongoing month is continuously calculated in order to determine the necessary actions. This control method can be applied to EV charging, where charging power is lowered if needed, and to BESS, which can be charged when free capacity is positive and discharged when free capacity is negative. The developed control method maximizes EV charging power while preventing unnecessary peak power increase. This could bring operational cost savings for apartment owners if a peak power-based distribution tariff component is used and the apartment building forms an energy community. To evaluate the viability of the introduced control method, potential cost savings will be calculated, and possible limitations are discussed.

The paper is organized as follows. In section II, the control method is introduced and discussed. In section III, the necessary initial data for the case study simulations are presented. Section IV represents the simulation results, and Section V finalizes the paper by presenting the conclusions and future work proposals.

II.   The Control Method

Without a proper control method for EV charging, monthly peak powers, for example of an apartment building, could increase notably. The monthly peak power

will likely be a popular basis to charge the power-based fee by DSOs in the future. The idea of this control method is that the total load of the whole real estate is measured in real-time, and the highest peak load of the ongoing month is memorized by the control system. The free capacity before exceeding the current peak load can then be continuously calculated to determine if EV charging power should be decreased or increased, or if BESS should be charged or discharged.

The main principle of the system structure is illustrated in Figure 1. According to the standard IEC 61851-1, this kind of control method is possible in mode 3 EV charging, where the charging station can restrict and adjust the maximum AC charging current (per phase) between 6 A and 80 A. Figures 2 and 3 illustrate the control method operation when applied to EV charging or BESS, respectively. The feeder limit shown in Figure 2 is there to ensure that the charging power would not exceed the limits of the fuse or the cable of the EV charging feeder. The highest memorized peak power should be reset at the beginning of each month so that previous months would not affect the peak power of the ongoing month.
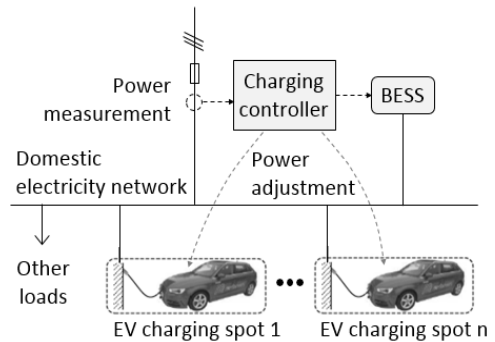
Fig. 1. The basic setup of the control method.
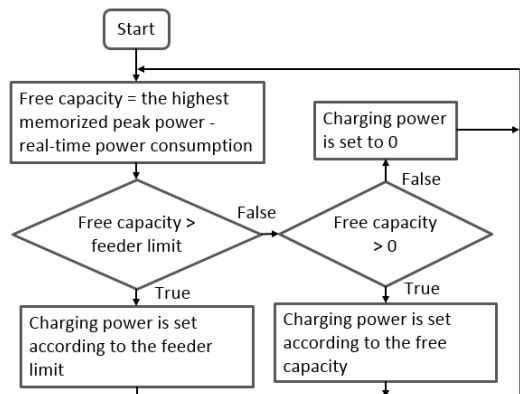
Fig. 2. Simplified block diagram of the control method for EV charging.
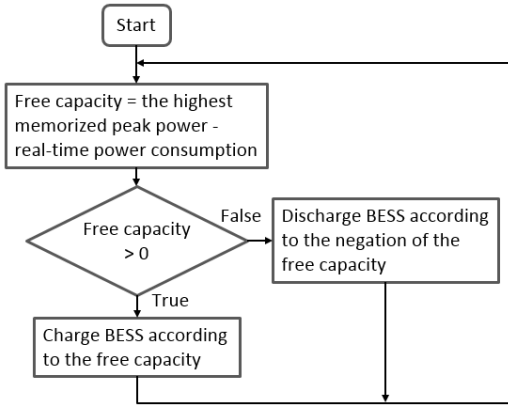
Fig. 3. Simplified block diagram of the control method for BESS.

As shown in Figure 3, BESS should be charged when the free capacity is positive and discharge when the free capacity is negative. Charging power should be limited according to the free capacity to increase the state of charge (SOC) of BESS as fast as possible without increasing monthly peak powers. Discharging power should be limited according to the free capacity to avoid increasing monthly peak powers while keeping the remaining SOC as high as possible. In addition to these, battery properties like the maximum charging and discharging powers and the maximum and the minimum SOC levels should also be taken into account.

In simulations of this case study, the total power consumption of the final hour of the previous month is used as a starting value for the memorized peak power of the new month. Another simple option would be to reset the memorized peak power of the new month to 0. However, preliminary simulations indicated that the selected method would result in lower monthly peak powers and lower uncharged energy of the EVs on average.

III.   Simulation Data and Modeling

III.1.   Case Description

The investigated case is called "Tammela," which is an apartment building built in 1980 in Finland. Between 2013 and 2015, various renovations have been made, which have resulted in a 67% reduction in purchased energy. However, the share of electrical energy has increased and resulted in electrical energy consumption to increase by around 30%. This is caused by the installation of exhaust air heat pumps, where produced heat energy replaces the purchase of energy from district heating. In the simulations, the models included eight charging points, a PV system, and a BESS for "Tammela." These eight charging points are modeled for daily use and equal to a local EV penetration of approximately 15%. Simulations

were carried out based on long-term electricity consumption measurements made in the apartment building and electricity production measurements of a 30 kW PV system. Consumption data were measured in 2013–2016 in one-hour intervals, and the PV production data was measured in 2017 in five-minute intervals.

Figure 4 illustrates the modeled system. The BESS is modeled so that it can be charged with energy from the PV system or from the grid. In the simulations, the BESS' usable energy capacity, maximum charging/discharging power, and charging/discharging efficiencies are selected to be 35 kWh, 10 kW, and 0.96, respectively. These parameters are based on a BESS found on the market [10] but multiplied by four (except the efficiency) to make it more impactful for the apartment building. Lithium-ion batteries typically have a high efficiency of 0.95–0.98 [11]–[13]. The selected BESS power and energy capacity is a few times larger than the ones meant for a single household mentioned in [11], [14], and [15]. Therefore, the BESS is assumed to be reasonable and yet its control method is expected to have an impact on the peak powers of the apartment building.

The simulation focuses on a charging power of 3.7 kW per charging point, which should be roughly suitable for almost every commercial EV. As EV charging presumably takes place mostly at night, there is no urgent need for a higher charging power. Furthermore, simulations investigate scenarios where the total charging power of the whole charging station group can be limited to 11 kW, or to 11 kW and according to the control method. By limiting the maximum total power of the EV charging system, cheaper feeding cables and smaller network connections can be used. This can result in lower investment costs and in some cases in smaller distribution fees without a notable effect on EV charging times. Even though the total charging power limit of 11 kW is under half of the combined power of all eight charging points, the simulations do not indicate that it has a negative impact on EV charging. This is likely due to long-available charging times and the reasonable energy demands of EVs, as presented in the following subsection.
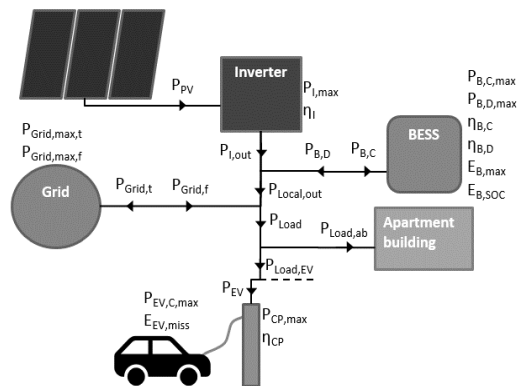
Fig. 4. System arrangement behind the simulations.

III.2. EV Load Modeling

According to Statistics Finland, the average travel distance per passenger car in Finland was 14 000 km/a in 2017 [16], which would be around 38.4 km/day on average. Assuming that a typical EV energy consumption is 0.25 kWh/km, this would lead to a daily charging energy need of 9.6 kWh, which is also close to the typical battery capacity of most common plug-in hybrid EVs in Finland. If charging losses in an EV are assumed to be 10%, the average daily energy needed from the charging point will be around 10.7 kWh. The investigated case is an apartment building, and EV charging is therefore assumed to occur in the afternoon and night.

To add variety to daily charging sessions, they are simulated to start between 16.30 and 20.00 and end between 6.00 and 8.30. The energy needed for the charging sessions has also been multiplied with factors of 0.5–2.0 in a way that the average energy need of an EV remains at 9.6 kWh. The schedule for the use of each charging point (CP) has been presented in Table I. Possible bigger energy needs for full electric vehicles (FEV) are left out of this study.

TABLE I
DAILY CHARGING SCHEDULE OF EVs

EV	Arrival	Departure	Missing energy (Wh)
1.	18:30	6:45	10416
2.	19:45	6:15	17904
3.	16:45	8:00	5040
4.	19:00	7:15	11424
5.	17:45	7:45	8256
6.	19:15	6:00	6384
7.	18:15	8:30	10560
8.	17:15	7:15	6816

III.3. System Modeling

The introduced control method discharges BESS when power taken from the grid is about to exceed the current month's highest peak power. The BESS is also controlled to discharge to allow a higher EV charging power when needed. If power taken from the grid is below the peak power, BESS will be charged. Power used for battery charging $P_{B,C}$ can be calculated according to (1),

$$P_{B,C} = \min(P_{B,C,max,p}, \max(0, P_{I,out} - P_{Load} + P_{Grid,f,mm})) \qquad (1)$$

where $P_{B,C,max,p}$ is the maximum power that BESS can receive, $P_{I,out}$ is power from the PV system after inverter losses, P_{Load} is the sum load of the building and EV charging, and $P_{Grid,f,mm}$ is the measured maximum peak power of the ongoing month. Power discharged from BESS $P_{B,D}$ can be calculated according to (2),

$$P_{B,D} = \min(P_{B,D,max,p}, \max(0, -P_{I,out} + P_{Load} - P_{Grid,f,mm})) \qquad (2)$$

where $P_{B,D,max,p}$ is the maximum power that BESS can discharge.

Power needed from the grid $P_{Grid,f}$ can be calculated according to (3),

$$P_{Grid,f} = \min(P_{Load} - P_{Local,out}, P_{Grid,max,f}, \max(P_{Grid,f,month,max}, P_{Load,ab} - P_{Local,out})) \qquad (3)$$

where $P_{Grid,max,f}$ is the limit of power taken from the grid due to the main fuse, $P_{Load,ab}$ is the consumption of the apartment building, and $P_{Local,out}$ is power coming from the PV system and BESS. Simulations use a time step of 15 minutes, which allows a whole year to be simulated within a reasonable amount of time. In order to use the measured consumption data of the apartment building in the simulations, an interpolation was necessary to change the time step of 1 hour to 15 min. This was done by simply dividing each of the 1-hour energy consumptions evenly for four parts.

IV. Simulation Results

To evaluate the effects of different settings, simulations have been carried out for 11 scenarios. These scenarios have been listed in Table II. Each simulation is done for a period of one year so that we can examine monthly peak powers for every month. At first, all scenarios are calculated using the newest consumption data of the apartment building (2016) in subsections IV.1.–IV.3. In subsection IV.4., simulations are carried out using consumption data of the apartment building during 2013 – 2016 to ensure that the results are repetitive.

TABLE II
SIMULATION SCENARIOS

Scenario	Explanation
1.	Only apartment building
2.	Uncontrolled EV charging with 3.7 kW CPs
3.	Uncontrolled EV charging with 1.8 kW CPs
4.	EV charging with 3.7 kW CPs, where the total EV charging power is limited to 11 kW
5.	EV charging with 3.7 kW CPs, where the total EV charging power is limited to 11 kW and the introduced peak saving control method is in use
6.	Apartment building with 30 kW PV system
7.	Scenarios 5 and 6 combined
8.	Apartment building with 35 kWh / 10 kW BESS, which is controlled with the control method
9.	Scenarios 5 and 8 combined
10.	Scenarios 6 and 8 combined
11.	Scenarios 5 and 10 combined

Each scenario includes the consumption for the apartment building.
CPs = Charging points

IV.1. EV Charging Scenarios

It is well known that uncontrolled EV charging can cause significant peaks in power consumption [4]–[6]. Figure 5 illustrates the EV charging load curves of scenarios 1–5. It can be seen that both the peak power of apartment building and that of an uncontrolled EV charging occur in the evening, resulting in increased peak power in the day, presented in Figure 5. In scenario 5, EV charging power is limited to the peak power of the ongoing month. This peak power is 30.9 kW in Figure 5, which causes EV charging to drop around 20:00–21:00.
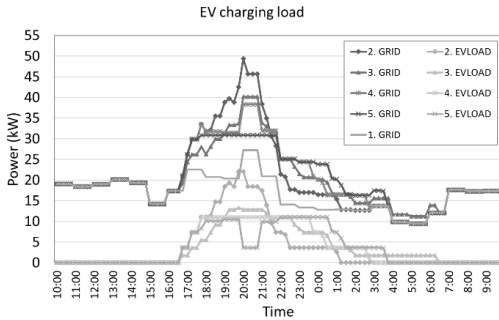
Fig. 5. Simulation results of scenarios 1–5.

As seen in Figure 6, scenario 2 results in quite a high increase in monthly peak powers, whereas in scenario 5, monthly peak powers will stay the same. For scenarios 2–5, the average relative increase in monthly peak power compared to scenario 1 is 23.9%, 13.1%, 16.6%, and 0.0%, respectively.
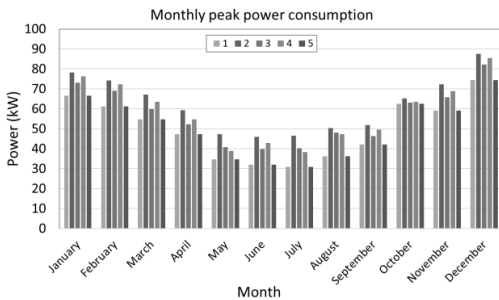
Fig. 6. Simulation results of scenarios 1–5.

IV.2. Effects of PV and BESS on Peak Powers of the Apartment Building

Figure 7 illustrates the effects of PV and BESS on the monthly peak powers of the apartment building. These scenarios (1, 6, 8, and 10) do not include EV charging and are therefore comparable to each other. The average

relative decrease in monthly peak powers compared to scenario 1 is 4.6%, 17.2%, and 22.0% for scenarios 6, 8, and 10, respectively. Although the PV system is more often seen as a way to reduce energy consumption, it can also reduce monthly peak powers in the summer. However, from the DSO's point of view, this might not be very useful as the grid must be planned according to the worst-case scenario, which is more often during the winter in Finland.
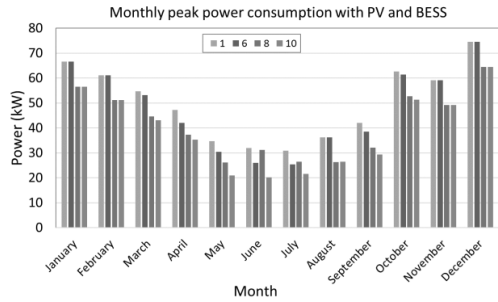
Fig. 7. Simulation results of scenarios 1, 6, 8, and 10.

IV.3. Effects of PV and BESS on Peak Powers of the Apartment Building with Controlled EV Charging

Figure 8 illustrates the effects of PV and BESS on the monthly peak powers of the real estate, which includes apartment buildings and controlled EV charging as in scenario 5. The average relative decrease in monthly peak powers compared to scenario 1 are 4.5%, 17.5%, and 21.5% for scenarios 7, 9, and 11, respectively. These results are close to the ones without EV charging that were stated above, which indicates that controlled EV charging would be possible without a notable increase to peak powers in real estate.
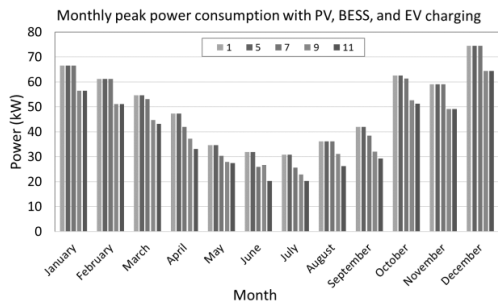
Fig. 8. Simulation results of scenarios 1, 5, 7, 9, and 11.

IV.4. Economic Effects of Different Scenarios

According to Figures 9 and 10, simulations give similar results when using different base power consumptions for

the apartment building. The economic effect of each scenario can be calculated using the sum of monthly peak powers. If the cost of the increase in monthly peak power is 3.72 €/kW (including VAT 24%) [17], the average cost increase in a month for scenarios 2–5 compared to scenario 1 would be 47.3 €, 24.9 €, 30.5 €, and 0.0 €, respectively. As a side note, scenarios 2 and 3 would also require more expensive investment costs on the feeding cable as they allow higher maximum power for EV charging.

As seen in Figure 10, the PV system would also reduce the monthly peak powers by about 2.02 kW on average, which results in cost savings of 7.5 €/month. In turn, BESS would similarly reduce peak powers by 7.97 kW/month on average, which would result in a cost savings of 29.7 €/month. Again, combining the PV system and BESS would result in an average of 10.07 kW/month and 37.4 €/month. It can be noticed that combining PV and BESS seems to reduce peak powers slightly more than the sum of using only the PV system and BESS. It is also worth noting that using this control method, BESS seem to be very effective in reducing peak powers. This can be deduced from the fact that BESS, with a maximum discharging power of 10 kW as used in the simulations, can reduce monthly peak power by no more than 10 kW. Therefore, the average peak power reduction of 7.97 kW/month would be quite good.

One reason for the high effect of BESS might be the usage of saunas in the examined apartment building, which is likely to cause high and relatively short peaks in power consumption. If the used BESS has enough capacity, it might be able to mitigate the peak power consumption taken from the grid in these occasions and therefore lead to noteworthy results.
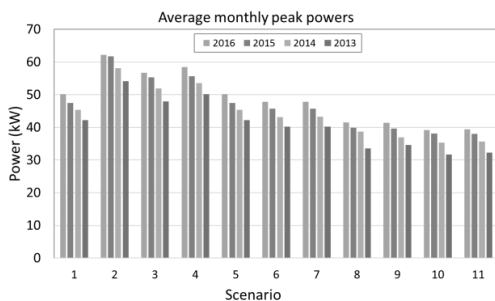
Fig. 9. Simulation results when using apartment building consumption data from 2013–2016.
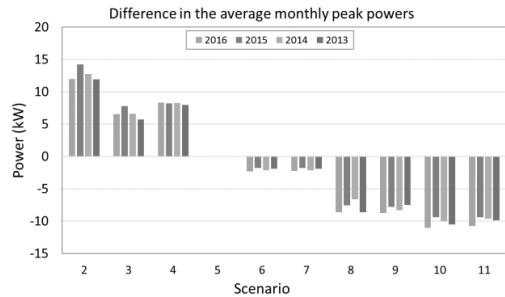
Fig. 10. Simulation results when using apartment building consumption data from 2013–2016.

IV.5. Limitations of the Control Method for EV charging

Figures 9 and 10 show that EV charging can be done without increasing the monthly peak powers of the real estate. The main downside of the introduced control method is the risk of EVs not being fully charged after a night of being plugged into a charging point. When using measured consumption data of the apartment building in 2013–2016, 11 of the 16 scenarios that used the control method for EV charging (scenarios 5, 7, 9, and 11) left some energy capacity of the EVs uncharged. The largest amount of uncharged energy occurred when simulating scenario 9 using the consumption data from 2013 for the apartment building. This energy was 11.2 kWh, which equals to 0.036% of the yearly total capacity of possible EV charging. This also means that an EV would still be completely uncharged 1.17 times per year on average after a night of being plugged into a charging point.

In the simulations, scenarios 9 and 11 use BESS to allow for higher power for EV charging. To execute this, the controller requires information from BESS about the available power that can be discharged. Besides that, this peak saving control method does require only smart metering of the real estate and charging points. Charging points require smart metering due to the fact that in mode 3 charging, the controller can only set the maximum current for a charging point, and the EV itself chooses a charging current below the limit. Therefore, the controller might not know the real power consumption of EV charging without smart metering.

V. Conclusion and Future Work

In conclusion, it can be stated that EV charging can be conducted alongside an apartment building without significantly increasing the monthly peak powers of the whole real estate. The control method, which uses memorized peak power for the ongoing month and real-time power measurements, can also be quite effective for controlling a BESS to reduce monthly peak powers. By assuming that the apartment building forms an energy

community and distribution tariff includes a component based on monthly peak power, this kind of control method could bring operational cost savings.

The problem with the control method for EV charging is the risk of EVs remaining uncharged after a night of being plugged into a charging point. Although the uncharged energy seems to be relatively small in the simulated scenarios, it might raise concerns among the users of the EV charging system. The control method, as it is presented in this paper, will be particularly unfavorable for operators of FEV.

To avoid this problem with increased penetration of EV or FEV, the control method should allow peak powers to increase if necessary. The allowed increase of peak powers should be executed in a way that results in the EVs being fully charged while peak powers remain as low as possible. This might be a challenge as there are multiple unknown factors like EV departure time and energy demand of the EV, which the EV charging system controller might not be able to use for the optimization of the charging system. It should also be noted that in order to fully charge a typical full electric vehicle in one night, a charging power of 3.7 kW would most likely not be enough. It might be enough, however, to carry on the next day.

Future work could investigate different options to allow higher energy to be charged with a minimal increase in peak powers in case of a higher energy demand of EVs. Also, a more detailed analysis of the method, which resets the memorized peak power, could be conducted as it seems to have an impact on the uncharged energy according to preliminary simulations. Future work could include a thorough techno-economic analysis for both EV charging and BESS as well. Furthermore, a more comprehensive investigation of the impacts of different variables, like charging point power, feeder limit, BESS attributes, or the time step of the simulations, might be useful.

References

[1] Ministry of Economic Affairs and Employment, "Strategy outlines energy and climate actions to 2030 and beyond," 2016, p. 1, Available: https://valtioneuvosto.fi/en/artikkeli/-/asset_publisher/1410877/strategia-linjaa-energia-ja-ilmastotoimet-vuoteen-2030-ja-eteenpain

[2] A. Rautiainen, K. Lummi, P. Järventausta, V. Tikka, A. Lana, Control of electric vehicle charging in domestic real estates as part of demand response functionality, Cired, p. 4, 2016.

[3] T. Bohn, C. Cortes, and H. Glenn, "Local automatic load control for electric vehicle smart charging systems extensible via OCPP using compact submeters," *IEEE Transportation Electrification Conference and Expo (ITEC)*, Chicago, IL, pp. 724–731, 2017.

[4] A. Dogan, M. Kuzlu, M. Pipattanasomporn, S. Rahman, and T. Yalcinoz, "Impact of EV charging strategies on peak demand reduction and load factor improvement," *9th International Conference on Electrical and Electronics Engineering (ELECO)*, Bursa, pp. 374–378, 2015.

[5] U. Reiner, C. Elsinger, and T. Leibfried, "Distributed self organising electric vehicle charge controller system: Peak power demand and grid load reduction with adaptive EV charging stations," *IEEE International Electric Vehicle Conference*, Greenville, SC, pp. 1–6, 2012.

[6] L. Hua, J. Wang, and C. Zhou, "Adaptive electric vehicle charging coordination on distribution network," *IEEE Transactions on Smart Grid*, vol. 5, no. 6, pp. 2666–2675, Nov. 2014.

[7] V. Aravinthan and W. Jewell, "Controlled electric vehicle charging for mitigating impacts on distribution assets," *IEEE Transactions on Smart Grid*, vol. 6, no. 2, pp. 999–1009, Mar. 2015.

[8] Y. Tang and J. Zhong, "System-level charging control strategy for plug-in electric vehicles," *IEEE Power & Energy Society General Meeting*, Denver, CO, p. 5, 2015.

[9] Energy Authority, "National Report 2018 to the Agency for the Cooperation of Energy Regulators and to the European Commission," p. 47, 2018, Available: https://www.energiavirasto.fi/documents/10191/0/National+Report+2018+Finland+1411-480-2018_20180726.pdf/10b8e538-2eef-4e97-8629-aafd4ad9ee02

[10] Solarwatt, Data sheet MyReserve 800, https://www.solarwatt.com/downloads/storage-myreserve [Accessed 4.9.2018]

[11] M. Naumann, R. C. Karl, C. N. Truong, A. Jossen, and H. C. Hesse, "Lithium-ion battery cost analysis in PV-household application," *Energy Procedia*, vol. 73, pp. 37–47, 2015.

[12] P. J. Hall and E. J. Bain, "Energy-storage technologies and electricity generation," *Energy Policy*, vol. 36, no. 12, pp. 4352–4355, 2008.

[13] V. F. Pires, E. Romero-Cadaval, D. Vinnikov, I. Roasto, and J. F. Martins, "Power converter interfaces for electrochemical energy storage systems – A review, Energy Conversion and Management," vol. 86, pp. 453–475, 2014.

[14] R. Martins, P. Kreimer, and P. Musilek, "LP-based predictive energy management system for residential PV/BESS," *2017 IEEE International Conference on Systems, Man, and Cybernetics (SMC)*, Banff, AB, pp. 3727–3732, 2017.

[15] X. Wu, X. Hu, Y. Teng, S. Qian, and R. Cheng, "Optimal integration of a hybrid solar-battery power source into smart home nanogrid with plug-in electric vehicle," Journal of Power Sources, vol. 363, pp. 277–283, 2017.

[16] Statistics Finland, "Henkilöautoilla ajettiin edellisvuosien lailla – maanteiden tavarankuljetukset tehostuivat," (In Finnish), Available: http://www.stat.fi/tietotrendit/artikkelit/2018/henkiloautoilla-ajettiin-edellisvuosien-lailla-maanteiden-tavarankuljetukset-tehostuivat/

[17] K. Lummi, A. Rautiainen, P. Järventausta, P. Heine, J. Lehtinen, and M. Hyvärinen, "Cost-causation based approach in forming power-based distribution network tariff for small customers," *EEM*, p. 5, 2016.

Authors' information

Tampere University of Technology.

Toni Simolin received his M.Sc. in electrical engineering from the Tampere University of Technology in 2018. At present, he works as a project researcher in the laboratory of Electrical Energy Engineering at the Tampere University of Technology. His research focuses on electric vehicle charging and its impacts on technical and economical points of view.

Antti Rautiainen received his M.Sc. and Dr.Tech. degrees in electrical engineering from the Tampere University of Technology in 2008 and 2015, respectively. At present, he works as a post-doctoral researcher in the laboratory of Electrical Energy Engineering at the Tampere University of Technology. His research focuses on various topics related to electricity grids and the electricity market.

Juha Koskela received his M.Sc. in electrical engineering from the Tampere University of Technology in 2016. At present, he works as a doctoral student in the laboratory of Electrical Energy Engineering at the Tampere University of Technology. His research focuses on electrical energy storages and their impacts on technical and economical points of view.

Prof. **Pertti Järventausta** received his M.Sc. and Licentiate of Technology degrees in electrical engineering from the Tampere University of Technology in 1990 and 1992, respectively. He received his Dr.Tech. in electrical engineering from the Lappeenranta University of Technology in 1995. At present, he is a professor at the Tampere University of Technology and leads the laboratory of Electrical Energy Engineering. His main interest focuses on the issues of Smart Grids from the grid and electricity market points of view.

PUBLICATION
2

Control of EV charging to reduce peak powers in domestic real estate

T. Simolin, A. Rautiainen, P. Järventausta

CONTROL OF EV CHARGING TO REDUCE PEAK POWERS IN DOMESTIC REAL ESTATE

Toni SIMOLIN
Tampere University – Finland
toni.simolin@tuni.fi

Antti RAUTIAINEN
Tampere University – Finland
antti.rautiainen@tuni.fi

Pertti JÄRVENTAUSTA
Tampere University - Finland
pertti.jarventausta@tuni.fi

ABSTRACT

The paper discusses electric vehicle (EV) charging control in apartment buildings in cases of high EV penetration. The introduced control method for EV charging utilizes real-time measurements and memorized peak power consumptions to determine a suitable charging power. The aim of the control method is to avoid an unnecessary increase to the peak powers of the whole property, while still allowing EVs to be charged sufficiently. This kind of control method could lead to cost savings if the power-based distribution tariff of distribution system operators (DSO) included a price component based on monthly peak power. Some Finnish DSOs have launched this kind of power-based distribution tariff for small-scale customers also. Simulations indicate that PHEVs can likely be sufficiently charged without increasing the monthly peak powers or controlling other loads of the property when EV penetration is around 40% or less.

INTRODUCTION

The Finnish government has set a target for Finland to have 250,000 EVs by 2030 [1], which is equivalent to an EV penetration of around 10%. However, with the relative growth of EV penetration during the last five years according to [2], this target could be achieved by 2023.

It is well known that uncontrolled EV charging can cause problems for power distribution networks [3–5]. Smart EV charging can be optimized from different perspectives, such as minimizing peak loads or electrical energy costs. Depending on the control method, various issues might occur. According to [6], use of real-time energy market pricing for the benefit of EV charging would likely increase the peak loads for the distribution networks. As the pricing information would be available to all customers at once, they would all receive the incentive for turning on loads at the same time. In [5] and [7] the smart charging method to reduce peak loads is based on an assumption where the state of charge (SOC) and departure of every EV is known, which is not typically the case.

In recent years, there has been ongoing discussion in Europe on shifting DSOs' distribution tariffs in a power-based direction. This means that in addition to or instead of traditional basic (€/month) and volumetric charges (€/kWh), there would be a tariff component (€/kW) based on peak power of some time period, i.e., the latest year or month. Power-based distribution tariffs are enabled by a rollout of smart meters. In Finland, the electricity consumption of over 99% of network customers including households is measured by smart meters [8]. As some distribution system operators in Finland have already started using power-based distribution tariffs for small-scale customers, suboptimal control of EV charging could cause an unnecessary increase in operational costs. Therefore, it is reasonable to investigate options to charge EVs with a minimal increase in the peak powers.

EV charging peak load management in an apartment building could result in cost savings for each apartment owner if the energy community model is used; the apartments form an energy community, which makes one contract with the energy retailer and another with the DSO. Each apartment should have its own electricity meter so the customers can divide the cost of all electricity purchased by the whole building from the grid. The law requires that every customer should have the possibility to tender out energy retailers, so the energy community model is possible only if all the apartment owners accept the energy community model.

This paper investigates the EV charging control method introduced in [9], which aims to keep total peak loads at minimum while charging EVs alongside an apartment building. Different scenarios are examined to evaluate the effects of various parameters and the general accuracy of the results. The paper includes discussion and simulation results.

THE CONTROL METHOD

The monthly peak power will likely be a popular basis for the power-based fee charged by DSOs in the future. By using fuse or cable capacity as the only limiting factor for EV charging, the peak powers of the whole property might increase significantly and thus the operational costs of EV charging might also increase.

The introduced control method is based on memorizing the peak power consumption of the month, measuring the present power consumption of the building, and then calculating the available power capacity. EV charging power should then be adjusted according to the available capacity. The main principle of the system structure is illustrated in Fig. 1 and the operation of the control method is illustrated in Fig. 2. This kind of control method is possible in mode 3 EV charging according to the standard IEC 61851-1, where the charging station can restrict and adjust the maximum AC charging current (per phase) between 6 A and 80 A. In Fig 2., the feeder limit is there to ensure that the charging power would not exceed the

limits of the cable or fuse of the EV charging feeder.

To prevent the previous month from affecting the peak power of the new month, the highest memorized peak power should be reset at the beginning of each month. However, the resetting method has a clear impact on the energy that can be charged to EVs. By setting the starting value of the memorized peak power too low, there might not be enough free capacity to charge EVs. And by setting the starting value too high, the peak powers of the month might increase more than is necessary. In the subsection "Resetting methods of the memorized monthly peak power," four simple resetting methods are investigated.
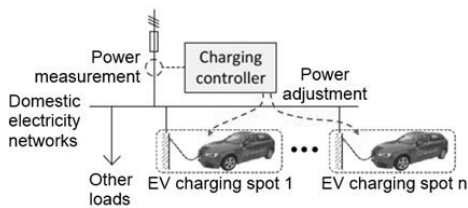
Figure 1. The basic setup of the control method.
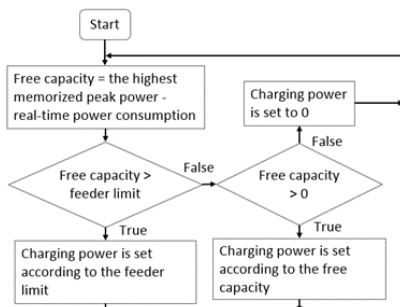
Figure 2. Simplified block diagram of the control method.

SIMULATION DATA AND MODELING

Case description

The investigated case is called "Tammela," which is an apartment building built in 1980 in Finland. Between 2013 and 2015, various renovations were made, which resulted in a 67% reduction in purchased energy. However, the share of electrical energy increased, resulting in electrical energy consumption increasing by around 30%. This was caused by the installation of exhaust air heat pumps, where produced heat energy replaces the purchase of energy from district heating.

Simulations were carried out based on long-term electricity consumption measurements made in the apartment building. This consumption data was measured from 2013–2016 at one-hour intervals. The apartment building has 53 parking spots. The property does not include any EV charging points at present in real practice, so all 53 charging points, one for each parking spot, are

modeled for simulations done in this study. Simulations focus on a charging power of 3.7 kW per charging point, which should be roughly suitable for almost every commercial EV.

EV load modeling

According to [2], the number of plug-in hybrid electric vehicles (PHEVs) is increasing much more rapidly than full electric vehicles (FEVs). With the average relative increase of PHEVs and FEVs during the last five years, there would be only around 4%–5% FEVs in Finland when the EV penetration reaches 100%. Therefore, simulations focus on PHEVs in this paper.

The average travel distance per passenger car was 14,000 km/a in Finland in 2017, according to Statistics Finland [10]. This equals around 38.4 km/day. To simplify the simulations, it is assumed that all PHEVs have the same maximum energy storage capacity of 8.0 kWh and energy consumption of 280 Wh/km. These are based on the most common PHEVs in Finland in [11] and data tables found in [12]. However, the real battery capacities and energy consumptions depend on the car and the operation conditions, so the simulations are repeated with slightly different parameters to improve the reliability of the results.

The case is an apartment building and, therefore, the EVs are assumed to depart in the morning and return later in the evening. Two different schedule types are investigated. The first assumes every EV departs at the same time and returns at the same time, e.g., depart at 0600 and return at 1900. This represents the worst-case scenario from the peak power point-of-view. The other schedule type includes random variations in the arrival and departure times. This random variation is normally distributed, where the median is 0 and the standard deviation is 2.0 hours. The same variation is added to both arrival and departure time so that the available charging time of each EV remains the same. The highest delay and advancement was 5 hours. Four other time variations were made based on this, but the variation is divided accordingly to get maximum delays or advancements of 1, 2, 3, or 4 hours. The effect of available charging time is investigated separately.

There are also three different driving schemes investigated in the simulations. The same driving scheme is assumed to occur daily through the whole year. The first driving scheme assumes every EV drives exactly 38.4 km/day. The second and the third driving schemes assume the average travel distance of EVs stays 38.4 km/day, but the travel distances varies between 0 km and 100 km with a standard deviation of 10 or 20 km, respectively. The needed charging energy of EVs can then be calculated using the energy consumption and the limitation set by the maximum usable battery capacity.

System modeling

Simulations use a time step of 15 minutes, which allows a whole year to be simulated within a reasonable amount of

time. In order to use the measured consumption data of the apartment building in the simulations, an interpolation was necessary to change the time step of 1 hour to 15 min. This was done by simply dividing each of the 1-hour energy consumptions evenly into four parts. Power loss in EV charging is assumed to be 10%, which is reasonable according to [13]. Acceptable charging speed for the EV is assumed to remain at the maximum during the whole charging time, which is relatively accurate for the slow charging of lithium-ion batteries [3].

In the simulations, for simplicity's sake the total available power capacity for EV charging is distributed for every EV that is connected to a charging point at the time. As there are often multiple EVs charging simultaneously and only a limited amount of available charging capacity, some of the EV charging currents fall below 6 A, which is not generally supported by the EVs. One solution to this would be to suspend some of the EV charging sessions so that there would be enough power for all active EV charging sessions. The suspended EV charging sessions could be rotated to achieve even distribution of charging energy. If the EVs would support all charging powers between e.g. 1.8 – 3.7 kW, roughly all available EV charging power capacity could be used as long as it is more than the said minimum charging power of 1.8 kW. The further investigation of this issue is, however, left out of this paper.

SIMULATION RESULTS

Resetting methods of the memorized monthly peak power

Four simple resetting methods are investigated, where the starting value of memorized peak power is

1. 0,
2. the apartment building power consumption of the final hour of the previous month,
3. a fraction of the previous month peak power of the apartment building, or
4. based on the previous month peak power and the relative monthly peak power difference of the previous years.

The resetting method could also use statistics from previous years more sophisticatedly to determine the new memorized peak power for each month. However, this was left out from this paper as there have been multiple renovations in this apartment building, which have affected the electrical energy consumption, as mentioned before.

According to the apartment building consumption data from 2013–2016, the highest decrease in monthly peak powers of two consecutive months was 27.4%. Therefore, the multiplier for the third resetting method was chosen to be 0.7. The fourth resetting method is similar to the third except that there is an individual multiplier for each month. Therefore, a maximum relative difference in monthly peak powers for each month was calculated. These were then

rounded down to one decimal place resulting in 0.8, 0.8, 0.7, 0.7, 0.7, 0.8, 0.9, 1.0, 1.1, 0.9, 1.1, and 0.8 for January to December, respectively. More accurate multipliers would likely give better results but also increase the risk of unnecessary increase in monthly peak powers. The ideal situation was also simulated, where the upcoming peak power of the apartment building of the new month is assumed to be perfectly forecasted and set as the starting value for the memorized peak power.

The impacts of these resetting methods were simulated in different EV penetrations using the 2016 consumption data of the apartment building. In these simulations the available charging time was 1900–0600 and the needed charging energy of each EV was 8.0 kWh. Results are shown in Fig. 4 and Table I. The uncharged energy shown in the following figures describes the proportion of the total charging energy need of the EVs that were not charged. The maximum EV penetration, where over 99% of the total energy need of all EVs were charged without increasing the peak powers of the apartment building, is referred to as "maximum EV penetration without peak power increase" for the rest of the paper.
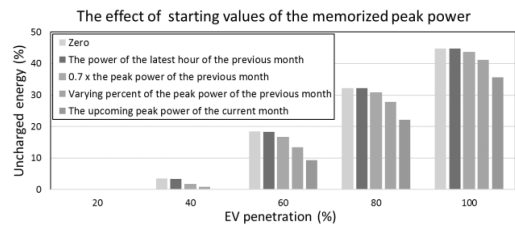
Figure 4. Simulation results with different starting values of the memorized peak power.

TABLE I
The maximum EV penetrations without peak power increase

Starting value for the memorized peak power	EV penetration
Zero	28.3%
The power of the latest hour of the previous month	28.3%
0.7 x the peak power of the previous month	35.8%
Varying percent of the peak power of the previous month	39.6%
Perfect forecast of the upcoming peak power of the current month	43.4%

Simulations indicate that excluding the perfect forecast, the fourth resetting method, where the starting value of memorized peak power is based on a fraction of the memorized peak power from previous years, clearly gives the best results. This resetting method was selected to be used in the simulations of the following subsections. The ideal situation, where the upcoming peak power of the month is perfectly forecasted, is notably better, but the selected resetting method reaches close to the same maximum EV penetration without peak power increase.

The effect of available EV charging time

To evaluate effects of the available charging time on charged energy, simulations were carried out using 14, 12.5, 11, 9.5, and 8 hours as the time that EVs can be charged per day. The daily charging energy need were 8.0 kWh for each EV. These results are shown in Fig. 5. The maximum EV penetrations without peak power increase were 47.2%, 43.4%, 39.6%, 35.8%, and 30.2% for the scenarios that had available EV charging time 14, 12.5, 11, 9.5, and 8 hours, respectively.

Simulations were also conducted on scenarios where the EV arrival and departure times included some variations, as mentioned in "EV load modeling." The available EV charging time for these scenarios was chosen to be 11 hours and the average arrival and departure time to be 1900 and 0600, respectively. These results have been illustrated in Fig. 6. The maximum EV penetrations without peak power increase were 39.6%, 43.4%, 45.3%, 49.1%, 50.9%, and 54.7% for the scenarios that had charging time variations of 0, 1, 2, 3, 4 and 5 hours, respectively. It can be seen that increased variation in EV charging schedule gives similar results to longer available charging time, which was expected.
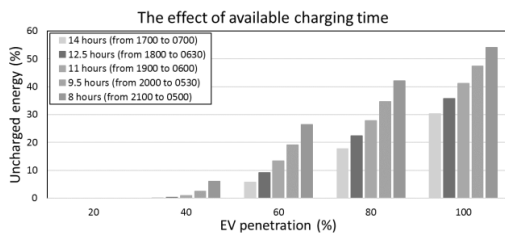
Figure 5. Simulation results with different charging times.
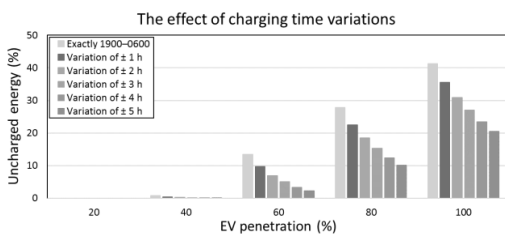
Figure 6. Simulation results with charging time variations.

The effect of the energy need of the EVs

To evaluate effects of the charging energy need of the EVs, simulations were carried out using the energy need based on the randomized daily travel distances of PHEVs mentioned in "EV load modeling" section and different fixed charging energy needs of PHEVs. The arrival and departure times were chosen to be 1900 and 0600, respectively. When the average daily travel distance is divided evenly for every PHEV, the usable battery capacity of PHEVs will be the limiting factor of the charging energy need. Therefore, longer driving distances will not increase the energy need of a PHEV, but a shorter driving distance may decrease the energy need of the PHEV. Therefore, more randomized travel distances results in lower total energy need of the PHEVs and thus more PHEVs can be charged without peak power increase. This can be seen from Fig. 7, where the scheme with more randomized travel distances will result in lower uncharged energies. The maximum EV penetrations without peak power increase were 39.6%, 41.5%, and 43.4% for the scenarios that had randomized driving distances with a standard deviation of 0, 10, and 20 km, respectively.

The effect of the actual charging energy need of PHEVs is illustrated in Fig. 8. The maximum EV penetrations without peak power increase were 39.6%, 32.1%, 26.4%, 22.6%, and 18.9% for the scenarios that had required EV charging energy 8.0, 10.0, 12.0, 14.0, and 16.0 kWh, respectively.
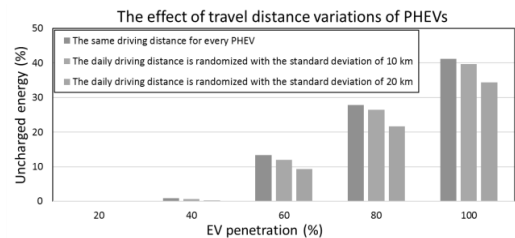
Figure 7. Simulation results with different daily driving distances of PHEVs.
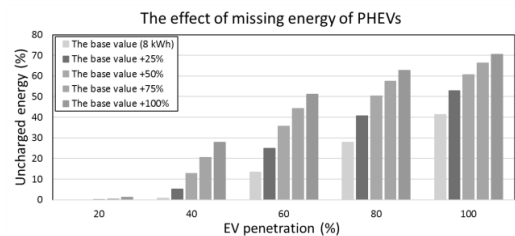
Figure 8. Simulation results with different charging energy needs of PHEVs.

EV charging using different consumption data of the apartment building

To investigate the reliability of the results, simulations were also carried out using the consumption data of the apartment building from 2013–2016. The simulation used the slightly randomized EV driving scheme mentioned earlier: average arrival time 1900, average departure time 0600, and ±2 as the maximum variation in arrival and departure times. The results have been illustrated in Fig. 9. The maximum EV penetrations without peak power

increase were 47.2%, 41.5%, 39.6%, and 35.8% for the years 2016, 2015, 2014, and 2013, respectively.

The annual growth in electricity consumption of the apartment building during 2013–2016 was around 10%. The average monthly peak power also increased each year about 6%. The increase in electricity consumption and the increase in monthly peak powers seems to correlate with the maximum EV penetration without peak power increase. The higher the electricity consumption and monthly peak powers an apartment building has, the more EVs can be charged, when the EV charging power is limited with this kind of control method.
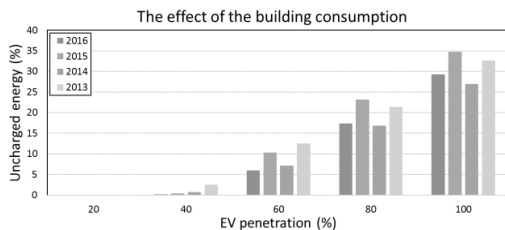
Figure 9. Simulation results using building consumption data from years 2013–2016.

CONCLUSION AND FUTURE WORK

According to the simulation results presented in this paper, EVs could be charged alongside an apartment building relatively well without notably increasing the peak powers, when using the introduced control method. The maximum EV penetration, where PHEVs can be charged at least 99% on average without peak power increase, would be up to around 30 – 50%. It can be seen that in case of 100% PHEV penetration, only around 25 – 35% of the energy need of PHEVs were left uncharged.

There are multiple assumptions and simplifications, which might affect the results one way or another. Also, the electricity consumption of apartment buildings, which is a key factor in this study, varies from case to case and year to year and thus has an impact on the results. The impacts of FEVs are also left out of this study. However, these simulations are somewhat pessimistic, because EV charging is assumed to occur only at the apartment building. The more EV charging occurs at the workplace and the more EVs are charged at fast charging stations, the less charging needs to be done at the residential area.

Future work could investigate smart options to increase peak power only when necessary to allow more EVs to be charged sufficiently. The EV charging outside of residential areas should also be assessed so that the required EV charging energy demand could be estimated more accurately. Future work should also confirm that the FEVs would have always enough energy to carry on after a night of charging when using this kind of control method. Modeling could also be improved in future studies by using, for example, the results of the national travel survey

data, where real departure and arrival times are recorded, or by taking into account that charging powers under 1.8 kW are not accepted.

REFERENCES

[1] Ministry of Economic Affairs and Employment, "Strategy outlines energy and climate actions to 2030 and beyond," 2016, Press release.

[2] Finnish Transport Safety Agency, (In Finnish) https://www.trafi.fi/tietopalvelut/tilastot/tieliikenne/ajoneuvokanta [Accessed 16.9.2018]

[3] K. Qian, C. Zhou, M. Allan and Y. Yuan, "Modeling of Load Demand Due to EV Battery Charging in Distribution Systems," in IEEE Transactions on Power Systems, vol. 26, no. 2, pp. 802-810, May 2011.

[4] G. Lacey, G. Petrus and E. Bentley, "Smart EV charging schedules: supporting the grid and protecting battery life," in IET Electrical Systems in Transportation, vol. 7, no. 1, pp. 84-91, 3 2017.

[5] U. Reiner, C. Elsinger and T. Leibfried, "Distributed self organising Electric Vehicle charge controller system: Peak power demand and grid load reduction with adaptive EV charging stations," 2012 IEEE International Electric Vehicle Conference, Greenville, SC, 2012, pp. 1-6.

[6] L. Kütt, E. Saarijärvi, M. Lehtonen, A. Rosin and H. Mõlder, "Load shifting in the existing distribution network and perspectives for EV charging-case study," IEEE PES Innovative Smart Grid Technologies, Europe, Istanbul, 2014, pp. 1-6.

[7] N. Leemput, F. Geth, J. Van Roy, A. Delnooz, J. Büscher and J. Driesen, "Impact of Electric Vehicle On-Board Single-Phase Charging Strategies on a Flemish Residential Grid," in IEEE Transactions on Smart Grid, vol. 5, no. 4, pp. 1815-1822, July 2014.

[8] Energy Authority, "National Report 2018 to the Agency for the Cooperation of Energy Regulators and to the European Commission," p. 47, 2018, National report.

[9] T. Simolin, A. Rautiainen, J. Koskela, P. Järventausta, "Control of EV charging and BESS to Reduce Peak Powers in Domestic Real Estate," Submitted for review in September 2018.

[10] Statistics Finland, "Henkilöautoilla ajettiin edellisvuosien lailla – maanteiden tavarankuljetukset tehostuivat," (In Finnish), Article.

[11] Finnish Transport Safety Agency, "Passenger cars in traffic by Area, Make and Driving power," Statistics database [Accessed 19.9.2018]

[12] Electric Vehicle Database, "Electric range of plug-in hybrids," Available: https://ev-database.uk/cheatsheet/electric-range-plugin-hybrid [Accessed 20.9.2018]

[13] lpiniki Apostolaki-Iosifidou, Paul Codani, Willett Kempton, "Measurement of power loss during electric vehicle charging and discharging," Energy, Volume 127, 2017, Pages 730-742.

PUBLICATION
3

Assessment of prediction uncertainties in EV charging management

T. Simolin, A. Rautiainen, P. Järventausta

Assessment of prediction uncertainties in EV charging management

T. Simolin[1], P. Järventausta[1], A. Rautiainen[2]

Abstract – *The share of electric vehicles (EVs) in the market has been growing rapidly during the past few years. A lot of research has been conducted to enable smart charging, which would fulfill EV user needs while considering technical limitations of the grid and incentives provided by the electricity market. However, the major part of the developed charging methods uses information of EV near-future driving profiles, e.g. departure time and energy need of the next trip, which can be problematic to achieve accurately enough. This kind of information will require either an extra communication link between the EV user and the EV charging controller, or EV tracking. Regardless of how the information is acquired, some uncertainty is likely in the predictions, which can cause undesired results. The aim of this paper is to assess these prediction error-related issues for distributing available charging capacity and to introduce alternative EV charging control methods that eliminate prediction error-related challenges. The results indicate that the EV battery state-based methods can distribute available charging capacity almost as effectively as the EV near future driving profile-based method with perfect predictions. Copyright © 2020 Praise Worthy Prize S.r.l. - All rights reserved.*

Keywords: *Control Algorithm, EV charging, Peak Power Limitation, Prediction uncertainty*

Nomenclature

DSO	Distribution system operator
EMS	Energy management system
EV	Electric vehicle
FEV	Full electric vehicle
HKDE	Hybrid kernel density estimator
PHEV	Plug-in hybrid electric vehicle
PV	Photovoltaic
SOC	State of charge
V2G	Vehicle-to-grid
E_{EV}	Energy stored in battery of the EV
$E_{EV,max}$	Maximum usable battery capacity
E_r	Predicted charging energy requirement for the next trip
N	Number of EVs currently charging
P_c	Charging power of an EV
P_{tc}	Total charging capacity available which can be used without increasing the monthly peak powers of the real estate
Δt_d	Predicted available charging time before departure

I. Introduction

Global warming is increasing pressure for green energy solutions. In the transportation sector, wide adoption of electric vehicles (EVs) is a key factor in reducing emissions. Finland has set a target of around 2 million EVs and 250,000 biogas vehicles by 2045 [1], which would form the basis for emission-free transportation. As the number of EVs in use increases, smart charging becomes increasingly more necessary to ensure maximum EV user satisfaction and optimize grid operation within technical limits.

I.1. Related Work and Motivation

Literature [2]–[26] describes multiple EV charging optimization methods investigated. In [2], an intelligent charging system is designed to efficiently manage charging process considering the interests of both customers and business. Additionally, battery charging characteristics are taken into account. In [3], an event driven model predictive control strategy, which provides cost-effective charging for EV users, is presented. In [4], EV charging is optimized considering uncertainty of electricity price. In [5], the developed control strategy minimizes electricity costs of photovoltaic (PV)-assisted charging station while guaranteeing completeness of EV charging demand. In [6], multi-agent trilayer EV charging framework is proposed. In the framework, each agent has its own objective function which it solves locally so that privacy is preserved. A centralized and a decentralized EV charging coordination are compared in [7]. The results demonstrate that the decentralized method achieves a satisfactory performance in improving the balance between the EV charging demand and locally generated wind power. In [8], approximate dynamic programming-based energy management system (EMS) is developed to determine optimal charging start time of each EV rather than controlling charging rates.

In [9], an algorithm to calculate optimal charging or discharging to reduce costs is proposed, and its effectiveness is demonstrated. Two algorithms that can fit multiple charging modes and diverse charging rate

T. Simolin[1], P. Järventausta[1], A. Rautiainen[2]

scenarios for distribution-side management is designed in [10]. Both algorithms are shown to be promising in terms of efficiency and accuracy. In [11], a single mixed integer linear programing formulation that considers local PV production, dynamic tariffs, and distribution network constraints for charging EVs is proposed. Simulations are used to demonstrate effectiveness of the EMS. An improved particle swarm optimization algorithm is proposed to control EV charging and discharging in [12]. Simulations were implemented to prove the effectiveness of the proposed algorithm. A pricing controlled EV charging and discharging strategy for households is proposed in [13]. The main advantage of the control strategy is that it can be utilized for different electricity markets to minimize electricity costs. In [14], a dynamic programming formulation is established by considering bidirectional energy flow, non-stationary energy demand, battery characteristics, and time-of-use electricity price. In [15], daily energy costs are minimized utilizing bidirectional EV charging and realistic EV battery model. Additionally, computational complexity is reduced by proving that a state-dependent four-threshold feedback policy is optimal for EV energy management. In [16], multiple heuristic algorithms are used to solve optimization problem, in which EV user profits are maximized while considering battery degradation. Numerical results are used to illustrate that genetic algorithm presents the most profitable charging scheduling for EV owners. In [17], a distributed EV charging coordination is proposed to allocate EV demand to valley period and minimize network load variance by utilizing vehicle-to-grid (V2G). In [18], a decentralized iterative algorithm is introduced to manage EV charging and discharging while considering EV charging demand. Additionally, a droop-based control algorithm is developed aiming to provide power regulation. An optimal EV charging scheduling with option of V2G and vehicle-to-vehicle energy transfer to increase customer satisfaction is proposed in [19]. The formulation is expanded so that additional battery storage is considered. In [20], a multi-objective EV charging and discharging method to minimize total operational costs and emissions is proposed. The Benders decomposition technique is used to solve the optimization model.

In [21], a closed-loop V2G control strategy which fulfills EV charging demand and offer frequency regulation is proposed. Simulations are conducted to ensure the expected operation. In [22], a control strategy for large-scale EVs, BESSs, and traditional FR resources is presented. Dynamic simulations of a power system are performed to verify its effectiveness. A coordinated sectional droop charging control strategy for frequency regulation is proposed in [23]. Simulations are used to verify the performance of the proposed strategy in a microgrid with high wind power penetration. A decentralized EV charging control for valley-filling is proposed in [24]. The control framework also considers grid constraints and allow flexible EV users to adjust the weighting factor between grid-level objective and their

individual objective. In [25], a concept of charging requirement index is proposed. The index is then used as a basis for an EV aggregation model to achieve valley-filling with low computational load. In [26], EV charging under limited power capacity is studied, and a new policy called least laxity ratio is introduced to balance EV charging capacity allocation.

In all these previously mentioned studies, the control method utilizes EV near future driving information to optimize the charging schedules. In most cases, this information includes the departure time and the energy need for the next trip. The major concerns with this information are acquisition and reliability. The EV driving profile-related data can be based on historical data or gained as an EV user input as mentioned, e.g., in [16]. Regardless of the acquisition method, the information will most likely contain some uncertainty. For example, future driving behavior does not always correspond to historical driving behavior or the user could estimate departure time incorrectly. Since there can be changes in driving/traveling plans or other unexpected occurrences, user input can also be seen as a prediction, which always contains uncertainty. This may have undesired effects if the uncertain information is used as a basis for charging optimization. Further analysis of the EV near future driving information acquisition methods in practice is left out of this paper.

It seems that relatively little effort has been made so far to assess the effects of the uncertainty of EV near future driving information. In [14], the EV driving profile is estimated by an exponentially weighted moving average algorithm in order to minimize energy costs while considering time-of-use pricing. The proposed scheme performs quite well compared to a scheme with prior knowledge of a person's EV driving profile. In [27], a trip prediction model is proposed to predict the next arrival location and the waiting time at the current location. The results indicate a mean prediction error of 4 hours in waiting time before the next trip, but the effect of the prediction error was not studied. In [28], hybrid kernel density estimator (HKDE) is proposed to address the uncertainties of EV user behavior by utilizing months of historical data. The HKDE prediction resulted in mean error deviation of 0.75 hours for stay durations and 1.68 kWh for energy consumption. The overall results based on the predicted behavior of EVs are close to the results utilizing real behavior of EVs, but the impacts for individual EVs were not mentioned.

To minimize the negative impacts of the EV charging demand uncertainty, there have been a few proposals. In [3], the uncertainties are taken into account by allowing the EV users to modify the original near future driving information and by establishing a minimum guaranteed charging profile. Similar minimum energy condition is used in [9]. The approach in [3] might be complex from the users' point-of-view. In [29] a stochastic dynamic programming method is developed, which gives a satisfactory dispatch even without perfect predictions of the hourly load demands. In [30], a reasonable level of EV user comfort is ensured by requiring a certain state of

T. Simolin[1], P. Järventausta[1], A. Rautiainen[2]

charge (SOC) within 3 hours of arrival time and a higher SOC at the expected departure time. However, these studies do not consider individual EVs.

The control strategies of the previously mentioned studies, which use the EV near future driving information in optimization, are minimizing electricity costs [2]–[16], enabling smart V2G operation [9]–[22], enhancing frequency stability [21]–[23], utilizing the valley-filling control method [17], [24], [25], or limiting peak loads [26]. Since electricity cost minimization can cause load peaks to the network as mentioned in [28] and [31], and the peak power-based grid tariff set by distribution system operators (DSO) is becoming more popular (e.g., in Finland), a peak power limitation control method is considered in this paper. Regardless of the control method, the EV near future driving information has been essential to ensure EV user comfort while pursuing the main objective.

As an alternative basis for the EV near future driving information, the control method could utilize information about the energy stored in the EV battery at the present moment. This information could be e.g. the actual energy (Wh) or the percentage SOC. This kind of information is less likely to include errors and can be more likely transmitted from an EV to a charging control system autonomously. Furthermore, this could simplify the control method and make it easier to adopt from the EV user point of view, as the logic of the control method can be understood more easily.

I.2. Contributions and Structure

The contribution of this paper is to assess the problems of using the EV near future driving information to distribute the available charging capacity among multiple EVs. In addition, alternative solutions are introduced and discussed. Simulations are conducted to enable comparison of these control methods.

The rest of the paper is organized as follows. Different control methods are presented in Section II. In Section III, the data used in the simulations and the simulation model are described. The simulation results are presented in Section IV. Practical implications of the results are discussed in Section V. In Section VI, the paper is finalized with conclusions and intended future work.

II. Control Methods

There has been growing interest in applying a power-based grid tariff charged by DSOs. There are variations in determining the peak power-based pricing component, but monthly peak power is emerging as the most popular basis for the fee in the present implementations. Therefore, peak power management can be an economically beneficial strategy for a customer. In this paper, the investigated control method is based on the one presented in [32], which acts similarly to the valley-filling control methods. In the control method presented in [32], the present power consumption of the real estate is measured, and the peak

power of the ongoing month is memorized. The available EV charging capacity, which will not increase the peak power of the real estate, can then be calculated. The operation of the control method is illustrated in Fig. 1. The feeder limit in Fig. 1 is there to ensure that the charging power would not exceed the limits of the cable or the fuse of the EV charging feeder.
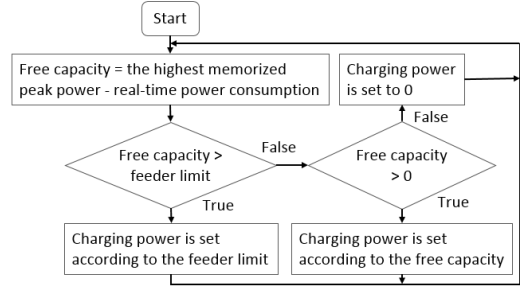
Fig. 1. Simplified block diagram of the control method

Only even distribution of the available charging capacity was considered in [32]. In addition to even distribution of the available charging capacity, five alternative methods are proposed in the following two subsections. The maximum available EV charging capacity remains the same, but the distribution method may affect the total energy that can be charged to EVs at home. This is due to the fact that available charging time of the EVs varies, and each EV has a limited battery capacity.

II.1. Utilizing EV Near Future Driving Information

The EV near future driving information-based (future prediction) charging method assumes departure time and energy requirement for the next trip to be known for each EV. The departure time can be used to calculate the available charging time. The aim of this charging method is to prioritize charging for those EVs that do not have enough energy for their next trip. After that, the available charging capacity is distributed evenly amongst all EVs since the trip after the next trip is unknown. Charging power P_c of an EV which requires energy for the next trip can be calculated as in (1),

$$P_c(n) = P_{tc} \times \frac{E_r(n)}{\Delta t_d(n)} / \sum_{k=1}^{N} \frac{E_r(k)}{\Delta t_d(k)}, \qquad (1)$$

where P_{tc} is the total charging capacity available that can be used without increasing the monthly peak powers of the real estate, E_r is the predicted energy charging requirement for the next trip, Δt_d is the predicted available charging time before the next departure, and N is the number of EVs currently charging. In addition to the selected distribution method, the charging is limited by the maximum charging power of the charging point.

T. Simolin[1], P. Järventausta[1], A. Rautiainen[2]

II.2. Utilizing EV Battery Information

One option for smart distribution of the available charging capacity would be using information about the energy stored in the batteries of the EVs. This information could be based on the actual energy (Wh), the percentual SOC (%), the actual missing energy (Wh), or the percentual missing SOC (%). The inverse of the actual energy stored in the battery of the EV (based on energy) could be used to distribute more energy for the EVs with less energy. In this case, the charging power for an EV can be calculated as in (2),

$$P_c(n) = P_{tc} \times \frac{1}{E_{EV}(n)} / \sum_{k=1}^{N} \frac{1}{E_{EV}(k)}, \qquad (2)$$

where E_{EV} is the actual energy (Wh) stored in the EV battery. Similarly, the inverse of the percentual SOC (based on SOC) could be used to distribute more charging energy for the EVs that have the least energy compared to their usable battery capacity. In this case, the charging power for an EV can be calculated as in (3),

$$P_c(n) = P_{tc} \times \frac{1}{SOC(n)} / \sum_{k=1}^{N} \frac{1}{SOC(k)}, \qquad (3)$$

where the SOC is percentual energy stored in the battery of the EV. When using distribution methods (2) or (3), charging of an almost empty EV would be highly prioritized at the beginning of its charging period. However, the prioritization falls relatively fast as the stored energy and SOC increases.

When using the actual missing energy of the EVs (based on missing energy) to distribute the available EV charging capacity, the charging power for an EV can be calculated as in (4),

$$P_c(n) = P_{tc} \times \frac{E_{EV,max}(n) - E_{EV}(n)}{\sum_{k=1}^{N}(E_{EV,max}(k) - E_{EV}(k))}, \qquad (4)$$

where the $E_{EV,max}$ is the maximum usable battery capacity. Similarly, when using the missing percentual SOC of the EVs (based on missing SOC) to distribute the available EV charging capacity, the charging power for an EV can be calculated as in (5),

$$P_c(n) = P_{tc} \times \frac{100\% - SOC(n)}{\sum_{k=1}^{N}(100\% - SOC(k))}, \qquad (5)$$

The distribution method based on the inverse of the percentual SOC (3) or the actual missing energy (4) can be favorable for the full electric vehicle (FEV) users compared to the plug-in hybrid electric vehicle (PHEV) users. This is because of the higher battery capacity of the FEVs, which will result in a higher inverse of the percentual SOC or a higher actual missing energy. Although these four battery energy state-based control methods do not guarantee the fulfilment of the needed charging requirements, the control methods can still be effective at distributing available charging capacity for EVs with low energy levels.

The utilization of information about the energy stored in the battery of the EV will require a communication link between the EV and the charging control system. However, if a suitable communication link exists, this kind of information could potentially be transmitted autonomously from the EV to the charging control system without risks of prediction errors.

III. Simulation Data and Modeling

III.1. Case Description

Simulations were carried out based on long-term electricity consumption measurements made in an apartment building called Tammela, which was built in 1980 in Finland. This consumption data was measured in 2016 at one-hour intervals. The monthly peak powers of the building are presented in Fig. 2. The property does not include any EV charging points at present in real practice, so all 53 simulated charging points, one for each parking spot, are modeled as including an EV for the simulations done in this study. The simulations focus on a charging power of 3.7 kW per charging point, which should be roughly suitable for almost every commercial EV. Since the available time for home charging is often quite long, the power limit of the charging points is not likely to be an issue.
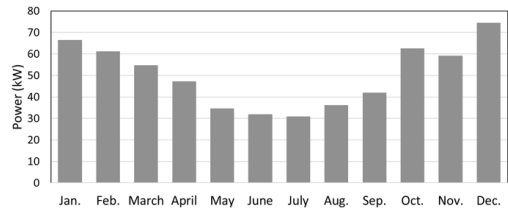
Fig. 2. Peak powers of the real estate

III.2. EV Properties and Driving Profiles

The average driving distance per passenger car for those who live in an apartment building was 13,650 km/year in Finland in 2016 [33]. The probability distribution for the yearly driving distances (real probability distribution) is presented in Fig. 3. The same probability is also applied to the driving distances of the 53 EVs considered in the simulations (used probability distribution). It is likely that FEVs with similar characteristics as used in the simulations of this paper would be driven roughly the same way as the present internal combustion engine cars. The data of [33] show that today >88% of the cumulative mileage consists of trips with length of < 300 km, which corresponds roughly with the average range of the FEVs simulated in our study. Yearly driving distances are divided into daily average distances and assigned to the 53 EVs in random order. These average daily travel distances are shown in Fig. 4.

T. Simolin[1], P. Järventausta[1], A. Rautiainen[2]
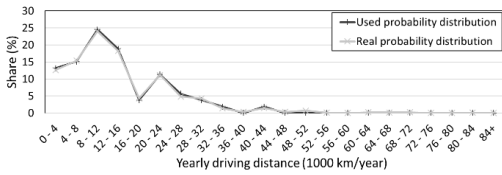
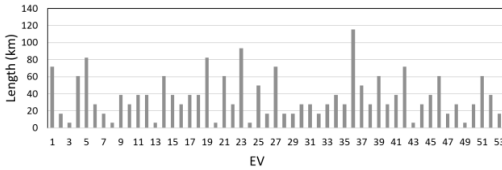Fig. 3. Passenger car driving distance probability

Fig. 4. Distribution of average daily travel distances

According to [34], the average daily travel distance per passenger car driver was around 110.7%, 103.0%, 107.6%, and 78.6% of the yearly average (23.4 km) in spring (March-May), summer (June-August), autumn (September-November), and winter (December-February), respectively. Also, the average daily travel distance per passenger car driver was around 101.7%, 107.3%, 85.9%, 106.0%, 122.6%, 78.6%, and 97.4% of the yearly average for Monday to Sunday, respectively [34]. Since there can be several drivers per vehicle throughout the day, the average travel distance of drivers and vehicles may differ. However, in this case, it is reasonable to assume a linear correlation between the travel distances of the vehicles and the drivers. The actual daily travel distances can then be calculated as a multiplication of the base daily travel distances shown in Fig. 4 and the factors based on the weekday and month.

The daily energy usage of each EV can be calculated as a multiplication of the daily travel distance and the energy consumption of the EV. The energy consumption is assumed to be a constant 180 Wh/km for each EV. This is close to the numbers used in, e.g., [7], [16]. The usable battery capacity of the FEVs is assumed to be normally distributed, where the average is 60 kWh and the standard deviation is 15 kWh. This is not the case in Finland currently, but since the battery capacity of FEVs may increase in the future, this assumption is reasonable when assessing future scenarios. The usable battery capacity of the PHEVs is assumed to be normally distributed, where the average is 9 kWh and the standard deviation is 1 kWh.

The simulation focuses on EV penetration of 100%, but the share of FEVs and PHEVs varies. The share of FEVs is either 0%, 33%, 66%, or 100%. Usable battery capacities in the case of 33% of EVs being FEVs are presented in Fig. 5. The order of the FEVs and PHEVs is randomly selected.

Since accurate information about passenger car departure and arrival times is not available and thus available home charging duration is not known, assumptions must be made. The departure and arrival times are assumed to be normally distributed. During weekdays, the average departure and arrival times are 07:00 and 19:00, respectively, and the standard deviations are 1 hour and 1.5 hours, respectively. For weekends, the average departure and arrival times are 11:00 and 18:00, respectively, with a standard deviation of 2.5 hours for both. The distribution of available home charging time for the weekdays and the weekends is presented in Fig. 6. These assumptions are somewhat in line with the trip timing distribution for the passenger car drivers mentioned in [34].
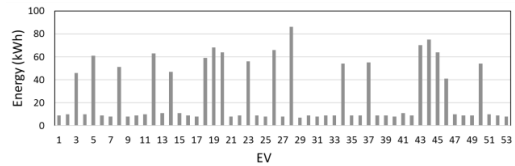
Fig. 5. Distribution of usable battery capacities in the case where 33% of EVs are FEVs and 67% are PHEVs
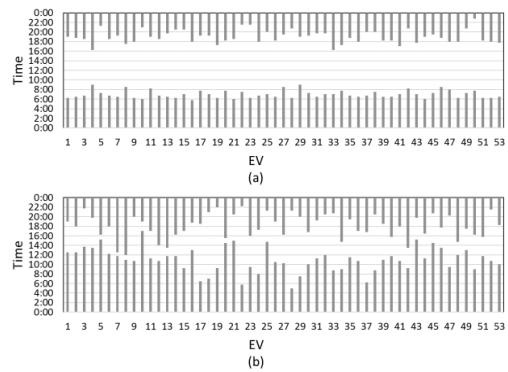
Fig. 6. Distribution of available home charging time during (a) weekdays and (b) weekends

III.3. System Modeling

Simulations use a time step of 15 minutes, which allows a whole year to be simulated within a reasonable amount of time. In order to use the measured consumption data of the apartment building in the simulations, an interpolation was necessary to change the time step of 1 hour to 15 min. This was done by simply dividing each of the 1-hour energy consumptions evenly into four parts. Power loss in the EV charging is assumed to be 10%, which is close to the efficiencies used in, e.g. [13], [14], [20], and [35]. Acceptable charging speed for the EV is assumed to remain at the maximum during the whole charging time. In the simulations, for simplicity's sake the EVs are assumed to support all charging powers between 0 and 3.7 kW.

The investigated EV charging control methods are only applied to home charging conducted while the EVs are parked at the apartment building. However, for some of the EV users, an optional slow charging at work is also considered. This charging is assumed to be a constant 1.84

T. Simolin[1], P. Järventausta[1], A. Rautiainen[2]

	EV11	EV14	EV30	EV42	EV45
Type	PHEV	FEV	PHEV	PHEV	FEV
Avg. travel distance (km/d)	38.7	60.6	27.8	71.5	38.7
Usable battery capacity (kWh)	10.0	47.0	9.0	9.0	64.0
All electric range (km)	55.6	261.1	50.0	50.0	355.6
Departure (weekdays)	8:15	6:15	7:15	8:15	7:15
Arrival (weekdays)	19:00	20:30	19:15	20:45	19:30
Departure (weekends)	11:15	11:45	10:00	9:15	14:30
Arrival (weekends)	17:00	16:15	16:45	13:30	20:45

kW (8 A, 230 V) and last for 8 hours, resulting in maximum energy drawn from the grid of 14.72 kWh. When taking the charging efficiency of 0.9 into account, the charged energy at work will be up to 13.2 kWh per day. The work charging is assumed to be possible only during weekdays. To properly calculate the need for extra charging or the use of gasoline, it is necessary to know the travel distance from home to work and vice versa. According to [34], work-related travel covers around 31.6% of the total average daily travel distances of passenger car drivers. If the EV users worked 5 days a week, the share of work-related travel would be around 44.27% during the workdays. By assuming that half of work-related travel occurs before work charging, 22.1% of the daily travel distance is covered in the morning from home to workplace and 77.9% is covered later in the evening from workplace to home during workdays. The home charging is assumed to start after the additional stops, e.g., shopping or other activities, and therefore the traveled distance between work charging and home charging is much longer.

IV. Simulation Results

The simulation results focus on the extra energy requirement, which indicates the amount of electrical energy that the EVs need, in addition to the home charging and the work charging, in order to travel the designated trips using only electrical energy. The required extra energy can be obtained by, e.g., using a fast charging station. Additionally, PHEVs may use gasoline to finish off a trip when the electricity runs out. PHEVs especially may require extra energy regardless of how much charging is done at home or at work if the trips are longer than their all-electric range.

The simulation results are compared in three scenarios, where in addition to the home charging, a slow charging at work is also possible for 0%, 40% (EVs 1–21), or 80% (EVs 1–42) of the EVs, respectively. Since car preheaters are widely used in workplaces in Finland, a high penetration of workplace EV charging is possible. The following subsections IV.1–IV.3 consider a FEV penetration of 33%. The impacts of different shares of FEVs and PHEVs are investigated in subsection IV.4.

To investigate the effects of prediction errors for individual EVs, five random EVs of the 53 are selected for closer look. These EVs are referred to as EV11, EV14, EV30, EV42, and EV45, which are based on their order number. The prediction errors examined in subsections

IV.2 and IV.3 are investigated by applying the prediction error either for all EVs or these five specific EVs. EV14 and EV45 are FEVs whereas EV11, EV30, and EV42 are PHEVs. The main characteristics of these five EV are presented in Table 1.

The results in the next subsections are based on the parameters presented in section III. The simulations were repeated twice using different randomly generated sets of EV-related parameters—i.e., travel distances, usable battery capacities, and available charging times. The results were very similar, but their detailed presentation is left out of this paper. The following conclusions were applicable for each simulation case.

IV.1. Comparison of Different Control Methods

As shown in Fig. 7(a), a major part, around 81–84%, of the total charging energy required by the EVs during the whole year can be charged at home in scenario 1 when taking the restrictions of the peak power management into account. When the available home charging capacity is distributed evenly, the share of the required extra energy is 18.9%. For all other algorithms the share of required extra energy is slightly lower, around 16.8–18.1%.
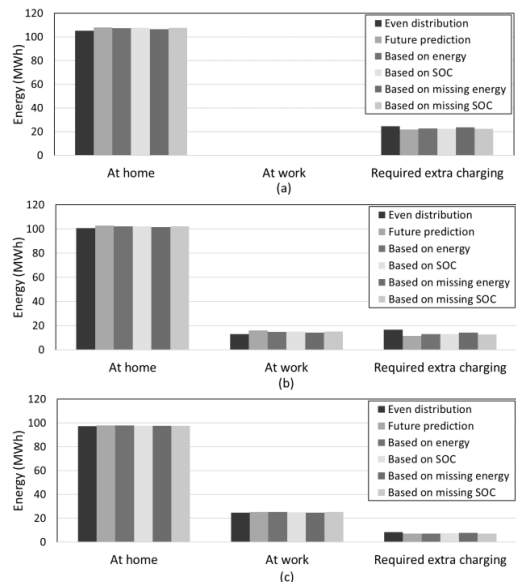
Fig. 7. Energy sources for EV charging in (a) scenario 1, (b) scenario 2, and (c) scenario 3

T. Simolin[1], P. Järventausta[1], A. Rautiainen[2]

If 40% or 80% of the EVs have an opportunity for 8 hours of slow charging during the workdays, as in scenario 2 or in scenario 3, respectively, the required extra charging for all EVs drops significantly compared to scenario 1. This can be seen from Fig. 7. The extra energy requirements of the EVs are between 1.12–1.28, 0.58–0.86, or 0.35–0.43 kWh per day on average for scenarios 1, 2 and 3 respectively. This is illustrated Fig. 8. In all three scenarios, the even distribution method seems to give the worst results whereas the future prediction gives the best results. The most notable difference can be seen in scenario 2, which was expected, as the uneven opportunity for work charging is causing more uneven charging demands at home. However, it should be noted that for the future prediction method, a precise prediction is assumed which is not likely to be the case most of the time.
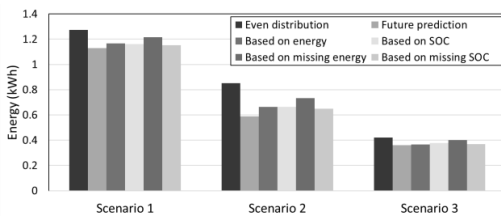
Fig. 8. Average daily extra energy requirement for scenarios 1–3

As mentioned earlier, distributing the available charging capacity based on the inverse of the percentual SOC or the actual missing energy (kWh) of the EV battery will be favorable for the FEVs (EV14 and EV45). Distributing the available charging capacity based on the inverse of the actual energy (kWh) or the missing SOC of the EV battery is fairer for the PHEVs (EV11, EV30, and EV42). This can be seen from Fig. 9 where the extra energy requirement is presented for the specific EVs in scenarios 1 and 2.
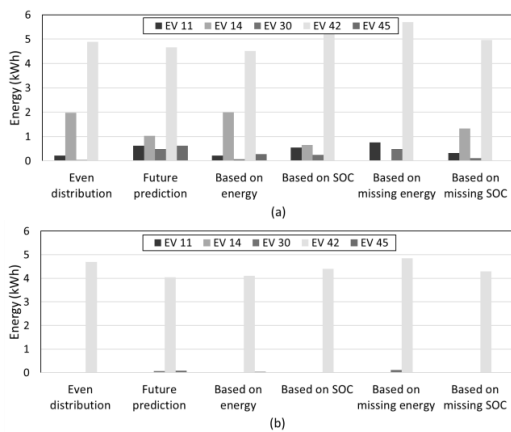
Fig. 9. The average daily extra energy requirement of the specific EVs in (a) scenario 1 and (b) scenario 2

The EV42 has notably higher daily trip distances than its all-electric range and thus some extra energy is required in order to complete the daily trips. The other specific EVs have nearly zero extra energy need in scenario 2 as seen in Fig. 9(b). When investigating the five specified EVs, scenario 3 is similar to scenario 2 but the EV42 requires less extra energy whereas the other specified EVs do not require any extra energy.

IV.2. Effects of Energy Requirement Prediction Error

To evaluate the prediction error effects of the future energy demand, different cases are considered. Prediction error range within ±30% of the energy consumption of the next trip is examined, which equals an average error of ±11.2 km or ±2.0 kWh. This is close to the mean prediction error deviation mentioned in [28]. The same prediction error is applied either to the five specified EVs, which represent roughly 10% of the EVs, or for all EVs. Depending on the EV near future driving information acquisition method, these kinds of cases could occur. For example, if the near future driving information is based on historical data, random prediction errors may be likely. On the other hand, if the information is based on user input, all EV users might be tempted to exaggerate the charging demand to ensure sufficient energy for the next trip.

Results of the cases where the same prediction error is applied to the five specified EVs or to all EVs are presented in Fig. 10. The prediction error does not seem to have a notable effect when considering average extra energy requirement for all EVs. This is most likely because the available charging capacity remains the same, but the intended distribution method is compromised as a result of the prediction error. Therefore, almost the same amount of energy can be charged to all EVs in total and thus the average extra energy requirement of all EVs might not be notably affected.
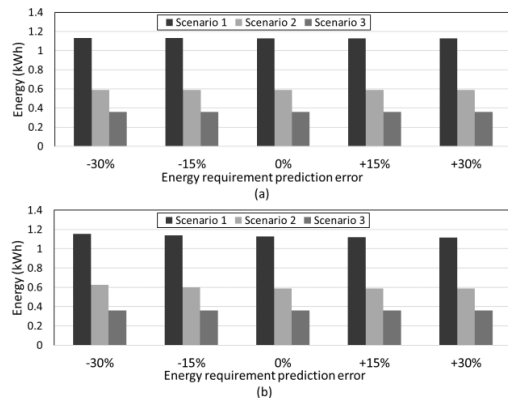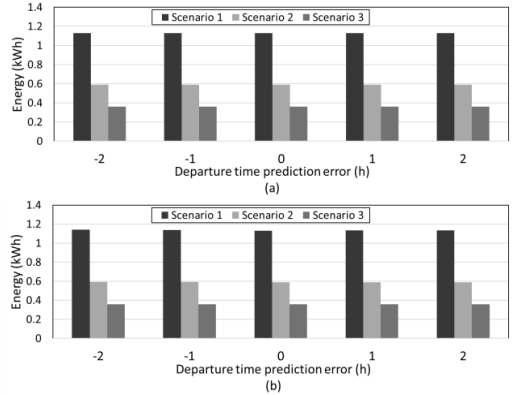

Fig. 10. The average daily extra energy requirement of all EVs when the energy demand is predicted similarly wrong (a) for the five specific EVs and (b) for all EVs
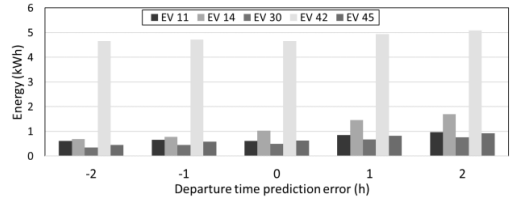
Even though the average extra energy requirement of all EVs remains the same, the prediction error may have

T. Simolin[1], P. Järventausta[1], A. Rautiainen[2]

notable impact on the individual EVs. In order to determine the effects of the prediction errors on the specific EVs, their extra energy requirements must be investigated separately. The prediction error impacts for the five specific EVs with the prediction error have been illustrated in Fig. 11 for scenario 1. There seems to be clear correlation with the prediction error and the extra energy need of the EVs. The lower the predicted consumption is compared to the real future consumption, the higher the extra energy requirement will be.

In Fig. 11, the energy consumption prediction error of -30% for the specific five EVs equals to an average error of 0.24 kWh when considering all EVs. However, the extra energy requirements of the EV11, EV14, EV30, and EV45 are almost double when compared to the case with prediction error of 0%. Due to the prediction error, the all-electric range would be reduced by up to 2.8, 5.9, 2.3, 0.2, and 2.2 km on average for the EV11, EV14, EV30, EV42, and EV45, respectively. Even though the prediction error will most likely vary from day to day and not remain the same as in these simulations, the effects of these prediction errors may seem displeasing from the EV user point of view.
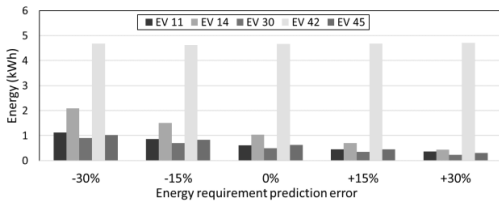
Fig. 11. The average daily extra energy requirement for the five specific EVs with energy demand prediction error in scenario 1

IV.3. Effect of Departure Time Prediction Error

Prediction error of the EVs' departure times has an effect similar to the prediction error of energy demand. With a prediction error of ±2 hours, the average extra energy requirement of all EVs remained almost the same. This is illustrated in Fig. 12 where the error is applied to the five specific EVs or to all EVs. When examining the effects for the specific EVs with the prediction error, more notable impacts can be seen. Predicting a later departure time than the real departure time seems to increase the extra energy requirement of the EV. This is illustrated in Fig. 13. Predicting a two hours later departure would mean around 2.0, 3.7, 1.5, 2.4, and 1.7 km reduced all-electric range on average for the EV11, EV14, EV30, EV42, and EV45, respectively.

Fig. 12. The average daily extra energy requirement of all EVs when the departure time is predicted similarly wrong (a) for the five specific EVs and (b) for all EVs

Fig. 13. The average daily extra energy requirement for the specific EVs with departure time prediction error in scenario 1

IV.4. Effects of Different FEV and PHEV Penetrations

Since some PHEVs have longer daily trips than their all-electric range, a higher FEV penetration may reduce the average extra energy need of EVs. On the other hand, FEVs cannot utilize traditional fuels, such as gasoline, to continue a trip after running out of electricity, and thus it is more important for FEVs to have enough electrical energy available. Simulation results for the cases with different shares of PHEVs and FEVs are shown in Fig. 14.
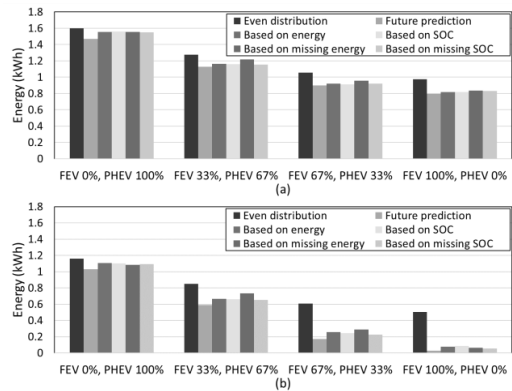
Fig. 14. The average daily extra energy requirement in different FEV and PHEV penetrations in (a) scenario 1 and (b) scenario 2

T. Simolin[1], P. Järventausta[1], A. Rautiainen[2]

V. Discussion

As seen from the results, the EV near future driving profile-based charging method can be used to effectively distribute available charging capacity for the EVs. When considering the total charging capacity distributed to all EVs, the prediction uncertainties do not seem to have notable impact. However, the prediction uncertainties can have more notable effects for individual EVs. As seen from the results in the previous section, moderate prediction errors in the departure time and the energy requirement cause some inconvenience to the EV users.

The most common methods to acquire EV near future driving profiles are EV user input and tracking of the EVs. From the EV user point of view, both methods can be problematic. Requiring users to input departure times or energy requirements could be burdensome and cause, e.g., response fatigue, which has been one of the most common barriers in demand response programs [36]. And as mentioned earlier, the users might, for example, exaggerate the charging requirements, which could diminish the efficiency of the control method. Additionally, it is worth mentioning that using EV user inputs in the charging controller requires an extra communication link between the EV user and the charging controller. Tracking of the EVs can be relatively accurate if there is enough data available. However, comprehensive data may not be easily accessible. Also, historical data-based prediction needs updating each time a resident or the behavior of a resident changes (change of workplace, etc.), which could happen quite often in an apartment building, as an example.

When considering the above, it might be reasonable to find other solutions to distribute available EV charging energy than EV near future driving profile-based methods. Depending on the investigated scenario, the efficiency of the presented EV battery-based control methods varied. However, their overall efficiency was relatively good compared to the EV near future driving profile-based method.

In the examined case, the monthly peak powers are limited to lower the peak power-based costs for the EV users. Depending on the availability of workplace charging, there may be a need to allow higher peak loads at the apartment building. Since higher peak loads are likely to cause higher costs as peak power-based demand charges are becoming more popular, the peak loads should be increased only the minimum amount which satisfies the EV users. Therefore, smart distribution of the available charging capacity will most likely still be necessary. Energy demand-based predictions could potentially still be suitable for predicting the required total EV charging energy, which could be used to determine, for example, the minimum necessary peak load that allows EVs to be charged sufficiently. This kind of prediction would again be prone to uncertainties, but the potential prediction error impacts could be distributed more evenly among all EVs, if, for instance, battery state-based charging distribution is used.

VI. Conclusions and Future Work

In this paper, relatively simple control methods, which utilize either EV near future driving information or information on the stored energy of the EV battery to distribute the available charging capacity between multiple EVs, are presented and discussed. The EV near future driving profile-based control method can be effective at distributing the available EV charging capacity. It is also not too sensitive to prediction errors when considering all EVs together. However, prediction errors can have more notable and unevenly distributed impacts for individual EVs. More complex prediction-based charging control methods might have even greater negative impact to the EVs with unexpected behaviors. Adopting such an EV charging control method which utilized future predictions might cause concerns amongst the EV users.

Alternatively, the available home charging capacity could be distributed based on the actual energy or the percentual SOC of the EV battery. This kind of control method can be almost as effective as the future charging demand-based control method with perfect predictions and notably more efficient compared to the charging method with even distribution when the EVs have uneven charging demands. Utilization of battery state-based information requires a simple communication link between EV and the charging control system. However, with the communication link, the information could be transmitted automatically. Since the information is about the present state, prediction errors, etc. do not influence the control method negatively. This kind of control method may seem a more attractive option from the EV user point of view.

Future work will investigate EV battery energy-based charging algorithms in different cases and scenarios. Also, options to utilize V2G without the EV near future driving information should be explored.

References

[1] Ministry of Transport and Communications, "Operational Program for Emission-free Transport 2045," 2018, p. 136, (In Finnish), http://urn.fi/URN:ISBN:978-952-243-559-0, accessed 29 October 2019.

[2] Z. Wei, Y. Li, Y. Zhang and L. Cai, Intelligent Parking Garage EV Charging Scheduling Considering Battery Charging Characteristic, *IEEE Transactions on Industrial Electronics*, vol. 65 n. 3, March 2018, pp. 2806–2816.

[3] A. Di Giorgio, F. Liberati, S. Canale, Electric vehicles charging control in a smart grid: A model predictive control approach, *Control Engineering Practice*, vol. 22 n. 1, January 2014, pp. 147–162.

[4] N. Korolko Z. Sahinoglu, Robust Optimization of EV Charging Schedules in Unregulated Electricity Markets, *IEEE Transactions on Smart Grid*, vol. 8 n. 1, January 2017, pp. 149–157.

[5] Q. Chen et al., Dynamic Price Vector Formation Model-Based Automatic Demand Response Strategy for PV-Assisted EV Charging Stations, *IEEE Transactions on Smart Grid*, vol. 8 n. 6, November 2017, pp. 2903–2915.

[6] B. Khaki, C. Chu, R. Gadh, Hierarchical distributed framework for EV charging scheduling using exchange problem, *Applied Energy*, vol. 241, May 2019, pp. 461–471.

[7] Y. Yang, Q. Jia, X. Guan, X. Zhang, Z. Qiu, G. Deconinck,

Decentralized EV-Based Charging Optimization With Building Integrated Wind Energy, *IEEE Transactions on Automation Science and Engineering*, vol. 16 n. 3, July 2019, pp. 1002–1017.

[8] Y. Wu, A. Ravey, D. Chrenko, A. Miraoui, Demand side energy management of EV charging stations by approximate dynamic programming, *Energy Conversion and Management*, vol. 196, September 2019, pp. 878–890.

[9] R. Rana, S. Prakash, S. Mishra, Energy Management of Electric Vehicle Integrated Home in a Time-of-Day Regime, *IEEE Transactions on Transportation Electrification*, vol. 4 n. 3, September 2018, pp. 804–816.

[10] T. Mao, X. Zhang, B. Zhou, Intelligent Energy Management Algorithms for EV-charging Scheduling with Consideration of Multiple EV Charging Modes, *Energies*, vol. 12 n. 2, February 2019, pp. 1–17.

[11] G. R. Chandra Mouli, M. Kefayati, R. Baldick, P. Bauer, Integrated PV Charging of EV Fleet Based on Energy Prices, V2G, and Offer of Reserves, *IEEE Transactions on Smart Grid*, vol. 10 n. 2, March 2019, pp. 1313–1325.

[12] Y., Zhou, G., Xu, M., Chang, Demand side management for EV charging/discharging behaviours with particle swarm optimization, Proceeding of the 11th World Congress on Intelligent Control and Automation, Shenyang, June 2014, pp. 3660–3664.

[13] U. Datta, N. Saiprasad, A. Kalam, J. Shi, A. Zayegh, A price-regulated electric vehicle charge-discharge strategy for G2V, V2H, and V2G, International Journal of Energy Research, vol. 43 n. 2, February 2019, pp. 1032–1042.

[14] H. Liang, B.J. Choi, W. Zhuang, X. Shen, Towards optimal energy store-carry-and-deliver for PHEVs via V2G system, Proceedings IEEE INFOCOM, Orlando, FL, March 2012, pp. 1674–1682.

[15] Wang, X., Liang, Q., Energy Management Strategy for Plug-In Hybrid Electric Vehicles via Bidirectional Vehicle-to-Grid, *IEEE Systems Journal*, vol. 11 n. 3, September 2017, pp. 1789–1798.

[16] A. Dogan, M. Alci, Heuristic Optimization of EV Charging Schedule Considering Battery Degradation Cost, *Electronics & Electrical Engineering*, vol. 24 n. 6, 2018, pp. 15–20.

[17] E. L. Karfopoulos, N. D. Hatziargyriou, Distributed Coordination of Electric Vehicles Providing V2G Services, *IEEE Transactions on Power Systems*, vol. 31 n. 1, January 2016, pp. 329–338.

[18] E.L. Karfopoulos, K.A. Panourgias, N.D. Hatziargyriou, Distributed Coordination of Electric Vehicles providing V2G Regulation Services, *IEEE Transactions on Power Systems*, vol. 31 n. 4, July 2016, pp. 2834–2846.

[19] A. Koufakis, E.S. Rigas, N. Bassiliades, S. D. Ramchurn, Towards an EV charging scheduling scheme with V2G and V2V energy transfer, IEEE International Conference on Smart Grid Communications (SmartGridComm), Sydney, NSW, November 2016, pp. 302–307.

[20] A. Zakariazadeh, S. Jadid, P. Siano, Multi-objective scheduling of electric vehicles in smart distribution system, *Energy Conversion and Management*, vol. 79, March 2014, pp. 43–53.

[21] H. Liu, J. Qi, J. Wang, P. Li, C. Li, H. Wei, EV Dispatch Control for Supplementary Frequency Regulation Considering the Expectation of EV Owners, *IEEE Transactions on Smart Grid*, vol. 9 n. 4, July 2018, pp. 3763-3772.

[22] J. Zhong, L. He, C. Li, Y. Cao, J. Wang, B. Fang, L. Zeng, G. Xiao, Coordinated control for large-scale EV charging facilities and energy storage devices participating in frequency regulation, *Applied Energy*, vol. 123, June 2014, pp. 253–262.

[23] X. Zhu, M. Xia, H-D. Chiang, Coordinated sectional droop charging control for EV aggregator enhancing frequency stability of microgrid with high penetration of renewable energy sources, *Applied Energy*, vol. 210, January 2018, pp. 936–943.

[24] M. Liu, P.K. Phanivong, D.S. Callaway, Customer-and Network-Aware Decentralized EV Charging Control, Power Systems Computation Conference (PSCC), Dublin, June 2018, pp. 1–7.

[25] M. Liu, Y. Shi, H. Gao, Aggregation and Charging Control of PHEVs in Smart Grid: A Cyber–Physical Perspective, *Proceedings of the IEEE*, vol. 104 n. 5, May 2016, 104, (5), pp. 1071–1085.

[26] M. Zeballos, A. Ferragut, F. Paganini, "Proportional Fairness for EV Charging in Overload," *IEEE Transactions on Smart Grid*, vol. 10 n. 6, November 2019, pp. 6792–6801.

[27] O. Sundström, O. Corradi, C. Binding, Toward electric vehicle trip prediction for a charging service provider, IEEE International

Electric Vehicle Conference, Greenville, SC, March 2012, pp. 1–6.

[28] Y. Chung, B. Khaki, C. Chu, R. Gadh, Electric Vehicle User Behavior Prediction Using Hybrid Kernel Density Estimator, IEEE International Conference on Probabilistic Methods Applied to Power Systems (PMAPS), Boise, ID, June 2018, pp. 1–6.

[29] Y. Liao, C. Lu, Dispatch of EV Charging Station Energy Resources for Sustainable Mobility, *IEEE Transactions on Transportation Electrification*, vol. 1 n. 1, June 2015, pp. 86–93.

[30] D. Wu, H. Zeng, C. Lu, B. Boulet, Two-Stage Energy Management for Office Buildings With Workplace EV Charging and Renewable Energy, *IEEE Transactions on Transportation Electrification*, vol. 3 n. 1, March 2017, pp. 225–237.

[31] L. Kütt, E. Saarijärvi, M. Lehtonen, A. Rosin, H. Mõlder, Load shifting in the existing distribution network and perspectives for EV charging-case study, IEEE PES Innovative Smart Grid Technologies, Europe, Istanbul, October 2014, pp. 1–6.

[32] T. Simolin, A. Rautiainen, P. Järventausta, Control of EV Charging to Reduce Peak Powers in Domestic Real Estate, 25th International Conference on Electricity Distribution (CIRED), Madrid, June 2019, pp. 1–5.

[33] Finnish Transport and Communications Agency Traficom, National passenger traffic survey 2016.

[34] Finnish Transport Agency, National Travel Survey 2016, (In Finnish),   https://julkaisut.vayla.fi/pdf8/lti_2018-01_henkiloliikennetutkimus_2016_web.pdf, accessed 29 October 2019

[35] T. Simolin, A. Rautiainen, J. Koskela, P. Järventausta, Control of EV Charging and BESS to Reduce Peak Powers in Domestic Real Estate, *International Review of Electrical Engineering (I.R.E.E),* vol. 14 n. 1, January 2019, pp. 1–7.

[36] J.-H. Kim, A. Shcherbakova, Common failures of demand response, *Energy*, vol. 36 n. 2, February 2011, pp. 873–880.

Authors' information

[1]Tampere University, Finland.
[2]Pohjois-Karjalan Sähkö Oy (North Karelian Electricity Ltd), Finland.

Toni Simolin received his M.Sc. in electrical engineering from the Tampere University of Technology in 2018. At present, he works as a doctoral researcher in the Unit of Electrical Energy Engineering at the Tampere University. His research focuses on electric vehicle charging and its impacts on technical and economic points of view.

Prof. **Pertti Järventausta** received his M.Sc. and Licentiate of Technology degrees in electrical engineering from the Tampere University of Technology in 1990 and 1992, respectively. He received his Dr.Tech. in electrical engineering from the Lappeenranta University of Technology in 1995. At present, he is a professor at the Tampere University and leads the Unit of Electrical Energy Engineering. His main interest focuses on the issues of Smart Grids from the grid and electricity market points of view.

Antti Rautiainen received his M.Sc. and Dr.Tech. degrees in electrical engineering from the Tampere University of Technology in 2008 and 2015, respectively. At present, he works as a project manager in Pohjois-Karjalan Sähkö Oy (North Karelian Electricity Ltd). His research interests are electricity grids and electricity market.

PUBLICATION
4

Load control of residential real estate to improve circumstances for EV charging

T. Simolin, A. Rautiainen, P. Järventausta, P. Santikko, H. Järvensivu

Load Control of Residential Real Estate to Improve Circumstances for EV Charging

Toni Simolin, Pertti Järventausta, Antti Rautiainen
Tampere University
Finland

Pasi Santikko, Hannu Järvensivu
Sandy Beach Oy
Finland

Abstract—**It is well known that uncontrolled EV charging may cause high peak loads and overloading. However, limiting the EV charging power may also reduce the total energy, which can be charged into the EV in a certain time period. This might raise concerns especially among full electric vehicle users as they cannot use traditional fuels e.g. gasoline to continue the trip after electricity runs out. In this paper, a control system which controls residential heating loads to enable higher EV charging powers without sacrificing comfort of living is introduced and discussed. Results of a real pilot system and two different simulations are presented. The results indicate that compared to the case with only EV charging current adjustment, up to around 30% more energy can be charged into the EV over a night by utilizing the presented control system.**

Index Terms—**EV charging, Load control, Peak load limitation, Residential real estate**

I. INTRODUCTION

There have been growing interest in electric vehicles (EVs). Although the amount of EVs in Finland is still low, the amount has almost doubled each year during the past few years [1]. Typical residential real estate e.g. detached house may not be suitable for a new high-power load like uncontrolled EV charging. To reduce the risk of overloading, there are at least a few simple options e.g. utilization of slow one-phase charging or charging current adjustment of mode 3 charging. Mode 3 charging can be adjusted according to the main fuse and the real time current consumption of the real estate, which eliminates the risk of EV charging related overloading completely.

As full-electric vehicles (FEVs) cannot utilize alternative fuels to continue the trip after electricity runs out, it becomes more important to charge energy into the FEVs as much as possible. By limiting charging current too much, the FEV users may need to use public charging stations more often than necessary. This can be a concerning factor and reduce the adoption rate of the emission free vehicles.

In Finland, heating is likely to be one of the largest energy consumers of a real estate. Since delaying heating load e.g. for an hour may not have a notable impact on the comfort of living, electric heating can be utilized as a controllable load quite well. For the same reason, hot water heater can be used

as a controllable load similarly. If these kinds of loads can be controlled optimally, the EV charging circumstances could be improved.

In the literature, there have been multiple studies related to EV charging in a residential real estate e.g. [2]–[6]. However, these studies focus mostly on energy cost minimization. In [7], domestic load management including EV charging control to limit peak loads have been discussed. To the best of the authors' knowledge, load control of a residential real estate to improve EV charging circumstances have not been studied properly. In this paper, the potential of a residential real estate heating load control to enable higher EV charging currents is investigated. A control system is developed and tested in a pilot case. Additionally, a simulation model of the control system is formulated. The performance of the control system is analyzed by examining the results of the pilot case and the simulation model.

The rest of the paper is organized as follows. Control method is introduced in section II. Pilot case and simulation model are described in section III. The simulation results and the pilot measurements are compared in section IV. In section, V the paper is finalized with conclusions and discussion.

II. CONTROL METHOD

The fundamental idea of the control method is to keep available current for EV charging in the suitable range (e.g. 8–16 A) by controlling the controllable loads (e.g. electric heating and hot water heater). The available EV charging current capacity is the difference between allowed peak current and measured real time currents. In case of three-phase EV charging, the available EV charging current is the minimum available current of the three phase currents. This paper focuses on three-phase EV charging. However, the control method could be applied to one-phase charging as well. The information about the available EV charging current is transmitted to actual EV charging point at short time intervals.

According to standard IEC 61851-1 [8], the maximum AC charging current per phase can be adjusted between 6 A and 80 A in mode 3 EV charging. Since 25 A is a typical main fuse size in Finland, a charging point with maximum charging current below 25 A (e.g. 16 A) might be feasible. There have

also been reports that some EVs cannot utilize currents lower than 8 A and thus the current which can be used for EV charging might be limited to 8–16 A. This acceptable charging current range is assumed within this paper. In addition to the minimum and maximum current, a target current is also included to the control method. This target current is used to determine if more controllable loads should be turned off to enable higher available EV charging current, or if some of the controllable loads should be turned on.

To secure comfort of living, there should be a limiting factor (e.g. timer) for each controllable load, which ensures that the load is not turned off too long. Depending on the nature of the controllable load and the required level of the comfort of living, acceptable controllability of the load may vary. Since there are multiple different potential use cases for the control system, it is important to retain flexibility. Different EVs can utilize different charging powers so the minimum and maximum current should be adjustable. The basic setup of the control system and a simplified block diagram of the most fundamental function of the control method are presented in Fig. 1 and 2 respectively.
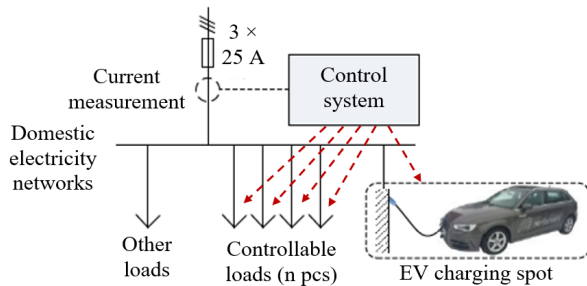
Fig. 1. The basic setup of the control system.
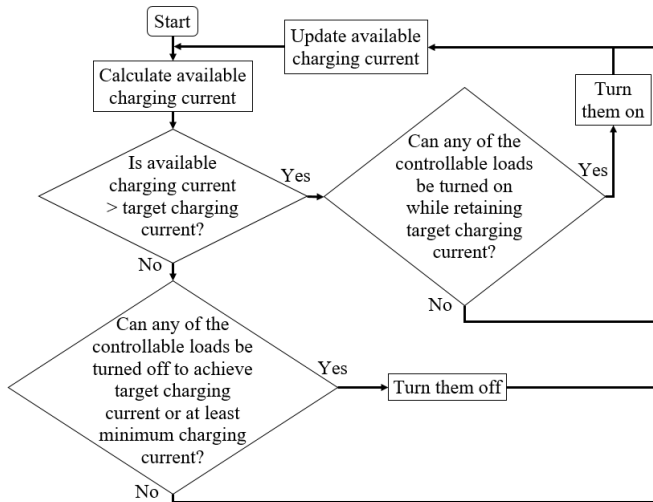
Fig. 2. Simplified block diagram of the main function of the control method.

By knowing the currents of the controllable loads, the control system can estimate new available charging current before the actual control action. However, the control system does not know whether the controllable load is on or off without separate feedback. To achieve lower investment and installation costs of the control system, separate feedbacks of the controllable loads are not considered in the control system in this paper. This can lead into a situation where the control system toggles a certain controllable load off which does not actually increase the available charging current as expected. However, this most likely does not have a notable negative impact as the control system can correct the potential problem in the next control cycle in e.g. 5 seconds.

III. PILOT CASE

In order to approximate the usefulness and effectiveness of the control system, a pilot case was implemented. The pilot case is an electrically heated detached house located in Satakunta area in Finland. The main fuse size of the real estate is 25 A and there are 6 underfloor heaters and a hot water heater which can be used as controllable loads. There is a two-time tariff in use, and these controllable loads can be forced by a separate switch to utilize only cheaper night-time electricity. In case of a forced utilization of night-time electricity, the loads can draw power only during the night-time (22:00–07:00). The pilot case did not include actual EV charging. However, the pilot system was operated in a way that EV charging circumstances would be improved.

A. Preliminary Measurements

To enable comparison of the pilot case to the original situation, preliminary measurements of the real estate were conducted. Based on the measurements, it was possible to simulate different scenarios and approximate the energy which could be charged into the EV over a night.

The total currents of the real estate were measured over a one-week long period for each phase. During this one-week period, all underfloor heaters were forced to utilize only the cheaper night-time electricity. The hot water heater was used without this limitation the first four days (Monday–Thursday) but was toggled on for the last three days (Friday–Sunday) to utilize only night-time electricity. This way the typical peak loads in both situations could be observed.

According to the measurements, the average current over the whole week for phase 1, 2, and 3 were 3.3 A, 5.9 A, and 7.0 A, respectively, whereas the highest one-hour peak currents were 20.0 A, 21.1 A, and 13.8 A, respectively. The measurements show that the night-time consumption is already relatively high without EV charging and thus uncontrolled EV charging may cause overloading.

During, e.g., Friday-Saturday, there won't be almost any current capacity left for three-phase EV charging around midnight when hot water heater is on simultaneously with space heating loads. Regardless of the utilization of night-time electricity, similar situation could occur anyway, and thus uncontrolled three-phase charging is inadvisable. The preliminary measurements indicate that around 12 A one-phase charging would be possible for the phase 3. This would occasionally cause minor overloading but might not trip the overload protection as the standard SFS-EN 60269-1 (IEC 60269-1:2006) defines that a fuse with a nominal current (I_n) between 16 A $\leq I_n \leq$ 63 A should withstand a current of 1.25×I_n for an hour (in 20 °C ambient temperature).

The current consumption of each controllable load was also measured separately. These are presented in Table I. It can be seen that most of the controllable load capacity is connected to phases 1 and 2, whereas the phase 3 has highest average loading.

TABLE I. PROPERTIES OF THE CONTROLLABLE LOADS

Load	Phase	Current consumption (A)
Underfloor heater 1	1	4.8
Underfloor heater 2	1	8.4
Underfloor heater 3	2	6.2
Underfloor heater 4	2	4.9
Underfloor heater 5	3	4.5
Underfloor heater 6	3	3.3
Hot water heater	1 and 2	6.9 and 7.1, respectively

B. Simulation Model

To evaluate the effects of different parameters and to demonstrate the operation of the control method before testing the pilot system, simulation model for the pilot house is formulated. Since the preliminary measurements of the pilot case only included the total phase currents of the real estate, the exact energy consumption of the controllable loads could not be deduced. Therefore, assumptions and simplifications have to be made in the simulation model. However, even a rough model enables estimating the operation and potential benefits of the control system.

Firstly, the hot water heater is not modeled as a controllable load as it is problematic to determine when it is on and off. For simplicity reasons, the controllable loads are assumed to be on during the night-time if the related phase current is over a certain threshold. Since the space heating is restricted to utilize night-time electricity only, it could be determined that the space heating is off during daytime. These thresholds ensure that the controllable loads will not be considered being on if the related phase current is not high enough. The downside of this assumption is that e.g. underfloor heater 1 is considered being on more than underfloor heater 2, which may not be the case. The thresholds are chosen based on the current consumptions of the controllable loads and the minimum currents of the corresponding phase. The thresholds have been presented in Table II. The assumption on how the controllable loads is on have been illustrated in Fig. 3.

If a certain controllable load is turned off by the control system to allow higher EV charging current or to limit peak loads, the control duration is calculated. In order to ensure the required level of the comfort of living, the duration of the off period is to be restricted using an adjustable timer. Depending whether the controllable load would be otherwise on or off, the missed heating duration is calculated and used to achieve the same indoor temperature later. In the simulation model and pilot system, the maximum control duration of each controllable load is limited to 2 hours per a four-hour period. For simplicity reasons, it is assumed that the load control only delays the amount of heating. The fact that indoor temperature may slightly decrease during the load rescheduling and thus

longer period of heating might be required afterwards to achieve the same peak indoor temperature is not considered in the simulation model.

TABLE II. SIMULATION ASSUMPTIONS OF THE CONTROLLABLE LOADS

Load	Phase	Current threshold (A)
Underfloor heater 1	1	4.8
Underfloor heater 2	1	13.2
Underfloor heater 3	2	6.6
Underfloor heater 4	2	11.5
Underfloor heater 5	3	5.5
Underfloor heater 6	3	8.8
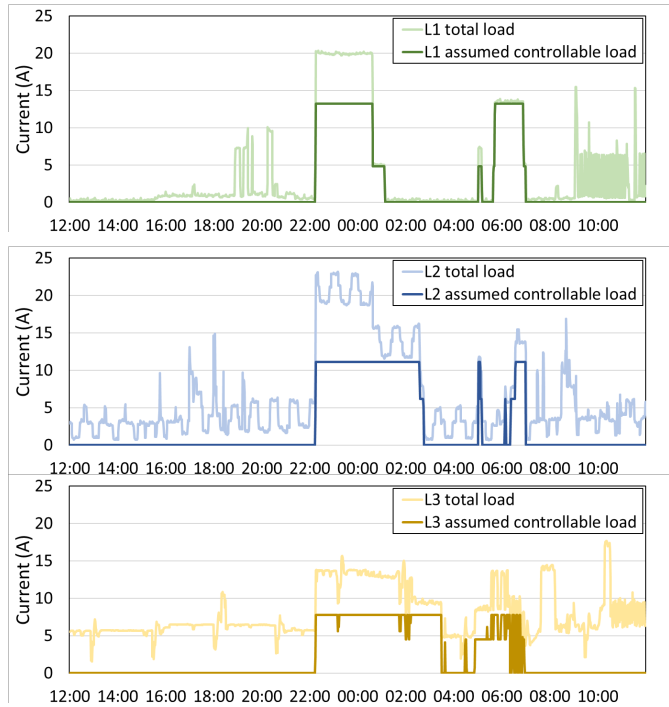
Fig. 3. Currents of the controllable loads on Friday–Saturday in the simulation model.

The impact of the control method is presented in Fig. 4. In Fig. 4, the maximum allowed total current of the real estate is 24.9 A and the target EV charging current is 12 A. Therefore, the control method attempts to limit phase currents to 12.9 A by rescheduling the controllable loads if necessary. If any of the phase currents rise above 16.9 A, there will be less than 8 A available EV charging capacity and thus EV charging must be halted. The available charging duration is assumed to be from 18:00 to 06:00. Fig. 4 shows that some of the controllable loads will be scheduled after 07:00. If the heating of the property is utilizing night-time electricity only, the heating load occurring after 7:00 would actually be scheduled to the later periods of the day, after 22:00. This may cause lower room temperatures. This could be solved e.g. by estimating the delayed heating load and restricting the EV charging current before morning to enable enough heating. However, this is not taken into account in the simulation model nor in the pilot system.
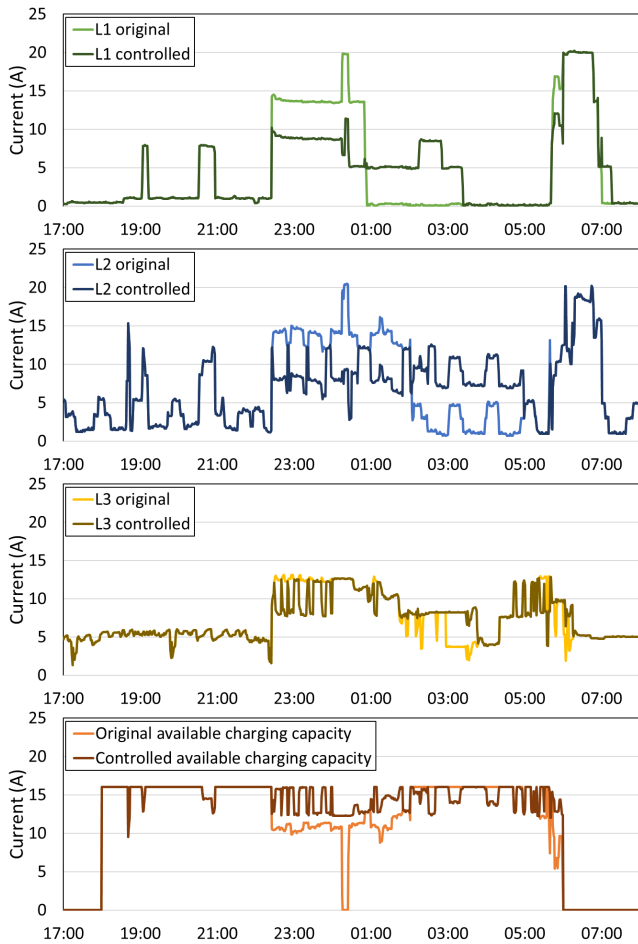
Fig. 4. Simulation results of the rescheduling of the controllable loads on Wednesday–Thursday in case of 24.9 A maximum total current of the real estate and 12 A as target EV charging current.

C. Pilot System

The pilot system consists of an automation system which controls 7 contactors, one for each controllable load. The controllable loads are still controlled by the original thermostats, but the pilot system is able to delay the heating loads when necessary by controlling the contactors. The pilot system utilizes the previously mentioned control method (illustrated in Fig. 2) and the system is tested in four different scenarios which are described in the next section.

IV. RESULTS

The idea of the pilot case is to test the core functions of the control system and estimate the benefits. Based on the measurements and simulations, four test scenarios are chosen. These scenarios have been presented in Table III. The duration of each scenario is around 72 hours, and the EV charging is assumed to be conducted between 18:00–06:00.

The effectiveness of the pilot system and the accuracy of the simulation model is assessed in the following subsections. All scenarios are investigated by comparing three cases:

1.   Pilot system measurements

2.   Results of the simulation model

3.   Without heating load control

In case 3, the heating loads are not controlled but the EV charging current is simply assumed to be adjusted according to the free capacity. Cases 2 and 3 are based on the preliminary measurements and thus there is likely to be some differences on the electricity consumption of the real estate compared to the pilot measurements. However, the average outdoor temperature was similar during the preliminary measurements and the pilot system testing (around 0˚C). For better comparison, same weekdays are chosen for each case. Available charging energy is calculated using a voltage level of 230 V and assuming that the EV could utilize any charging current between 8–16 A.

TABLE III.   TEST SCENARIOS FOR THE PILOT SYSTEM

Scenario	Forced night-time electricity utilization	Total current limit of the real estate (A)	Target current of EV charging (A)
1.	Hot water heater and underfloor heaters	24.9	12
2.	Only underfloor heaters	22.5	10
3.	Only underfloor heaters	20.0	9
4.	None	18.0	9

To examine the comfort of living, floor temperatures were measured from several different locations before and during the pilot system testing.   The temperature measurements were conducted in the morning and the results indicate that the pilot system did not have noticeable impact on the temperatures in any of the following scenarios. The variation in the floor temperatures were mostly within ±0.5˚C range from the preliminary measurements.

A. Scenario 1

The idea of the scenario 1 is to utilize night-time electricity as much as possible for controllable loads and EV charging without risk of overloading. In Fig. 5, one-minute averages of the phase currents and available charging current of the pilot system case have been presented. It can be seen that the phase currents are kept relatively steady through the night and there will be plenty of available charging capacity during the whole charging period. The numerical results for this scenario are presented in Table IV.

When comparing the case without heating load control and the simulation model, it can be seen that heating load controlling enables around 6.8% (7.8 kWh) higher EV charging energy. This percentage is relatively low due to the fact that average EV charging current over the charging period is already close to the maximum and the charging current does not need to be restricted very much. In the pilot system, the energy consumption is 21.7% (10.9 kWh) higher, but the available EV charging energy is about the same than in the case without heating load control.

TABLE IV.   Results of Scenario 1

	Pilot system[a]	Simulation model[a]	Without heating load control[a]
L1 (A)	6.0	4.0	4.0
L2 (A)	8.0	6.8	6.9
L3 (A)	8.2	7.3	7.3
Available charging current (A)	13.9	14.8	13.9
Available charging energy (kWh)	114.8	122.8	115.0
Required charging interruption (min)	3.8	0.6	17.6

a. Daily average values of the three charging periods (18:00–06:00) between Monday–Thursday. The maximum current of the real estate and the target charging current were 24.9 A and 12.0 A, respectively.
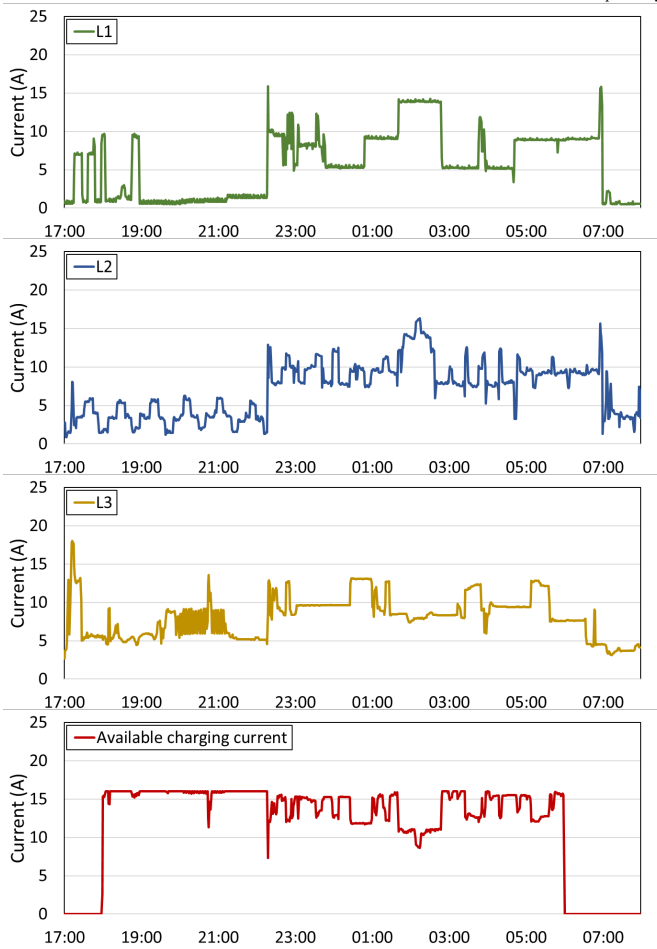
Fig. 5. Measured currents of the real estate and the available EV charging capacity in the pilot system case on Wednesday–Thursday.

B. Scenario 2

In scenario 2, the peak current is limited to 22.5 A. According to the preliminary measurements, the real estate peak current average of one-hour period are 20.0, 21.1, and 13.8 for phases 1 to 3, respectively. Therefore, this peak current limitation could be possible regardless of the heating load controlling if the EV charging current is controlled.

The energy consumption of the simulation model is around 8.1% (5.1 kWh) lower than in the case without heating load control, which means that the control system is scheduling the controllable loads partly outside of the investigated charging period (18:00–06:00). Also, the control system allows about 18.8% (16.2 kWh) more energy to be charged to the EV when comparing the simulation model to the case without heating load control. In the pilot system, the energy consumption of the real estate is 6.0% (3.4 kWh) and 13.6% (8.5 kWh) lower than in the case of simulation model and the case without heating load control, respectively. However, the available EV charging energy is also 6.1% (6.3 kWh) and 26.0% (22.5 kWh) higher, respectively.

Lower energy consumption of the real estate during the pilot system case is likely because the hot water heater is utilizing only night-time electricity between Friday–Sunday during the preliminary measurements. For a better comparison, the results of Thursday–Friday are investigated separately and presented in Table V.

From Table V, it can be seen that while the energy consumption of the real estate is 11.7% (6.6 kWh) higher in the pilot system case than the case without heating load control, the available charging energy is 4.3% (4.3 kWh) higher for the pilot system. When comparing the simulation model case and the case without heating load control, 10.9% (6.2 kWh) of the total load is scheduled outside of the investigated charging period and 16.1% (16.1 kWh) higher charging energy is achieved.

TABLE V.   Results of Scenario 2 on a Specific Day

	Pilot system[a]	Simulation model[a]	Without heating load control[a]
L1 (A)	6.6	4.1	4.4
L2 (A)	9.0	6.4	7.2
L3 (A)	7.3	7.8	9.0
Available charging current (A)	12.6	14.0	12.1
Available charging energy (kWh)	104.1	115.9	99.8
Required charging interruption (min)	14.8	0.3	53.5

a. Daily average values of the charging period (18:00–06:00) between Thursday–Friday. The maximum current of the real estate and the target charging current were 22.5 A and 10.0 A, respectively.

C. Scenario 3

The idea of the scenario 3 is to investigate if the peak currents could be limited to 20.0 A, which is less than the peak-hour current of phase 2 in the preliminary measurements, while allowing reasonable amount of energy to be charged into EV. In Table VI the results of scenario 3 is presented. According to the pilot system measurements, currents for phases 2 and 3 are successfully limited to 20.0 A. However, the peak average current of a one-hour period for phase 1 was 22.0 A. According to the data collected from the pilot system, this unexpected peak current could have been avoided. Due to unknown reason, the pilot system was not able to schedule the controllable loads of phase 1 to a later time period.

TABLE VI.   Results of Scenario 3

	Pilot system[a]	Simulation model[a]	Without heating load control[a]
L1 (A)	5.1	4.0	4.0
L2 (A)	6.5	6.6	6.9
L3 (A)	6.0	6.9	7.3
Available charging current (A)	11.5	11.7	9.1
Available charging energy (kWh)	94.8	96.6	75.0
Required charging interruption (min)	80.3	30.9	236.3

a. Daily average values of the three charging periods (18:00–06:00) between Monday–Thursday. The maximum current of the real estate and the target charging current were 20.0 A and 9.0 A, respectively.

In scenario 3, the simulation model schedules 4.8% (2.4 kWh) of the real estate load outside of the investigated charging period and enabled 28.8% (21.6 kWh) higher EV charging energy. In pilot system case, the energy consumption is 3.9% (2.0 kWh) lower but the available EV charging energy is 26.4% (19.8 kWh) higher when compared to the case without heating load control.

D. Scenario 4

In scenario 4, the aim is to reduce peak currents even more by allowing all controllable loads to utilize also daytime electricity. The pilot system results cannot be compared properly to the simulation model or to the case without heating load control since the preliminary measurements were not conducted for this kind of scenario where all controllable loads could utilize either night-time or daytime electricity.

According to the pilot system measurements, the peak currents were successfully limited to 18.0 A while reasonable amount of energy could have been charged into the EV. This suggests that even higher peak power reduction could possibly be achieved with the control system in the pilot case.

V.   Conclusions and Discussion

The core function of the presented control system is to limit peak currents while improving the circumstances for EV charging. Besides the unexpected peak current in scenario 3, the pilot system executed the core functions well. Since the energy consumption of the real estate vary from day to day, the accuracy of the simulation model cannot be directly proven by comparing current consumptions of the pilot system and simulation model. However, the results of the pilot system and simulation model in scenarios 1–3 are at least somewhat in line with each other even though the simulation model included a few simplifications.

When comparing the scenarios 1–3, it can be seen that the control system is more effective compared to the case without heating load control when the real estate energy consumption is relatively high compared to the peak power limit. In the selected scenarios, the heating load control enabled around 6–30% more energy to be charged to an EV. It should be noted

that different EVs can utilize different charging currents and thus the actual gain may vary even more.

While enabling higher average charging powers, the control system can also limit peak loads and provide better utilization of cheaper night-time electricity. In addition to eliminating the risk of overloading related issues, the peak load control can bring operational cost savings if a power-based tariff component (€/kW of some period) is used by the distribution system operator. According to [9], these kinds of demand-based distribution tariffs are likely becoming more popular as they are potentially more cost-reflective than the present distribution tariffs of small-scale customers.

In each scenario, the potential charging energy is quite high, around 50–120 kWh. This would be more than enough to fully charge a typical FEV. However, the assumed 12-hour charging period may not always be possible and thus the potential charging energy may be notable lower. Depending on the driving requirements and available charging time, the control system could, for example, reduce the need to use public charging stations notably.

Encouraged by the good results, an application for a patent was filed [10]. The intention is to continue developing flexible energy management systems suitable for different real estates.

References

[1] J Traficom, "Vehicles in traffic by Vehicle class, Driving power and Quarter," [Accessed 13.8.2019] (Available: http://trafi2.stat.fi/PXWeb/pxweb/en/TraFi/TraFi__Liikennekaytossa_olevat_ajoneuvot/040_kanta_tau_104.px/table/tableViewLayout1/?rxid=d44ee935-a646-4c12-85d6-766dc63e196d)

[2] X. Liang, T. T. Lie, and M. H. Haque, "A cost-effective EV charging method designed for residential homes with renewable energy," 2014 International Conference on Connected Vehicles and Expo (ICCVE), Vienna, 2014, pp. 207-208.

[3] Z. Wan, H. Li, H. He, and D. Prokhorov, "A Data-Driven Approach for Real-Time Residential EV Charging Management," 2018 IEEE Power & Energy Society General Meeting (PESGM), Portland, OR, 2018, pp. 1-5.

[4] Y. Ogata and T. Namerikawa, "Energy Management of Smart Home by Model Predictive Control Based on EV State Prediction," 2019 12th Asian Control Conference (ASCC), Kitakyushu-shi, Japan, 2019, pp. 410-415.

[5] U. Datta, N. Saiprasad, A. Kalam, J. Shi, and A. Zayegh, "A price-regulated electric vehicle charge-discharge strategy for G2V, V2H, and V2G," International Journal of Energy Research, vol. 43, (2), pp. 1032-1042, Feb. 2019.

[6] A. Dargahi, S. Ploix, A. Soroudi, and F. Wurtz, "Optimal household energy management using V2H flexibilities," Compel, vol. 33, (3), pp. 777-792, 2014.

[7] A. Rautiainen, "Aspects of Electric Vehicles and Demand Response in Electricity Grids," Ph.D. dissertation, Department of Electrical Energy Engineering, Tampere University, Tampere, 2015.

[8] International Standard IEC 61851-1: "Electric vehicle conductive charging system - Part 1: General requirements," 2017.

[9] K. Lummi, A. Mutanen, P. Järventausta, "Upcoming changes in distribution network tariffs – potential harmonization needs for demand charges," 25th International conference on electricity distribution (CIRED), Madrid, June 2019.

[10] Sandy Beach Oy, "An apparatus and a method for managing residential electrical loads," Finnish Patent 20195394, May 13, 2019.

PUBLICATION
5

Optimized controlled charging of electric vehicles under peak power-based electricity pricing

T. Simolin, K. Rauma, A. Rautiainen, P. Järventausta

Optimised controlled charging of electric vehicles under peak power-based electricity pricing

Toni Simolin[1] ✉, Kalle Rauma[2], Pertti Järventausta[1], Antti Rautiainen[3]

[1]*Unit of Electrical Engineering, Tampere University, Korkeakoulunkatu 7, 33720 Tampere, Finland*
[2]*Institute of Energy Systems, Energy Efficiency and Energy Economics, TU Dortmund University, Emil-Figge-Str. 76, 44227 Dortmund, Germany*
[3]*Pohjois-Karjalan Sähkö Oy, Rantakatu 29, 80100 Joensuu, Finland*
✉ *E-mail: toni.simolin@tuni.fi*

Abstract: This study presents a practical control method for electric vehicle (EV) charging optimisation for detached and attached houses. The developed EV charging control method utilises real-time measurements to minimise charging costs of up to two EVs in a single household. Since some Finnish distribution system operators have already launched peak power-based distribution tariffs for small-scale customers and because there is a lot of discussion on this kind of tariff development, the control method considers peak power-based charges. Additionally, the proposed smart charging control method utilises charging current measurements as feedback to reallocate unused charging capacity if an EV does not utilise the whole capacity allocated for it. The control method is implemented and tested with commercial EVs. The conducted hardware-in-the-loop simulations and measurements confirm that the control method works as intended. The proposed smart charging control reduces EV charging electricity distribution costs around 60% when compared to the uncontrolled EV charging.

1 Introduction

According to [1], the share of detached houses and attached houses of all Finnish dwellings are 38 and 14%, respectively. Furthermore, 50 and 22% of the households living in detached or attached houses, respectively, include two cars [2]. As electric vehicles (EVs) are emerging and more traditional internal combustion engine vehicles are being replaced by EVs, a notable number of detached and attached houses in Finland are likely to include two EVs in the future. The number of EVs in Finland have almost doubled every year since 2012 [3], and thus, the need for smart charging solutions is quickly increasing. The amount of EVs was around 30,000 at the end of 2019 [3]. Although a block of flats is the most common type of dwelling in Finland [1], only under 7% of these households include a second car [2]; therefore, EV charging in a block of flats is left out of this paper. Due to range anxiety, which is discussed further in [4], and the practicality of home charging, it is likely that many EV owners prefer to charge at home. Therefore, it is of great importance to enable cost-effective and practical domestic charging solutions.

It is a well-known fact that uncontrolled EV charging can negatively impact electric networks due to the daily load peak in a residential area and often occur soon after people arrive home after work [5, 6]. Peak load management could be a key incentive for decentralised EV charging control methods to prevent potential congestions caused by uncontrolled EV charging. In Finland, three distribution system operators already use peak power-based tariffs for households and other small-scale customers [7–9]. According to [10, 11], peak power-based tariffs are becoming more popular as they can improve the electricity pricing cost reflectivity. Therefore, peak load management as the main objective of the home charging control should be investigated. Since peak power-based tariff structures also tend to include traditional time-of-use (TOU) pricing, as seen in [7–9], night-time charging should be preferred. In Finland, there are currently no tariffs that combine demand charges and real-time (RT) electricity pricing, and thus, RT pricing is not considered in this paper.

1.1 Related work

Several studies in the literature, such as [12–15], have optimised EV charging in residential real estates. These studies optimise charging cost under TOU electricity pricing [12] or RT pricing [13–15]. However, these studies did not consider modern peak power-based tariffs. Several studies, such as [16–18], have already stated that solely TOU or RT electricity price minimisation-based EV charging can cause even higher load peaks than uncontrolled charging.

EV charging peak load limitations have been studied from different viewpoints, e.g. in cases of non-residential building [19], apartment building energy community [20], and residential real estate [21]. In [19], a real-time valley-filling algorithm to reduce peak demand in commercial and industrial buildings is proposed. Data such as charging time and energy dispensed from real EV charging sessions is used to determine the maximum flexibility of the EV charging. In [20], EV charging powers are adjusted to limit total monthly peak loads of an apartment building energy community. The peak power limit for a new month is estimated based on historical data, and then, if necessary, the limit is adjusted to a new level based on real-time measurements. In [21], the EV charging scheduling objective is to flatten the net load profile of a residential real estate with a photovoltaic (PV) generator. The charging scheduling problems were formulated and solved with quadratic programming approaches.

The algorithms presented in these studies limit peak loading, but they share common shortcomings when it comes to real-life solutions. EVs are often assumed to use the charging current set by the EV supply equipment (EVSE) as in [19–21], but the EVSE can only set the maximum charging current, and the EV on-board charger (OBC) decides the charging current below this limit. Therefore, an EV might not utilise the whole charging capacity allocated to it. This is discussed further in Section 2.1. If there is more than one EV, as opposed to [21], this can result in a non-ideal utilisation of the available charging capacity. Furthermore, many studies, such as [19, 21], assume that plug-in durations or energy requirements are known by the EVSE. Since an accurate historical data-based prediction is not always available and the EV owners might not be willing to actively input their driving needs due to
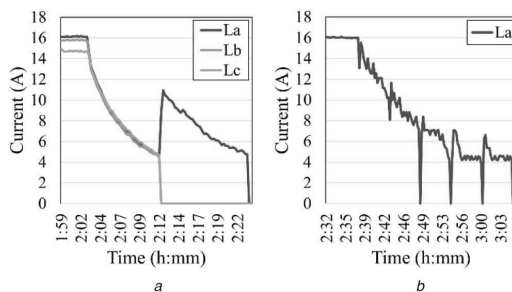
Fig. 1. *Measure of charging currents (phases A–C) at final state of charges for*
(a) BWM i3, *(b)* Nissan Leaf

response fatigue [22], access to this kind of information may be difficult to obtain. Some EV models allow the user to track the battery SOC via a mobile application. However, there is currently no standardised method to transfer the data, and not all EV models have such a feature. Therefore, the utilisation of such information is excluded from this paper.

Load control implementations with commercial EVs are studied, e.g. in [23, 24]. Study [23] presents a practical EV charging load control solution in which the total EV charging load limit is based on PV input and the maximum constant loading of the transformer. However, due to the high total charging capacity and the low number of charging points, there is no need to pause any charging sessions. Additionally, the load control does not consider the fact that EVs may not utilise the whole charging capacity allocated to them. Therefore, the control algorithm can be more simplified. In [24], a unique physical testbed for large-scale EV charging research is described, and a practical framework for online scheduling based on model predictive control and convex optimisation is presented. For optimisation purposes, the control system utilises a mobile application to collect user inputs, such as their expected departure and energy demand. Additionally, the charging currents are measured and used as feedback for the control algorithm. However, there was no mention of allocating the unused capacity for other EVs. It also remains to be seen how actively the EV users are willing to keep reporting their departure times and energy demands.

It is also worth mentioning that the EV charging peak loads could be mitigated by using, e.g. a battery energy storage system (BESS) as in [25]. Additionally, vehicle-to-grid (V2G) can be used for peak shaving and valley-filling as mentioned in [26]. However, this paper focuses solely on grid-to-vehicle charging, which ensures that battery degradation is not increased due to more frequent charging and discharging sessions. Additionally, at present, most of the commercial EVs and charging controllers, including the ones mentioned in Section 3.3, do not support V2G operation, and thus, V2G is excluded from this paper. Auxiliary energy storages for the household are not considered in this paper either, as they would increase the total system costs notably.

Based on the literature review, there does not seem to be an optimised but practical home charging solution, which considers modern peak power-based tariffs and the fact that a household might very likely include a second EV. This fact is the major motivation for this paper.

1.2 Contributions and structure

The contribution of this paper is to develop a smart charging control algorithm, which minimises the charging costs in a residential real estate under a modern peak power-based tariff and reallocates the unused charging capacity if an EV does not utilise the whole capacity allocated to it. According to the authors' best knowledge, there are no similar works presented in the literature. The effectiveness of the proposed control algorithm is demonstrated with commercial EVs through hardware-in-the-loop (HIL) simulations. The proposed control algorithm includes

advantages such as the suitability for households with one or two EVs and the ease of implementation. The control algorithm does not rely heavily on predictions nor knowledge about the future. It is only assumed that the EVs are connected to charging points during the night time.

The rest of the paper is organised as follows. In Section 2, EV charging control is discussed, and the smart charging algorithm is introduced. In Section 3, the investigated case, related parameters, and laboratory setup are described. The results are presented in Section 4. Section 5 discusses the control system requirements, the assumptions made in the case study, and the suitability of the control system in other countries. In Section 6, the paper is finalised with conclusions.

2 Charging control

In the next subsection, the relevant properties of EV charging control are discussed. After that, the developed smart charging method and two simpler control strategies are described. These simpler control strategies are only used for comparison purposes. The idea is that the simpler control strategies do not require a separate control system, and thus, their implementation would be easier. However, the simpler control strategies do not dynamically limit currents nor peak powers, and they do not prevent overloading nor an increase in the peak power-based costs. This paper focuses on single-phase charging as it is often sufficient when considering the long parking duration and the moderate charging requirements of domestic charging. However, the smart charging algorithm could be extended to be suitable for three-phase charging with moderate modifications.

2.1 Controllability of EV charging

According to IEC 61851-1, the allowed charging current limits in mode 3 charging are 6–80 A [27]. An EVSE can use pulse-width modulation (PWM) through a control pilot circuit to indicate the charging current limit for the EV. By changing the duty cycle of the PWM signal, the EVSE can indicate a new maximum charging current limit. The standard limits the EVSE from initiating a new charging current limit within 5 s of the previous current limit.

IEC 61851-1 also determines that an EV shall indicate the readiness to receive energy. This is done by adjusting the EV side resistance of the control pilot circuit, which affects pilot voltage measured at the EVSE output. The information can be transferred forward from the charging controller to the control unit so that the number of EVs requiring charging energy can be calculated. This can be used to distribute the available charging capacity more effectively.

As mentioned in [24], an EV can charge with a lower rate than the pilot signal indicates for multiple reasons. For example, the maximum charging rate of the vehicle's OBC or the charging cable might cause a lower limit. Also, the OBC charger may choose a lower charging rate to protect the battery from overheating, or the battery might require slower charging when it is nearly fully charged. In Fig. 1, an example is given for the BMW i3 and Nissan Leaf (technical characteristics are shown in Section 3.3), where the charging currents decrease in the last ~20 and ~26 min, respectively, before becoming fully charged. The initial SOCs are about 33 and 40% for the BMW and Nissan, respectively. The charging currents are constant for about 2:02 and 2:37 h, respectively, before the batteries are close to being fully charged. Additionally, some EVs may be able to use only a few specific charging currents. For example, according to the measurements, the BMW i3 used in this study can only utilise 6 or 16 A currents for charging. Therefore, if a charging current limit of 15 A is set by the charging controller, the BMW would start charging with 6 A.

It is reasonable to assume that EVs can utilise different charging currents more flexibly in the future as OBCs will go through technical improvements. However, it is likely that there will be more opportunities for charging at different locations, such as homes, workplaces, and within the vicinity of commercial buildings. Therefore, it will be more likely that EVs are often close to their final SOCs, and in order to fully utilise available charging
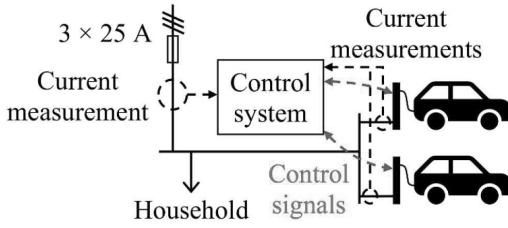
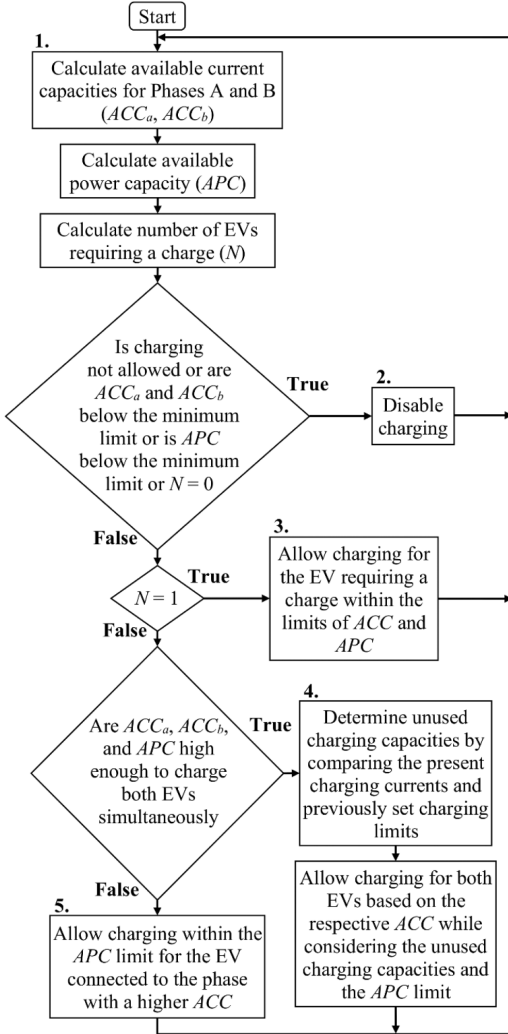**Fig. 2** *Basic setup of the control system*

Fig. 3 *Block diagram of the control method*

capacity in the case of multiple EVs, it becomes necessary to measure the actual charging currents drawn by the EVs.

Even though this paper does not consider V2G, it is worth mentioning that the V2G operation is likely to include similar non-ideal characteristics, where e.g. the vehicle's OBC might choose a lower discharging rate to protect the battery. Therefore, future V2G studies should be carried out using commercial EVs, which supports the V2G operation.

2.2 Proposed smart charging algorithm

The objective of the smart charging control method proposed in this paper is to reactively limit the peak loads and currents if necessary while ensuring that the available power capacity (APC) is used as effectively as possible. Additionally, the control method delays the EV charging to night-time hours (22:00–7:00) to reduce charging energy costs. Therefore, the EVs should be parked at home and plugged in to the charging points during the night. To balance phase loads, the control method gives priority to the phase with the lowest non-controllable load when only one EV can be charged at a time. The restriction to limit the total peak power of the real estate includes an acceptance that by using the charging algorithm, the EV charging process will take a longer time than without the algorithm.

To limit peak loading, it is necessary for the control method to know the highest non-controllable load peak of the building and its real-time electricity consumption. These can then be used to calculate the APC for EV charging, which will not increase the peak loads and thus peak power-based costs. It should be mentioned that the selected tariff [7] accounts for only 80% of the peak powers during night time, which effectively allows 25% higher peak loads during those hours without additional costs. It is expected that demand charges will be more notable in the future, and thus, the tariff with the highest demand charge is selected. The night-time peak power limit P_{limit} can be determined according to the following equation:

$$P_{limit} = \max \begin{cases} \dfrac{P_{peak}(t)}{0.8} \times \text{SF}, & 7 \leq t < 22 \\ P_{peak}(t) \times \text{SF}, & t < 7 \text{ or } t \geq 22 \end{cases}, \quad (1)$$

where P_{peak} is the highest measured peak load, SF is a safety factor, and t is hour. The control method is chosen to adjust charging currents every 10 s. Since the charging currents cannot be adjusted more frequently according to the peak load limit and the real-time energy consumption of the household, a peak power safety factor of 0.99 is used to limit the highest allowed peak load to 1% under the target peak load. The highest non-controllable load peak can be estimated, and the control method can use the measurement data to detect whether the non-controllable loads reach a new peak value. A similar peak load management principle is used in [20].

The setup of the control system is presented in Fig. 2, and the block diagram of the control method is presented in Fig. 3. The control system can be, e.g. a microcomputer that runs the algorithm script. The control system requests EV charging states and realised charging current information from EVSEs and then sends new current limits calculated using the algorithm. Household electricity consumption and line voltages are measured using the household's smart meter and are sent to the control system when requested.

The algorithm starts (part 1 in Fig. 3) by calculating the available current capacities for phases A and B (ACC$_a$, ACC$_b$, respectively), the APC, and the number of EVs requiring a charge (N). ACC$_a$ and ACC$_b$ represent the currents that are available for EV charging while considering the household electricity consumption and the limit set by the main fuse of the building (25 A). APC represents the power available for EV charging while considering the household power consumption and the highest allowed peak load. The equations for ACC$_a$, ACC$_b$, and APC are presented in (2), where I_{fuse} represents the current limit of the main fuse of the household (25 A), I_{sf} is safety marginal (0.1 A) for the fuse, I_a–I_b are phase currents, and $P_{household}$ is the power consumption of the household

$$\begin{cases} \text{ACC}_a(t) = I_{fuse} - I_a(t) - I_{sf} \\ \text{ACC}_b(t) = I_{fuse} - I_b(t) - I_{sf} \\ \text{APC}(t) = P_{limit}(t) - P_{household}(t) \end{cases} \quad (2)$$

If both ACC$_a$ and ACC$_b$ are below the minimum current limit (6 A), the APC is too low, it is daytime, or there are no EVs requiring

a charge, the EV charging should be disabled (part 2 in Fig. 3). To allow charging, APC should be high enough so that there are at least 6 A for EV charging with the present voltage level (~230 V), which is measured in real time. If only one EV requires charging, the charging current should be limited according to APC and the respective ACC (part 3 in Fig. 3). The conditions and the charging current limits C_{limit} for the EVs that are connected to phases A and B, respectively, are presented in (3), where S represents the charging state of an EV in accordance to the IEC 61851-1 standard, V is phase voltage, and $I_{\text{cp,max}}$ is the maximum current allowed by the charging point. Charging is only allowed if the charging state is C (EV is ready to receive energy) or D (EV is ready to receive energy but requires charging area ventilation) [27]. In most cases, the charging area ventilation is only necessary with higher charging powers (>32 A), and thus, its further analysation is excluded from this paper

$$\begin{cases} \text{if } (S_a(t) = C \text{ or } S_a(t) = D) \text{ and } ACC_a(t) \geq 6 \\ \text{and } N = 1 \text{ and } APC(t)/V_a(t) \geq 6 \text{ then} \\ C_{\text{limit},a}(t) = \min\left(ACC_a(t), \ APC(t)/V_a(t), \ I_{\text{cp,max}}\right) \\ C_{\text{limit},b}(t) = 0 \end{cases} \quad (3a)$$

$$\begin{cases} \text{if } (S_b(t) = C \text{ or } S_b(t) = D) \text{ and } ACC_b(t) \geq 6 \\ \text{and } N = 1 \text{ and } APC(t)/V_b(t) \geq 6 \text{ then} \\ C_{\text{limit},a}(t) = 0 \\ C_{\text{limit},b}(t) = \min\left(ACC_b(t), \ APC(t)/V_b(t), \ I_{\text{cp,max}}\right) \end{cases} \quad (3b)$$

To allow two EVs to charge simultaneously, both ACC_a and ACC_b should be at least the minimum limit (6 A). Additionally, APC should be high enough so that the minimum charging current (6 A) for both EVs does not cause a new load peak in the given phase voltage levels (part 4 in Fig. 3). Available charging currents of up to 16 A could be used effectively to charge one EV. However, the algorithm prefers to charge two EVs, if possible, as it promotes phase load balancing within the real estate network. As mentioned earlier, an EV may not be able to utilise the whole charging current set by the EVSE. Therefore, the realised charging currents are measured and used as a feedback. If an EV is drawing less current than the set limit, the difference should be allocated to the other EV.

The condition to allow two simultaneous charging sessions is presented in (4). To allocate available charging capacity effectively, preliminary allocations $C_{\text{pre,limit}}$ are calculated first based on (5). After that, the algorithm calculates the unused charging capacity C_{unused} of the previous control cycle from both EVs, as shown in (6), where C_{measured} is the measured charging current. A margin of 1 A is used to determine whether the OBC is limiting the charging current below the set charging current limit. If the OBC limits the charging current, the expected charging currents C_{expected} are calculated based on (7), which assumes that the charging current will stay on the same level set by the OBC even if its limit is increased. Finally, the charging current limits are updated according to (8)

$$\begin{aligned} \text{if } N = 2 \text{ and } APC(t)/\text{avg}(V_a(t), \ V_b(t)) \geq 12 \\ \text{and } ACC_a(t) \geq 6 \text{ and } ACC_b(t) \geq 6 \text{ then} \end{aligned} \quad (4)$$

$$\begin{cases} C_{\text{pre,limit},a}(t) = \min\left(ACC_a(t), \ I_{\text{cp,max}}, \ APC(t)/2/V_a\right) \\ C_{\text{pre,limit},b}(t) = \min(ACC_b(t), \ I_{\text{cp,max}}, \\ (APC(t) - C_{\text{limit},a}(t) \times V_a)/V_b)) \end{cases} \quad (5)$$

$$\begin{cases} C_{\text{unused},a}(t-1) = C_{\text{limit},a}(t-1) - C_{\text{measured},a}(t) \\ C_{\text{unused},b}(t-1) = C_{\text{limit},b}(t-1) - C_{\text{measured},b}(t) \end{cases} \quad (6)$$

$$\begin{cases} C_{\text{expected},a}(t+1) = \min\left(C_{\text{pre,limit},a}(t), \ C_{\text{measured},a}(t)\right) \\ C_{\text{expected},b}(t+1) = \min\left(C_{\text{pre,limit},b}(t), \ C_{\text{measured},b}(t)\right) \end{cases} \quad (7)$$

$$\begin{cases} C_{\text{limit},a}(t) = \ \min\left(ACC_a(t), \ I_{\text{cp,max}}, \right. \\ C_{\text{pre,limit},a}(t) + C_{\text{pre,limit},b}(t) - C_{\text{expected},b}(t+1), \\ \left. (APC(t) - C_{\text{expected},b}(t+1) \times V_b)/V_a(t) \right) \end{cases} \quad (8a)$$

$$\begin{cases} C_{\text{limit},b}(t) = \ \min\left(ACC_b(t), \ I_{\text{cp,max}}, \right. \\ C_{\text{pre,limit},b}(t) + C_{\text{pre,limit},a}(t) - C_{\text{expected},a}(t+1), \\ \left. (APC(t) - C_{\text{expected},a}(t+1) \times V_a)/V_b(t) \right) \end{cases} \quad (8b)$$

If ACC_a or ACC_b is below the minimum limit (6 A) or if APC is not high enough to allow charging for the two EVs, only one EV can be charged (part 5 in Fig. 3). The conditions and charging current limits are presented in the following equations:

$$\begin{cases} \text{if } (ACC_b(t) < 6 \text{ or } (ACC_a(t) > ACC_b(t) \text{ and} \\ APC(t)/\text{avg}(V_a(t), V_b(t))) < 12) \text{ and } N = 2 \text{ then} \\ C_{\text{limit},a}(t) = \ \min\left(ACC_a(t), \ APC(t)/V_a(t), \ I_{\text{cp,max}}\right) \\ C_{\text{limit},b}(t) = 0 \end{cases} \quad (9a)$$

$$\begin{cases} \text{if } (ACC_a(t) < 6 \text{ or } (ACC_b(t) > ACC_a(t) \text{ and} \\ APC(t)/\text{avg}(V_a(t), V_b(t))) < 12) \text{ and } N = 2 \text{ then} \\ C_{\text{limit},a}(t) = 0 \\ C_{\text{limit},b}(t) = \ \min\left(ACC_b(t), \ APC(t)/V_b(t), \ I_{\text{cp,max}}\right) \end{cases} \quad (9b)$$

This case study does not consider a distributed generation such as solar power. However, optimal solar power use would be relatively simple in this case. The same algorithm, shown in Fig. 3, can be used during the daytime if it is modified so that the available charging capacity is equal to the excess solar energy that is not consumed by the household.

2.3 Simpler charging strategies

Naturally, the simplest EV charging strategy is the uncontrolled charging, where the EVs start charging immediately after being plugged in after arriving home. This would be the easiest solution for EV owners as this would not require any extra effort or any kind of charging control system at the charging station.

As TOU electricity pricing is commonly used in detached households in Finland, the next most obvious simple control strategy would be to delay charging until night time (uncontrolled night-time charging). However, this would not likely lower the peak loads that much. In fact, if controllable loads, e.g. space heating and the hot water heater, are already utilising only night-time electricity, night-time EV charging could cause even higher peak loads, as mentioned in [18].

3 Case description

The developed charging algorithm is tested using HIL simulations with a modified commercial charging station and two commercial EVs. A detailed description about the simulation environment is presented in the following subsections.

3.1 Detached house under study

The studied case is a detached house located in Pirkanmaa, Finland. It was built in 2010. The floor area of the building is 158 m², and a geothermal heat pump is used as the main heating system. This represents a typical Finnish detached house.

The electricity consumption was measured in December 2018 in 1 s intervals. The daily average outdoor temperature was between −1 and −5°C throughout the measurement period. Wintertime was chosen to be investigated in this case study so that the heating load would be high, with a limited capacity for EV charging. The highest measured hourly peak load was 6.88 kW. For phases A–C, the average currents over the whole measurement period were 2.9, 2.3, and 3.6 A, whereas the highest 1 h peak currents were 12.7, 12.4, and 13.8 A, respectively. The highest
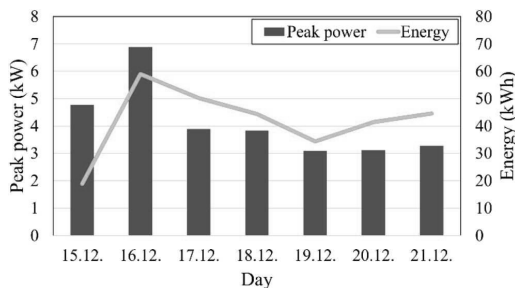
Fig. 4 *Household electricity consumption*

Table 1 EV departure and arrival times

Day	EV	Departure	Arrival
Sat 15.12.	A	10:00	15:00
	B	11:00	16:00
Sun 16.12.	A	10:00	15:00
	B	11:00	16:00
Mon 17.12.	A	7:00	17:00
	B	7:30	18:00
Tue 18.12.	A	7:00	17:00
	B	7:30	18:00
Wed 19.12.	A	7:00	17:00
	B	7:30	18:00
Thu 20.12.	A	7:00	17:00
	B	7:30	18:00

Table 2 Technical characteristics of the EVs

Vehicle	Nissan Leaf (A)	BMW i3 (B)
model	2014–15	BMW i3 (94 Ah)
battery capacity	67 Ah	94 Ah
battery rated voltage	360 V	353 V
battery energy capacity	24.1 kWh	33.2 kWh
OBC efficiency	0.89%	0.925%
connector IEC 62196	Type 1	Type 2
max charging current	16 A	32 A
max supported AC charging	1-phase AC	3-phase AC

hourly peak loads and daily electrical energy consumptions are presented in Fig. 4.

The electricity consumption measurement started on Saturday (15.12.) at 12:53 h, which explains the low energy consumption during that day. There is notable loading every day around 18:00–20:00 h, but three of the highest daily load peaks occurred at 9:00, 12:00, and 22:00 h. The main fuse is sized as 3×25 A.

The residents own two passenger cars. Due to the limits set by the main fuse, the study focuses on charging points with a maximum charging current of 16 A. As phase *C* has the highest average loading, phases *A* and *B* are chosen for EV charging. Phase *B* has the lowest average and peak loading, so it is logical to use it to charge the EV with a higher charging requirement.

3.2 EV driving profiles

According to [28], passenger cars were driven almost 33,000 km/a in total in Finnish households with two cars in 2016. Car (B), driven the most, had an average distance of 21,900 km/a, whereas the other (A) had 11,000 km/a. The yearly driving distances equal to around 59.8 and 30.1 km/day, respectively. Passenger car trips most often start around 7:00 or 16:00 h on weekdays, according to [28]. During weekends, the most active passenger car usage is between 10:00 and 16:00 h [28]. The departure and arrival times used in this study are presented in Table 1. These values are used
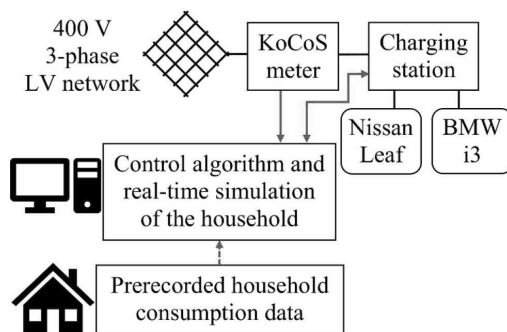
Fig. 5 *Simplified scheme of the laboratory setting*

Fig. 6 *Laboratory setup*

as a basis for this study. However, the impacts of different driving behaviours are discussed in Section 5.1.

3.3 Laboratory setup

The practical implementation of the EV charging control system is carried out at the Smart Grid Technology Lab [29] at TU Dortmund University. The lab included Nissan Leaf (A), BMW i3 (B), and a charging station, which made it possible to conduct the study. The technical characteristics of the EVs are presented in Table 2. The used charging point is a modified RWE eSTATION charging station with two independent charging sockets. Both charging sockets are suitable for charging powers up to 22 kW (400 V AC), but one of them is modified into a one-phase socket by disconnecting phases *A* and *C*. This was necessary to make sure that the BMW would charge using only phase *B*. The Nissan Leaf uses one-phase (phase *A* in this case) charging regardless of the opportunity for three-phase charging. As charging controllers, there were two Phoenix Contact Advanced EV charge controllers (type EM-CP-PP-ETH), which are fully compatible with the IEC 61851-1 standard and allow limiting the charging currents and reading the charging states through Modbus TCP/IP.

The control algorithm and the household simulations are run on a computer that was connected to the same local area network with a KoCoS EPPE CX power quality meter and charge controllers. The algorithm is implemented using the Python programming language and a Modbus library (ModbusTcpClient). The KoCoS meter measured the total electricity consumption and line voltages. In a real-life case, a smart meter could provide the same measurements as the KoCoS meter in this case. The KoCoS meter and the charging station are connected to the 400 V laboratory network. The pre-recorded household electricity consumption data are simulated and read from an Excel file in real time. The lab setup topology and the setup of the lab are presented in Figs. 5 and 6, respectively. The laboratory has been previously used in, e.g. [30], where the EVs were controlled to limit voltage violations and network congestion.
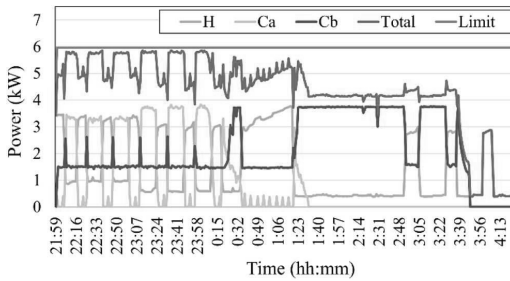
Fig. 7 Charging sessions for Saturday
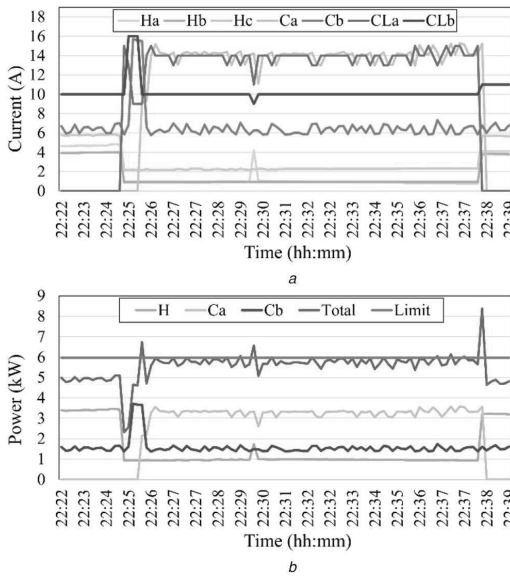
Fig. 8 Operation of the proposed charging control algorithm

4 Results

The results of the HIL simulations are presented in this section. Table 3 presents the driving distances of the measurement period as well as the energy consumptions, which are calculated by using the values (currents and voltages) measured throughout the charging sessions.

The energy consumptions shown in Table 3 are the electrical energy drawn from the residential network, including losses, such as OBC and EVSE losses.

4.1 Analysing the operation of the proposed control algorithm

According to the results, the smart charging algorithm works as intended. This is illustrated in Fig. 7, where the peak load is successfully limited below 5.97 kW during the night time.

In Figs. 7–9, notations a–c represent phases, H is for household, C is for charging, and CL is for charging current limit set by the charging controller. Fig. 7 is presented in 1 min resolutions. A peak load of 4.77 kW was measured earlier on the same day during the daytime, resulting in the peak power limit of 5.97 kW according to (1). Fig. 7 shows that the EV charging load is increased and reduced depending on the electricity consumption of the household.

During the charging sessions, several unideal characteristics are identified, as illustrated in Fig. 8. Fig. 8a shows that there is always a delay of a few seconds between the current limit set by the charging controller and the actual charging current. This can cause short load peaks if the household consumption suddenly rises as in

Table 3 EV driving statistics

Day	EV	Driving distance, km	Average speed, km/h	Energy consumption, kWh
Sat 15.12.	A	28.3	67.4	5.3
	B	66.1	76.1	13.5
Sun 16.12.	A	37.9	35.8	6.6
	B	58.2	51.7	9.2
Mon 17.12.	A	29.3	37.9	5.3
	B	72.0	55.9	12.6
Tue 18.12.	A	30.0	44.1	5.6
	B	58.1	69.6	11.1
Wed 19.12.	A	28.8	41.1	5.3
	B	62.6	71.3	10.4
Thu 20.12.	A	33.2	46.6	6.1
	B	62.7	80.3	12.3
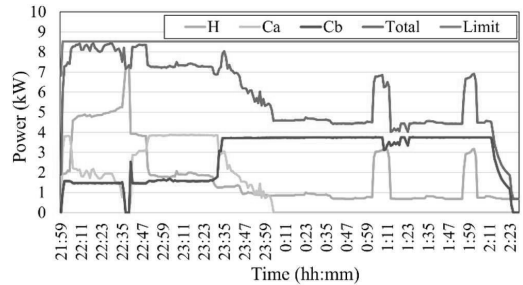
Fig. 9 Charging sessions for Monday

Fig. 8b at 22:38 h. However, this kind of peak load only lasts for about one control cycle which, in this case, is 10 s and thus its impact is negligible. In Fig. 8a, there is a slight anomaly in the behaviour of the Nissan (connected to phase A) at 22:25 h. The algorithm allows a 9–15 A charging current for the Nissan at 22:25:10 h, but the charging starts after 40 s (22:25:50 h). Within this time, the algorithm notices the unused charging capacity and allocates it for the BMW (connected to phase B). This causes a slight charging current peak for the BMW at 22:25 h. The measurements show that the control algorithm can reallocate unused charging capacity, but the used control cycle of 10 s might be unnecessarily short and result in a high number of control actions.

As shown in Fig. 4, there is a notable load peak (6.88 kW) in the real estate on Sunday. Therefore, the peak load limit is 8.60 kW during the night time according to (1) for the rest of the measurement period. Since the limit is quite high, the EVs are charged relatively fast. In Fig. 9, the charging sessions are illustrated for Monday.

4.2 Comparing the control strategies

For practical reasons, simpler control strategies are only simulated. The charging currents are assumed to stay at a constant 16 A for the bulk part of the charging sessions. The charging currents at high SOCs are modelled based on measurements of uncontrolled charging sessions. For the Nissan and the BMW, the charging currents start to decrease when there is under 0.90 and 0.39 kWh of energy, respectively, remaining to be charged. The charging curves at the final SOCs are presented in Fig. 10 in 1 min resolution.

The total charging energy is 103.2 kWh during the six days that were studied. By assuming that the average daily charging requirement stays the same, the total charging energy requirement would be 533.4 kWh for all of December. For the sake of simplicity, the peak power of 6.88 kW is assumed to be the peak power that determines monthly demand charges for the case where EV charging is not considered. These values can then be used to
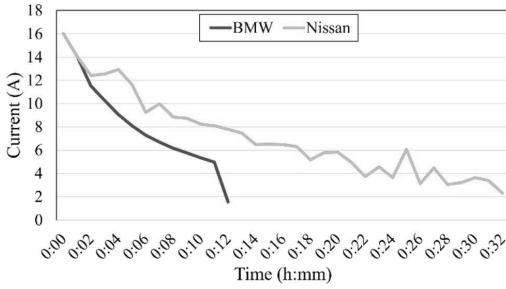
Fig. 10 *Charging currents at final SOCs*
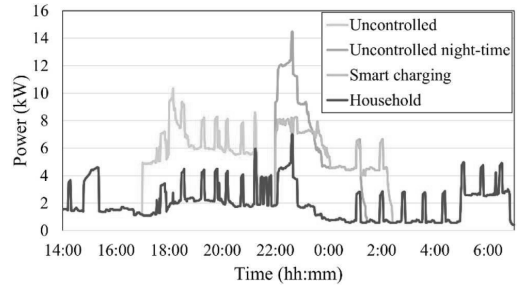
Fig. 11 *Total power consumptions for Monday*

Table 4 EV charging-related monthly electricity distribution costs

Control strategy	Cost type	Increment	Cost
uncontrolled charging	daytime electricity	533.4 kWh	13.8 €
	night-time electricity	0.0 kWh	0.0 €
	peak power	2.5 kW	4.1 €
uncontrolled night-time charging	daytime electricity	0.0 kWh	0.0 €
	night-time electricity	533.4 kWh	7.2 €
	peak power	2.2 kW	3.5 €
proposed smart charging	daytime electricity	0.0 kWh	0.0 €
	night-time electricity	533.4 kWh	7.2 €
	peak power	0.0 kW	0.0 €

calculate the monthly electricity distribution cost increments, when EVs are charged using different control strategies. The selected tariff presented in [7] includes demand charge ($\varnothing_{peak,power} = 1.59$ €/kW,month) and TOU pricing ($\varnothing_{energy,day} = 2.59$ c/kWh during the daytime and $\varnothing_{energy,night} = 1.35$ c/kWh during the night time). The equations to calculate peak power-based costs caused by EV charging are presented in (10), where $X_{energy,day}$ is the costs of daytime energy consumption, $X_{energy,night}$ is the costs of night-time energy consumption, X_{peak} is the peak power-based costs, E_{day} is the daytime energy consumption, and E_{night} is the night-time energy consumption. The cost increments are presented in Table 4

$$\begin{cases} \Delta X_{energy,day} = \varnothing_{energy,day} * \Delta E_{day} \\ \Delta X_{energy,night} = \varnothing_{energy,night} * \Delta E_{night} \\ \Delta X_{peak} = \varnothing_{peak} * \Delta P_{peak} \end{cases} \qquad (10)$$

The proposed smart charging algorithm reduces charging costs by around 59.8% (10.7 €) when compared to uncontrolled charging. The uncontrolled night-time charging mostly affects the volumetric electricity costs instead of the peak demand charges. In Fig. 11, the total power consumptions in 1 min resolutions are presented for Monday.

It is worth mentioning that one of the uncontrolled night-time charging sessions could be delayed to later hours of the night. This could give time for the first sessions to finish before the second starts. Therefore, it reduces the probability of two simultaneous charging sessions and could reduce peak power-based costs. However, in practice, this could be an unreliable solution and inconvenient from the EV user's perspective. A very late charging start time could result in a higher probability that the EV would not be fully charged in the morning, and an earlier charging start time would more likely cause a similar peak load increase.

5 Discussion

This section discusses the requirements of the control system, the suitability of the control system in other countries, and the potential impacts of different EV usage. The discussions are divided into two separate subsections.

5.1 Requirements and suitability

The control system requires that the household consumption be measured with a smart meter. The smart meter is also a key component to enable more complex tariffs, such as peak power-based tariffs. In Finland, the electricity consumption is measured by smart meters for over 99% of the network customers [31]. According to [32], 35% of households in the EU were equipped with smart meters in 2018. The current expectation is that smart meter penetration will reach 77 and 92% in 2024 and 2030, respectively. However, there are already several countries with smart meter penetrations of >80%, such as Denmark, Estonia, Italy, Malta, Spain, and Sweden [32].

The control system also requires that the realised charging currents be measured. Usually, this cannot be done by the charging controller itself, and thus, a separated energy meter is required on the EVSE. However, it is becoming more common that even the low-cost EVSEs include an energy meter as it does not notably affect the total costs of the EVSE.

The presented control method is suitable for detached houses and attached houses that include one or two EVs. Only 5% of the detached or semi-detached households include a third vehicle [2]; thus, they have been excluded from this paper. According to Eurostat [33], around 57% of the European population lives in detached or semi-detached houses, stating the importance of smart EV charging control in detached and attached houses. In Fig. 12, the 15 countries with the highest percent of residents living in detached houses or semi-detached houses are presented [33].

5.2 Impact of different driving behaviours

In this paper, it is assumed that the EVs would be charged solely at home. In reality, there are an increasing number of charging opportunities in, e.g. workplaces and shopping centres. Therefore, the real home charging requirement might be lower in most cases. However, a shorter driving distance would mostly decrease the electricity volumetric costs, and a home charging energy requirement of >3.6 kWh (~20 km) could still cause the same maximum peak power increase. Additionally, in case of uncontrolled charging, it takes only 1 day where the household peak consumption and the EV charging load coincide to cause unnecessarily high monthly demand charges. Therefore, from a
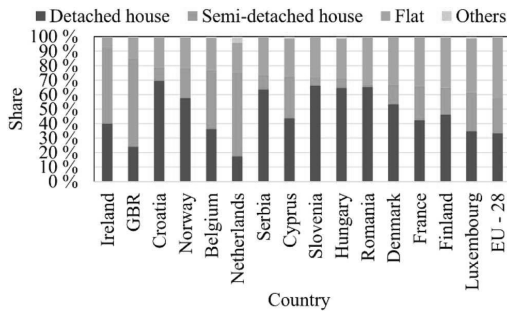
Fig. 12 *Distribution of population by dwelling type in 2018*

demand charge point-of-view, longer or shorter driving distances may not have notable effects.

According to the household electricity consumption measurements, the household consumes electrical energy around 10.5–16.0 kWh at night (22:00–7:00 h). As mentioned earlier, the highest load peak of the household is 6.88 kW. Since it occurs during the day, a loading of 8.60 kW can be allowed at night time without increasing the monthly peak power-based costs. Based on this loading limit and the night-time energy consumptions of the household, there is around 45.9–51.5 kWh of energy capacity for EV charging. This means that there would be enough charging capacity even if the daily driving distance of the EVs is doubled. The results shown in Fig. 9 also support this claim, as both EVs are fully charged before 2:30 h, which is the midpoint of the night time (22:00–7:00 h).

In this paper, it is also assumed that EVs are connected to the charging points at night (22:00–7:00 h). However, depending on the case (different charging requirements and different household electricity consumption), occasional late-night arrivals or early morning departures might not have any negative impacts. This is because the charging sessions finish before 2:10 h on average, so the required parking duration is not likely to be an issue.

When the EVs are driven notably more than average, or if they should be charged as fast as possible regardless of the costs, the residents should be allowed to manually override the charging load management. During this kind of event, the control system should only limit currents to avoid overloading. This would maximise the EV charging rates within the safe limits and thus minimise the charging need outside of home.

6 Conclusions

In this paper, a practical EV charging control method for detached and attached households is presented. Additionally, its operation is demonstrated using HIL simulations with commercial EVs. The control method is able to optimise the charging of two EVs under a peak power-based tariff.

The results of the HIL simulations show that the proposed smart charging algorithm successfully limits peak loading of the real estate and reallocates unused charging capacities for the other EV. When considering a modern peak power-based tariff, the algorithm reduces peak loads by 2.5 kW and offers around a 59.8% cost savings compared to uncontrolled charging. The objective for the charging control optimisation is based on Finland's specific needs. However, based on the statistical analysis, the control method will be useful in several other countries once peak power-based tariffs become more common for small-scale customers.

This paper does not consider V2G charging, BESS, or distributed generation, e.g. solar power. However, these topics will be studied in future works. Additionally, the presented charging algorithm accounts for a maximum number of two EVs, but it will be extended to be suitable for a higher number of EVs.

7 Acknowledgments

8 References

[1] 'Dwellings and living conditions': https://www.stat.fi/tup/suoluk/suoluk_asuminen_en.html#Dwellingsandlivingconditions, accessed 28 April 2020

[2] Finnish Transport and Communications Agency Traficom.: 'National passenger traffic survey, 2016

[3] 'Vehicles in use by gategory and propulsion': https://www.traficom.fi/fi/tilastot/ajoneuvokannan-tilastot?toggle=Käyttövoimat, (In Finnish: 'Liikennekäytössä olevat ajoneuvot ajoneuvoluokittain ja käyttövoimittain'), accessed 26 March 2020

[4] Melliger, M.A., van Vliet, O.P.R., Liimatainen, H.: 'Anxiety vs reality – sufficiency of battery electric vehicle range in Switzerland and Finland', *Transp. Res. D, Transp. Environ.*, 2018, **65**, pp. 101–115

[5] Wang, H., Zhou, W., Qian, K., *et al.*: 'Modelling of ampacity and temperature of MV cables in presence of harmonic currents due to EVs charging in electrical distribution networks', *Int. J. Electr. Power Energy Syst.*, 2019, **112**, pp. 127–136

[6] Lacey, G., Putrus, G., Bentley, E.: 'Smart EV charging schedules: supporting the grid and protecting battery life', *IET Electr. Syst. Transp.*, 2017, **7**, (1), pp. 84–91

[7] 'Electricity distribution tariffs'.: https://www.helensahkoverkko.fi/globalassets/hinnastot-ja-sopimusehdot/hsv---enkku/Distribution-tariffs.pdf, accessed 28 April 2020

[8] 'Network service price list'.: https://www.lahtienergia.fi/fi/sahkoverkko/hinnastot-sopimusehdot/verkkopalveluhinnasto, (In Finnish: 'Verkkopalveluhinnasto'), accessed 28 April 2020

[9] 'Prices of electricity distribution'.: https://www.kuopionenergia.fi/wp-content/uploads/2020/07/S%C3%A4hk%C3%B6nsiirtohinnasto-01012020.pdf, (In Finnish: 'Sähkönsiirtohinnat 1.1.2020'), accessed 13 August 2020

[10] Lummi, K., Mutanen, A., Järventausta, P.: 'Upcoming changes in distribution network tariffs – potential harmonization needs for demand charges'. 25th Int. Conf. on Electricity Distribution (CIRED), Madrid, Spain, June 2019, pp. 1–5

[11] Öhrlund, I., Schultzberg, M., Bartusch, C.: 'Identifying and estimating the effects of a mandatory billing demand charge', *Appl. Energy*, 2019, **237**, pp. 885–895

[12] Datta, U., Saiprasad, N., Kalam, A., *et al.*: 'A price-regulated electric vehicle charge-discharge strategy for G2 V, V2H, and V2G', *Int. J. Energy Res.*, 2019, **43**, (2), pp. 1032–1042

[13] Yoon, S.G., Choi, Y.J., Park, J.K., *et al.*: 'Stackelberg-game-based demand response for at-home electric vehicle charging', *IEEE Trans. Veh. Technol.*, 2016, **65**, (6), pp. 4172–4184

[14] Wan, Z., Li, H., He, H., *et al.*: 'A data-driven approach for real-time residential EV charging management'. IEEE Power and Energy Society General Meeting, Portland, OR, USA, August 2018, pp. 1–5

[15] Aragon, G., Werner-Kytola, O., Gumrukcu, E.: 'Stochastic optimization framework for online scheduling of an EV charging station in a residential place with photovoltaics and energy storage system'. 2019 IEEE Milan PowerTech, Milan, Italy, June 2019, pp. 1–6

[16] Chung, Y. W., Khaki, B., Chu, C., *et al.*: 'Electric vehicle user behavior prediction using hybrid kernel density estimator'. 2018 Int. Conf. on Probabilistic Methods Applied to Power Systems (PMAPS), Boise, ID, USA, June 2018, pp. 1–6

[17] Mobarak, M. H., Bauman, J.: 'Vehicle-directed smart charging strategies to mitigate the effect of long-range EV charging on distribution transformer aging', *IEEE Trans. Transp. Electri.*, 2019, **5**, (4), pp. 1097–1111

[18] Kutt, L., Saarijarvi, E., Lehtonen, M., *et al.*: 'Load shifting in the existing distribution network and perspectives for EV charging – case study'. IEEE PES Innovative Smart Grid Technologies Conf. Europe, Istanbul, Turkey, October 2014, pp. 1–6

[19] Zhang, G., Tan, S. T., Gary Wang, G.: 'Real-time smart charging of electric vehicles for demand charge reduction at non-residential sites', *IEEE Trans. Smart Grid*, 2018, **9**, (5), pp. 4027–4037

[20] Simolin, T., Rautiainen, A., Järventausta, P.: 'Control of EV charging to reduce peak powers in domestic real estate'. 25th Int. Conf. on Electricity Distribution (CIRED), Madrid, Spain, June 2019, pp. 1–5

[21] Fachrizal, R., Munkhammar, J.: 'Improved photovoltaic self-consumption in residential buildings with distributed and centralized smart charging of electric vehicles', *Energies*, 2020, **13**, (5), pp. 1153–1161

[22] Kim, J. H., Shcherbakova, A.: 'Common failures of demand response', *Energy*, 2011, **36**, (2), pp. 873–880

[23] Bohn, T., Cortes, C., Glenn, H.: 'Local automatic load control for electric vehicle smart charging systems extensible via OCPP using compact submeters'. 2017 IEEE Transportation and Electrification Conf. and Expo (ITEC), Chicago, IL, USA, June 2017, pp. 724–731

[24] Lee, Z.J., Chang, D., Jin, C., *et al.*: 'Large-scale adaptive electric vehicle charging'. 2018 IEEE Int. Conf. on Communications, Control, and Computing Technologies for Smart Grids (SmartGridComm), Aalborg, Denmark, October 2018, pp. 1–7

[25] Gjelaj, M., Hashemi, S., Bach Andersen, P., *et al.*: 'Optimal infrastructure planning for EV fastcharging stations based on prediction of user behaviour', *IET Electr. Syst. Transp.*, 2020, **10**, (1), pp. 1–12

[26] Najafi, S., Shafie-khah, M., Siano, P*., et al.*: 'Reinforcement learning method for plug-in electric vehicle bidding', *IET Smart Grid*, 2019, **2**, (4), pp. 529–536

[27] International Standard IEC 61851-1: 'Electric vehicle conductive charging system – part 1: general requirements', 2017

[28] 'Passenger Traffic survey'.: https://julkaisut.vayla.fi/pdf8/lti_2018-01_henkiloliikennetutkimus_2016_web.pdf, (In Finnish: 'Henkilöliikennetutkimus 2016'), accessed 28 April 2020

[29] Spina, A., Rauma, K., Aldejohann, C*., et al.*: 'Smart grid technology lab – a full-scale low voltage research facility at TU Dortmund University'. 2018 AEIT Int. Annu. Conf., Bari, Italy, October 2018, pp. 1–6

[30] García Veloso, C., Rauma, K., Fernandez Orjuela, J*., et al.*: 'Real-time agent-based control of plug-in electric vehicles for voltage and thermal management of LV networks: formulation and HIL validation', *IET Gener. Transm. Distrib.*, 2020, **14**, (11), pp. 1–12

[31] Energy Authority.: 'National Report 2018 to the Agency of Cooperation of Energy Regulators and to the European Commission', 2018, pp. 1–47

[32] European Commission.: 'Benchmarking smart metering deployment in the EU-28', Tractebel Impact, 2019, pp. 1–141

[33] 'Distribution of population by degree of urbanisation, dwelling type and income group – EU-SILC survey', http://appsso.eurostat.ec.europa.eu/nui/show.do?query=BOOKMARK_DS-057122_QID_1BA00AC6_UID_-3F171EB0&layout=TIME,C,X,0;BUILDING,L,X,1;GEO,L,Y,0;INCGRP,L,Z,0;DEG_URB,L,Z,1;INDICATORS,C,Z,2;&zSelection=DS-057122INDICATORS,OBS_FLAG;DS-057122INCGRP,TOTAL;DS-057122DEG_URB,TOTAL;&rankName1=INDICATORS_1_2_-1_2&rankName2=INCGRP_1_2_-1_2&rankName3=DEG-URB_1_2_-1_2&rankName4=TIME_1_0_0_0&rankName5=BUILDING_1_2_1_0&rankName6=GEO_1_2_0_1&sortC=ASC_-1_FIRST&rStp=&cStp=&rDCh=&cDCh=&rDM=true&cDM=true&footnes=false&empty=false&wai=false&time_mode=ROLLING&time_most_recent=false&lang=EN&cfo, accessed 28 April 2020

PUBLICATION
6

Overcoming non-idealities in electric vehicle charging management

K. Rauma, T. Simolin, A. Rautiainen, P. Järventausta, C. Rehtanz

IET Electrical Systems in Transportation

IET The Institution of Engineering and Technology WILEY

ORIGINAL RESEARCH PAPER

Overcoming non-idealities in electric vehicle charging management

Kalle Rauma[1] | Toni Simolin[2] | Antti Rautiainen[2] | Pertti Järventausta[2] | Christian Rehtanz[1]

[1]Institute of Energy Systems, Energy Efficiency and Energy Economics, TU Dortmund University, Dortmund, Germany

[2]Unit of Electrical Engineering, Tampere University, Tampere, Finland

Correspondence

Kalle Rauma, Institute of Energy Systems, Energy Efficiency and Energy Economics, TU Dortmund University, Emil-Figge-Straße 76, 44227 Dortmund, Germany.
Email: kalle.rauma@tu-dortmund.de

Abstract

The inconvenient nature of non-ideal charging characteristics is demonstrated from a power system point of view. A new adaptive charging algorithm that accounts for non-ideal charging characteristics is introduced. The proposed algorithm increases the local network capacity utilization rate and reduces charging times. The first unique element of the charging algorithm is exploitation of the measured charging currents instead of ideal or predefined values. The second novelty is the introduction of a short-term memory called expected charging currents. This makes the algorithm capable of adapting to the unique charging characteristics of each vehicle individually without the necessity to obtain any information from the vehicle or the user. The proposed algorithm caters to various non-idealities, such as phase unbalances or the offset between the current set point and the real charging current but is still relatively simple and computationally light. The algorithm is compatible with charging standard IEC 61851 and is validated under different test cases with commercial electric vehicles.

1 | INTRODUCTION

Because of the increasing popularity of electric vehicles (EVs), charging them is expected to have a notable impact on the power distribution network [1, 2]. To avoid overinvestment in network components, charging management will become a necessity in the future [3]. Insufficient charging infrastructure and long charging times are regarded as obstacles for EVs [4–6]. That is why capacity-efficiency and reduced charging times should be relevant considerations when designing a charging algorithm. With a more efficient algorithm, the charging system operator can minimize the idle capacity of the power network, which leads to shorter charging times and a higher-quality charging service. To the authors' knowledge, this efficiency is not considered under realistic conditions in the charging algorithms that have been presented in the research literature.

By network capacity, we refer to the capacity of the power network at the charging site. Usually, this is part of the electricity network at the real estate (parking hall etc.). Several algorithms for EV charging management are offered in the scientific literature. However, the shortage of most is that they do not

focus on the efficient use of network capacity, with the result that many of these proposed solutions may lead to low usage rates in real life. In addition, most available algorithms are tested only through computer simulations, which may not guarantee that they work as efficiently in reality as in the simulation. In reality, there are significant differences in the behaviour of EVs that in the worst case could jeopardize the correct functioning of a charging algorithm or reduce its efficiency.

The work presented in [7] focuses on developing an online charging algorithm and testing it with a fleet of 55 real charging stations. A time step of 5 min is used for the operation of the algorithm. A distinguishing aspect of the work is that it considers real-life constraints such as a non-ideal charging curve, unbalanced phase conductors, and unknown state-of-charge (SoC) of the EV battery. The charging current is measured at the charging station, but it is not used for control purposes. The batteries are charged according to a predefined two-stage model. First, a constant current is allowed up to 80% of the SoC followed by a decreasing current model. A benefit of this approach is that it is closer to the real load curve of most EVs than a completely constant load curve. However, each EV

model has a different load curve, which means that applying the same load model for all EVs will inevitably decrease the efficiency of the charging algorithm. The great advantage of this paper in comparison with [7] is that it handles each EV separately in real time without relying on predefined models, which makes it more adaptive and reliable.

In [8], an adaptive charging algorithm is presented. The work also considers unbalanced charging and is able to carry out phase balancing. The algorithm is run every 10 min. Unlike this paper, the studies in [8] are based on simulations and the compatibility with the standards is not discussed. It is not clearly explained, how the currents are measured and how they are applied in the charging management. In [9], an adaptive charging algorithm with the objective of peak-load management is introduced. The major lacks in [9] are that unbalanced charging is not considered and the actual charging currents are not used as an input to the algorithm. The operation of the algorithm is validated through simulations and no dynamic charging characteristics of the EVs are mentioned, which makes the work much less detailed than this paper.

In [10, 11], a charging management algorithm to cope with fluctuating available power is presented. It also considers various user groups through prioritization. The algorithm does not consider different phases or the fact that EVs may not charge according to the current value used as a set point. The algorithm is tested in a hardware-in-the-loop simulation using three electronic loads that mimic EVs but not with real EVs or charging hardware. Neither does the work discuss its suitability on practical applications or compatibility with current charging standards.

The article [12] tackles a similar problem of EV charging under changing power capacity. The algorithm is tested through simulations with a time step of 10 min. Herein, the different phases are not taken into account. The charging stations used have a maximum charging power of 50 kW, which means the algorithm is oriented towards DC charging stations.

Another algorithm that uses predefined load curves to control the charging algorithm is presented in [13]. A neural network–based algorithm is trained with a dataset that consists of data from more than 10,000 charging session and includes 18 different EV models. The algorithm performs well, but the drawbacks are the large amount of data and computationally heavy data processing. Data from all EV models has to be available so that the neural network model can be trained to accommodate all EVs, which may not be realistic in a practical setting. The SoC is used in the algorithm and is estimated based on the dataset. The algorithm does not account for different phases separately as the work done here. In contrast to our work, the algorithm presented in [13] can be computationally burdensome and prone to errors in real life.

Different phases and the problem of phase unbalance is considered in [14]. The problem is solved by using a phase switcher at each charging station. The approach is verified through simulations with a time step of 15 min. The work does not include tests on real EVs. The results lack the real measured charging curves that would likely impact the results significantly. The work in [15] introduces a new EV charging algorithm with

the main objective to reduce losses in the low voltage distribution network and considers phase balancing for domestic single-phase chargers. In addition, the impact of loss minimization, load flattening, and phase balancing on the increased charging times is not included in the work. Likewise, compatibility with common charging standards is not mentioned.

As seen in the state of the art, there are no algorithms that use the actual measured current as feedback to the algorithm and are compatible with the commercial charging standards as well as validated with real EVs. The non-idealities considered by the algorithm presented include the following:

- At three-phase charging stations, a customer can charge by using one, two, or three phases.
- The charging phase(s) can be any, or any combination, of the three phases.
- Charging can be unbalanced—different currents drawn from different phases.
- The charging system operator does not know beforehand which phases the EV uses for charging.
- The current drawn by the EV is altered during a charging session.
- The EV can use any current for charging below the maximum current limit, or set point, at the charging station.
- There is always an offset (positive or negative) between the current set point and the real charging current.
- There is always a time delay from the moment the current set point is changed to the moment that the desired charging current is reached.

Accounting for the above non-idealities will improve the efficiency of any adaptive charging algorithm. To the knowledge of the authors, no paper considering all of the above non-idealities in charging management can be found in the literature. This is the major difference between this work and the previous works. The aim of this work is to provide a strategy for how the non-idealities of EV charging can be accounted for to make each charging process more capacity efficient. The algorithm presented can be used with a fixed maximum current for the charging site. In addition, the algorithm can be used with any other strategy that determines the maximum current of the charging site according to an external signal, such as the price of electricity. That is to say, the algorithm of this work does not replace, but complements, other charging algorithms. Thus, this paper addresses this previously unstudied topic, and the proposed algorithm answers different questions from those of most other research on EV charging algorithms. The main contributions of this paper are the following:

- Demonstrate that non-idealities exist in EV charging that have not been considered in previous research.
- Identify the impact of these non-idealities on EV charging management.
- Provide a novel strategy how the non-idealities can be handled in a commercial EV charging application.
- The strategy considers the above-mentioned factors and improves the use rate of network capacity at the charging

site significantly in comparison with the previously suggested algorithms.

- The strategy is tested using commercial EVs and charging infrastructure.

The remaining parts of this paper are organized as follows. Section 2 describes the experimental setup used. Section 3 introduces the proposed charging algorithm. Section 4 presents the experimental results. Section 5 discusses the obtained results. Finally, Section 6 presents the conclusion and suggests ideas for future work.

2 | EXPERIMENTAL SETUP

This section covers the descriptions of the experimental laboratory setups. The first subsection describes the organization of the current set point response test. The second subsection describes the experimental setup of the algorithm validation by using two real EVs. The third subsection covers the experimental testing of the proposed algorithm under a real test case. All laboratory tests are carried out at TU Dortmund University [16].

2.1 | Current set point response test

The purpose of the current set point response test is to measure how quickly popular commercial EV models react when the current set point is changed at a charging station. In addition to the time delays, the offsets between current set points and the real charging currents are observed. The measurements are coordinated by a Python script that sends the current set points to the charging station and reads the current measurement. The communication is carried out by using Modbus TCP/IP protocol. The used charging station is an RWE eStation equipped with a Phoenix Contact Advanced EV Charge Controller. The controller supports the standard IEC 61851-1. The currents are measured at the charging station once per second with a KoCoS EPPE PX power quality analyzer and KoCoS ACP 300 current probes.

During the first 10 s of the test, the charging is disabled. At the beginning of the 11th second, the charging process is enabled, and the current set point is set to 6 A. At the beginning of the 21st second, the current is set to 7 A. The current set point is increased every 10 s until it reaches 16 A. After that, it is again reduced by 1 A every 10 s until it reaches 6 A and finally the charging is disabled. The used charging controller supports integer values with a minimum resolution of 1 A when controlling the charging current. Thus, steps smaller than 1 A are not possible. That is why a current step of 1 A is used thorough in all experiments and in the presented charging algorithm. For additional clarification, the idea of current set point response test is to assess the behaviour of the EVs at all possible current set points that a commercial charging controller can have between 0 and 16 A.

A Modbus signal is registered and sent to the charging station once it is executed by the Python programme. However, there

TABLE 1 Characteristics of the used electric vehicles

Vehicle model	Charging phase	Max. charging current	Connector
Nissan Leaf	Phase A	16 A	Type 1
BMW i3	3-phase	16 A ('max.')	Type 2
BMW i3	3-phase	16 A ('reduced')	Type 2
BMW i3	3-phase	16 A ('low')	Type 2

TABLE 2 The differences between the different charging modes of BMW i3 according to the manufacturer [17]

Current set point	'Maximum' mode	'Reduced' mode	'Low' mode
8 A	8 A	6 A	6 A
10 A	10 A	7.5 A	6 A
12 A	12 A	9 A	6 A
15 A	15 A	11.25 A	7.5 A

are communication delays before the signal reaches the EV, such as the mechanical movement of the contactor at the charging station, when enabling and disabling the charging, causes an additional time delay. Thus, these delays are in the range of 2–4 s and are included in the delays seen in the measurement results. The used EV models are shown in Table 1.

A charging controller at a charging station sets the current set point, but an EV can charge with any current below that set point. It should be noticed that an EV can have charging modes or settings. The purpose of the different charging modes may be to increase the energy efficiency or safety. For example, the BMW i3 has three charging modes for AC charging: 'low', 'reduced' and 'maximum' mode [17]. These modes cannot be changed from the charging station. The current is measured only at the charging phases: for the Nissan Leaf phase A and BMW i3 phases A, B, and C.

Table 2 shows the differences between the different charging modes of the BMW i3 [17]. The settings are country-specific and vary between different areas [17].

2.2 | Validation of the charging algorithm

Here the experimental setup of the second test is explained. The objective is to validate the algorithm in a laboratory environment by using two real EVs so that the behaviour of the EVs is easy to observe. Moreover, this test proves that the algorithm is compatible with the standard IEC 61851.

The laboratory setting is similar to the one of the current set point response test with the exception that now both charging sockets are measured with KoCoS EPPE PX power quality analyzers that communicate with the controlling computer via Modbus TCP/IP. The control algorithm is written in Python and runs on a computer in the laboratory. In the algorithm, measured current less than 1 A is considered as noise and set to 0. This is to prevent a noise-originated malfunction of the algorithm. Even if the algorithm runs in the time steps of 1 min, the current measurements are taken every 20 s. The
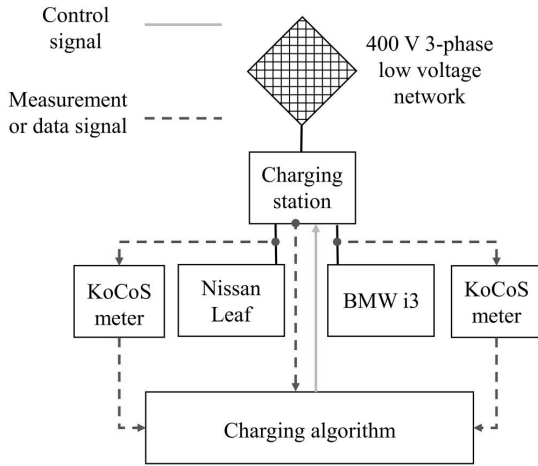
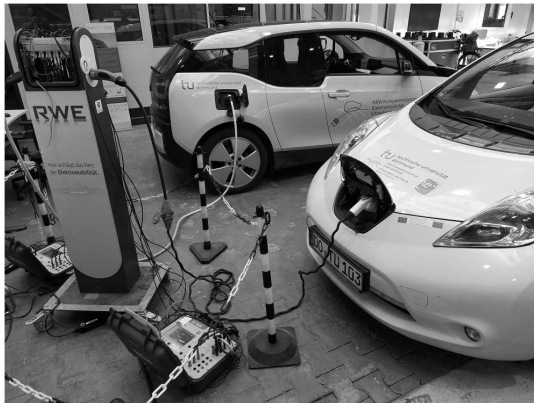**FIGURE 1** Experimental setup of the charging algorithm validation

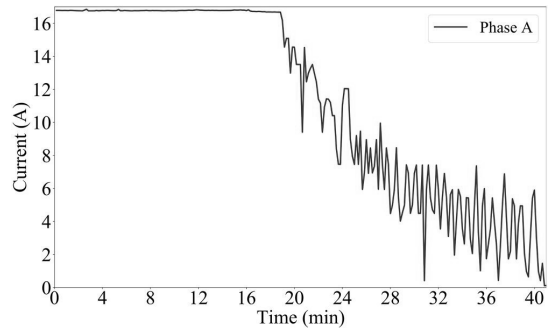**FIGURE 2** Laboratory setting in the algorithm validation

FIGURE 3 Decreasing-current part of the uncontrolled charging curve of Nissan Leaf
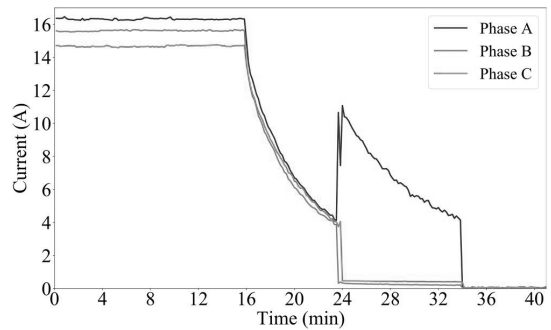
FIGURE 4 Decreasing-current part of the uncontrolled charging curve of BMW i3

scheme of the experimental setup is illustrated in Figure 1. The setup with the charging station, the measurement equipment and the used EVs can be seen in Figure 2.

To understand the details of the following Tests 1, 2, and 3, the uncontrolled charging curves of the Nissan Leaf and BMW i3 are presented in Figures 3 and 4.

In Figures 3 and 4, not the complete charging curve, but the part of decreasing current is presented. The starting SoC of the Nissan Leaf is 92% and the SoC of the BMW i3 is 87%. The current measurement is taken every 10 s. The BMW i3 is in 'maximum' mode. It is important to point out that by using two EVs, the details of the functioning of the proposed algorithm are distinguishable. The common purpose of the tests is to demonstrate in a detailed manner that the algorithm works with real hardware.

In continuation, the used three test cases are presented. The tests are selected so that the performance of the proposed charging algorithm can be observed in detail under challenging

circumstances. In each test case, a limit for the total current (current drawn by the Nissan Leaf summed by current drawn by the BMW i3) is set. This is the total current that the charging site uses to supply EVs. In Tests 1 and 3, the limit is 20 A, and in Test 2, it is 15 A. In reality, this limit would be defined by a selected electro-technical limit, such as the rating of the fuses, cables or a transformer. In the following tests, two EVs are used, so the limit is set lower than it would be in a reality to increase the complexity of the test cases and to verify the operation of the algorithm.

2.2.1 | Test 1

The purpose of this test is to demonstrate the dynamic performance of the charging algorithm. In this test, the BMW i3 is set to 'low' mode to see the functioning of the algorithm as evidently as possible. This is because in this mode, the BMW i3 has fewer current steps than in other modes, and as a consequence, the offset between the current set point at a charging station and the real charging current is larger and thus better observable. Before the start of the test, the initial SoC of the Nissan Leaf is 50% and the SoC of the BMW i3 is 85%. In this test, the maximum limit for both EVs is selected as 20 A,

which means that both EVs cannot charge at full current simultaneously and the algorithm has to limit the charging.

2.2.2 | Test 2

This test shows the performance of the algorithm in another situation with a lower current limit and with different starting SoCs of the EVs than in Test 1. In addition, the BMW i3 is in a different charging mode. The total limit of the current is set to 15 A, which means that any of the two EVs is not able to charge with maximum current. The BMW i3 is set to 'maximum' mode. The starting SoC of the BMW i3 is 73% and of the Nissan Leaf is 90%.

2.2.3 | Test 3

The objective of this test is to show how the algorithm detects that two EVs charge at different phases, so charging current does not need to be limited. The total current limit is 20 A. On the side of the BMW i3, phase A and phase C are disconnected at the charging station, so the BMW i3 can only charge using phase B. The Nissan Leaf is charged at phase A as in all tests. The BMW i3 is set to 'maximum' mode. The initial SoC of Nissan Leaf is 85%, while the BMW i3 has 70%.

3 | CHARGING ALGORITHM

Before the description of the algorithm, it is important to underline that the objective is to form a set of practices that create a basis for other charging management algorithms. The proposed algorithm is illustrated in Figure 5. The algorithm is executed in 1 min time steps.

The algorithm is divided into two parts. Firstly, the 3-phase capacity is divided evenly between all EVs in state C or D, meaning that they are ready to receive energy (see Table 3). An even division of the 3-phase charging capacity means that total charging capacity (in amperes) is divided by the number of active charging sessions. The decimals of the division are eliminated, and the remaining natural number is given as a set point to all active charging sessions. Secondly, the remaining capacity is divided between 1-phase EVs, repeating phases A, B, and C (phase p). This means that the 1-phase charging sessions may receive higher allowed current. However, 3-phase charging sessions are still likely to receive higher charging powers.

When an EV is connected, the algorithm supposes that the EV charges at three phases. The algorithm gives one-time step to the EV to react. During this time, the algorithm memorizes which phase(s) the EV uses for charging. Because some EVs react slowly, one time step is required to avoid a malfunction.

A core feature of the algorithm is that it learns the behaviour of the EV that is currently charging through the
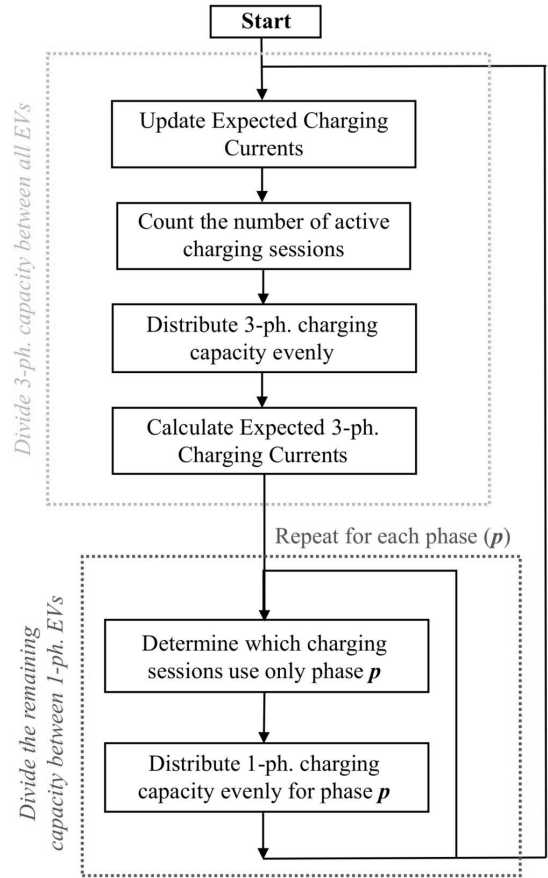
FIGURE 5 Flowchart of proposed charging algorithm

TABLE 3 Simplified charging states according to IEC 61851

State	Message
A	EV not connected
B	EV or Electric Vehicle Supply Equipment not ready to receive energy
C	EV is charging
D	Charging is possible. EV requires charging area ventilation.
E	Error
F	Fault

Abbreviation: EV, electric vehicle.

use of expected charging currents. For clarity, this is described in an own subsection. Simplified explanations of the charging states according to the standard IEC 61851 are explained in Table 3. It is important to notice that even though each EV is modelled separately by means of expected charging currents, the algorithm is computationally light, which makes it easily scalable to cover large charging sites.

TABLE 4 Expected charging currents during the first time step of the algorithm for every charging station. All values in amperes

Set point	Phase A	Phase B	Phase C
6	6.0	6.0	6.0
7	7.0	7.0	7.0
8	8.0	8.0	8.0
9	9.0	9.0	9.0
⋮	⋮	⋮	⋮
32	32.0	32.0	32.0

TABLE 5 Expected charging currents during second time step of the algorithm for BMW i3 after updating first-row values. All values in amperes

Set point	Phase A	Phase B	Phase C
6	6.3	5.8	5.7
7	7.0	7.0	7.0
8	8.0	8.0	8.0
9	9.0	9.0	9.0
⋮	⋮	⋮	⋮
32	32.0	32.0	32.0

3.1 | Expected charging currents

The idea of expected charging currents is to make the algorithm capable of memorizing the unique charging characteristics of a charging session without the need for obtaining any information from the vehicle. Expected charging currents keeps track on each EV of which phases are being used and how much current is drawn from each phase. It is important to underline that expected charging currents are not calculated, but they are direct measurements of phases A, B, and C at the charging station.

When an EV is connected to a charging station and changes from state A to state B, the behaviour of the EV is expected to be 'ideal' and three-phase connected. This means that the EV draws exactly the current indicated by the current set point at each phase. Expected charging currents of each charging session are updated every time the algorithm is executed. An update means that the three-phase currents at the given current set point are added to expected charging currents. An illustration of how expected charging currents are structured and updated as illustrated in Tables 4 and 5. During the very first time step of the algorithm, the EV is expected to be 'ideal'. In this case, expected charging currents for any charging station are as presented in Table 4.

During the second execution of the algorithm, expected charging currents is updated according to the measured current. The measured current values are stored in the columns labelled according to the phases as A, B, and C. In the case of the BMW i3, for example, the expected charging currents after the first update are presented in Table 5.

The BMW i3 charges at 3 × 6 A, but in reality, offsets in the phase currents exist. This procedure is continued through
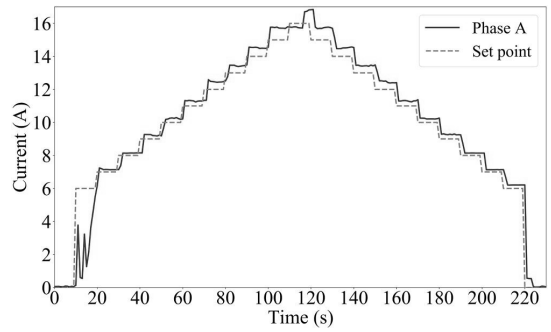
FIGURE 6 Measured current of Nissan Leaf and current set point

the whole charging process. If the algorithm detects that current flows only during one phase (a single-phase EV), the values of the other phases are set to 0. Allowing each EV to start charging with 6 A means that the algorithm allows temporary overload of maximum 6 A per EV. However, this overload will last 1 min as maximum. In case of a failure when reading a current measurement, the algorithm uses the previously measured value. This alleviates the impacts of short communication failures while still allowing the algorithm to operate on each control cycle.

4 | RESULTS

This section first presents the results of the current set point response test. Subsequently, the results of the algorithm validation are introduced.

4.1 | Current set point response test

The results of the current set point response test of the EVs in Table 1 are presented in Figures 6–9. The current of phase A of the Nissan Leaf and the current set point are illustrated in Figure 2.

In Figure 6, it is observed that the Nissan Leaf starts to react within 2 s after the charging is enabled. It takes 10 s to reach 6 A charging current from the disabled position. Once the charging is enabled, the next charging current is reached within the maximum time of 2 s. Similar time delays are seen thorough the increasing part (0 to 110 s) as well as the decreasing part (110 to 220 s) of the test.

The current offset is higher with a higher charging current. When the current set point is 7 A, the maximum measured current is 7.24 A. The largest offset is measured when the current set point is at 16 A, in this case the current is 16.84 A. According to the standard IEC 61851, the maximum current drawn by the EV does not include inrush or leakage currents. The currents of phases A, B, and C of the BMW i3 under different charging modes and the current set point are shown in Figures 7 ('low' mode), 8 ('reduced' mode), and 9 ('maximum' mode).
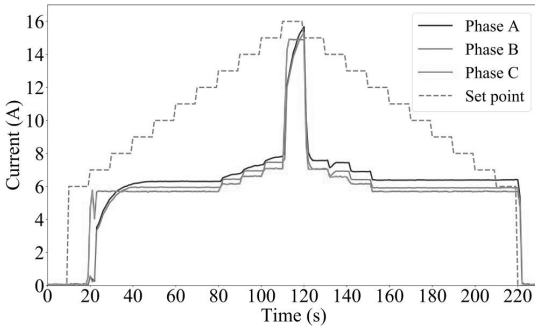
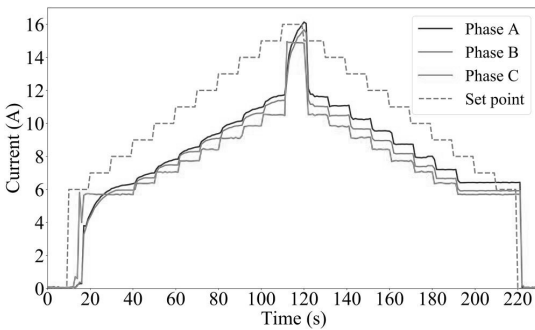**FIGURE 7** Measured current of BMW i3 ('low' mode) and current set point

FIGURE 8 Measured current of BMW i3 ('reduced' mode) and current set point
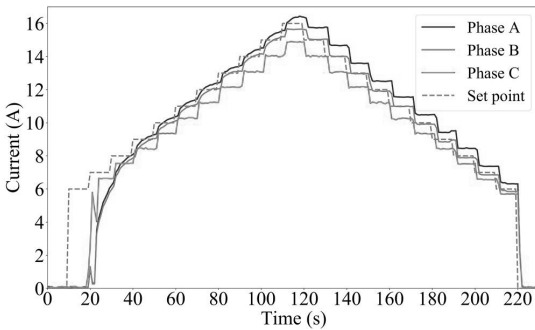

FIGURE 9 Measured current of BMW i3 ('maximum' mode) and current set point

Through all three charging modes, phase C has the shortest response time. When the BMW i3 is on the 'low' mode, five levels of charging currents are measured at phase C with the following set points: 6, 7, 8, 9 and 16 A. In 'reduced' mode, different current levels are measured with the set points 6, 7, 8, 9, 10, 11, 12, 13 and 16 A.

Most of the time, current at phase A has the most elevated values. In 'low' mode, the largest measured difference of the
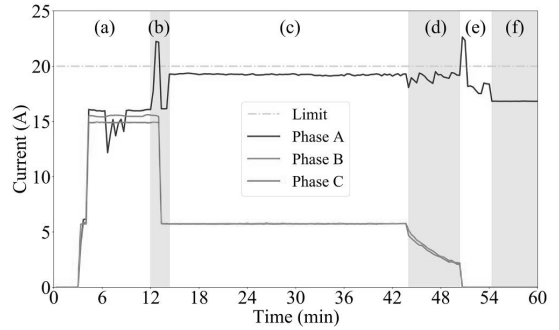
FIGURE 10 Sum of the measured phase currents of both electric vehicles and the limit in Test 1

current between phase A and phase C is 2.3 A. In 'reduced' mode it is 3.3 A and in 'maximum' mode, it is 2.3 A. However, these values are measured during the transient times when the current is changing from one set point to another one. Most of the time, the current difference between phase A and phase C is around 1 A.

In 'low' mode, the differences between the measured phase currents and the current set point is the largest. At steady state, the largest measured offset between phase C and the set point is 7.96 A at the time step 124 s (in Figure 7). In 'reduced' mode, the measured currents are closer to the set point (Figure 8) and in 'maximum' mode, even more (Figure 9). However, it is crucial to consider that at 'low' and 'reduced' modes, the EV is not designed to charge at the set point current but has its internal limitations [17]. These limitations cannot be changed by the charging controller at the charging station.

When the Nissan Leaf mostly draws current that is higher than the set point, in the case of the BMW i3, it depends on the phase. On the 'maximum' mode, during the time when the charging is enabled, phase A has an average bias of 0.93 A, phase B 0.73 A and phase C 1.03 A from the set point. Therefore, once the current has reached the desired level, phase B follows the set point most accurately.

4.2 | Validation of charging algorithm

The results of Tests 1, 2, and 3 are presented in the following three subsections to validate the correct functioning of the algorithm with real EVs. The results from Figure 10 onwards are shown in corresponding order. Only the phase currents where the EVs draw energy are illustrated. The solid lines present currents and the non-solid lines present the limit (light blue) or the corresponding current set point (grey).

To increase the readability, each test is divided into steps (a), (b), (c) etc. and highlighted by a grey or white background colour, all of which is clarified in detail following the figures.
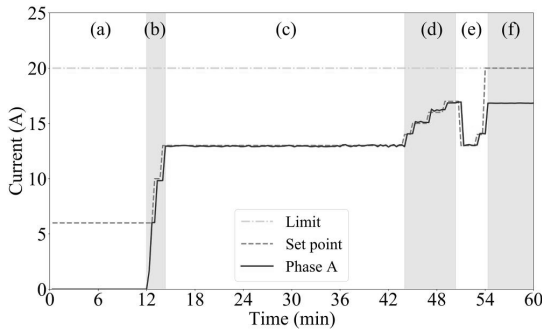
FIGURE 11 Measurements of Nissan Leaf in Test 1
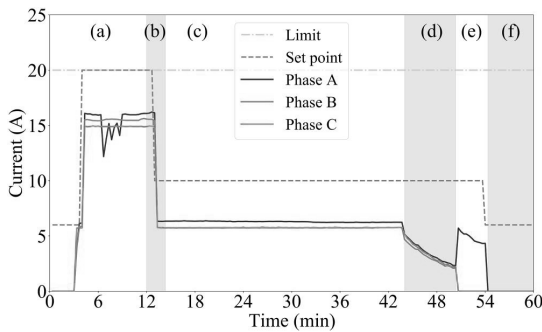
FIGURE 12 Measurements of BMW i3 in Test 1

4.2.1 | Test 1

Results of Test 1 are observed in Figures 10 (the sum of the currents), 11 (Nissan Leaf), and 12 (BMW i3).

(a) At the beginning, no EV is connected. At about 3.5 min, the BMW is connected. The algorithm allows the BMW to charge with 6 A using all three phases. During this minute, the algorithm verifies how much free charging capacity the charging site has. Because no other vehicles are connected, the algorithm gives 20 A to the BMW. Thus, BWM increases the charging current to full capacity (~16 A). The measured ripple at phase A between 6 and 9 min (Figures 10 and 12) is characteristic behaviour of the BMW i3 and is not caused by the algorithm.

(b) At minute 12, the Nissan Leaf is connected to the charging station. Since the algorithm allows the Nissan to start charging at ~6 A, and the BMW is using ~16 A at phase A, the total current of the charging site at phase A increases to ~22 A. In the next control cycle, the algorithm notices that the current limit is exceeded and calculates new current set points to both EVs. By design, the algorithm aims at dividing the charging current as evenly as possible between the EVs. Thus, it establishes a set point of 10 A to both EVs. However, in 'low' mode, BMW charges at ~6.3 A (measured in Figure 7) with the set point

of 10 A. Hence, ~3.7 A of the charging capacity allocated to BMW is not used. The algorithm allocates 3 A more to the Nissan, and it starts charging at ~13 A. This is the maximum capacity that can be allocated to the Nissan without exceeding the total limit of the charging site (20 A).

It is important to notice that in (b), the efficiency of the algorithm is easily observable. If the algorithm did not have an adaptive nature, the real charging current of the BMW (~6.3 A) could not be detected, and as a consequence, additional current (3 A) could not be allocated to the Nissan. Thus, the Nissan would have continued to charge at ~10 A instead of ~13 A, representing a longer charging time.

(c) The Nissan is charging at ~13 A and the BMW at ~6.3 A. Due to the used charging controller, current is regulated in the steps of 1 A, the total current is slightly less than 20 A (Figure 10).

(d) At minute 44, BWM starts the decreasing-current phase of charging since the battery is close to be full. This characteristic can be also clearly seen in Figure 4. Decreasing charging current of the BMW means that more capacity can be allocated to the Nissan. As the BMW frees the charging capacity, the algorithm allocates more charging capacity to the Nissan. This is seen as stepwise increase of the set point and the charging current in Figure 11.

(e) The Nissan charges at ~16.9 A. At minute 51, phase A current of the BMW increases to ~5.7 A. This is characteristic of the BMW i3, and the same phenomenon is visible also in Figure 4. The increasing current of the BMW can be seen as a peak of ~22.7 A in Figure 10. The algorithm reacts to this by decreasing the set point of the Nissan to 13 A. When the BMW naturally decreases the charging current, more charging capacity is allocated to the Nissan by increasing the set point of the Nissan to 14 A. When the BMW stops charging as a result of its fully charged battery at minute 53, the whole charging capacity of the charging site (20 A) is allocated to the Nissan. However, the Nissan can charge at ~16.8 A, as measured also in Figure 3.

4.2.2 | Test 2

Results of Test 2 are presented in Figures 13, 14, and 15.

(a) At minute 0, no EV is connected. During minute 1, the Nissan Leaf is connected to the charging station. Directly when the Nissan is connected, 6 A is allocated to it. During this minute, the algorithm calculates the capacity that can be allocated to the Nissan. Since the limit of the charging site is 15 A and there are no other EVs connected, the algorithm allocates 15 A to the Nissan. Consequently, the charging current of the Nissan increases. However, with the set point of 15 A, the Nissan Leaf actually charges at ~15.2 A, which would mean
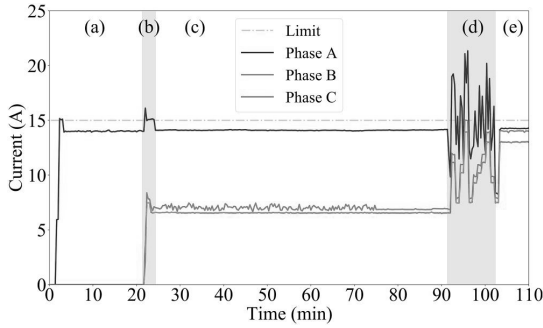
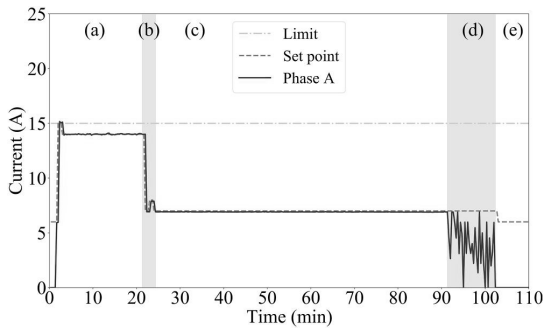**FIGURE 13** Sum of the phase currents of both electric vehicles in Test 2

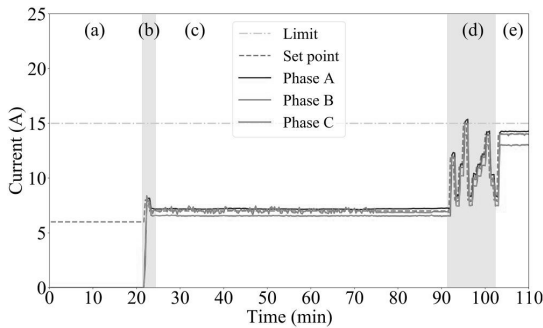**FIGURE 14** Measurements of Nissan Leaf in Test 2

FIGURE 15 Measurements of BMW i3 in Test 2

~0.2 A overload. This behaviour is also measured in Figure 6. As a consequence, the algorithm reduces the set point of the Nissan to 14 A, and the Nissan actually charges at ~13.9 A. This is an inherent characteristic of the algorithm to guarantee that the total current limit of the charging site is not exceeded over several minutes.

(b) At minute 22, the BMW i3 is connected to the charging station. Since the Nissan is already charging at ~14 A and 6 A is allocated to the BMW when connected, and the

BMW slowly increases its charging current, a maximum peak of ~16.1 A is experienced at phase A. Other phases are not overloaded. The algorithm corrects the overload situation by dividing the charging capacity between both EVs as evenly as possible. Thus, it allocates 7 A to the Nissan and 8 A to BWM. However, it notices that with the set point of 8 A, the BMW actually draws ~8.2 A and the Nissan ~6.9 A, so the algorithm reduces the set point of the BMW to 7 A and increases the set point of the Nissan to 8 A. Then, the algorithm learns that the Nissan charges ~7.9 A with the set point of 8 A and that the BMW charges ~7.2 with the set point of 7 A, so it reduces the set point of the Nissan to 7 A, resulting in a charging current of ~6.9 A. Thus, the set point of both EVs is set to 7 A with the total resulting charging current of ~14.1 A.

(c) Both EVs are charging with a constant charging current.

(d) During minute 91, the Nissan Leaf starts to reduce its charging current because of the high SoC of the battery. Throughout this time, the current oscillates. This is a characteristic of the Nissan Leaf, which is seen also in Figure 3. This causes stepwise increments and reductions of the current set point of the BMW i3. During this time, short overloading occur (Figure 13), with the highest peak of ~21.1 A. At minute 102, the battery of the Nissan Leaf is full and it stops charging.

(e) Since the Nissan Leaf does not charge anymore, the total capacity (15 A) could be allocated to the BMW i3. However, during (d), the algorithm has memorized that with the set point of 15 A, the BMW i3 charges slightly more than 15 A at phase A. This has been registered in expected charging currents of the BMW i3. Thus, the algorithm fixes the set point of the BMW i3 to 14 A instead of 15 A with the aim at avoiding a long-term overload. The BMW i3 continues to charge with the set point at 14 A.

4.2.3 | Test 3

Lastly, the results of Test 3 are presented in Figures 16, 17, and 18. It should be noticed that in this test, the BMW i3 uses only phase B to charge because of the physical disconnection of phase A and phase C. That is why only the measurements at phase B of the BMW i3 are presented. The current limit of the charging site is set to 20 A.

(a) At the beginning, no EV is connected to the charging station. Before minute 2, the Nissan Leaf is connected. During the first minute of connection, the algorithm has set the set point of the Nissan Leaf to 6 A.

(b) Approximately at 2 min 20 s, the set point of the Nissan is set to maximum of 20 A, since no other EVs are connected to phase A. The Nissan continues charging with the maximum current, which is measured at ~16.7 A. In the moment of 5 min 20 s, the BMW i3 is connected to the charging station. In this case, the BMW i3 is charging only at phase B, but the algorithm does not have such
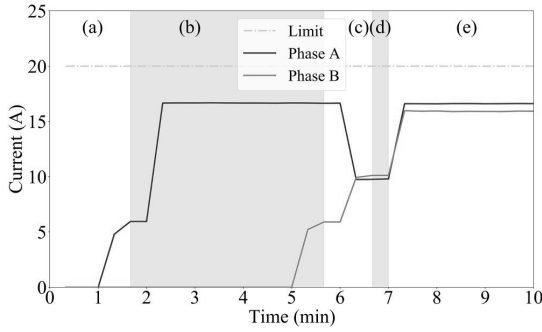
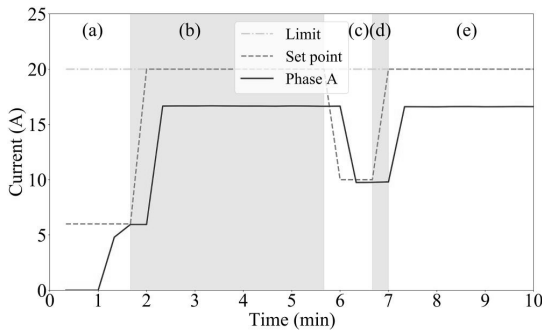**FIGURE 16** Sum of the phase currents of both electric vehicles in Test 3

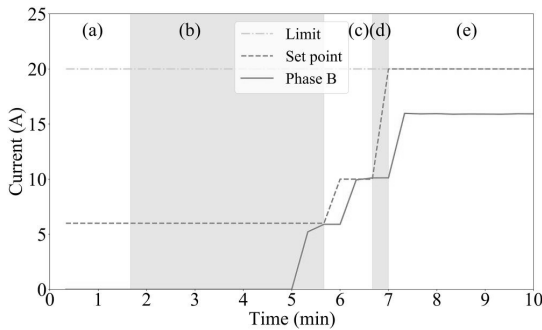**FIGURE 17** Measurements of Nissan Leaf in Test 3

FIGURE 18 Measurements of BMW i3 in Test 3

information, so it supposes that the BMW will charge in 3-phase manner as explained in Section 4.1.

(c) The algorithm expects that the BMW i3 charges 3-phase and divides the charging capacity evenly to both EVs. Thus, it increases the set point of the BMW i3 from 6 to 10 A and reduces the set point of the Nissan Leaf from 20 to 10 A.

(d) The algorithm learns that the BMW i3 charges only at phase B. In addition it knows that the Nissan Leaf uses only phase A. In addition, from expected charging

currents of the Nissan Leaf it knows that with the set point at 20 A, the Nissan Leaf does not exceed 20 A. As a consequence, it increases the set points of both vehicles to the maximum of 20 A.

(e) Both EVs continue charging with the full capacity because they are connected to different phases.

5 | DISCUSSION

The measurements demonstrate that the delays from a change in the current set point to a steady state are mostly a matter of a few seconds. Standard IEC 61851 defines 5 s as the time an EV has to react to a new current limit, and during this time, the charging controller shall not change the current limit. This sets the absolute minimum limit for the time step that can be used to execute the algorithm. To guarantee the correct functioning of the charging algorithm, a time step shorter than 5 s should not be used. Otherwise, not all EVs may have time to reach a new current set point. The used communication technology, the charging controller, and the charging station can have an impact on delays.

In the current set point response test, the current set points are changed in 1 A steps. The charging dynamics may be different if, for instance, the set point is set from 6 to 16 A. This should be verified in further development work. The current set point test illustrates that there is always a difference between the current set point and the real charging current. With the measured EV models and charging modes, there is a great variety of offset. The largest measured offset at a steady state with the BMW i3 is 7.96 A, which was measured in the 'low' mode at the time step 124 s (in Figure 7) in phase C. From the point of view of the EV, this is really not an offset, because the EV is not even meant to be charged at the current indicated by the set point. In this case, the EV is designed to charge at 7.5 A [17] and in reality, it charges at 7.04 A in phase C, while the algorithm would like it to charge at 15 A. The issue is that the charging algorithm is not aware of the internal limitations of the EV and does not know that by changing the charging mode, a higher charging current can be used. Thus, from the viewpoint of the EV, the offset is 0.46 A, and from the viewpoint of the charging algorithm, the offset is 7.96 A.

Such an extreme offset can have a fundamental reducing impact on the efficiency of a charging algorithm, especially, when controlling several EVs at the same charging site. Otherwise, when the difference between the current offset and the measured current is, say, less than 1 A, it probably will not have much impact small charging sites. Another story is in the case of large sites with tens of simultaneous charging sessions. In that case, even offsets of 1 A may accumulate up to tens of amperes. If the charging current was not measured at all but expected that the EVs charge exactly the current defined by the set point, it could lead to overloading cables or a distribution transformer.

In reality, the EV fleet consists of different models with different load curves and offsets. This leads to a balancing

effect at a large charging site and reduces the risk of malfunction of the algorithm due to the accumulation of the offsets at the same phase. For better general knowledge, the current set point response test covering more EV models should be repeated to see the variations between different EV models in this regard. However, the proposed charging algorithm takes the offsets into account.

The validation of the proposed algorithm through three tests show that the algorithm works as intended with commercial EVs, under various circumstances. The algorithm adapts well in situations, where current drawn by EV or EVs increases or decreases suddenly. The proposed algorithm complies well with the charging standard IEC 61851.

EV models possess different characteristics with regard to charging [18]. Even the same EV can behave in different ways depending on its charging settings. The charging system operator does not know what kind of charging curve the EV connected to a charging station has. It is also possible that even the EV driver is not aware of the charging settings. This poses a potential reduction in efficiency of the charging management algorithm applied by the charging operator. If the charging management algorithm is unable to regulate the charging current as intended or if the gap between the current set point and the real charging current is overlooked, it is likely that there is network capacity allocated to an EV that in reality is not used completely. Perhaps this unused capacity could be allocated to another EV. For instance, if 10 A is allocated to an EV, but it charges with only 6 A, the resting 4 A could be used by another vehicle.

While in the case of most EVs, the load curve starts to decrease during the last 1%–3% of the SoC. Keeping in mind the average daily distances, a large part of the time, the EVs are charged during this decreasing phase [19]. As one EV releases network capacity because of the decreasing current phase of the charging process, this free capacity is reallocated to other EVs. This is an inherent and efficient characteristic of using measured currents in the charging algorithm. In this regard, the efficiency of the proposed algorithm is assessed in Tests 1 and 2.

In essence, the less accurately the charging operator can regulate the charging current of the charging EVs, the higher is the inefficiency of the charging system as a whole because the charging management algorithm does not perform as it was designed to. The problem of phase imbalance can be mitigated through phase swapping [20] at difference charging stations. This helps to alleviate the problem but does not guarantee that it will be eliminated. The algorithm handles well sudden unbalances as seen in Test 1. In addition, it operates even under a case of long-term unbalance as seen in Test 3.

Even if the algorithm allows a temporal overload of maximum 6 A per vehicle, in a real case, it is very unlikely that it would pose a problem because of two reasons. Firstly, the fuses of a charging site do not react immediately to small overloads. For example, a widely used gG fuse must withstand 25% overcurrent at least 1 h, according to the standard IEC 60269. In addition, such short-term overcurrent does not have time to overheat the network components. Secondly, it is unlikely that many EVs are connected to the charging station exactly within the same minute at the same charging site. The performance of the algorithm under overloads is seen in Tests 1 and 2.

It can be argued that from the customer point of view, it might be important that the charging process starts as soon as possible when the EV is connected to the charging station. In this way, a customer notices immediately that the EV starts charging and does not worry that the EV will not charge because of a malfunction, for example. This may improve the user experience.

The proposed algorithm is especially suitable for large charging sites with tens or hundreds of charging stations. This is because it may not be economically feasible to size the network of such site to be able to cover the peak demand. Apart from that, many large charging sites, such as shopping centres, have a high percentage of short charging sessions [19]. Thus, an efficient charging management is likely to be reflected as higher SoCs of the batteries and improved customer experience.

Even if the algorithm focuses on the network capacity at the charging site, more efficient use of this capacity may be also indirectly beneficial for the distribution network upstream. With a view to practical applications, an advantage of the proposed algorithm is that it is mathematically easy to understand and computationally lightweight. It does not include computationally demanding algorithms, such as neural networks.

6 | CONCLUSION AND FUTURE WORK

An original algorithm for EV charging management is presented. The proposed algorithm creates a basis for further charging algorithms to become more efficient in real charging solutions. The novelty of the algorithm is twofold.

Firstly, the proposed algorithm considers several non-ideal charging behaviours of EVs in which no comprehensive solutions have previously been proposed. These non-idealities are the unknown charging phase or phases, the offset between the real charging current and the current set point at the charging station, unbalanced charging, and the otherwise unknown charging curve. The key to the algorithm is that it is based on measurements of the actual charging current and does not rely on predefined load curves. Thus, no modelling or data about the EVs is necessary.

Secondly, the algorithm focusses on maximizing the charging current within the capacity limits of the power network or otherwise set limit. This leads to a high use rate for the power network and a reduction in charging times.

According to the test with commercial EVs, the algorithm is robust, straightforward, and computationally light. These are positive aspects with a view towards practical applications. In addition, the algorithm does not need any additional information from the vehicle or user. The only requirement is that the vehicle must fulfil charging standard IEC 61851. The

algorithm is tested experimentally by using commercial EVs and charging infrastructure. Consequently, the algorithm is suitable for real applications and compatible with charging standard IEC 61851. For communication amongst the algorithm, charging controllers, and measurements devices, Modbus TCP/IP is used, which is a well-established and robust communication protocol.

To the best knowledge of the authors, no other algorithm in the published research literature uses measured phase currents in the operation of charging management. Neither has any other algorithm had the main objective to maximize used network capacity to overcome the non-ideal behaviour of EVs. Therefore, the presented work fills a gap in research knowledge.

In the future, new strategies to improve expected charging currents will be studied, and the algorithm will be improved against oscillations. The performance of the algorithm will also be compared with other charging management algorithms. Additionally, the algorithm will be tested using a larger number of real EVs and charging stations to prove its scale capabilities. Lastly, the algorithm will be validated by a commercial charging system operator in a field test.

ACKNOWLEDGEMENTS

ORCID

Kalle Rauma https://orcid.org/0000-0002-5553-8751
Toni Simolin https://orcid.org/0000-0002-0254-1113

REFERENCES

1. Calearo, L., et al.: Grid loading due to EV charging profiles based on pseudo-real driving pattern and user behaviour. IEEE Trans. Transp. Electrification. 5(3), 683–694 (2019)
2. Lillebo, M., et al.: Impact of large-scale EV integration and fast chargers in a Norwegian LV grid. J. Eng. 18(7), 5104–5108 (2019)
3. Szinai, J., et al.: Reduced Grid Operating Costs and Renewable Energy Curtailment with Electric Vehicle Charge Management. Energy Policy. 136, 136 (2020). https://doi.org/10.1016/j.enpol.2019.111051
4. Mellinger, M., van Vliet, O., Liimatainen, H.: Anxiety vs reality – sufficiency of battery electric vehicle range in Switzerland and Finland. Transport Res. Transport Environ. 65, 101–115 (2018)
5. Noel, L., Zarazua de Rubens Gerardo, Kester Johannes, Sovacool Benjamin K. et al.: Understanding the socio-technical nexus of Nordic electric vehicle (EV) barriers: A qualitative discussion of range, price, charging and knowledge. Energy Policy. 138, 111292 (2020). https://doi.org/10.1016/j.enpol.2020.111292
6. Miele, A., et al.: The Role of Charging and Refuelling Infrastructure in Supporting Zero-emission Vehicle Sales, pp. 81. Transportation Research Part D (2020)
7. Lee, Z., et al.: Large-Scale Adaptive electric vehicle charging. In: Proceedings of the IEEE International Conference on Communications, Control, and Computing Technologies for Smart Grids, Aalborg (2018)
8. Rautiainen, A., Järventausta, P.: Load control system of an EV charging station group. In: Proceedings of the 11th Nordic Conference on Electricity Distribution System Management and Development, Stockholm (2014)
9. Alinia, B., Hajiesmaili Mohammad H., Lee Zachary J., Crespi Noel, Mallada Enrique et al.: Online EV Scheduling Algorithms for Adaptive Charging Networks with Global Peak Constraints. IEEE Transactions on Sustainable Computing. 1–1 (2020). https://doi.org/10.1109/tsusc.2020.2979854
10. Alsabbagh, A., Yin, H., Ma, C.: Distributed charging management of multi-class electric vehicles with different charging priorities. IET Gener., Transm. Distrib. 13(22), 5257–5264 (2019)
11. Alsabbagh, A., Ma, C.: Distributed charging management of electric vehicles considering different customer behaviours. IEEE Trans. Ind. Inf. 16(8), 5119–5127 (2020)
12. Wang, Y., Thompson, J.S.: Two-stage admission and scheduling mechanism for electric vehicle charging. IEEE Trans. Smart Grid. 10(3), 2650–2660 (2019)
13. Frendo, O., et al.: Data-driven smart charging for heterogeneous electric vehicle fleets. Energy AI. Journal Pre-proof 1, 1–13 (2020). https://doi.org/10.1016/j.egyai.2020.100007
14. Kikhavani, M.R., Hajizadeh, A., Shahirinia, A.: Charging coordination and load balancing of plug-in electric vehicles in unbalanced low-voltage distribution systems. IET Gener., Transm. Distrib. 14(3), 389–399 (2020)
15. Crozier, C., Deakin Matthew, Morstyn Thomas, McCulloch Malcolm Coordinated electric vehicle charging to reduce losses without network impedances. IET Smart Grid. 3(5), 677–685 (2020). https://doi.org/10.1049/iet-stg.2019.0216
16. Spina, A., et al.: Smart grid technology lab – a full-scale low voltage research facility at TU Dortmund University. In: Proceedings of the AEIT International Annual Conference, Bari (2018)
17. Bayerische Motoren Werke AG: The BMW i3. Owners Manual, pp. 183. BMW AG, München (2016)
18. Dronia, M., Gallet, M.: Field test of charging management system for electric vehicle - state of the art charging management using ISO 61851 with EV from different OEMs. In: Proceedings of the 5th Conference on Future Automotive technology, Fürstenfeldbruck (2016)
19. Fenner, P., Rauma Kalle, Rautiainen Antti, Supponen Antti, Rehtanz Christian, Järventausta Pertti et al.: Quantification of peak shaving capacity in electric vehicle charging – findings from case studies in Helsinki Region. IET Smart Grid. 3(6), 777–785 (2020). https://doi.org/10.1049/iet-stg.2020.0001
20. Fang, L., Ma, K., Zhang, X.: A statistical approach to guide phase swapping for data-scarce low voltage networks. IEEE Trans. Power Syst. 35(1), 751–761 (2020)

PUBLICATION
7

Foundation for adaptive charging solutions: Optimised use of electric vehicle charging capacity

T. Simolin, K. Rauma, A. Rautiainen, P. Järventausta, C. Rehtanz

IET The Institution of Engineering and Technology WILEY

ORIGINAL RESEARCH PAPER

Foundation for adaptive charging solutions: Optimised use of electric vehicle charging capacity

Toni Simolin[1] 🄳 | Kalle Rauma[2] | Antti Rautiainen[1] | Pertti Järventausta[1] | Christian Rehtanz[2]

[1]Unit of Electrical Engineering, Tampere University, Tampere, Finland

[2]Institute of Energy Systems, Energy Efficiency and Energy Economics, TU Dortmund University, Dortmund, Germany

Correspondence

Toni Simolin, Unit of Electrical Engineering, Tampere University, Korkeakoulunkatu 7, 33720 Tampere, Finland.
Email: toni.simolin@tuni.fi

Abstract

As electric vehicles (EVs) are emerging, smart and adaptive charging algorithms have become necessary to ensure safe and efficient operation of the grid. In the scientific literature, most of the proposed charging control algorithms focus solely on EV usage-related behaviour, while the charging characteristics of EVs are overlooked. Herein, realistic charging characteristics are illustrated and discussed. More notably, to overcome the issues caused by the non-idealities in charging characteristics, a new adaptive charging characteristics expectation algorithm is proposed. The objective of this algorithm is to enable accurate estimation of the non-ideal charging characteristics. This can be used to reallocate any unused charging capacity and to ensure that the intended total capacity is used effectively. The effectiveness of the proposed algorithm is demonstrated using hardware-in-the-loop simulations with commercial EVs and real charging data. The results show that the proposed algorithm achieves an 88%–97% capacity usage rate, while the current benchmark solution achieves only 45%.

1 | INTRODUCTION

As electric vehicles (EVs) are emerging at a fast pace, smart charging solutions are becoming increasingly important. When it comes to real-life EV charging solutions, there are often numerous unknown variables to be considered. These unknown variables include the EV user-dependent charging behaviour (available charging time and energy requirement) and the EV technology-dependent charging characteristics, which define the current consumption at each moment of time. Herein, the term 'charging characteristics' is used to describe the complex correlation of the realised charging currents to the factors, such as the current limit set by the electric vehicle supply equipment (EVSE), the temperature and state-of-charge (SOC) of the EV battery, and the limitations of the on-board charger (OBC). For the development of efficient smart charging solutions, consideration of realistic charging behaviours and charging characteristics is imperative.

1.1 | Related research and motivation

In the scientific literature, the EV charging behaviour has been analysed from the EV use perspective (hourly/daily level) by using, for example, traffic survey data [1–8], energy metre-level data [9], and actual measurements of charging sessions [6, 10–13]. However, in addition to the differences in EVs' usage, the EVs also have different charging characteristics. It is often assumed that the EV charging current can be fully controlled, but in reality, the EVSE can only set the maximum charging current, and the EV can choose any charging current below the limit. There are several reasons for an EV to charge with a lower current than the limit set by the EVSE such as the vehicle's maximum charging rate being lower than the limit or the OBC may choose a lower charging rate to protect the battery from overheating [14]. The impacts of all these reasons are referred to as non-ideal charging characteristics as the charging current deviates from the current limit set by the EVSE.

From previous studies [1–14], only [4, 14] mention non-ideal charging characteristics, whereas the rest focus solely on EV usage-related behaviour. In [14], the realised charging currents are measured to determine the energy levels of the EVs more accurately. However, there is no mention of real-locating the unused charging capacity when an EV is drawing less current than the set limit. In [4], experimental measurements of a Citroen C-Zero are used to form a simplified model for the final charging curve. However, no other non-ideal charging characteristics are considered, and the same model is assumed for each EV in the simulations.

The issue regarding the non-idealities has recently been brought up in [15–17] and a solution is presented in [16, 17]. In [15], the final charging curves of 304 charging sessions are analysed. According to the analysis the different charging curves can be classified into six types with reasonable accuracy. In [16], a data-driven approach for integrating a machine learning model to predict the charging profiles is proposed. According to that study, the realised utilisation rate of the charging capacity was 65.8% of the planned utilisation when the EVs are assumed to draw the maximum power, whereas the proposed prediction algorithm achieves a 94.4% utilisation rate. The increased capacity usage rate leads to a higher charging energy dispatch and higher final SOC for the EVs in a limited infrastructure without the need for costly upgrades of the charging infrastructure [16]. Thus, these results signify the importance of the consideration of the non-ideal characteristics. However, even though the results of the proposed solution are very promising, there is a notable drawback. The approach requires a large data set of the charging processes of the EVs and the trained model only reflects the charging characteristics of the models included in the data set. Therefore, its usability might be restricted if the necessary data are not available. In [17], a capacity reallocation algorithm is proposed for a case considering two EVs and a peak power-based tariff. The algorithm is tested using hardware-in-the-loop (HIL) simulations with commercial EVs. The results show that the algorithm effectively reallocates unused charging capacity. However, the algorithm is limited to only two single-phase EVs and the reallocation method is not scalable to a larger charging site.

In public charging stations, it is not reasonable to assume that the charging characteristics of individual EVs can be accurately predicted in advance. In addition, the charge point operators do not have access to internal battery variables [16]. A control system can be made without feedback of the charging current measurements, but this does not enable the control algorithm to observe the realised charging load. The potential deviation between the planned loading and the realised loading is especially significant when considering three-phase charging points [16], because a notable share of all EVs (include both full EVs and plug-in hybrid EVs) support only single-phase charging. By measuring the charging currents, the control algorithm can learn or adapt to the charging characteristics of each EV during the charging sessions, which can then be used for optimisation purposes. Control algorithms with an ability to adapt and learn have been studied

before in, for example, [18–27]. However, the adaptation and learning in these studies focus on the usage-related behaviour, while the limitations caused by the non-ideal charging characteristics are overlooked.

When it comes to practical solutions that are compatible with the charging standards and commercial EVs, the present state-of-the-art solution is to assume that each active EV draws the current indicated by the EVSE, as in [28, 29]. An EV being active refers to a situation where it is plugged in and ready to receive energy. Both these studies acknowledge the fact that the realised charging currents of the EVs may be well below the limit set by the EVSE. In [28], the realised charging currents are measured and used to calculate the realised energy consumption of the EVs, but neither of the studies offers any solutions to reallocate the unused charging capacity.

Based on the literature review, it seems that the non-ideal charging characteristics and their impacts are attracting more attention. However, according to the best knowledge of the authors, practical and scalable solutions to overcome the potential deviation between the planned and realised loading have not been proposed. This kind of solution can increase the charging capacity utilisation rate, which may reduce the necessary investment cost of the local electric grid or improve the quality of the charging service (QoCS), that is, increase the charged energy [16]. A greater charged energy also improves the utilisation rate of the charging points and can lead to higher revenues for the charging operator if a volumetric charging energy pricing is used. In addition, the deviation between the planned and realised loading may have negative impacts on smart charging objectives, such as frequency regulation.

1.2 | Contributions

The aim herein is to thoroughly illustrate the non-ideal charging characteristics and discuss their impacts. More importantly, an adaptive charging characteristics expectation (CCE) algorithm is proposed to minimise the wasted capacity caused by the non-idealities. This is a crucial step towards capacity-efficient charging sites. The proposed algorithm is compared to the ideal situation, where the charging characteristics are perfectly predicted, and to the present benchmark situation where the charging currents are assumed to be equal to the limit set by the EVSE. To ensure the intended operation under realistic conditions, the experiment is carried out using HIL simulations with two commercial EVs and measured data of real charging sessions.

The contributions are as follows:

1. *Illustrating the complexity of the non-ideal charging characteristics.* Unlike other previously mentioned studies regarding the non-idealities, the non-ideal charging characteristics under different current limits set by the EVSE are analysed herein.
2. *Development of an adaptive CCE algorithm* that enables the charging control system to estimate the potentially

unused three-phase charging capacity and reallocate it effectively among the active EVs.

3. *Formulating a simulation model that considers non-ideal charging characteristics*. The simulation model can be used with real EVs (HIL simulation) or without (only simulated EVs).

4. *Comparing the proposed algorithm to the present benchmark solution and to the ideal case*. This can be used to determine the usefulness and optimality of the proposed algorithm.

1.3 | Structure

The controllability of EV charging and the non-ideal charging characteristics are discussed in Section 2. The control algorithm basis and the proposed CCE algorithm are described in Section 3. Section 4 presents the experiment setup, including the HIL simulation model, the used data and the laboratory setup. In Section 5, the results are presented and discussed. Finally, the conclusions are provided in Section 6.

2 | BACKGROUND FOR EV CHARGING CONTROL

The focus herein is on the charging mode 3 defined in the Standard IEC 61851-1. The charging mode 3 includes extended control options while still being cost-efficient, and it is meant to be the basic charging mode for EVs. There may be a need for a charging control also in a fast charging site, but the objective of a fast-charging station is often to provide as much charging power as is safely possible. Consequently, the charging control objective may be different, for example, to utilise an auxiliary battery energy storage system to reduce charging demand peaks from the grid point of view [30]. Therefore, further consideration of fast-charging solutions is not discussed here.

2.1 | Controllability

As stated in [31], mode 3 charging supports currents between 6 and 80 A. To indicate a charging current limit for the EV, the EVSE can adjust the duty cycle of the pulse width modulation signal through the control pilot circuit. The EV should then adjust its charging current to the limit or below it. The same charging current limit is for each phase and thus the EVSE cannot control phases separately.

There are several non-ideal characteristics that can cause a phase current to be lower than the limit indicated by the EVSE. In a three-phase charging point, the most trivial and yet the most impactful issue is the fact that some EVs support only single-phase or two-phase charging. In addition, the OBC or the charging cable may limit the maximum charging current to, for example, 16 A. Other reasons include the OBC reducing the charging current to protect the battery from overheating or the vehicle's battery being nearly fully charge and thus requiring slower charging [14].

2.2 | Nonideal charging characteristics

It may be trivial that different EVs have different charging characteristics. However, an EV may also have different internal charging modes which can affect the charging characteristics of the EV. For example, BWM i3 has three different charging modes: 'maximum', 'reduced' and 'low' [32]. Only the EV user can change the charging mode. Table 1 summarises the examined EVs [33]. Since there are no accurate data available regarding their charging efficiencies, the OBC efficiency is assumed to be the same for each mode of the BMW. Comprehensive details regarding the differences between the three modes of the BMW are not available as it is presumably a trade secret.

The same Smart Grid Technology laboratory [34] and equipment (including the two EVs, the charging point and two energy analysers) are used to measure the realistic non-ideal charging characteristics and to conduct the HIL simulation experiment. The equipment is described in more detail in Section 4.3.

The aim here is not to assess the technical details of the EVs which define their charging characteristics. Instead, the authors illustrate different charging characteristics and discuss their impacts from the charging control system point of view.

2.2.1 | Steady state charging currents

Based on the conducted charging current measurements with different current limits, the charging current seems to be steady (variation of <0.5 A) until around 98% SOC. However, the steady-state currents might be slightly over or notably under the limit set by the charging controller. This is illustrated in Figure 1, where the charging current limit for the BMW in low mode is changed every 20 s. The symbols I1–I3 in the legend represent phase currents. In Figure 1, the largest difference between the limit and the realised charging currents after a 20-s adjustment period is 7.7 A. This is the largest measured deviation between the current limit and the realised charging current of the considered EVs. Similar currents were seen even with longer adjustment periods. This means that the BMW in low mode would charge with currents of around 7.6 A (I1), 7.5 A (I2) and 7.3 A (I3) when the current limit is 15 A. More importantly, Figure 1 shows that all EVs may not be able to use all charging currents between their minimum and maximum supported charging currents, which has been assumed in [16].

For the other BMW modes (i.e. reduced mode and maximum mode), the deviation between the current limit and the realised current is smaller. For the Nissan Leaf, the steady-state single-phase charging currents deviate ±0.8 A from the current limit. For the sake of conserving space, these are not illustrated.

While the charging characteristics of, for example, BWM's low mode are likely to be more energy efficient or safer from the EV perspective they pose a challenge from the charging control system point of view. This is because there is no standardised way for a charging control system to gain access to the information regarding the charging characteristics of the EVs.
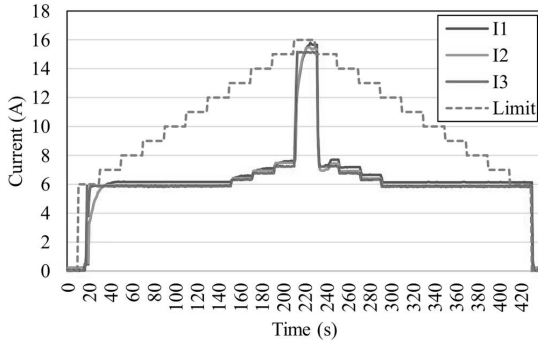
TABLE 1 EV models and charging modes

EV model	Charging mode	Battery capacity	OBC efficiency
BMW i3 (94 AH)	Maximum mode	33.2 kWh	0.865[a]
	Reduced mode		
	Low mode		
Nissan Leaf	–	24.1 kWh	0.899[b]

Abbreviations: EV, electric vehicle; OBC, on-board charger.

[a]Efficiency for model BMW i3 (120 Ah).

[b]Efficiency for model Nissan Leaf Acenta (40 kWh).

FIGURE 1 Charging characteristics of BMW i3 in low mode

2.2.2 | Adaption time to a new current limit

The steady-state charging current measurements show that it takes around 2–15 s for an EV to reach the new steady state after the current limit changes. The reaction time to decreased current limit seems to be faster, around two seconds for both EVs. A greater change of the current limit does not seem to impact the adaption time. This was seen in the measurements where the current limit is changed in steps of 5 and 10 A. An illustration of these measurements is not included here due to space restrictions.

There seems to be a relatively consistent delay when the charging is supposed to start. This delay is often around 10 s as seen in Figure 1. In three-phase charging, there may also be notable differences between the phases. As shown in Figure 1, one phase current (I3) may react much faster than the others. This characteristic was seen in each measurement of the BMW.

2.2.3 | Charging currents in the final SOCs under a constant current limit

Different EVs may have dissimilar charging characteristics also at the final SOCs. To illustrate this, the final charging curves of both EVs are presented in Figure 2. In this figure, BMW maximum mode is chosen as its final charging curves depend more notably on the current limit compared to the other modes. The illustration of the remaining two modes is excluded to conserve space. The final charging curves are measured for all current limits (6–16 A), but for the sake of clarity, only the curves with 6, 9, 12 and 16 A limits are presented. In Figure 2b, the three-phase charging of BMW changes into a single-phase charging at around the mid-point of the final charging curve. After the change, the current I1 triples quickly. There seems to be a clear correlation between the steady-state charging current and the point where the three-phase charging changes into a single-phase charging.

The energy drawn during the final charging curve depends notably on the current limit. For the Nissan and the BMW this energy varies between 0.09–0.71 and 0.16–0.91 kWh, respectively. Assuming the efficiencies presented in Table 1, the final charging curves start at around 97.5%–99.7% and 97.5%–99.6% SOC for the Nissan and BMW, respectively.

3 | CHARGING CONTROL ALGORITHM

To overcome the challenges posed by the non-ideal charging characteristics, an adaptive CCE algorithm is proposed. The algorithm utilises real-time charging current measurement as feedback to memorise and deduct the charging characteristics. As opposed to the solution presented in [16], this solution does not require any preliminary data and is computationally light, which are valuable qualities in real-life implementations. The CCE algorithm is designed to complement other charging algorithms to ensure that they operate as intended, even when the EVs have non-ideal charging characteristics. Therefore, an algorithm basis is needed to demonstrate the efficiency of the CCE algorithm. The main objective of the algorithm basis is to:

1. Limit the charging currents according to the limits of the local electricity network
2. Distribute the whole charging capacity evenly between the active EVs.

The algorithm basis is essentially the same as the current benchmark solution used in, for example, [28, 29]. The algorithm does not require any user inputs or preliminary knowledge about the arriving EVs. The following subsection presents the CCE algorithm.

3.1 | Proposed charging characteristic expectation algorithm

In short, the idea of the CCE algorithm is to use charging current measurements to determine the charging characteristics of each active EV, and then use that information to reallocate any potentially unused charging capacity of an EV to other EVs. Modelling each charging session separately makes the algorithm scalable, which is the main issue in the solution presented in [17]. In addition, the modelling considers three-phase charging as opposed to the solution presented in [17] that focuses only on single-phase charging.
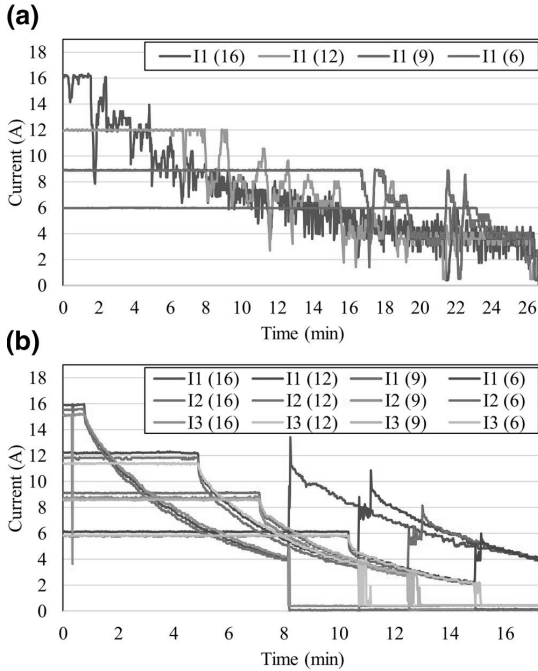
FIGURE 2 Final charging curves for (a) Nissan Leaf and (b) BMW i3 in maximum mode

$$\begin{array}{cccccc} & I_{L} & I_{M,1} & I_{M,2} & I_{M,3} & Boolean \\ I_{max} & \begin{bmatrix} 6 \\ 7 \\ 8 \\ \vdots \\ 32 \end{bmatrix} & \begin{array}{c} 6.0 \\ 7.0 \\ 8.0 \\ \vdots \\ 32.0 \end{array} & \begin{array}{c} 6.0 \\ 7.0 \\ 8.0 \\ \vdots \\ 32.0 \end{array} & \begin{array}{c} 6.0 \\ 7.0 \\ 8.0 \\ \vdots \\ 32.0 \end{array} & \begin{array}{c} False \\ False \\ False \\ \vdots \\ False \end{array} \end{array}$$

[32.0, ...]

FIGURE 3 Initial charging characteristics model

the number of EVs present. This can be done by accessing the charging state information known by the IEC 61851-1 compliant mode 3 charging controller.

After calculating the number of active EVs, the algorithm allocates the available three-phase charging capacity evenly. The capacity distribution process is iterative and considers the charging characteristics memorised and deducted by the CCE algorithm. At the beginning of the distribution process, a 6 A limit is assumed for each active charging session as it is the minimum current limit according to [31]. In each iteration step, the capacity distribution process considers allocating 1 A higher charging current limit for a certain charging session and evaluates whether the expected total charging currents for the charging site will be within the intended limits. If the 1 A higher current limit can be allocated for the charging session, the algorithm updates the considered current limit for the charging session and moves to the next charging session to maintain an even capacity allocation. This will be repeated until a current limit incrementation will result in too high expected total charging currents or until all active charging sessions have the maximum current limits supported by the charging points. This ensures that the non-ideal charging characteristics of each EV are taken into account and the charging capacity will be reallocated if necessary.

Afterwards, there may be single-phase capacity available for allocation and thus the algorithm carries out a similar iterative distribution process for each phase separately. The CCE algorithm deducts the phase usage of each charging session, which makes it possible to optimise phase-specific capacity utilisation. After the algorithm has determined the current limits that are expected to lead to optimal capacity usage rate, the current limits will be sent to the corresponding EVSEs to be put into effect. A simplified block diagram of the control algorithm is presented in Figure 4.

3.1.1 | Direct memorisation

Each time the charging currents are measured, the measurements are updated for the corresponding current limit and the Boolean variable is set to true. An example is given in Figure 5, where the current limit is 10 A and currents of 10.2, 10.1 and 9.9 A are measured afterwards. It should be noted that it may take around 10 s for an EV to properly react to the current limit. Therefore, using a shorter time step may result in an inaccurate charging characteristics model.

The direct memorisation is only memorising the measured values. To improve the rate at which the charging
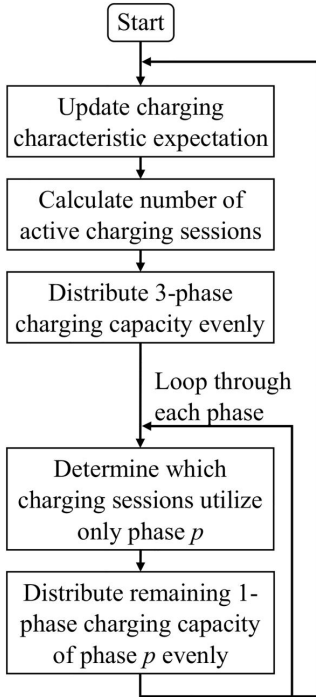
The charging characteristics model is constituted of a maximum current and a matrix of all current limit-correspondences from 6 A to the maximum current supported by the charging point (e.g. 16 or 32 A). Each current limit-correspondence is constituted of the current limit, phase currents and a Boolean variable. In the beginning of a charging session, when the algorithm notices a change of a charging state from 'A' to 'B', 'C', or 'D', the charging characteristics model is initialised, and ideal charging characteristics are assumed. If the charging state is 'B', 'C' or 'D', an EV is connected to the charging point, whereas the state 'A' means that an EV is not connected [31]. Further explanation of the standard is not presented here due to space restrictions. The initial charging characteristics model is presented in Figure 3. In the figure, the currents $I_{M,1}$, $I_{M,2}$ and $I_{M,3}$ in the matrix present the presumed currents when the corresponding current limit (I_L) is set by the EVSE. The Boolean variable is used to keep track of which values are actual measurements and which are initial assumptions.

The algorithm begins by updating the charging characteristics model of each active EV based on the current measurements. The updating process is constituted of four different functions: *direct memorisation*, *phase detection*, *maximum current deduction* and *indirect deduction*. These functions are described in the next subsections. After updating the expected charging characteristics, the algorithm calculates

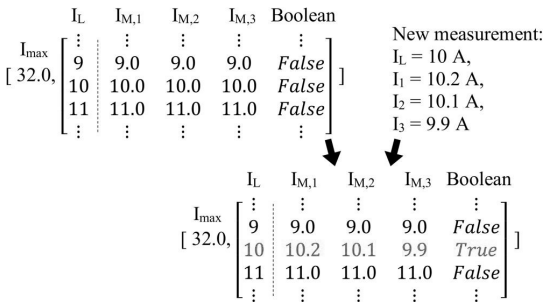**FIGURE 4** Simplified block diagram of the control algorithm

FIGURE 5 Direct memorisation of newly measured charging currents

characteristics modelling evolves, the following three functions use reasonable assumptions made based on the analysis of the non-ideal charging characteristics presented in Section 2.2.

3.1.2 | Phase detection

This function aims to determine which phases are used in the charging session. If one phase current is clearly above zero, while a current on another phase is zero, it means that the phase with zero current is not used. After recognising an unused phase, the charging characteristics model is updated so that there are not assumed to be currents on the phase

regardless of the current limit. An illustration is presented in Figure 6.

There are two key factors which should be considered in this function. First, there may be noise measured by the current metre and thus a small threshold, for example, 1 A, should be used to determine whether a current is zero or not. Second, as mentioned earlier, it may take longer than 10 s for an EV to start charging after the charging is allowed. Therefore, the phase detection function should not be used without a clear delay after the charging is allowed.

3.1.3 | Maximum current deduction

The goal of this function is to determine the highest current that an EV can use. Public charging points may very well be suitable for charging currents of up to 3×32 A, but EVs with ≤ 16 A maximum supported charging current in mode 3 (IEC 61851-1) are very common. Since it is very likely that most EVs cannot utilise the higher end currents, the accuracy of the charging characteristics model may be improved notably after deducting the maximum charging current.

The maximum current deduction function checks if the measured charging current is clearly below the set current limit. And, if so, the measured current is assumed to be the maximum charging current for the present EV. As shown in Figure 1, there may be notable differences (>7 A) between the current limit and the charging current even though the current has not reached its maximum value. Therefore, a threshold of a couple of amperes should be used to determine whether there is a clear difference between the current limit and the measured charging current. However, since the algorithm can always relearn the maximum charging current for each session, there is no need for a remarkably high threshold (e.g. >7 A) which would minimise the risk of erroneous maximum charging current deduction.

The maximum current is taken into account according to Equation (1), where I_E represents the expected charging current, I_M represents the corresponding currents in the matrix, I_{max} represents the maximum current, L denotes the considered current limit, and the subscript p denotes the phase.

$$I_{E,p}(L) = \min\left[I_{M,p}(L), I_{max}\right]. \tag{1}$$

3.1.4 | Indirect deduction

The aim of this function is to improve the modelling accuracy of those current limit-correspondences which are yet not directly measured but which are between two directly measured current limit-correspondences. Since the non-measured current limit-correspondences are assumed to be ideal, they may be significantly inaccurate (potentially over 7 A difference as shown in Figure 1). The current limit-correspondences seems
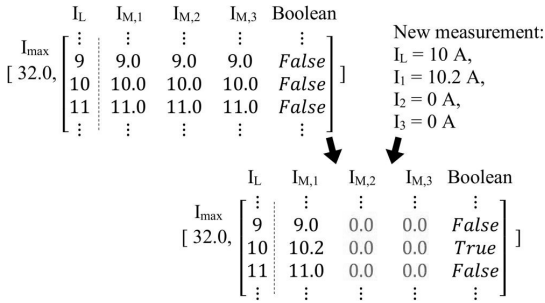
I_{max} [32.0,

I_L	$I_{M,1}$	$I_{M,2}$	$I_{M,3}$	Boolean
⋮	⋮	⋮	⋮	⋮
9	9.0	9.0	9.0	*False*
10	10.0	10.0	10.0	*False*
11	11.0	11.0	11.0	*False*
⋮	⋮	⋮	⋮	⋮

]

New measurement:
I_L = 10 A
I_1 = 10.2 A,
I_2 = 0 A,
I_3 = 0 A

I_{max} [32.0,

I_L	$I_{M,1}$	$I_{M,2}$	$I_{M,3}$	Boolean
⋮	⋮	⋮	⋮	⋮
9	9.0	0.0	0.0	*False*
10	10.2	0.0	0.0	*True*
11	11.0	0.0	0.0	*False*
⋮	⋮	⋮	⋮	⋮

]

FIGURE 6 Detection of unused phases in the present charging session

I_{max} [32.0,

I_L	$I_{M,1}$	$I_{M,2}$	$I_{M,3}$	Boolean
⋮	⋮	⋮	⋮	⋮
9	8.9	8.8	8.6	*True*
10	10.0	10.0	10.0	*False*
11	11.0	11.0	11.0	*False*
⋮	⋮	⋮	⋮	⋮

]

New measurement:
I_L = 11 A,
I_1 = 10.7 A,
I_2 = 10.6 A,
I_3 = 10.2 A

I_{max} [32.0,

I_L	$I_{M,1}$	$I_{M,2}$	$I_{M,3}$	Boolean
⋮	⋮	⋮	⋮	⋮
9	8.9	8.8	8.6	*True*
10	9.8	9.7	9.4	*False*
11	10.7	10.6	10.2	*True*
⋮	⋮	⋮	⋮	⋮

]

FIGURE 7 Indirect charging characteristics deduction

to be logical in a way that a higher current limit results in equal or higher charging currents, whereas a lower current limit results in equal or lower charging currents. Therefore, two directly measured current limit-correspondences can be used to determine boundaries for all non-measured correspondences between them. Since more accurate prediction becomes very complex and requires more input data, it is reasonable to assume that the non-measured current limit-correspondences are settled linearly between the two directly measured correspondences.

After receiving a current measurement, the indirect deduction function is used to check whether there are non-measured current limit-correspondences between the adjacent directly measured correspondences. This is made possible with the Boolean variables. If a measured correspondence is found after one or more non-measured correspondences, the non-measured correspondences are updated. The operation of this function is illustrated in Figure 7.

4 | EXPERIMENT

In order to ensure compliance with commercial EVs, the verification of the charging control algorithm is carried out using HIL simulations. To further improve the overall accuracy of the simulation model, real charging behaviour data and realistic charging characteristics (illustrated in Section 2.2) are used. The following subsections describe the used simulation model, modelling of charging characteristics, the laboratory setup and the simulation case.

4.1 | Simulation model

The experiment consists of up to two HIL charging points, which are described in Section 4.3, and a necessary amount of fully simulated charging points. The key feature of the simulation model is the coupling of realistic charging profiles (Section 4.2) and real charging session data (Section 4.4). The simulation model and the used algorithms are implemented using Python programming language, and a time step of 10 s is
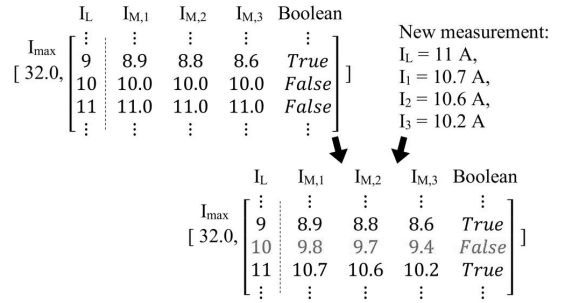
used to calculate the values of the simulated EVs and to measure the charging currents of the HIL charging points.

The control algorithm is run every 60 s unless a new EV arrival is observed. To avoid potential overloading, the control algorithm does not allow charging for a new charging session until the control algorithm has allocated the charging capacity properly. In the case of a new EV arrival, the control algorithm is run on the very next time step. This improves the EV user convenience as the charging will start with minimal delay.

As mentioned in Section 2.2, there may be a delay of over 10 s before a charging session starts properly. Therefore, the algorithm waits 1 min after the start of the charging sessions before enabling *phase detection* and *maximum current deduction* functions to avoid erroneous characteristics deduction.

4.2 | Modelling of EV charging profiles

This subsection describes the modelling of the charging profiles in the simulation model and should not be confused with charging characteristics modelled by the CCE algorithm. The charging profiles are modelled based on the measurements illustrated in Section 2.2. Another option to model battery behaviour would be the use of equivalent circuit models (ECM). However, this approach is problematic as the detailed parameters of an ECM as well as the battery pack composition are generally trade secrets of the manufacturers and cumbersome to determine via experimental battery measurements and reverse engineering [16]. The charging profiles are measured for each current limit for both EVs and for each BMW charging mode mentioned in Table 1. The currents, voltages and time are then used to calculate the missing energy of the EV battery. The energies, currents and current limits are then used to determine realistic charging profiles for each EV (and for each BMW's charging mode) in which the charging current depends on the EV battery energy level and the charging current limit set by the charging controller.

The impacts of the battery temperature and other external factors are not considered in these models. Therefore, a slight deviance between the modelled charging currents and the

laboratory measurements is expected. However, the charging profiles can still be used to introduce realistic non-ideal charging characteristics to the simulation model.

4.3 | Laboratory setup

The experiment was carried out at the Smart Grid Technology Lab [34] at TU Dortmund University. The HIL simulations used the same EVs described in Table 1. A modified RWE eSTATION charging station with two charging sockets suitable for up to 22 kW (400 V AC) charging power was used. The charging station included two Phoenix Contract Advanced EV Charge Controllers (type EM-CP-PP-ETH) which are compatible with IEC 61851-1 standard.

The algorithm uses a Modbus library (PyModbus [35]) which enables it to control the charging current limits of the charging controllers and to read registers such as the charging state. A similar Modbus connection is used for two KoCoS EPPE PX power quality analysers with KoCoS ACP 300 current probes to measure phase voltages and charging currents. The setup for the HIL simulations is illustrated in Figure 8, and a photograph of the setup is presented in Figure 9.

While the run time of one loop of the script (including the proposed CCE algorithm) is a fraction of a second, the queries through the Modbus connection may occasionally take several seconds. The selected time step of 10 s works well without any issues but the tests with shorter time steps does show an increasing chance of the queries not having enough time to receive a response.

4.4 | Simulation case

The simulation case uses real charging data measured at Mall of Tripla [36], which is located in Helsinki, Finland. There are nearly 300 charging points, and the charging points for public use can supply charging powers up to 22 kW. The data consist of around 5000 charging sessions recorded over a 6-month period (October 2019–March 2020). The charging sessions were uncontrolled. The data include start time, stop time, energy consumption and peak power of each charging session.

According to the charging data, there were up to 20 simultaneous charging sessions. Since the utilisation rate of the charging infrastructure was so low, the simulations consider only 20 charging points and a total charging capacity limit of 3×120 A. As a consequence, the algorithm basis mentioned in Section 3 is needed to limit the charging currents during congestions. Since there are always at least 3×6 A charging capacity for each charging session, there is no need to temporarily disable any charging sessions.

The simulations consider three scenarios. These scenarios are based on the 3 days with the highest number of charging sessions and the highest total energy consumptions. By assuming that the peak power of three-phase charging would be over 10 kW, the EV types (single-phase or three-phase) can be estimated. Scenarios 1 and 2 represent the days with the highest
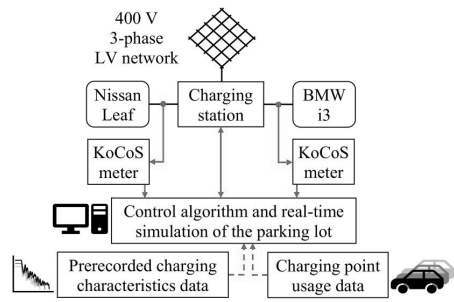
FIGURE 8 The setup for the hardware-in-the-loop (HIL) simulations. HIL, hardware-in-the-loop

FIGURE 9 The laboratory setup

number of single-phase and three-phase charging sessions, respectively, whereas Scenario 3 represents the day with the highest energy consumption. All single-phase charging sessions are modelled based on the Nissan, whereas all three-phase charging sessions are modelled based on the BMW. The BMW modes for the three-phase charging sessions are chosen arbitrarily. The scenarios are presented in Table 2, and the charging point occupation rate is illustrated in Figure 10. Since these charging sessions are uncontrolled, their total charged energies are used as a reference value to represent the 100% QoCS level used herein for comparison purposes. For each examined algorithm, the QoCS is calculated by dividing its total charged energy with the total charged energy of the uncontrolled case.

In addition to these scenarios, simulations are conducted to provide an example of a peak power-based charging control algorithm and to demonstrate its differences regarding the capacity allocation. This example is based on Scenario 3, but the charging capacity is limited to 82.8 kW, which equals an average phase current of 120 A (230 V). However, in this case, the fuse size is assumed to be higher, and thus, the currents on the individual phases are allowed to rise above 120 A as long as the total charging load is within the power limit. In the future, peak power-based electricity tariffs are likely to become more popular as they improve the cost-reflectivity of the electricity pricing [37]. As a result, there will be an incentive to limit peak loading in charging sites and thus effective capacity utilisation becomes more valuable.

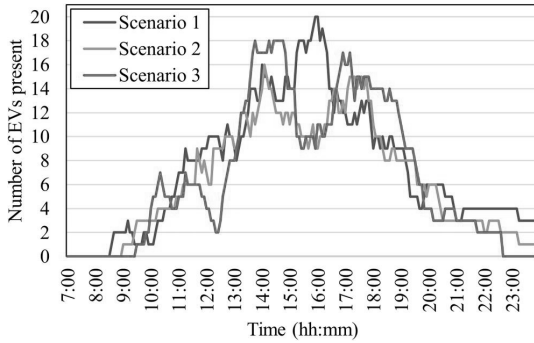| Number of electric vehicle charging sessions	Three-phase charging sessions	Single-phase charging sessions	Total charged energy	Date
1. 66	4	62	372 kWh	22 Feb 2020
2. 61	12	49	428 kWh	19 Oct 2019
3. 59	10	49	454 kWh	14 Dec 2019

F I G U R E 1 0   Charging point utilisation for Scenarios 1–3

5 | RESULTS

The simulations are carried out using four different algorithms:

Algorithm 1 *Uncontrolled charging*

Algorithm 2 *Control without an adaptive CCE algorithm (the present benchmark solution),*

Algorithm 3 *Control with the proposed CCE algorithm*

Algorithm 4 *Control with perfect knowledge of the charging characteristics*

The same algorithm basis (presented in Section 3) is used for Algorithms 2–4, and only the adaption method to the different charging characteristics varies. The second algorithm does not include an adaptive CCE algorithm and thus the control algorithm essentially assumes charging characteristics of each EV to stay ideal. The third algorithm utilises the proposed CCE algorithm. The fourth algorithm has perfect knowledge about the charging characteristics and battery energy levels. Due to the required preliminary knowledge, the fourth algorithm can only be simulated. As the first two algorithms are less complex, only the third algorithm is carried out as an HIL simulation. However, the charging requirements of the EVs are kept the same regardless of the chosen algorithm. The fourth algorithm is used to assess the optimality of the proposed CCE algorithm and to determine the upper bound of the possible capacity usage rate without the risks of overloads. The capacity usage rate (C_{usage}) is calculated according to Equation (2), where t is time index, P is

the realised power consumption and P_{max} is the maximum allowed power determined based on, for example, the fuse size or other peak load limit.

$$C_{\text{usage}}(t) = \frac{P(t)}{P_{\text{max}}(t)}. \tag{2}$$

5.1 | Scenarios 1–3

The results of Scenarios 1–3 are summarised in Table 3. The charging loads in Scenario 1 and 2 are naturally spread over the day, and thus, even the uncontrolled charging load peak is relatively modest. However, Algorithm 2 simply divides the available charging capacity among the EVs without recognising that some of the EVs draw much lower currents than the limit set by the EVSEs. Since the unused capacity is not reallocated to other EVs, it is essentially wasted, resulting in lower QoCS.

In Scenario 3, there is a notable charging load congestion between 13:30 and 14:48 h and a smaller congestion between 16:42 and 17:13 h. In the case of uncontrolled charging, the highest current peaks at 144 A, which means an overload of 24 A (20%), and thus, a peak load limitation is necessary. The currents in case of Algorithms 3 and 4 are very similar and thus the proposed CCE feature seems to operate near ideally. According to the simulations, even Algorithm 4 results in a slight QoCS reduction of 8.1 kWh (1.8%), whereas Algorithms 2 and 3 resulted in a QoCS reduction of 148.2 (32.6%) kWh and 9.7 (2.1%) kWh, respectively. The currents in Scenario 3 are presented in Figure 11.

To illustrate the charging currents in more detail, the moment of the more notable congestion is presented in Figure 12. Algorithms 3 and 4 result in very similar charging currents. Since the control algorithms are run only every 60 s or in the case of a new EV arrival, neither algorithms can fully utilise the whole charging capacity without the risk of a slight overload. In addition, the charging sessions are not likely to be equally distributed for the three phases, which may lower the optimal capacity usage rate. The average capacity usage rates during 13:30–14:40 h are 45.4%, 87.9% and 88.9% for the Algorithms 2–4, respectively.

5.2 | Peak power-based capacity allocation

This example demonstrates that a peak power limit-based charging capacity allocation is more straightforward than, for example, fuse size-based capacity allocation. This is because a

TABLE 3 Results of Scenarios 1–3

Scenario	Algorithm	QoCS	Charged energy	Uncharged energy
1.	1.	100.0%	372.1 kWh	0.0 kWh
	2.	77.6%	288.8 kWh	83.3 kWh
	3.	100.0%	371.9 kWh	0.2 kWh
	4.	100.0%	372.0 kWh	0.1 kWh
2.	1.	100.0%	427.8 kWh	0.0 kWh
	2.	84.5%	361.4 kWh	66.4 kWh
	3.	100.0%	427.8 kWh	0.0 kWh
	4.	100.0%	427.8 kWh	0.0 kWh
3.	1.	100.0%	454.3 kWh	0.0 kWh
	2.	67.4%	306.0 kWh	148.2 kWh
	3.	97.9%	444.6 kWh	9.7 kWh
	4.	98.2%	446.1 kWh	8.1 kWh

Abbreviation: QoCS, quality of the charging service.

power-based capacity allocation does not require perfectly balanced load for each phase. Therefore, a higher capacity usage can be achieved. However, it is still necessary to consider each phase separately to avoid phase-specific overloading, and an adaptive CCE algorithm is still required to effectively allocate the intended total charging capacity. In this case, 96.5% average capacity usage is achieved during 13:30–14:40 with the proposed CCE algorithm. The charging currents are presented in Figure 13. Without an adaptive CCE algorithm, the capacity usage would be 45.4%, whereas the ideal algorithm would result in 98.0% capacity usage rate over the same period. The QoCS for Algorithms 2–4 are 67.4%, 99.8% and 99.9%, respectively.

It is worth mentioning that even a higher capacity usage percent is possible by exploiting the fact that in some cases, such as [17], the objective is to limit the average power of a 1-h long period to a certain level, and thus, the power is allowed to momentarily be higher than the targeted level.

5.3 | Discussion

Based on the results, by not considering an adaptive CCE algorithm over half of the charging capacity would remain unused. In addition, even an ideal algorithm may not achieve higher a fuse size-based maximum capacity usage rate than 89%. This is because of the unevenly balanced charging loads and the non-ideal EV charging characteristics, which reduces the controllability of the charging load. When comparing Algorithm 3 (the proposed CCE algorithm) and Algorithm 2 (the present benchmark solution), the average charged energy is increased by 96.0 kWh by the CCE algorithm. Consequently, the average QoCS is improved from 76.5% to 99.3%. These results underline the usefulness of the CCE algorithm to maximise the QoCS while minimising the investment costs of the required charging infrastructure. When comparing the
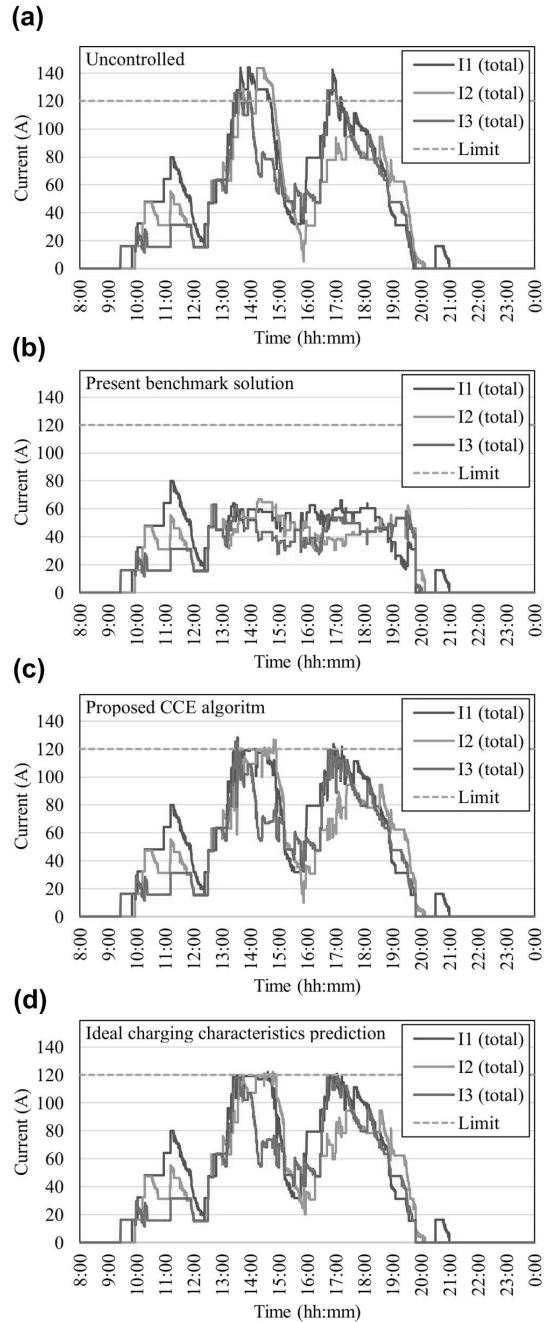
FIGURE 11 Charging currents in Scenario 3 in the case of (a) Algorithm 1, (b) Algorithm 2, (c) Algorithm 3 and (d) Algorithm 4

CCE algorithm to Algorithm 4 (perfect preliminary knowledge of the charging characteristics), the average charged energy is only 0.6 kWh higher with Algorithm 4. The average QoCS is

(a)

(b)
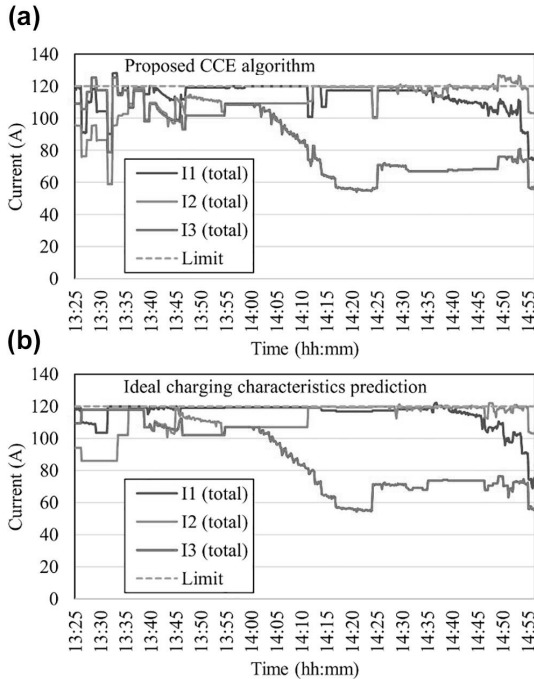
FIGURE 12 Charging currents in Scenario 3 between 13:25 and 14:55 in case of (a) Algorithm 3 and (b) Algorithm 4
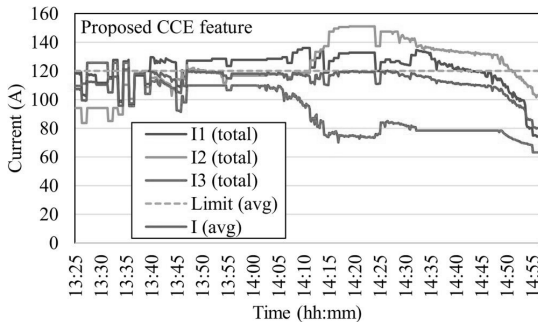
FIGURE 13 Charging currents in a power capacity allocation example utilising the proposed charging characteristics expectation (CCE) algorithm in Scenario 3. CCE, charging characteristics expectation

99.4% with Algorithm 4. Based on these results, it can be seen that the proposed CCE algorithm overcomes the issues posed by the non-ideal charging characteristics near ideally.

The non-ideal charging characteristics would particularly affect the algorithms that schedule the charging of EVs based on their individual energy requirements and departure times, such as the algorithms presented in [1, 2, 4, 11, 24]. The impacts to the individual EVs cannot be completely avoided but the proposed CCE algorithm could be used to ensure that the

whole intended charging capacity is used efficiently, which will improve the average QoCS of all EVs.

It is worth mentioning that the charging standard IEC 61851 supports digital data communication between the EV and the EVSE which, in theory, could replace the need for the proposed CCE algorithm. However, this communication approach is problematic from two perspectives. First, the charging characteristics are complex, and the charging current depends on variables such as the temperature. In addition, the correlation between the charging current and the current limit set by the EVSE is not always linear as presented in Figure 1. Thus, in order to accurately keep track of the charging characteristics of an EV, the control system requires multiple updated data sets of the charging characteristics throughout every charging session. This would increase the data transfer between EV, EVSE, and the control system notably. Second, even if the data transfer would be supported by some of the EVs in the near future, it might take a long time for all EVs to be able to support this data transfer. In the meantime, the proposed solution will be very valuable. Based on the optimality of the proposed solution, it may even be argued that there is no need for EVs to be able to inform the EVSE or the main control system about their charging characteristics.

The vehicle-to-X (V2X) is not considered herein as it is not supported by the used EVs and charging point. It is reasonable to assume that the V2X operation also includes non-ideal characteristics that will limit its controllability. The proposed CCE algorithm could be modified relatively easily to consider V2X operation. However, to ensure its effective operations, it should be tested using EVs and charging points that support bidirectional power flow.

6 | CONCLUSIONS AND FUTURE WORK

The often-overlooked issues caused by the non-ideal charging characteristics of commercial EVs have been illustrated and discussed herein. While the non-ideal charging characteristics may make the charging safer and more energy efficient from the EV's perspective, they pose a challenge from the charging control system point of view. There is currently no standardised way for a control system to gain access to the information regarding the EVs' charging characteristics. Therefore, an adaptive CCE algorithm seems to be a prominent solution to ensure that the intended charging capacity is effectively used in public charging sites.

An adaptive CCE algorithm is proposed herein. The algorithm utilised charging current measurements to memorise and deduct charging characteristics of the EVs without any preliminary knowledge. This information is then used to ensure that the intended capacity is effectively used resulting in a higher quality of charging service. The proposed CCE algorithm is tested using HIL simulations with commercial EVs to ensure compliance with the standard IEC 61851-1. In order to test the operation in a larger charging site, a simulation model is developed that couples realistic charging profiles

(charging current over time) with real charging data (arrival time, departure time and energy requirement). Thus, the simulation model ensures that the non-ideal charging characteristics, which cause the charging current to deviate from the current limit set by the EVSE, are realistically modelled.

According to the simulation results, the proposed CCE algorithm operates almost as well as the ideal algorithm with perfect knowledge. When compared to the present benchmark solution, the total daily charging energy is increase by 96 kWh on average, resulting in the average QoCS increasing from 76% to 99%. In addition, the results show that the proposed CCE algorithm reaches up to 88% maximum charging capacity usage rate over the congestion hour if the capacity is determined by a fuse size, whereas the ideal control algorithm reaches 89% and the present benchmark solution reaches only 45%. If the available charging capacity is limited to a certain peak power, the capacity allocation does not require perfectly balanced phase loading. Therefore, the capacity allocation is simpler and a higher capacity usage rate is possible. In this case, the proposed CCE algorithm reaches the 97% maximum capacity usage rate.

The result also gives an indication that over 98% QoCS can be achieved in a public charging site with multiple 22 kW charging points even if the total charging capacity per charging point results in 3×6 A. To determine more comprehensive guidelines to maximise the QoCS while minimising the investment costs of the necessary charging infrastructure at public charging sites, extended simulations will be carried out for different charging sites. Additional future works include testing of the proposed CCE algorithm in a pilot case with multiple charging points and analysis of non-ideal discharging characteristics in V2X operation.

ACKNOWLEDGEMENTS

CONFLICT OF INTEREST

The authors declare that they have no known competing financial interests or personal relationships that could have appeared to influence the work reported herein.

ORCID

Toni Simolin https://orcid.org/0000-0002-0254-1113

REFERENCES

1. Yang, Y., et al.: Decentralised EV-based charging optimization with building integrated wind energy. IEEE Trans. Automat. Sci. Eng. 16(3), 1002–1017 (2019)
2. Koufakis, A.M., et al.: Offline and online electric vehicle charging scheduling with V2V energy transfer. IEEE Trans. Intell. Transport. Syst. 21(5), 2128–2138 (2020)
3. Bryden, T.S., et al.: Electric vehicle fast charging station usage and power requirements. Energy. 152, 322–332 (2018)
4. Wei, Z., et al.: Intelligent parking garage EV charging scheduling considering battery charging characteristic. IEEE Trans. Ind. Electron. 65(3), 2806–2816 (2018)
5. Su, J, Lie, T.T., Zamora, R.: Modelling of large-scale electric vehicles charging demand: a New Zealand case study. Electr. Power Syst. Res. 167, 171–182 (2019)
6. Calearo, L., et al.: Grid loading due to EV charging profiles based on pseudo-real driving pattern and user behavior. IEEE Trans. Transp. Electrific. 5(3), 683–694 (2019)
7. Liu, Y., Deng, R., Liang, H.: A stochastic game approach for PEV charging station operation in smart grid. IEEE Trans. Ind. Inf. 14(3), 969–979 (2018)
8. Bulut, E., Kisacikoglu, M.C., Akkaya, K.: Spatio-temporal non-intrusive direct V2V charge sharing coordination. IEEE Trans. Veh. Technol. 68(10), 9385–9398 (2019)
9. Kim, J.D.: Insights into residential EV charging behavior using energy metre data. Energy Pol. 129, 610–618 (2019)
10. Fotouhi, Z., et al.: A general model for EV drivers charging behavior. IEEE Trans. Veh. Technol. 68(8), 7368–7382 (2019)
11. Zhang, G., Tan, S.T., Wang, G.G.: Real-time smart charging of electric vehicles for demand charge reduction at non-residential sites. IEEE Trans. Smart Grid. 9(5), 4027–4037 (2018)
12. Quiros-Tortos, J., et al.: Statistical representation of EV charging: real data analysis and applications. 20th Power Systems Computation Conference (PSCC), pp. 1–7. Dublin, Ireland, June (2018)
13. Zeng, T., Zhang, H., Moura, S.: Solving overstay and stochasticity in PEV charging station planning with real data. IEEE Trans. Ind. Inf. 16(5), 3504–3514 (2020)
14. Lee, Z.J., et al.: Large-scale adaptive electric vehicle charging. IEEE Global Conference on Signal and Information Processing (GlobalSIP), Anaheim, CA, USA, 863–864 (2018)
15. Sun, C., et al.: Classification of electric vehicle charging time series with selective clustering. Electr. Power Syst. Res. 189, 106695 (2020)
16. Frendo, O., et al.: Data-driven smart charging for heterogeneous electric vehicle fleets. Energy AI. 1, 100007 (2020)
17. Simolin, T., et al.: Optimised controlled charging of electric vehicles under peak power-based electricity pricing. IET Smart Grid. 3(6), 751–759 (2020)
18. Ucer, E., et al.: An Internet-inspired proportional fair EV charging control method. IEEE Syst. J. 13(4), 4292–4302 (2019)
19. Xydas, E., Marmaras, C., Cipcigan, L.M.: A multi-agent based scheduling algorithm for adaptive electric vehicles charging. Appl. Energy. 177, 354–365 (2016)
20. Lam, A.Y.S., Leung, K.C., Li, V.O.K.: Capacity estimation for vehicle-to-grid frequency regulation services with smart charging mechanism. IEEE Trans. Smart Grid. 7(1), 156–166 (2016)
21. Wan, Z., et al.: Model-free real-time EV charging scheduling based on deep reinforcement learning. IEEE Trans. Smart Grid. 10(5), 5246–5257 (2019)
22. Ma, W.J., Gupta, V., Topcu, U.: Distributed charging control of electric vehicles using online learning. IEEE Trans. Automat. Control. 62(10), 5289–5295 (2017)
23. Lopez, K.L., Gagne, C., Gardner, M.A.: Demand-side management using deep learning for smart charging of electric vehicles. IEEE Trans. Smart Grid. 10(3), 2683–2691 (2019)
24. Sadeghianpourhamami, N., Deleu, J., Develder, C.: Definition and evaluation of model-free coordination of electrical vehicle charging with reinforcement learning. IEEE Trans. Smart Grid. 11(1), 203–214 (2020)
25. Zhang, X., et al.: Deep-learning-based probabilistic forecasting of electric vehicle charging load with a novel queuing model. IEEE Trans. Cybern. 1–14 (2020)

26. Li, H., Wan, Z., He, H.: Constrained EV charging scheduling based on safe deep reinforcement learning. IEEE Trans. Smart Grid. 11(3), 2427–2439 (2020)

27. Silva, F.L.D., et al.: Coordination of electric vehicle charging through multiagent reinforcement learning. IEEE Trans. Smart Grid. 11(3), 2347–2356 (2020)

28. Heredia, W.B., et al.: Evaluation of smart charging for electric vehicle-to-building integration: a case study. Appl. Energy. 266, 114803 (2020)

29. Zhang, T., et al.: Real-time renewable energy incentive system for electric vehicles using prioritisation and cryptocurrency. Appl. Energy. 226, 582–594 (2018)

30. Gjelaj, M., et al.: Optimal infrastructure planning for EV fast-charging stations based on prediction of user behaviour. IET Electr. Syst. Transp. 10(1), 1–12 (2020)

31. International Standard IEC 61851-1: Electric vehicle conductive charging system—Part 1: General requirements (2017)

32. BMW AG: The BMW i3. Owners Manual, pp. 183. Munich, Germany (2015)

33. Electric vehicles in test: this is how high the power consumption is. (In germany: Elektroautos im Test: So hoch ist der Stromverbrauch).

https://www.adac.de/rund-ums-fahrzeug/tests/elektromobilitaet/strom verbrauch-elektroautos-adac-test/. Accessed 13 April 2021

34. Spina, A., et al.: Smart grid technology Lab - a full-scale low voltage research facility at TU Dortmund university. 2018 AEIT International Annual Conference, Bari, Italy. pp. 1–6 (2018)

35. PyModbus—A Python Modbus Stack. https://pymodbus.readthedocs. io/en/latest/readme.html#. Accessed 13 April 2021

36. Parking at Tripla. https://malloftripla.fi/en/pysakointi. Accessed 13 April 2021

37. Lummi, K., Mutanen, A., Järventausta, P.: Upcoming changes in distribution network tariffs—potentialharmonisation needs for demand charges. 25th International Conference on Electricity Distribution (CIRED), Madrid, Spain, pp. 3–6. (2019)

PUBLICATION
8

Realistic QoS optimization potential at commercial EV charging sites through pricing-based prioritization

T. Simolin, K. Rauma, A. Rautiainen, P. Järventausta

REALISTIC QOS OPTIMIZATION POTENTIAL AT COMMERCIAL EV CHARGING SITES THROUGH PRICING-BASED PRIORITIZATION

Toni Simolin[1], Kalle Rauma[2], Antti Rautiainen[3], Pertti Järventausta[1]*

[1]*Unit of Electrical Engineering, Tampere University, Tampere, Finland*
[2]*Institute of Energy Systems, Energy Efficiency and Energy Economics, TU Dortmund University, Dortmund, Germany*
[3]*Pohjois-Karjalan Sähkö Oy, Joensuu, Finland*
*toni.simolin@tuni.fi

Keywords: CONTROL ALGORITHM, EV CHARGING, HARDWARE-IN-THE-LOOP, QUALITY OF CHARGING SERVICE

Abstract

At present, EVs are emerging at a fast pace. This may cause pressure for commercial buildings to offer electric vehicle (EV) charging services for their customers. In a cost-efficient charging site, it is necessary to find a balance between the costs and the offered quality of charging service (QoCS). This may be a difficult task as the charging requirements of the customers are unpredictable and vary daily. In this paper, an algorithm using a charging price–based prioritization is proposed and discussed. This can be used to take unpredictable charging requirements into account and to improve the QoCS while requiring a minimal effort from the EV users. To ensure an improvement in the QoCS and the practicality of its implementation, the algorithm is tested using hardware-in-the-loop simulations with two commercial EVs and real charging data. The results verify that the QoCS can be improved by 2% on average and by up to 16% for a single EV user. This leads to a more attractive and more cost-efficient charging site.

1 Introduction

Due to their environmentally friendly nature, electric vehicles (EVs) are emerging at a fast pace. Since the range anxiety is common among the EV users [1], commercial buildings, e.g. shopping centres, may want to offer charging services to attract customers. However, it can be a challenging task to design a cost-efficient charging site that provides a high quality of charging service (QoCS) with minimum investment costs.

In this paper, the charged energy of an uncontrolled case is chosen to represent the level of 100% QoCS. Since the uncontrolled charging represents the maximum charged energy under the limitations set by, e.g., the on-board charger (OBC) of the EV, the maximum charging power of the EV supply equipment (EVSE), and the available charging time, it is a reasonable reference value to evaluate the negative impacts of a charging control algorithms.

The QoCS could be optimized using the driving schedules and the charging demands. However, requesting such information from the EV users could be burdensome and requires a suitable interface [2]. Additionally, it may be difficult for an EV user to predict an accurate duration of their stay at commercial locations, such as shopping centres. And, if the users are requested to report their parking time and charging demand, they may be tempted to exaggerate their needs to improve their own convenience. Therefore, a price-based prioritization could be used to allocate charging

capacity to those with more urgent demand. This can also increase the utilization rate of the total charging capacity, and thus, lead to a more cost-efficient charging site.

In the scientific literature, several algorithms to improve QoCS are presented [3]–[6]. However, these studies [3]–[6] share common deficiencies: the limitations of the OBCs of the EVs or the compatibility with commercial EVs are not considered. Therefore, the practicalities of the proposed solutions are not thoroughly assessed. As mentioned in [7], there are several non-ideal charging characteristics, such as the EV's on-board charger reducing the charging current to protect the battery from overheating or the vehicle's maximum charging rate being lower than the current limit indicated by the charging controller. These factors may impact the QoCS. According to [8], more than 76% of the EV users see a high QoCS as more important factor than the price of the charged energy. Thus, these factors should be considered in order to accurately evaluate the operation of the proposed charging solution in a real-life implementation.

This paper proposes a charging control algorithm that considers prioritization levels to distribute the available charging capacity between the EVs. The proposed solution is partly similar to the mechanism presented in [6]. However, the proposed algorithm offers more flexible prioritization options, ensures high capacity usage rate while considering non-ideal charging characteristics, and operates in real-time. The algorithm is tested using

hardware-in-the-loop (HIL) simulations with two commercial EVs and real charging data to ensure practicality and compatibility with the IEC 61851 charging standard. The algorithm does not require any user inputs other than the request of whether to prioritize or not.

The remainder of the paper is organized as follows. The proposed control method is presented in Section 2. The details of the experiment are presented in Section 3. The results are presented and discussed in Section 4. Finally, the conclusions are provided in Section 5.

2   EV charging control method

To know whether the OBC of the EV limits the realized charging current, the control method uses a charging current measurement feedback of all EVSEs. The measurements are used to detect the number of used phases and memorize the correlation between the current limit set by the EVSE and the realized charging currents. This function is referred to as charging characteristics expectation (CCE) algorithm that enables the control algorithm to adapt to the charging profile of each EV without any preliminary knowledge.

The algorithm utilizes prioritization levels to distribute the total charging capacity between all EVs. The prioritization levels could be linked to charging prices so that a higher charging price equals a higher prioritization level. This leaves the decision to the customers and guides them to choose a higher priority only when it is necessary. The proposed control method could be applied into charging algorithm that focuses on determining the available charging capacity to improve its capacity utilization rate and enable prioritization-based capacity distribution.

The charging capacity allocation algorithm is illustrated in Algorithm 1. It begins by gathering a list of charging points with an active charging session (list_ACP). After that, the current limit of each charging session is initialized to 6 A which is the minimum current limit (IEC 61851). The available charging capacity (ACC) to be allocated in the main loop can then be calculated based on the total charging current limit (TCCL) and the minimum value returned by total_CCE function. This total_CCE function returns the expected charging currents of each phase (A, B, and C) of all EVs which can then be used to calculate remaining available charging capacity.

To allocate the remaining charging capacity, the algorithm considers a priority index (p_i) that is determined based on the prioritization level (p_l) and the currently allocated capacity (p_c) according to Eq. 1. The charging current limit of the charging session with the lowest p_i will be increased by one ampere in each cycle of the loop until the total capacity is allocated or until there are no more suitable charging sessions remaining. A charging session becomes unsuitable if the allocated charging current limit reaches the maximum current of the charging point (row 7) or if at least one of the phase currents would rise above the total charging current limit when the current limit of the charging session increases (row 12).

$$p_i(n) = \frac{p_c(n)}{p_l(n)}. \quad (1)$$

Algorithm 1 prioritization-based capacity allocation

---

def distribute_capacity_based_on_priority():
1. list_ACP = check_CPs_with_active_charging_session()
2. **for** i in range(length(list_ACP)):
3.   list_ACP[i].current_limit = 6
4. ACC = TCCL - min(total_CCE())
5. **while** ACC > 0 and length(list_ACP) > 0:
6.   list_ACP.sort(key = priority_index, order = ascending)
7.   **if** list_ACP[0].max_current <= list_ACP[0].current_limit:
8.   delete list_ACP[0]
9.   **else**:
10.   list_ACP[0].current_limit = list_ACP[0].current_limit + 1
11.   list_ACP[0].priority_index = list_ACP[0].current_limit / list_ACP[0].prioritization_level
12.   **if** max(total_CCE()) > TCCL:
13.   list_ACP[0].current_limit = list_ACP[0].current_limit - 1
14.   delete list_ACP[0]
15.   ACC = TCCL - min(total_CCE())
16.   return

---

3   Experiment

In the following subsections, the used charging data, the simulation model, the scenarios, and the laboratory setup are described. The use of commercial EVs and real charging data ensures compliancy with the charging standard IEC 61851 and that the scenarios are realistic.

3.1 Data

The experiment utilizes real charging data measured at Mall of Tripla [9] located in Helsinki, Finland. At the charging site, there are almost 300 charging points suitable for 22 kW charging power. The data was measured between 10/2019–3/2020 and consists of nearly 5,000 uncontrolled charging sessions. The data include information such as arrival and departure times, active charging times, energies charged, and charging peak powers.

3.2 HIL simulation model

The HIL simulation model includes two real charging points and a necessary amount of fully simulated charging points. The simulation model utilizes preliminary measured EV charging profiles in the modelling. The charging profiles of both EVs (Nissan Leaf and BMW i3) are measured for all possible charging current limits (integers) set by the EVSE to build a simulation model for the charging profiles where the charging current depends on the current limit set by the EVSE and the energy that is missing from the battery of the EV. This ensures that the non-ideal charging characteristics (e.g. on-board charger starts limiting the charging current

when the battery becomes nearly fully charged) are taken fully into account. The algorithm uses a time step of 10 seconds. At each time step, all values of the simulated EVs are calculated and the charging currents of the HIL charging points are measured. The control algorithm is run every 60 seconds or in the next time step after a new EV is plugged into a charging point.

3.3 Laboratory setup

Besides the EVs (Nissan Leaf and BMW i3), the laboratory equipment includes a charging station (a modified RWE eSTATION) with two charging sockets (22kW, 3×32 A, 400 V) and charge controllers (Phoenix Contact Advanced EV charge Controllers, type EM-CP-PP-ETH). The charging currents are measured with KoCoS EPPE PX power quality analysers with KoCoS ACP 300 current probes. The algorithm is implemented by using Python programming language, and a Modbus library (PyModbus [10]) is used to enable communication with the charging controllers and the metering devices. The experiment is carried out at the Smart Grid Technology Lab at TU Dortmund University [11]. The laboratory setup is shown in Fig. 1.
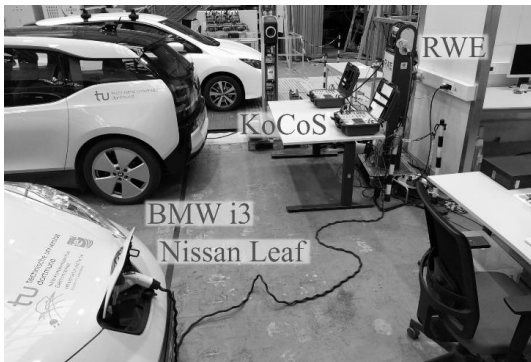
Fig. 1. Laboratory setup

3.4 Scenarios

According to the charging data, the charging point utilization rates are currently very low at the Mall of Tripla. Therefore, to investigate realistic scenarios with higher EV penetrations, charging sessions of two consecutive days are grouped into one day. Three scenarios are considered which represents the days with the highest energy consumption. The scenarios are illustrated in Table 1. To increase the need for peak load management that may also reduce the QoCS, the charging capacity of each three phase is limited to (n_{max}×6 A), where the n_{max} is the highest number of simultaneously present EVs.

The data does not contain information whether a charging session is a single-phase or a three-phase. However, if the peak power of a charging session is higher than 10 kW, it is likely to be a three-phase one. Two-phase charging sessions are also possible but, for the simplicity's sake, all charging sessions are assumed to be single-phase or three-phase depending on whether their peak power is under or over 10 kW. This information is then used to couple each charging sessions with the modelled charging profile of either the Nissan (single-phase) or the BMW (three-phase).

Since the priority preference of the EV users and the willingness to pay for it are unknown, the priority levels have to be assumed. For demonstration purposes, two prioritization levels are assumed: either 1 or 5. This means that the algorithm tries to allocate 5 times more capacity for the more prioritized charging sessions. In each scenario, the higher prioritization level is given to 0%, 20%, 40%, 60%, or 80% of the EVs. The higher prioritization levels are given to the EVs with the highest energy requirement indexes ($E_{r,i}$), which are calculated according to Eq. 2, where E_c is the energy consumption, t_p is the parking time, and P_{max} the maximum charging power (3.68 kW for a single-phase and 11.04 kW for a three-phase charging session).

$$E_{r,i}(n) = E_c(n) - t_p(n) \times P_{max}(n). \quad (2)$$

It is worth mentioning that all charging sessions will receive at least the minimum capacity (3×6 A) and the algorithm always tries to allocate the whole available charging capacity. This means that both prioritized and non-prioritized sessions receive the same minimum capacity during peak congestion hours or the same maximum capacity if there are only a few EVs present.

Table 1 Scenario data

Scenario	1.	2.	3.
Charging sessions (3-p / 1-p)	96 (16 / 80)	106 (21 / 85)	101 (12 / 89)
Total charged energy	760 kWh	707 kWh	692 kWh
n_{max}	37	22	31
Date	14–15th Dec. 2019	18–19th Oct. 2019	18–19th Jan. 2020

4   Results

As mentioned earlier, the uncontrolled charging is used as a reference to represent 100% QoCS level. The average QoCS of all EVs in each scenario and case are presented in Fig. 2. The results show that by offering an option for a prioritized charging, the charging system operator can improve the average QoCS. According to Fig. 2, the QoCS is the highest when the prioritization is requested by around 20% of the customers. This information can be used to design optimal pricing levels for commercial charging sites. Determination of the actual pricing levels (€/kWh) is excluded from this paper. In Fig. 2, it can be seen that when comparing the cases with 0% and 20% prioritization in Scenario 1, the prioritization increases the QoCS up to 1.9% which results in 14.9 kWh higher charged energy.
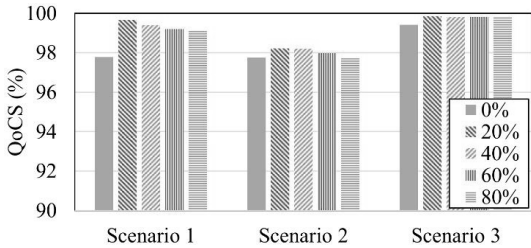
Fig. 2. QoCS in each scenario and case

In Fig. 3, the total charging currents in Scenario 1 between 13:50–15:50 are presented for the cases where none of the EV users request prioritization and where 20% of the users request prioritization. During the congestion hour between 14:00–15:00, the currents in Phase 2 and 3 are higher for the case with 20% of users requesting prioritization (Fig. 3 b) which explains the higher QoCS. The prioritization has more notable impacts on the individual EVs than the average of all EVs. This is illustrated in Fig. 4, where the charging currents of a BMW i3 in Scenario 1 are presented. In Fig. 4 a and Fig. 4 b, none of the EVs and 20% of the EVs (including the BMW i3) are prioritized, respectively. The QoCS for the BMW in these cases are 83.9% and 100.0%, respectively. The request of the prioritization results in 3.5 kWh higher charged energy for the BMW.
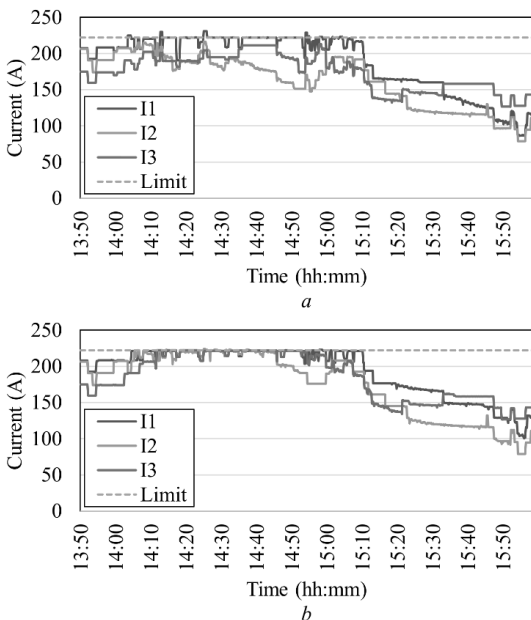
Fig. 3. Charging currents in Scenario 1 when (a) none of the EV users and (b) 20% of the EV users request prioritization
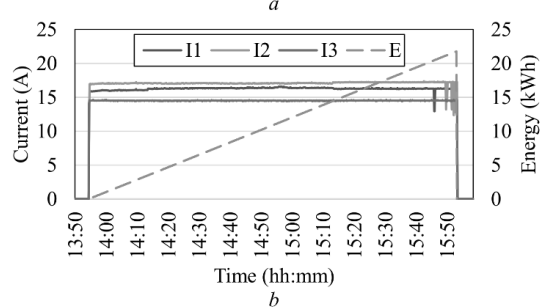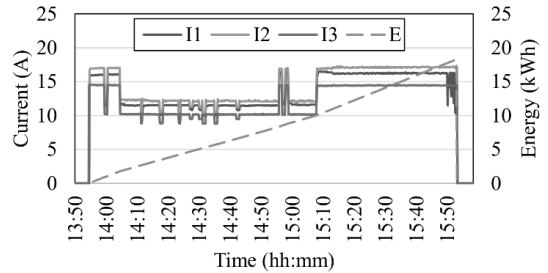
Fig. 4. Charging currents of a BMW i3 in Scenario 1 (a) without prioritization and (b) with prioritization

As mentioned earlier, prioritized and non-prioritized charging sessions receive the same capacity during peak congestion hours or if there are only a few EVs present. Therefore, it might be reasonable to increase the price of the charged energy of a prioritized charging session only when the prioritization increases the charging power compared to the non-prioritized sessions. This could simplify the situation from the EV user perspective as a customer would not have to pay extra in case of the prioritization is not possible.

5   Conclusion

This paper proposes a price–based prioritization algorithm for EV charging. The algorithm is tested by using HIL simulations with two commercial EVs and real charging data. The strengths of the proposed algorithm include the ease of implementation and its convenience from the user perspective as the only required information is whether to prioritize or not.

The results show that the highest QoCS is achieved when around 20% of the EVs users with the highest charging requirement are requesting prioritization. This increases the average QoCS up to 1.9% which means 14.9 kWh increase in the daily total charged energy. More notably, the QoCS of an individual EV user increases up to 16.1%.

6   Acknowledgement

7 References

[1] Melliger, M. A., van Vliet, O. P. R., Liimatainen, H.: 'Anxiety vs reality – Sufficiency of battery electric vehicle range in Switzerland and Finland', Transp. Res. Part D Transp. Environ., 2018, 65, pp. 101–115

[2] Tuchnitz, F., Ebell, N., Schlund, et al.: 'Development and Evaluation of a Smart Charging Strategy for an Electric Vehicle Fleet Based on Reinforcement Learning', Applied Energy, 2021, 285

[3] Zhang, G., Tan, S. T., Gary Wang, G.: 'Real-Time Smart Charging of Electric Vehicles for Demand Charge Reduction at Non-Residential Sites', IEEE Trans. Smart Grid, 2018, 9, (5), pp. 4027–4037

[4] Wei, Z., Li, Y., Zhang, Y., et al.: 'Intelligent parking garage EV charging scheduling considering battery charging characteristic', IEEE Trans. Ind. Electron., 2018, 65, (3), pp. 2806–2816

[5] Bayram, I. S., Tajer, A., Abdallah, M., et al.: 'Capacity Planning Frameworks for Electric Vehicle Charging Stations With Multiclass Customers', IEEE Trans. Smart Grid, 2015, 6, (4), pp. 1934–1943

[6] Bayram, I. S., Ismail, M., Abdallah, M., et al.: 'A pricing-based load shifting framework for EV fast charging stations', IEEE Int. Conf. Smart Grid Comm., Venice, Italy, Nov. 2014, pp. 680–685

[7] Lee, Z. J., Chang, D., Jin, C., et al.: 'Large-scale adaptive electric vehicle charging', IEEE Int. Conf. Smart Grid Comm., Aalborg, Denmark, Oct. 2018, pp. 863–864

[8] Wang, Y., Yao, E., Pan, L.: 'Electric vehicle drivers' charging behavior analysis considering heterogeneity and satisfaction', Journal of Cleaner Production, 2021, 286

[9] 'Mall of Tripla', https://malloftripla.fi/en/pysakointi, accessed 18 November 2020

[10] 'PyModbus - A Python Modbus Stack', https://pymodbus.readthedocs.io/en/latest/readme.html#, accessed 18 November 2020

[11] Spina, A., Rauma, K., Aldejohann, C., et al.: 'Smart Grid Technology Lab - A Full-Scale Low Voltage Research Facility at TU Dortmund University', AEIT Int. Annu. Conf., Bari, Italy, Oct. 2018, pp. 1–6

PUBLICATION
9

Charging powers of the electric vehicle fleet: Evolution and implications at commercial charging sites

T. Simolin, K. Rauma, R. Viri, J. Mäkinen, A. Rautiainen, P. Järventausta

ELSEVIER
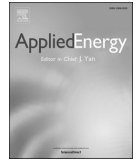
Charging powers of the electric vehicle fleet: Evolution and implications at commercial charging sites

Toni Simolin [a],[*], Kalle Rauma [b], Riku Viri [c], Johanna Mäkinen [c], Antti Rautiainen [a], Pertti Järventausta [a]

[a] *Unit of Electrical Engineering, Tampere University, P.O. Box 692, FI-33014, Finland*
[b] *Institute of Energy Systems, Energy Efficiency and Energy Economics, TU Dortmund University, Emil-Figge-Straße 76, 44227 Dortmund, Germany*
[c] *Transport Research Centre Verne, Tampere University, P.O. Box 600 FI-33014, Finland*

HIGHLIGHTS

- The charging powers of the current electric vehicle fleet are analyzed.
- Almost 80% of the electric vehicles support only around 4 kW charging powers.
- The development of the electric vehicle fleet during 2020–2040 is modelled.
- The energy requirement in commercial locations is predicted to increase by 134%.
- The peak of the normalized power is predicted to increase by 77%.

ARTICLE INFO

ABSTRACT

Electric vehicle (EV) charging is widely studied in the scientific literature. However, there seems to be a notable research gap regarding the charging power limitations of the on-board chargers of the EVs. In this paper, the present state of the maximum charging powers of the on-board chargers is thoroughly analysed using data from two commercial charging sites. Furthermore, the results of the analysis are used along with an EV fleet development model to form realistic future scenarios, which are then used for a simulation model that couples the charging sessions with measured charging profiles. The results of the simulations show that, due to the evolution of the EV fleet, the average energy consumption in commercial locations will increase by 134% on average from 5.6 to 8.7 kWh/EV to 13.0–19.6 kWh/EV during 2020–2040. Similarly, the peak of the normalized power increases by 77% on average from 1.1 to 1.4 kW/EV to 1.6–2.9 kW/EV. These values are essential to guide long-term decisions such as optimal sizing of charging infrastructure and parking policies.

1. Introduction

Electric vehicles (EVs) are seen as a major establisher of environmentally friendlier mobility, both globally and in Finland. Previous studies show that charging infrastructure is one of the concerns hindering users from investing in electric vehicles [1,2]. Although the shift towards electric vehicles does not create a large increase in total energy demand, the effects in low voltage networks are major as they are not designed to work with large and sudden power peaks caused by vehicle charging. This may cause problems within the low-voltage networks feeding large parking areas, and therefore, electric vehicle parking should be considered when organizing the parking in general.

Parking policy can be used to guide where and when cars are parked and, consequently, where and when electric cars are charged. Limitations in a building's electrical systems and parking availability may lead to a lack of charging points, thus creating barriers to the uptake of EVs [3]. Therefore, the development of EV charging infrastructure should be aligned with the parking policy. Several studies have investigated how charging infrastructure affects the uptake of EVs, but there is a clear research gap in the alignment of parking policy and the development of EV charging infrastructures. Many cities have set strategies to increase the number of EV charging points, but there is a lack of knowledge about

---

* Corresponding author.
E-mail address: toni.simolin@tuni.fi (T. Simolin).

how the charging powers of the EVs will evolve, how this will affect the development of charging sites, and how this should be taken into account in parking policy.

Over the past few years, the modelling of the EV charging load has improved significantly. Accurate prediction of the electric vehicle load is of great importance for the optimal dispatching and safe operation of the power grid [4]. Several studies have recently contributed to analysing or predicting the EV charging loads in terms of energy (kWh) and charging time. However, according to the authors' knowledge, there are two notable research gaps:

- the charging peak powers of individual EVs are not analysed, and
- the development of the EV fleet in terms of the supported charging powers is not examined to further increase the prediction accuracy of the future charging loads.

In a commercial charging station, charging powers of up to 22 kW (charging mode 3, IEC 61851) are typical in Europe. However, in such locations, to accurately predict or model the charging load, it is important to consider the limits of the EVs' on-board chargers (OBC). This is due to the fact that accounting for only the nominal powers of the charging stations does not reflect the real charging behaviour, since most EVs cannot use the full 22 kW capacity. At present, a relatively small percentage of EVs support such charging powers. Therefore, without considering the limits of the individual EVs, the modelled charging load is likely to be significantly inaccurate.

1.1. Literature review

The most common solution for modelling the EV charging loads is based on travelling traditional passenger vehicles [5], e.g. using travel surveys, as in [6–12]. In [5], the effectiveness of travel surveys to model EV charging demand is evaluated by comparing the modelling results with the measurements obtained from several EV field tests. The study states that travel surveys can be used to model EV charging loads with reasonable accuracy. However, the sensitivity analysis highlights the importance of accurately modelling input parameters, such as charging power. Furthermore, the fact that OBCs of the EVs may constitute the actual bottleneck in the charging process is acknowledged but not analysed.

In [6], the EV charging simulations are conducted while considering people's demographics and social attributes. According to the results, the attributes have a considerable effect on the magnitude and peak time of the charging load. The study [9] uses an artificial neural network to improve the forecasting accuracy of EV travel behaviour. The results show that an aggregator's financial losses could be reduced compared to conventional forecasting methods. In [11], a mixed-integer linear programming model for decisions is proposed to control EV charging and the use of an energy storage system. The results show that the operational costs of a charging hub microgrid can be significantly reduced. The study [12] establishes a spatial–temporal distribution model to assess charging loads. Monte Carlo simulation is used to show that the charging loads vary notably between different charging sites.

Previously mentioned approaches based on travel surveys, such as [6,7,9,11,12], often tend to overlook the impacts of charging powers. In [10], two scenarios with different charging powers are compared. The main conclusions of the effects of increased charger powers are that the charging demand peak will occur 1–2 h earlier, and the number of simultaneous charging sessions decreases in the scenario with higher charging powers. In [8], three charging powers (3.7 kW, 6.9 kW and 22 kW) are considered. From the charging power perspective, the study concludes that higher charging power results in higher variability in the charging load and requires smaller time resolution to accurately evaluate the load peaks.

Real EV charging data are used in, e.g. [4,13–16]. In [4], state of charge (SOC) curves of different types of EVs are analysed to evaluate

charging prediction models. In [13] and [14], datasets of 1.5 M and 2.6 M charging sessions, respectively, are used to thoroughly analyse arrival, sojourn and idle times. In [15], the driving profile is based on real data of EVs including SOC, ambient temperature, driving distance and charging time. In [16], the data of 55 electric taxis, including accumulated range, velocity and position of the vehicle and SOC, are used to analyse and predict energy consumption. In real EV data–based solutions that have the information of plug-in time and charging energy, e.g. [13,15], the data can be used to calculate the average charging power. However, the charging peak powers of the EVs are not assessed in these studies.

Additionally, as the technology evolves, it is reasonable to assume that more EVs adopt more powerful OBCs, which naturally impacts the EVs' charging loads. Forecasting the number of EVs in the future is discussed in [7,17], and different EV penetrations are considered in [8,18]. In [7], the future demand of EVs from 2020 to 2050 is investigated by using country-specific projections of the EV fleet development while assuming separate shares for battery electric vehicles (BEVs) and plug-in hybrid electric vehicles (PHEVs). In [17], the number of EV adopters is based on the potential market size, the coefficient of innovation (influenced by external factors, such as monetary subsidy, non-monetary policies, oil price, charging infrastructure and industry maturity) and the coefficient of imitation (reflecting the impacts of previous adopters). However, none of the previously mentioned studies considers the development of the OBCs of the EVs in terms of maximum supported charging powers.

In simulations, it is also common to model linear charging profiles, i. e. assume that EVs can be charged with a fixed power over the whole charging session as in [6–10,12,13,18,19]. Study [17] simply assumes that the power decreases linearly after the SOC reaches 85% in charging sessions with a charging power of over 20 kW. In reality, there are several factors, such as a nearly-fully charged battery or high battery temperature, that can cause the OBC to limit the charging current [20]. In this paper, the non-linear charging profile refers to a situation where the charging current decreases as the battery is becoming fully charged. In [21], it is shown that the real daily charging load considering non-linear profiles can deviate up to 34.2% from the case that assumes that EVs can utilize constant maximum power. This emphasizes the need to consider realistic charging profiles.

Since the EV charging infrastructure is located in parking spaces, the development of charging infrastructure and parking policy are intertwined. The challenges of building charging infrastructure can hinder the uptake of EVs [3]. Many cities have recognized the importance of building charging infrastructure and have made requirements for new buildings to have charging points installed or at least to have readiness for charging points so that they can be installed afterwards. In Finland, there is a new law that regulates the number of charging points in new buildings and buildings undergoing major renovations [22].

However, these charging infrastructure requirements consider only the number of charging points. So far, there has been little discussion about the development of charging power limitations of the EVs' OBCs and how this will affect the low-voltage network and the cost-efficient ways of building charging infrastructures. Additionally, it is important to study how this should be taken into account in parking policy.

1.2. Contributions and structure

Based on the research gaps identified in the literature review, four research questions were formed. The contribution of the paper is to address these questions and provide useful perspectives and numeric results to further improve future studies relating to EV charging. Additionally, the results can be used by policymakers to enhance the sustainability of private-sector transportation from the charging solution point of view. The research questions are as follows:

1. *What is the influence of different charging powers on the charging sessions at commercial charging sites?* To address this question, we thoroughly analyse charging session data from the charging power perspective (Section 2.1).

2. *How does the EV fleet develop in terms of supported charging powers (charging mode 3, IEC 61851)?* To answer this, a car fleet development model is utilized along with the gathered information of existing EV models to estimate the development until 2040 (Section 2.2).

3. *What are the impacts of the development of the EV fleet in commercial charging sites in terms of charging energy and peak loading?* To answer this question, different simulation cases and scenarios are formed based on the analysis of the charging characteristics and the EV fleet (Section 3). In this study, to model the charging loads, a simulation model that considers non-linear charging profiles is used. In the simulation model, preliminary laboratory measurements of four commercial EVs are used to determine the correlation between the charging power and the SOC of the battery. Therefore, the model produces realistic non-linear charging profiles where the charging power decreases before the battery becomes fully charged. After the simulations, the results are analysed (Section 4).

4. *How should the development of the charging energy and peak loads be taken into account in parking policy?* To address this question, we discuss how our findings in relation to the development of the charging energy and peak loads should be considered while making long-term decisions related to charging infrastructure and parking (Section 5).

The paper is finalized in Section 6 by stating the main conclusions and key findings. In this section, the research questions are briefly addressed separately.

2. Data analysis

This section describes the data used in the analysis and presents key findings. The analysis is done separately for the EV charging data and the development of the EV fleet in the following subsections. The analysis focuses on commercial charging sites in the Finnish capital region.

2.1. Charging data

The charging analysis uses real data measured at the Mall of Tripla and the shopping centre REDI, which are both located in Helsinki, Finland. There are nearly 300 [23] and 200 [24] charging points at Tripla and REDI, respectively. In both locations, the charging points provide three-phase charging up to 22 kW. Additionally, the parking areas in both locations are warm, which reduces the need to use the charging energy to warm up the EV or the battery of the EV. Thus, the charging energy can be used mostly for charging the EV batteries. The data consist of charging sessions recorded over a 6-month period (10/2019–3/2020). However, there seem to be notably fewer charging sessions recorded during March 2020 compared to previous months, assumably due to COVID-19. This is also assumed to have impacted parking and charging behaviours and, therefore, the data for March 2020 are excluded. Since the EV penetration increases exponentially, a subset of data (including 3518 sessions from Tripla and 5107 sessions from REDI) measured between 1.11.2019 and 29.2.2020 is selected to represent the average charging behaviour at the beginning of 2020. The charging sessions are uncontrolled, and thus, the charging powers are only limited by the OBCs of the EVs or by the charging point (22 kW). The data include plug-in time, connection time, active charging time, energy consumption and peak power of each charging session.

The data show that most of the charging sessions have a peak charging power of around 4 kW. Two other clear clusters are also seen: ~7.5 and ~ 11 kW. These are expected, as the charging powers of
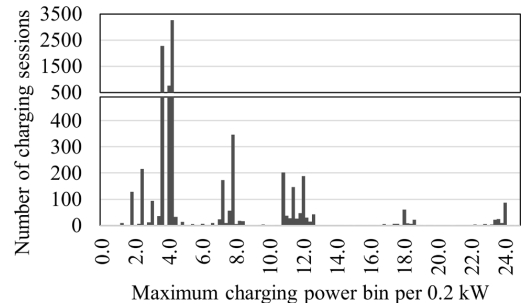

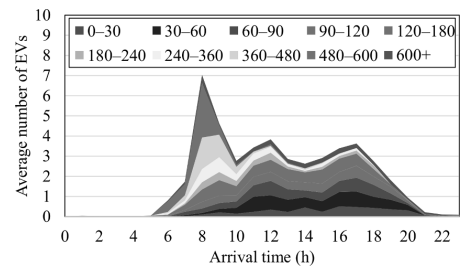**Fig. 1.** Distribution of charging peak powers.

Fig. 2. Average number of EVs arriving each hour, where the colours indicate the categories for the stay durations (min) on a typical weekday at REDI.

commercial EVs in charging mode 3 (IEC 61851) often tend to be 3.7 kW (equalling a single phase 16 A at 230 V), 7.4 kW (1 × 32 A), or 11.0 kW (3 × 16 A) charging. New models are also likely to support 22 kW (3 × 32 A) charging. However, the share of these models is currently marginal. The share of charging sessions with maximum a power of 0–4.5 kW is 79.4%, 4.5–10 kW is 8.1%, 10–15 kW is 9.0%, and 15–25 kW is 3.5%. The distribution of the charging peak powers is shown in Fig. 1.

In Fig. 1, it can be seen that some EVs actually charge with a power greater than 22 kW. This can be explained by the natural variation in voltage levels, which affects the exact charging power. Furthermore, as observed in [25], EV charging currents may slightly exceed the limits set by the charging point.

In the analysis, the charging behaviour is separated into weekdays and weekends for both charging sites, resulting in four different cases. It is assumed that in each case, the probability distribution of the arrival and parking times remain the same when the EV penetration increases. Furthermore, it is assumed that seasons do not substantially impact the sojourn and idle time, as stated in [13]. In this paper, idle time refers to the time that an EV is connected to a charging point, but the charging process is stopped due to a fully charged battery. The data show a correlation between arrival time and parking duration. For example, on a weekday at REDI, there is a noticeable peak in the arrival times in the morning around 8:00; most importantly, a notable share of these EVs stay 8–10 h. It is likely that these EVs are used for commuting. Park & Ride, which is available at REDI on weekdays between 06:30 and 17:30 [24], is a parking facility with public transport connections, allowing commuters to leave their cars outside the city centre and continue their journey via public transport. REDI is located next to Kalasatama metro station, which offers connection to Helsinki city centre. The average number of EVs arriving each hour is presented in Fig. 2 for the case of a weekday at REDI. In the figure, the colour indicates the category of the stay duration, where the unit for the durations is a minute. For example, on average, 7.0 EVs arrive during 8–9 h, and 2.7 of them stay 480–600 min.
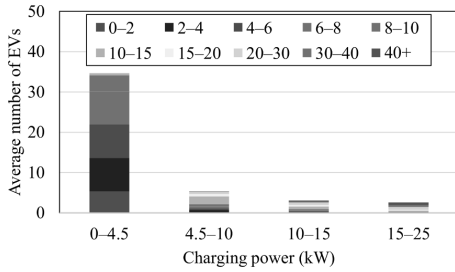
Fig. 3. Average number of EVs with certain charging powers, where the colours indicate the categories for the amount of charged energy (kWh) on a typical weekday at REDI.
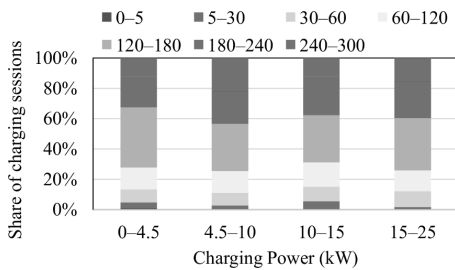

Fig. 4. Distribution of parking time (min) over charging peak powers.
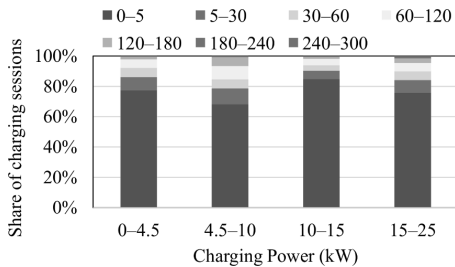

Fig. 5. Distribution of idle time (min) for charging peak powers.

According to the data, a clear correlation exists between the charging peak power and the charging energy of the session. The charging sessions with low charging powers tend to charge less than 10 kWh, whereas a large share of charging sessions with high charging powers charge over 15 kWh. This can be seen in Fig. 3, which presents the average number of EVs with certain charging powers during weekdays at REDI. In the figure, the colour indicates the category for the amount of charged energy, where the unit for the energy is a kWh. The arrival hours with plug-in durations and charging powers with charging energies for other cases are presented in Figs. A.1 and A.2 in the Appendix.

In Fig. 4, the distribution of parking times over charging peak powers of both charging sites is illustrated. In the figure, only the charging sessions with fewer than 5 h of parking time are included to better represent the behaviour of the customers at the shopping centres instead of work charging behaviour. The figure shows that the charging power does not seem to correlate with the stay duration. The study in [14] supports this claim by concluding that the parking time at charging stations (up to 11 kW) are mostly aligned with the parking behaviour and preferences instead of the energy requirement.
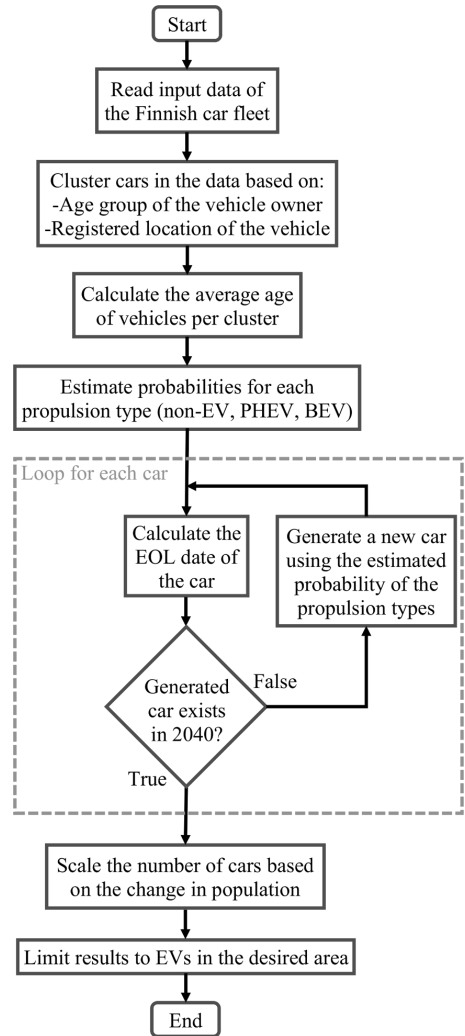
Fig. 6. Block diagram of the EV fleet model to forecast the number of PHEVs and BEVs in 2040.

According to the data, EVs rarely become fully charged, as the parking time and supported charging power act as bottlenecks. This is also true even for the charging sessions that utilize charging powers of 11–22 kW. Therefore, when the share of EV models that support higher charging powers (charging mode 3, IEC-61851) increases, the charging energy will also increase in these kinds of locations. In Fig. 5, the distribution of idle time is presented for both charging sites. Again, only the charging sessions with parking times below 5 h are included. It can be seen that 68.0–84.7% (average 77.4%) of the charging sessions with a plug-in time of fewer than 5 h have idle time of less than 5 min, and fewer than 8.2% have an idle time of 1 h or more. Most importantly, higher charging power does not seem to increase the idle time. The study in [12] is aligned with the results by stating that fulfilling the charging demand at commercial locations, such as shopping centres, often requires a higher charging power compared with home and work charging.

In other types of locations such as the home or workplace, long parking time enables EVs to be fully charged with a moderate charging power. In those cases, a higher charging power will lead to increased flexibility, as the charging can be scheduled more freely from the EV user perspective.

2.2. Development of EV fleet in Finnish Capital Region

To estimate the number of EVs in the Finnish Capital Region during the next 20 years, the baseline scenario results of a prior developed Finnish car fleet model were used. The results of the EV fleet analysis are limited to BEVs and PHEVs located in 4 cities (Helsinki, Espoo, Vantaa and Kauniainen) forming the Finnish Capital region, so that it would respect the expected catchment areas of Tripla and REDI. The model provides both the current car fleet as well as the estimated yearly car fleet development to the year 2040. The model uses disaggregate single-vehicle data from the Finnish vehicle register and combines it with the socio-demographic data of the vehicle owner to calculate the average speed of car renewal within different user and area groups. The average age of cars and EV-acquisition probabilities differ between user and area groups, and they are based on a statistical analysis of car fleet history and survey results regarding EV adoption [26,27].

In Fig. 6, an outline of the car fleet model is presented. As the starting dataset, open data from the Finnish car fleet [28] were used. In addition to the open data fields, the dataset in this study obtained additional fields containing basic information about the registered users of cars. The additional fields were the gender of the registered user (male/female/na), the area the car is registered to (first three digits of the Finnish postal code), year of birth of the registered user (yyyy), age of the registered user, and the datetime-stamp of last inspection of the car, when the mileage of the car was last recorded.

However, not all fields of the open data were needed. The car introduction dates were used to track the age of the cars and technical details were used to see the propulsion type of each car. The postal code was used to categorise the cars in within different area types (according to urban–rural classification by Finnish Environment Institute) and the municipality code was used to track the population development. The area type, age groups (18–24, 25–34, 35–44, 45–54, 55–64, 65–74, over 75), and gender information were used to form categories of every combination of age, gender and area type. This categorisation was chosen as the urban–rural classification is widely used in Finland to reflect differences between areas at the level of a regional structure. Age and gender groups were defined as such because those have been widely used in other research (for example Finnish research and surveys regarding future car use), but they are still wide enough to have large sample size for each category.

The average age of the cars was calculated for each category to produce the end-of-life (EOL) date for every car in that category. Even though this method loses some of the details of a single car, it allows large scale modelling, where only the total composition of the fleet is forecasted. It also takes into account that the average age of cars in Finland varies largely between different areas [29]. The EOL was calculated based on the averages as the data only had a snapshot of Finnish car fleet (for 31st of July 2018), and therefore it did not allow to have more specific calculation method. In the study, it is assumed that the average age of the cars in every category is stable to the end of the simulation. When a car exits the fleet on EOL-day, a replacement enters into the fleet on EOL + 1 day, so there is no overlap or gaps between generations. Whenever a car exits the fleet, it can no longer re-enter.

After defining the EOL of every car, an estimation was made on how the probability to obtain a non-EV, a BEV, or a PHEV changes over time in the future. The yearly probabilities are estimated based on the Finnish national forecasts [30] so that the yearly number of new cars with certain propulsion (non-EV, PHEV, BEV) follows the estimated path. If a car has an EOL estimate before 2040, a new replacement at the EOL point is generated as many times as needed so that the new replacement
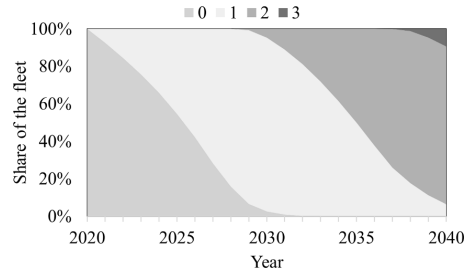

Fig. 7. Model estimated renewal speed of the car fleet in the Finnish Capital Region, where the colours represent the number of times the car owners have replaced their cars since 2020.

Table 1
Supported charging powers of new EVs.

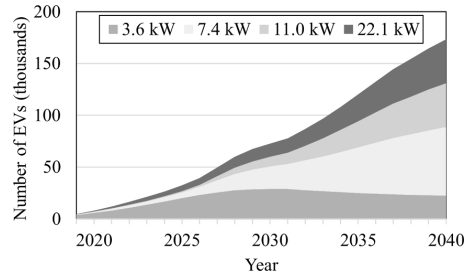| Charging powers		3.7 kW	7.4 kW	11.0 kW	22.1 kW
Scenario 1	PHEVs	70%	30%	–	–
	BEVs	–	50%	25%	25%
Scenario 2	PHEVs	70%	30%	–	–
	BEVs	–	40%	30%	30%
Scenario 3	PHEVs	70%	30%	–	–
	BEVs	–	20%	40%	40%

Fig. 8. Development of the EVs according to Scenario 2.

exists at the year 2040. As the model memorizes each car, the number of PHEVs and BEVs in use in any given year during 2020–2040 can be obtained.

In the car fleet model, it was assumed that the ratio between the population and cars stays stable. To consider the change in the population, the Finnish population forecast [31] was used to calculate yearly changes of population in every municipality to correct the car amounts to respect the forecasted population development. Finally, the results were limited to BEVs and PHEVs for the desired area to know the annual number of EVs.

In Fig. 7, the average car fleet renewal speed in the Finnish Capital Region is presented. The number of cars used in 2020 is assumed as iteration zero, and the figure depicts how large a share of the car fleet has been upgraded to a newer model at any given year.

According to the car fleet model, the total number of EVs in the Finnish Capital region will increase from 7,972 to 72,712 by 2030 and to 173,319 by 2040. In this paper, we assume that the average number of charging sessions at REDI and Tripla will increase in the same proportion.

For the current car fleet, where specific car models are known, the EV Database [32] is used to gather information about the charging power and technology in existing EV models. This information was used to classify every existing EV in the area based on its maximum charging

power, which was either 3.7, 7.4, 11.0 or 22.1 kW.

For new PHEVs, it is assumed that 70% will have an OBC with a maximum power of 3.7 kW and 30% with a 7.4 kW max. The BEVs are assumed to be 7.4 kW, 11.0 kW or 22.1 kW. The exact shares will depend on the scenario. Three different scenarios are studied to assess uncertainty regarding the charging powers of new EVs. The distribution of the charging powers of new EVs for each scenario is shown in Table 1, and the number of EVs with certain charging powers for Scenario 2 are shown in Fig. 8.

Due to the relatively slow renewal speed of the car fleet, the share of EVs that support only 3.7 kW seems to be dominant for the next 5–10 years. After that, the share of the higher charging powers takes over. In Scenario 2, the share of EVs that support 3.7 kW is 12.9%, 7.4 kW is 38.2%, 11.0 kW is 24.5%, and 22.1 kW is 24.5% in 2040.

3. Modelling power demand

This section describes the generation of the simulation cases and the used simulation model that generates the power consumption profiles for all EVs. Both the cases and the model are described in separate subsections.

3.1. Simulation cases

By combining the development of the EV fleet and the average number of charging sessions in each case (REDI/Tripla and weekday/weekend), the number of charging sessions can be estimated for the following years. In this paper, the charging load for 2020, 2025, 2030, 2035, and 2040 are studied. As mentioned earlier, it is assumed that the average daily number of charging sessions in REDI and Tripla increases by the same proportion as the total number of EVs in the Finnish Capital Region. The charging powers of the new EVs in each scenario are determined using the shares presented in Table 1. The exact number of charging sessions separated by their charging powers are presented in Table A.1 in the Appendix.

After determining the total amount of EVs with certain charging powers, the correlation between the charging powers and the charged energies presented in Fig. 3 (for the case of a weekday in REDI) and in Fig. A.2 (for all cases) is used to determine the amounts of energy to be charged. However, since there have been only 12 charging sessions with charging powers of 15–25 kW at Tripla in the data, it does not form a well scalable probability distribution. Therefore, the combined data of both REDI (includes 289 charging sessions with charging powers of 15–25 kW) and Tripla are used to determine the amounts of energy to be charged for the EVs with charging powers of 15–25 kW for Tripla.

As the charging power does not have a clear correlation with the arrival hours or stay durations, the arrival timings and stay durations are generated separately and are randomly allocated for the EVs. The generation is done using the correlation between the arrival hours and stay duration categories presented in Fig. 2 (for the case of a weekday in REDI) and in Fig. A.1 (for all cases). The exact minute of the arrival times and the exact charging energy within the category (i.e. "0–2 kWh", "2–4 kWh", etc.) are randomly generated.

As mentioned earlier, EVs rarely become fully charged at the investigated charging locations as the parking time and supported charging power act as bottlenecks. This means that the charged energies in the datasets determine only the lower bound for the actual missing energies of the EVs. To carry out the simulations, it is assumed that the charged energy in the data is the exact energy that was initially missing from the EV when it was plugged in. This assumption is likely to reduce the total charging loads. However, since the same assumption is made for each simulation case, the results are comparable with each other.

3.2. Simulation model

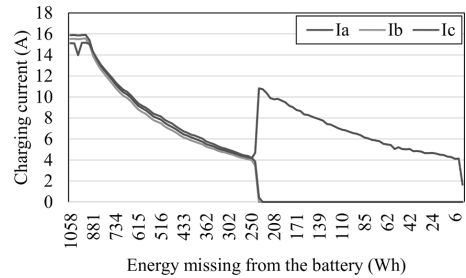The used simulation model couples realistic charging profiles (phase

Fig. 9. Correlation between the realized charging current and the energy that is missing from the battery for BMW i3.
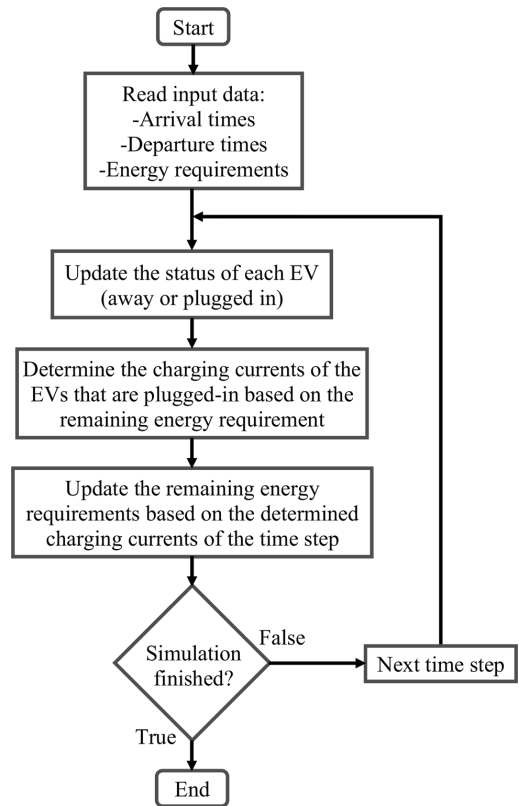

Fig. 10. Block diagram of the simulation model.

currents for each time step) with charging session data (arrival time, departure time and charging energy requirement). The charging profiles of the EVs are modelled based on real measurements of uncontrolled charging sessions of four different commercial EVs with a time-resolution of one second. These measurements are then used to calculate the energies that are missing from the batteries of the EVs (i.e. charging energy requirements) of each time step. The process goes backwards from the end of the charging sessions where the missing energies are zero. Then, a lookup table is formed separately for each EV to represent the correlation between the realized charging currents and the missing energy. Thus, the simulation model takes the limitations of

Table 2
Electric vehicles.

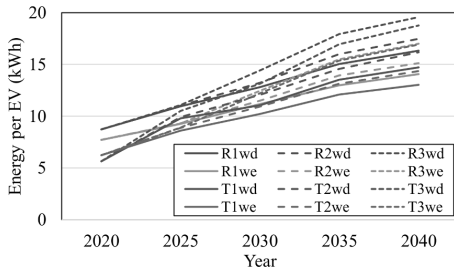| Model	Max charging current	Max charging power	Charging power group
Nissan 2012	1x16 A	3.7 kW	0–4.5 kW
Nissan 2019	1x32 A	7.4 kW	4.5–10 kW
BMW i3	3x16 A	11.0 kW	10–15 kW
Smart forfour	3x32 A	22.1 kW	15–25 kW

Fig. 11. Average charging energy consumption per EV.

the OBCs fully into account and is able to produce realistic non-linear charging profiles where the charging current decreases before the battery becomes fully charged. Instead of percentual SOC, the simulation model considers only the energy in Wh that is missing from the batteries of the EVs as this method does not require the maximum battery capacities to be known.

As an example, the charging profile model for BMW i3 is illustrated in Fig. 9. If the missing energy is greater or equal to 1058 Wh, the charging currents are 15.9 (phase a), 15.5 (phase b) and 15.1 A (phase c). According to the conducted measurements, the charging currents have very little variation (less than 0.5 A) until the battery is close to being fully charged. Therefore, the charging profile model of BMW i3 assumes constant charging currents when the missing energy is greater than 1058 Wh. As seen in the figure, the BMW utilizes mostly three-phase charging but switches to a single-phase charging when the missing energy is around 235 Wh.

As mentioned in [20], the charging currents also depend on the temperature of the battery. However, due to the increasing complexity, it is left out of the modelling. The operating principle of the simulation model is illustrated in Fig. 10.

The used EV models include Nissan Leaf 2012, Nissan Leaf 2019, BMW i3, and Smart forfour EQ. These EVs have different charging characteristics, thus enabling a comprehensive basis for the modelling of large EV fleets. According to the ablation study in [21], when considering charge profiles in heterogeneous EV fleets, the number of phases used for charging and the maximum current are much more important than the exact EV model. Therefore, the EVs shown in Table 2 can be used to model most EV charging profiles with a reasonable accuracy.

As mentioned in [8], a time resolution of 1 min is notably more accurate than one of 5 min when modelling momentary peak loads in 22 kW charging powers. However, since the study did not consider finer time resolutions, a finer time resolution may yield even more accurate results. Therefore, the model uses a time resolution of 10 s.

The simulation model considers three phase charging points. The phase order of the charging point alternates, as it is common practice to avoid unnecessary phase imbalance, which may occur especially if there are multiple EVs that utilize only a single phase for charging. In the simulations, the arriving EVs are assigned randomly for available charging points.
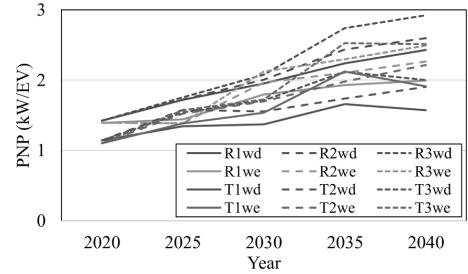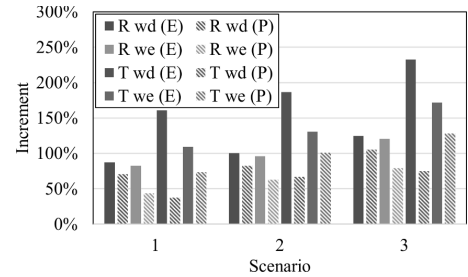

Fig. 12. Peak of normalized power (PNP).

Fig. 13. Increment of the average charging energy and the PNP.

4. Results

The key numeric results of the simulations are presented in Table A.2 in the Appendix. From the results, it can be seen that the total charging load and the highest peak load in commercial locations will increase at a faster pace than the number of EVs. For example, the total daily charging energy and the highest daily peak power increase over the 20 years by factors of 39.2–71.5 and 29.0–48.1, respectively, while the number of EVs increases by a factor of 20.6–21.1. This is due to the increased share of EVs with more powerful OBCs, which allows the EVs to charge more energy within the very limited amount of available plug-in time.

To enable a more straightforward comparison with other charging sites and locations, the average charged energy per EV and the peak of the normalized power (PNP) are calculated and presented in Figs. 11 and 12, respectively. In the figures, 'R' denotes REDI, 'T' denotes Tripla, the numbers 1–3 denote the scenario, 'wd' denotes weekday, and 'we' denotes weekend. The peak of the normalized power is defined in [8] and can be calculated according to Eq. (1),

$$PNP = \frac{P_{max}}{n_{EV}} \tag{1}$$

where P_{max} is the highest peak load and n_{EV} is the total number of EVs.

In Fig. 11, it can be seen that the average charging energy per EV is expected to increase relatively linearly over the next 20 years, from 5.6 to 8.7 kWh to 13.0–19.6 kWh. As the PNP depends heavily on the timings of the charging sessions, it includes a higher variability. Nonetheless, the PNP rises from 1.1 to 1.4 kW/EV to 1.6–2.9 kW/EV. The results also show that the average charging energy per EV increases more than the PNP. This is illustrated in Fig. 13, where the increment of the average charging energy per EV (E) and the PNP (P) over the 20 years can be compared. The figure shows that the solid bars (increment of the energy) are consistently higher than the striped bars (increment of the PNP), i.e. the average charging energy clearly increases at a faster pace than the PNP in next 20 years. This is assumed to be due to the fact that the higher the daily number of charging sessions, the less likely it is that most of
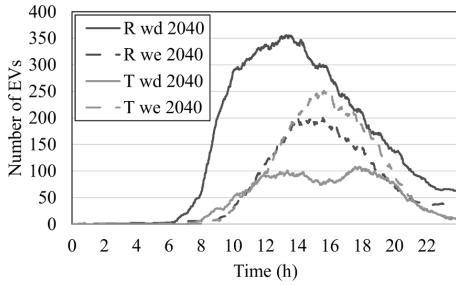
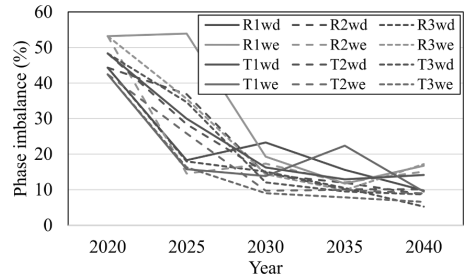**Fig. 14.** The average number of charging sessions.

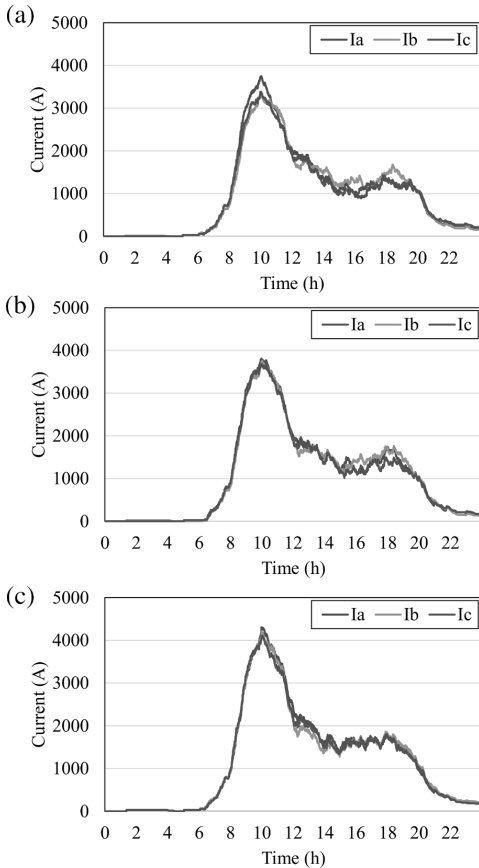**Fig. 16.** Phase imbalance of the charging load.

behaviour from a timing perspective. To illustrate this, the number of charging sessions for each case in 2040 is presented in Fig. 14. Although the average daily number of charging sessions for a weekday at REDI (993) and a weekend at Tripla (949) are relatively close, the use of charging points in terms of time of occupancy are very different. This can be explained by the different distribution of arrival times over plug-in durations, as illustrated in Fig. A.1. On the weekend at Tripla, EV users tend to arrive later and stay for a shorter amount of time compared to weekdays at REDI.

The charging loads on weekdays at REDI in 2040 are illustrated in Fig. 15. Contrary to the results mentioned in [10], the charging peak demand does not seem to be earlier for scenarios where the average charging power of the EVs is higher. Instead, the charging peak demand is higher for the scenarios where the average charging power of the EVs is higher. From the figure, it can also be seen that the loading imbalance of the three phases varies between the scenarios.

Further phase imbalance analysis is carried out using Eq. (2), where I_u represents the percentual phase imbalance for each time step t, $\Delta I_{max,avg}$ is the maximum deviation of any phase current from the average current I_{avg}. In each simulation case, the average phase imbalance of each time step is calculated. To avoid potential distortion caused by, e.g. a random single-phase EV charging at nighttime, the average phase imbalance is limited to time steps with at least three EVs present. The average phase imbalance for each simulation case is presented in Fig. 16. In the figure, the phase imbalance is shown to decrease over the years, and Scenario 3 tends to lead to a slightly lower phase imbalance compared with Scenario 1. This indicates that the decreasing phase imbalance correlates more notably with the increasing number of EVs than the increasing share of EVs that support three-phase charging.

$$I_u(t) = \frac{\Delta I_{max,avg}(t)}{I_{avg}(t)} \times 100\% \qquad (2)$$

5. Discussion

The simulation results promote the idea of centralized charging locations from two perspectives. Firstly, as seen in Fig. 13, an increasing number of EVs in a charging site will increase total energy consumption more than the peak power demand. Secondly, the average phase imbalance decreases as the number of EVs increases, as seen in Fig. 16. Therefore, to ensure a certain level of user satisfaction, the total charging capacity per charging point can be lower in larger charging sites than in smaller charging sites. The centralization of small charging sites into larger ones may also result in lower infrastructure costs per EV. If the site is large enough, it can also be connected directly to a higher voltage level, eliminating the potential bottlenecks of the low voltage network.

Regardless of the size of the charging site, the development of the charging energy demand and the peak power demand obviously impact the optimal sizing of charging infrastructure. This may also include other components such as PV systems and energy storage systems (ESSs)
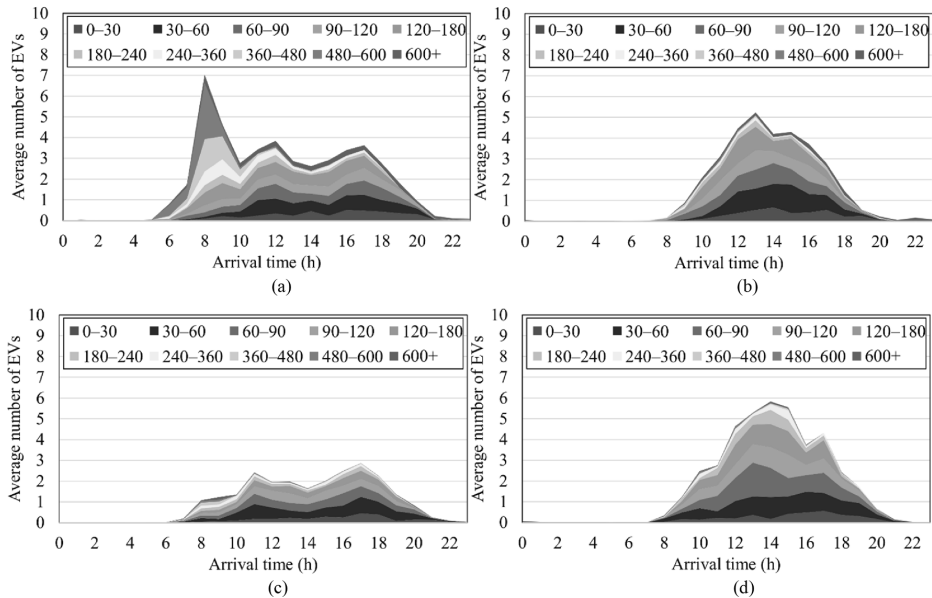

Fig. 15. Current consumption on a weekday at REDI in 2040 for (a) Scenario 1, (b) Scenario 2 and (c) Scenario 3.

them will be charging with maximum power at the same time. The results shown in Table A.2 support this claim as the highest number of EVs simultaneously plugged in in a day (N_{max}) per the total number of EVs in a day (N_{EV}) decreases over the years in most cases as the total number of EVs in a day increases. On average, the increment of the average charging energy per EV is $+133.5\%$, whereas the increment of the PNP is $+77.1\%$.

According to the simulations, each case results in different charging

Fig. A1. Average number of EVs arriving each hour where the colours indicate the categories for stay durations (min) in the case of (a) REDI weekday, (b) REDI weekend, (c) Tripla weekday and (d) Tripla weekend.

that are coupled with the charging site. Since the lifetime of PV systems and ESSs are quite long, the development of the EV fleet in terms of size and charging powers will impact the total benefits. Therefore, studies considering the sizing of the charging capacity [33], PV systems [19] or ESS [11] could benefit from the results presented in this paper to enhance the accuracy of the calculations. Besides avoiding potential overinvestments, the accurate load modelling can be used to ensure satisfying quality of the charging service, i.e. the energy charged to the EVs. According to the survey presented in [34], the quality of the charging service is seen as a more important factor than the charging costs.

As the charging powers of the EVs and the average energy consumption of the charging sessions in commercial locations increases, a larger part of the home charging load is fulfilled by commercial charging. This means that the load is shifted from later evening to daytime, which can be beneficial from a renewable energy perspective as the solar energy can be utilized more efficiently by the EV fleet. To take full advantage of this, commercial charging sites should use charging points that support powers up to 22 kW along with a cost-effective PV system. It would be worth considering the use of subsidies or policies to encourage such arrangements in commercial charging locations as it would be a logical step towards fully renewable energy-powered EVs.

6. Conclusions

This paper has analysed the charging characteristics in commercial charging locations in terms of supported charging powers. Additionally, two simulation models are used. The first model estimates the development of the electric vehicle (EV) fleet and the supported charging powers of the EVs. The second model simulates the charging loads in fine detail. Based on the results, it is evident that the supported charging powers of the EVs have a significant impact on the charging loads when considering charging points with a nominal power of > 3.7 kW.

The investigated research questions and the findings of the study are listed below:

1. *What is the influence of different charging powers on the charging sessions at commercial charging sites?* According to the data analysis, 77% of the charging sessions on average have idle time of less than 5 min in commercial locations, which means that the charging process continues throughout the whole plug-in duration in most cases. Importantly, a higher supported charging power of the EV does not seem to increase the idle time, which indicates that the available charging time together with the charging power forms a bottleneck for the charged energy. As a consequence, when the EV fleet develops and EVs begin to support higher charging powers, the average charging energy per EV will also increase in these locations. Since most of the analysed charging sessions (79%) support only charging powers below 4.5 kW, the increase is likely to be notable. Meanwhile, the flexibility of the EVs may not increase remarkably unless both the charging site and the EVs begin to support over 22 kW charging powers.

2. *How does the EV fleet develop in terms of supported charging powers?* The results indicate that the share of EVs with ~ 3.7 kW maximum charging powers will dominate the next 5–10 years. However, after that, most EVs begin to support higher charging powers. In 2040, the estimated share of EVs that support around 3.7 kW is 12.9%, 7.4 kW is 38.2%, 11.0 kW is 24.5% and 22.1 kW is 24.5%.

3. *What are the impacts of the development of the EV fleet in commercial charging sites in terms of charging energy and peak loading?* According to the simulations, both the average charging energy per EV and the peak of the normalized power will increase notably over the next 20 years. The average energy will increase from 5.6 to 8.7 kWh/EV to 13.0–19.6 kWh/EV (+133.5% on average), while the peak of the normalized power increases from 1.1 to 1.4 kW/EV to 1.6–2.9 kW/EV (+77.1% on average).

4. *How should the development of the charging energy and peak loads be taken into account in parking policy?* According to the results, centralized charging solutions could lead to a more cost-effective utilization of charging capacity, thus lowering the infrastructure costs per EV. If the site is large enough, it can also be connected directly to a higher voltage level. Additionally, centralized parking
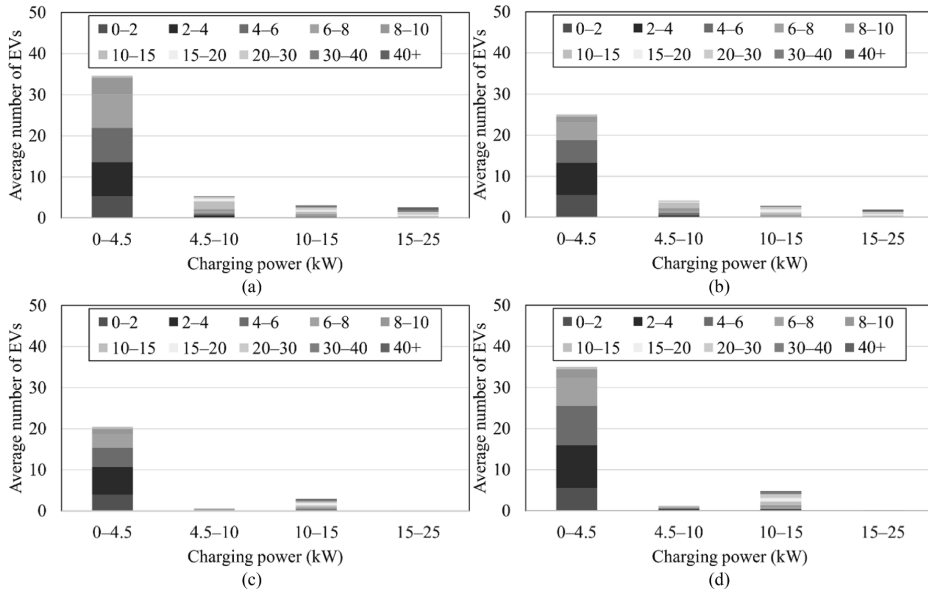
Fig. A2. Average number of EVs with certain charging powers, where the colours indicate the categories for the amount of charged energy (kWh) in the case of (a) REDI weekday, (b) REDI weekend, (c) Tripla weekday and (d) Tripla weekend.

allows new forms of city development, as it frees the parking spaces from the street level to be used by other sustainable forms of transport. These factors should be considered when planning the implementation and location of new parking spaces.

Overall, the results of the study are quite valuable. They can be used to improve the accuracy and reliability of future simulations related to topics such as load forecasting, flexibility evaluation, and optimal sizing of charging infrastructure. Additionally, policymakers can use these findings to improve parking policies from the charging solution

perspective. Future work aims to investigate the impacts of the increasing charging powers of the EVs in other charging sites, such as homes and workplaces. Furthermore, the influence of the charging loads of different charging sites on each other will be studied.

CRediT authorship contribution statement

Toni Simolin: Conceptualization, Software, Data curation, Formal analysis, Investigation, Methodology, Visualization, Writing – original draft, Writing – review & editing, Validation. **Kalle Rauma:**

Table A1
The number of EVs in the simulation cases separated by their charging powers.

Charging power (kW)					3.7	7.2	11.0	22.1					Total
2020	**REDI**	Weekday			35	5	3	3					46
		Weekend			26	4	3	2					35
	Tripla	Weekday			20	1	3	0					24
		Weekend			37	1	5	0					44
			Scenario 1				Scenario 2				Scenario 3			
Charging power (kW)			3.7	7.2	11.0	22.1	3.7	7.2	11.0	22.1	3.7	7.2	11.0	22.1	Total
2025	**REDI**	Weekday	117	31	9	29	117	30	9	30	117	29	10	30	186
		Weekend	91	24	7	23	90	24	8	23	91	23	8	23	145
	Tripla	Weekday	64	14	6	14	64	14	6	14	64	13	6	15	98
		Weekend	116	26	11	25	116	25	11	26	117	24	11	26	178
2030	**REDI**	Weekday	168	140	47	62	168	124	55	70	167	91	72	87	417
		Weekend	130	109	37	48	129	96	44	55	130	71	56	67	324
	Tripla	Weekday	90	72	26	31	90	63	30	36	90	46	39	44	219
		Weekend	164	130	47	57	164	114	55	65	164	83	71	80	398
2035	**REDI**	Weekday	144	300	123	120	144	252	147	144	144	156	195	192	687
		Weekend	111	234	96	93	111	196	115	112	112	121	152	149	534
	Tripla	Weekday	78	156	66	62	78	131	79	74	78	80	104	100	362
		Weekend	142	283	119	112	142	237	142	135	142	145	188	181	656
2040	**REDI**	Weekday	130	460	204	199	130	378	245	240	130	217	326	320	993
		Weekend	101	357	159	155	101	294	191	186	101	168	254	249	772
	Tripla	Weekday	71	240	109	103	71	197	130	125	71	112	173	167	523
		Weekend	129	435	197	188	129	358	236	226	129	203	313	304	949

Table A2

Key numeric results of the simulations.

			REDI				Tripla		
2020	Weekday	N_{EV} (N_{max})	46 (20)			N_{EV} (N_{max})	24 (6)		
		P_{max} (kW)	65.5			P_{max} (kW)	27.4		
		E (kWh)	401.4			E (kWh)	135.4		
		E/N_{EV} (kWh)	8.73			E/N_{EV} (kWh)	5.64		
		P_{max}/N_{EV} (kW)	1.42			P_{max}/N_{EV} (kW)	1.14		
	Weekend	N_{EV} (N_{max})	35 (8)			N_{EV} (N_{max})	44 (13)		
		P_{max} (kW)	48.7			P_{max} (kW)	48.5		
		E (kWh)	270.0			E (kWh)	274.1		
		E/N_{EV} (kWh)	7.71			E/N_{EV} (kWh)	6.23		
		P_{max}/N_{EV} (kW)	1.39			P_{max}/N_{EV} (kW)	1.10		
			Scenario 1	Scenario 2	Scenario 3		Scenario 1	Scenario 2	Scenario 3
2025	Weekday	N_{EV} (N_{max})	186 (72)			N_{EV} (N_{max})	98 (21)		
		P_{max} (kW)	319.7	320.6	326.4	P_{max} (kW)	131.6	154.6	151.0
		E (kWh)	2040.2	2050.6	2063.3	E (kWh)	959.6	970.8	1030.1
		E/N_{EV} (kWh)	11.97	11.02	11.09	E/N_{EV} (kWh)	9.79	9.91	10.51
		P_{max}/N_{EV} (kW)	1.72	1.72	1.75	P_{max}/N_{EV} (kW)	1.34	1.58	1.54
	Weekend	N_{EV} (N_{max})	145 (40)			N_{EV} (N_{max})	178 (49)		
		P_{max} (kW)	209.0	201.1	201.1	P_{max} (kW)	246.4	271.5	280.0
		E (kWh)	1341.77	1352.42	1345.41	E (kWh)	1529.3	1581.1	1587.0
		E/N_{EV} (kWh)	9.25	9.33	9.28	E/N_{EV} (kWh)	8.59	8.88	8.92
		P_{max}/N_{EV} (kW)	1.44	1.39	1.39	P_{max}/N_{EV} (kW)	1.38	1.53	1.57
2030	Weekday	N_{EV} (N_{max})	417 (154)			N_{EV} (N_{max})	219 (46)		
		P_{max} (kW)	814.0	835.8	866.2	P_{max} (kW)	299.83	340.31	374.91
		E (kWh)	5344.6	5514.1	6018.2	E (kWh)	2422.9	2639.3	2873.8
		E/N_{EV} (kWh)	12.82	13.22	14.43	E/N_{EV} (kWh)	11.06	12.05	13.12
		P_{max}/N_{EV} (kW)	1.95	2.00	2.08	P_{max}/N_{EV} (kW)	1.37	1.55	1.71
	Weekend	N_{EV} (N_{max})	324 (91)			N_{EV} (N_{max})	398 (103)		
		P_{max} (kW)	581.9	637.4	687.9	P_{max} (kW)	611.9	676.3	686.8
		E (kWh)	3619.6	3726.6	4037.6	E (kWh)	4064.2	4352.3	4854.7
		E/N_{EV} (kWh)	11.17	11.50	12.46	E/N_{EV} (kWh)	10.21	10.94	12.20
		P_{max}/N_{EV} (kW)	1.80	1.97	2.12	P_{max}/N_{EV} (kW)	1.54	1.70	1.73
2035	Weekday	N_{EV} (N_{max})	687 (252)			N_{EV} (N_{max})	362 (76)		
		P_{max} (kW)	1536.9	1672.1	1882.5	P_{max} (kW)	600.6	629.5	767.3
		E (kWh)	10329.9	10987.7	12317.0	E (kWh)	4898.4	5268.9	6134.7
		E/N_{EV} (kWh)	15.04	15.99	17.93	E/N_{EV} (kWh)	13.53	14.55	16.95
		P_{max}/N_{EV} (kW)	2.24	2.43	2.74	P_{max}/N_{EV} (kW)	1.66	1.74	2.12
	Weekend	N_{EV} (N_{max})	534 (138)			N_{EV} (N_{max})	656 (165)		
		P_{max} (kW)	1031.7	1123.6	1227.1	P_{max} (kW)	1391.9	1297.4	1657.5
		E (kWh)	6927.2	7451.1	8272.1	E (kWh)	7929.0	8621.2	10092.7
		E/N_{EV} (kWh)	12.97	13.95	15.49	E/N_{EV} (kWh)	12.09	13.14	15.39
		P_{max}/N_{EV} (kW)	1.93	2.10	2.30	P_{max}/N_{EV} (kW)	2.12	1.98	2.53
2040	Weekday	N_{EV} (N_{max})	993 (356)			N_{EV} (N_{max})	523 (108)		
		P_{max} (kW)	2412.0	2578.6	2902.1	P_{max} (kW)	821.7	995.5	1046.7
		E (kWh)	16213.6	17353.0	19435.8	E (kWh)	7696.4	8462.0	9814.5
		E/N_{EV} (kWh)	16.33	17.48	19.57	E/N_{EV} (kWh)	14.72	16.18	18.77
		P_{max}/N_{EV} (kW)	2.43	2.60	2.92	P_{max}/N_{EV} (kW)	1.57	1.90	2.00
	Weekend	N_{EV} (N_{max})	772 (204)			N_{EV} (N_{max})	949 (251)		
		P_{max} (kW)	1539.9	1748.0	1923.4	P_{max} (kW)	1813.2	2102.1	2382.9
		E (kWh)	10859.5	11676.6	13128.0	E (kWh)	12366.7	13626.9	16062.9
		E/N_{EV} (kWh)	14.07	15.13	17.01	E/N_{EV} (kWh)	13.03	14.36	16.93
		P_{max}/N_{EV} (kW)	1.99	2.26	2.49	P_{max}/N_{EV} (kW)	1.91	2.22	2.51

N_{EV} is the total number of EVs in a day, N_{max} is the highest number of EVs simultaneously plugged in a day, E is the total charged energy (kWh) in a day, P_{max} is the highest peak load (kW) in a day

Conceptualization, Data curation, Investigation, Validation, Resources, Writing – original draft, Writing – review & editing. **Riku Viri:** Conceptualization, Data curation, Formal analysis, Investigation, Methodology, Writing – original draft, Writing – review & editing, Validation. **Johanna Mäkinen:** Conceptualization, Investigation, Methodology, Writing – original draft, Writing – review & editing, Validation. **Antti Rautiainen:** Writing – review & editing. **Pertti Järventausta:** Writing – review & editing.

Declaration of Competing Interest

The authors declare that they have no known competing financial interests or personal relationships that could have appeared to influence the work reported in this paper.

charging data.

Appendix

See Figs. A1 and A2
See Table A1 and A2

References

[1] Melliger MA, van Vliet OPR, Liimatainen H. Anxiety vs reality – Sufficiency of battery electric vehicle range in Switzerland and Finland. Transportation Research Part D: Transport and Environment 2018;65:101–15. https://doi.org/10.1016/j.trd.2018.08.011.

[2] Scorrano M, Danielis R, Giansoldati M. Dissecting the total cost of ownership of fully electric cars in Italy: The impact of annual distance travelled, home charging and urban driving. Res. Transp. Econ. 2020;80:100799. https://doi.org/10.1016/j.retrec.2019.100799.

[3] Lopez-Behar D, Tran M, Mayaud JR, Froese T, Herrera OE, Merida W. Putting electric vehicles on the map: A policy agenda for residential charging infrastructure in Canada. Energy Res. Soc. Sci. 2019;50(November 2018):29–37. https://doi.org/10.1016/j.erss.2018.11.009.

[4] Ge X, Shi L, Fu Y, Muyeen SM, Zhang Z, He H. Data-driven spatial-temporal prediction of electric vehicle load profile considering charging behavior. Electr. Power Syst. Res. 2020;187:106469. https://doi.org/10.1016/j.epsr.2020.106469.

[5] Pareschi G, Küng L, Georges G, Boulouchos K. Are travel surveys a good basis for EV models? Validation of simulated charging profiles against empirical data. Appl. Energy 2020;275:115318. https://doi.org/10.1016/j.apenergy.2020.115318.

[6] Zhang J, Yan J, Liu Y, Zhang H, Lv G. Daily electric vehicle charging load profiles considering demographics of vehicle users. Appl. Energy 2020;274:115063. https://doi.org/10.1016/j.apenergy.2020.115063.

[7] Gunkel PA, Bergaentzlé C, Græsted Jensen I, Scheller F. From passive to active: Flexibility from electric vehicles in the context of transmission system development. Appl. Energy 2020;277:115526. https://doi.org/10.1016/j.apenergy.2020.115526.

[8] Shepero M, Munkhammar J. Spatial Markov chain model for electric vehicle charging in cities using geographical information system (GIS) data. Appl. Energy 2018;231(June):1089–99. https://doi.org/10.1016/j.apenergy.2018.09.175.

[9] Jahangir H, Tayarani H, Ahmadian A, Golkar MA, Miret J, Tayarani M, et al. Charging demand of Plug-in Electric Vehicles: Forecasting travel behavior based on a novel Rough Artificial Neural Network approach. J. Clean. Prod. 2019;229:1029–44. https://doi.org/10.1016/j.jclepro.2019.04.345.

[10] Dixon J, Bell K. Electric vehicles: Battery capacity, charger power, access to charging and the impacts on distribution networks. eTransportation 2020;4:100059. https://doi.org/10.1016/j.etran.2020.100059.

[11] Haupt L, Schöpf M, Wederhake L, Weibelzahl M. The influence of electric vehicle charging strategies on the sizing of electrical energy storage systems in charging hub microgrids. Appl. Energy 2020;273:115231. https://doi.org/10.1016/j.apenergy.2020.115231.

[12] Yi T, Zhang C, Lin T, Liu J. Research on the spatial-temporal distribution of electric vehicle charging load demand: A case study in China. J. Clean. Prod. 2020;242:118457. https://doi.org/10.1016/j.jclepro.2019.118457.

[13] Sadeghianpourhamami N, Refa N, Strobbe M, Develder C. Quantitive analysis of electric vehicle flexibility: A data-driven approach. Int. J. Electr. Power Energy Syst. 2018;95:451–62. https://doi.org/10.1016/j.ijepes.2017.09.007.

[14] Wolbertus R, Kroesen M, van den Hoed R, Chorus C. Fully charged: An empirical study into the factors that influence connection times at EV-charging stations. Energy Policy 2018;123(August):1–7. https://doi.org/10.1016/j.enpol.2018.08.030.

[15] Zhao Y, Wang Z, Shen Z-J, Sun F. Data-driven framework for large-scale prediction of charging energy in electric vehicles. Appl. Energy 2021;282:116175. https://doi.org/10.1016/j.apenergy.2020.116175.

[16] Zhang J, Wang Z, Liu P, Zhang Z. Energy consumption analysis and prediction of electric vehicles based on real-world driving data. Appl. Energy 2020;275(5):115408. https://doi.org/10.1016/j.apenergy.2020.115408.

[17] Zheng Y, Shao Z, Zhang Y, Jian L. A systematic methodology for mid-and-long term electric vehicle charging load forecasting: The case study of Shenzhen, China. Sustain Cities Soc. 2020;56(September 2019):102084. https://doi.org/10.1016/j.scs.2020.102084.

[18] Xiang Y, Jiang Z, Gu C, Teng F, Wei X, Wang Y. Electric vehicle charging in smart grid: A spatial-temporal simulation method. Energy 2019;189:116221. https://doi.org/10.1016/j.energy.2019.116221.

[19] Deshmukh SS, Pearce JM. Electric vehicle charging potential from retail parking lot solar photovoltaic awnings. Renew. Energy 2021;169:608–17. https://doi.org/10.1016/j.renene.2021.01.068.

[20] Lee ZJ, Chang D, Jin C, Lee GS, Lee R, Lee T. et al., "Large-scale adaptive electric vehicle charging," 2018 IEEE Glob. Conf. Signal Inf. Process. Glob. 2018 - Proc., pp. 863–864, 2019, doi: 10.1109/GlobalSIP.2018.8646472.

[21] Frendo O, Graf J, Gaertner N, Stuckenschmidt H. Data-driven smart charging for heterogeneous electric vehicle fleets. Energy AI 2020;1:100007. https://doi.org/10.1016/j.egyai.2020.100007.

[22] "Hallituksen esitys eduskunnalle laeiksi sähköajoneuvojen latauspisteistä ja latauspistevalmiuksista rakennuksissa sekä rakennusten automaatio- ja ohjausjärjestelmistä ja maankäyttö- ja rakennuslain 126 §:n muuttamisesta" ("Law on charging points for electric vehicles and readiness for charging points in buildings, as well as a system for property automation and property management and a law amending section 126 of the Land Use and Building Act"), https://www.eduskunta.fi/FI/vaski/EduskunnanVastaus/Sivut/EV_108+2020.aspx [Accessed 8 April 2021].

[23] "Parking at Mall of Tripla," https://malloftripla.hyperin.com/en/web/mall-of-tripla-2019/pysakointi [Accessed 8 April 2021].

[24] "Parking at REDI," https://www.redi.fi/parking/?lang=en [Accessed 8 April 2021].

[25] Rauma K, Simolin T, Rautiainen A, Järventausta P, Rehtanz C. "Overcoming non-idealities in electric vehicle charging management," accepted in IET Electrical Systems in Transportation 28.3.2021.

[26] "Ladattavien autojen käyttötutkimus - selvitys ladattavien hybridien ja täyssähköautojen käyttötavoista" ("User survey of electric vehicles – user habits of plug-in hybrid and battery electric vehicles in Finland"), https://www.aut.fi/ajankohtaista/julkaisuja/ladattavien_autojen_tutkimus [Accessed 8 April 2021].

[27] "Suomalaisten autoilu 2019" ("Driving in Finland 2019"), https://www.aut.fi/ajankohtaista/julkaisuja/suomalaisten_autoilu [accessed 8 April 2021].

[28] "Open data for vehicles version 5.14," https://www.traficom.fi/en/news/open-data?toggle=Open%20data%20for%20vehicles%20version%205.14 [Accessed 8 June 2021].

[29] Viri R. "Different Characteristics of Finnish Car Fleet and its Development," European Transport Conference, Dublin, Ireland, Oct. 2019, p. 12.

[30] Ministry of Transport and Communications, "Liikenteen kasvihuonekaasupäästöjen perusennuste 2020–2050" ("Baseline forecast of greenhousegas emissions of transportation 2020–2050"), https://api.hankeikkuna.fi/asiakirjat/d99a3ae3-b7f9-49df-afd2-c8f2efd3dc1d/1ab511f1-aa06-45c0-b3ef-9ac9650838c9/MUISTIO_20200422120412.pdf [Accessed 8 June 2021].

[31] "Population projection 2019: Demographic dependency ratio by area, 2019–2040," https://pxnet2.stat.fi/PXWeb/pxweb/en/StatFin/StatFin_vrm_vaenn/statfin_vaenn_pxt_128x.px/table/tableViewLayout1/ [Accessed 8 June 2021].

[32] "Electric Vehicle Database," https://ev-database.org/ [Accessed 8 April 2021].

[33] Dong Houqi, Wang Liying, Wei Xuan, Xu Yanbin, Li Weikang, Zhang Xiaochun, et al. Capacity planning and pricing design of charging station considering the uncertainty of user behavior. Int. J. Electr. Power Energy Syst. 2021;125:106521. https://doi.org/10.1016/j.ijepes.2020.106521.

[34] Wang Yue, Yao Enjian, Pan Long. Electric vehicle drivers' charging behavior analysis considering heterogeneity and satisfaction. J. Clean. Prod. 2021;286:124982. https://doi.org/10.1016/j.jclepro.2020.124982.

PUBLICATION
10

Network-adaptive and capacity-efficient electric vehicle charging site

K. Rauma, T. Simolin, P. Järventausta, A. Rautiainen, C. Rehtanz

IET Generation, Transmission & Distribution

IET The Institution of Engineering and Technology WILEY

ORIGINAL RESEARCH PAPER

Network-adaptive and capacity-efficient electric vehicle charging site

Kalle Rauma[1] | **Toni Simolin[2]** | **Pertti Järventausta[2]** | **Antti Rautiainen[2]** | **Christian Rehtanz[1]**

[1] Institute of Energy Systems, Energy Efficiency and Energy Economics, TU Dortmund University, Emil-Figge-Str. 76, Dortmund 44227, Germany

[2] Unit of Electrical Engineering, Tampere University, Korkeakoulunkatu 7, Tampere, Finland

Correspondence
Kalle Rauma, Institute of Energy Systems, Energy Efficiency and Energy Economics, TU Dortmund University, Emil-Figge-Str. 76, 44227 Dortmund, Germany.
Email: kalle.rauma@tu-dortmund.de

Abstract
The adaptive charging algorithms of today divide the available charging capacity of a charging site between the electric vehicles without knowing how much current each vehicle draws in reality. Thus, they are not able to detect deviations between the current set point at the charging station and the real charging current. This leads to a situation where the charging capacity of the charging site is not used optimally. This paper presents an algorithm including a novel feature, Expected Characteristic Expectation and tested under realistic circumstances. It is demonstrated that the proposed algorithm enhances the adaptability of the charging site, increasing the efficiency of the used network capacity up to about 2 kWh per charging point per day in comparison with the previous benchmark algorithm. The algorithm is able to increase the average monetary benefits of the charging operators by up to around 5.8%, that is 0.6 € per charging point per day. No input, such as departure time, is required from the user. The proposed algorithm has been tested with real electric vehicles and charging stations and is compatible with the IEC 61851 charging standard. The charging algorithm is applicable in practice as it is described in this paper.

1 | INTRODUCTION

With an increasing need to build new charging sites for electric vehicles (EVs), a remarkable consideration is that most of the new charging sites must be retrofitted to an already existing network infrastructure [1]. This is likely to pose challenges with the current capacity, particularly during the daily peak hours. In most cases, a reinforcement of the network results in high costs and is not economically feasible [2]. Regardless of the limited network capacity, the charging time is a critical constraint in order to provide a charging service of high quality. Another issue is that each EV possesses different charging characteristics, or non-idealities [3]. Ignoring this aspect will reduce the charging efficiency when it comes to the use of network capacity and increase charging times [4–6]. It is shown that about 76% of the users of public charging stations find a high-quality charging service more important than the price of charging [7]. With such restrictions from the side of the network and from the side of

the customers, a highly efficient and adaptive charging algorithm is a key element to improve the quality of the charging service.

In the literature review of this paper, six requirements to develop a practical charging algorithm are considered. These requirements are used to highlight the differences between already published research works and this paper. The requirements are as follows:

1. Is the algorithm tested by applying real charging data? Commercial EVs have a wide range of charging characteristics and the charging habits of the users are strongly dependent on the type of the charging site.
2. Are the non-ideal charging characteristics considered? In practice, this means the use of charging curves that are measured on real EVs with sufficient accuracy. If the goal is to develop an algorithm to manage charging in a time frame of seconds or a few minutes, real, session-based charging data does not reveal the dynamic charging characteristics of each

TABLE 1 Comparison of related research works

Reference	1) Tested using real charging data	2) Non-ideal charging considered	3) Compliancy with charging standards tested	4) Tested with real EVs	5) Control time-step ≤ 1 min	6) Utilizes measured current of EVs as feedback for the real-time charging management algorithm
[9]	yes	no	yes (J1772)	yes	no (15 min)	no
[10]	yes	no	yes (J1772)	yes	not mentioned	no
[11]	no	no	yes (IEC 61851)	yes	yes (30 s)	no
[5]	yes	yes	no	no	yes (1 min)	no
[12]	no	no	no	no	yes (1 min)	no
[13]	yes	no	no	no	no (15 min)	no
[14]	no	no	no	no	no (30 min)	no
[15]	no	no	no	no	no (60 min)	no
[16–20]	no	no	no	no	no (15 min)	no
[21–23]	no	no	no	no	not mentioned	no

vehicle that could cause undesirable decisions of the algorithm in practice.

3. Is the compliancy of the algorithm with the charging standards verified? It is important to ensure that the algorithm is able to work with commercial charging stations and electric vehicles as well as to rule out any unrealistic features of the algorithm.
4. Is the algorithm tested with real EVs and charging stations, either directly or via hardware-in-the-loop simulations?
5. Is the time step applied by the algorithm short enough so that no meaningful dynamic phenomena, such as sudden power peaks, remain unnoticed? The results in [8] suggest that a time step longer than one minute may not be accurate enough to observe the load peaks when operating charging stations with nominal powers up to 22 kW.
6. Does the algorithm utilize measured charging currents of the EVs in its operation? In order to make the algorithm agile and adaptive, it should use as accurate values of currents as possible.

In the best case, all six abovementioned requirements are included when developing a practical algorithm for charging management that works with the commercial hardware of today. Table 1 summarizes related works found in the literature where real-time charging management algorithms are developed and evaluates their matching with the abovementioned six requirements. Then, the contribution of our work is stated against the papers that the authors consider the most relevant for this work.

In [5], a real-time charging management algorithm with a focus on non-ideal charging characteristics is presented. The algorithm is based on neural network models, which means that the neural network must be trained with the charging characteristics of each EV model before the algorithm works in an optimal manner. The study overlooks the fact that the charging curve is different at each current set point [4], but the same charging curve is used for all current set points, which will result in a reduced accuracy to predict charging profiles in a practical application. Also, the simulation or the algorithm, does not take

into account that the charging curve depends on the temperature and the lifetime of the battery, which will further reduce the performance of the algorithm. In order to reach the optimal operation, all EV models should be measured at all possible set points in different temperatures. This would be extremely laborious and unpractical. Because of the fact that the operation of the algorithm is based on predefined charging curves, all abnormalities in the charging curve are automatically ignored. The algorithm in [5] requires a certain computation time between the connection of the EV to the charging point and the start of the charging session to schedule the charging sessions. If this computation time becomes too long, customer experience may be reduced. The scheduling algorithm in [5] works in time slots of 15 min, which means that if an unexpected charging behaviour occurs, the scheduler must wait until the end of the time slot to consider the behaviour, which can be too long time for some applications.

In [10] it is mentioned that the individual charging characteristics of each EV complicate priority sharing. This is due to the fact that the EVs do not always charge according to the indicated maximum power. However, no solution for the issue is offered. In [9], an adaptive charging algorithm is presented, where the charging current is used to measure the energy consumption of each vehicle, but is not used as an input to the charging algorithm. The algorithm is tested with single-phase AC chargers and a fast charger, not with three-phase AC chargers. In [17], constant-current and constant-voltage charging stages are included in the mathematical modelling of the EVs. This makes the scheduling algorithm more efficient than considering only a constant charging curve. However, only one generic load curve is used, which makes it inaccurate in a real application.

The work in [21], presents a real-time adaptive charging algorithm. The algorithm uses discrete charging powers: 0 kW, 20 kW, 40 kW and 62.5 kW, for every EV, which can be inefficient from the network-capacity viewpoint. In [24], the capacity utilization rates of the charging stations are increased by changing their physical locations in the network, but these are rather

fixed solutions than algorithms, as the solution presented in this paper.

The second study with a focus on non-ideal charging behaviour of EVs is presented in [6]. In the work, an offline method for clustering charging curves is presented. Even if the work does not present a real-time method to deal with non-idealities, it underlines the importance of considering non-idealities in charging management.

The literature review in Table 1 shows that non-ideal charging characteristics are taken into account only in one study developing a real-time algorithm for charging management. In addition, no algorithm uses the measured charging current as an input to the charging management algorithm. Three works are identified where the algorithm is proven to be functional with real electric vehicles and charging stations or is otherwise proven to be compatible with the charging standards. What is also noticeable in Table 1 is that most real-time algorithms have a fixed operating time-step of 15 min or more. This is rather long for many applications of demand response [8].

In this paper, the term 'network adaptivity' means that the charging current that is available for a charging site changes over time and, consequently, the current drawn by the charging site adapts to these changes. The term 'capacity efficiency' describes how many percent of the charging current that is available for the charging site is used by the charging site (consisting of one or more charging points). To the best of the authors' knowledge, no other paper has considered the capacity efficiency related to EV charging as it is done in this work.

To fill the identified gaps in research, the contribution of this paper is as follows:

1. Propose a novel adaptive charging algorithm, called CCE (charging characteristic expectation) algorithm that employs actual charging currents and has a capacity to learn the charging characteristics of the charging EV. The CCE algorithm would enhance the operation of the charging algorithms, for example the ones presented in [9, 10, 17] and [21], by reducing idle network capacity and charging times. The charging algorithm is extended to function with a prioritized fast-charging station or under varying load in the network.
2. Test the functionality of the algorithm with four real electric vehicles, charging stations and a fast-charging station emulator via hardware-in-the-loop simulations. The hardware testing guarantees that the algorithm is compatible with the IEC 61851 charging standard. All data used in the hardware-in-the-loop simulations are real, measured data.
3. Compare the proposed charging algorithm with a commonly used reference algorithm.
4. Demonstrates that the CCE algorithm outperforms the reference algorithm in terms of efficient use of the charging capacity.

Non-idealities of EV charging and their impacts on charging management, supported by detailed laboratory measurements, are studied in [3], where an initial version of such adaptive algorithm is also presented. The benefits of an adaptive charging algorithm on a larger simulation case are further explored in [4]. In comparison with [3] and [4], in this paper, the algorithm is further developed by a complete reorganization and including a load prioritization. Also, new features, such as metrics on the performance of the algorithm are added. In addition, new EV models are added to the simulation model as well as used in the experiments as hardware. Further, an extent comparison between the CCE algorithm and the reference algorithm is carried out.

The remainder of the paper is structured as follows. Section 2 presents the complete algorithm step-by-step. CCE, which is a remarkable feature of the algorithm, is explained in its own sub-section. Also, the reference algorithm is separated as a sub-section. Section 3 describes the used data and the modelling in the hardware-in-the-loop simulations as well as the laboratory setup. Section 4 provides the results of the experiments and Section 5 discusses the results and their implications. Section 6 concludes the paper and gives directions to the future work.

2 | PROPOSED CHARGING ALGORITHM

This section explains the functioning of the proposed charging algorithm. Henceforth, the algorithm is referred to as the CCE algorithm according to its distinctive feature called CCE. The reference algorithm that is used for comparison purposes, is briefly explained in Section 2.1. A flowchart of the CCE algorithm is presented in Figure 1. The main idea of the algorithm is to find the most suitable current set points for each charging station so that the current capacity available for the charging site is used as efficiently as possible without causing an overload. The time step of the algorithm is 10 s. The algorithm does not require any input from the user. The maximum current that is shared between the prioritized load(s) and the charging points can be a fixed value, for example an ampacity of the feeder where the charging stations are connected, or non-fixed, such as the free current capacity at the feeding secondary substation. In order to enhance the readability of Figure 1, the steps of the algorithm are numbered and explained separately in the text.

Step 1–2: The currents of the prioritized load(s) are read. In the experiments of this study, the prioritized load is a DC fast charging station, but it could be any other network load, such as a current measurement from a building that is connected to the same feeder. The fast-charging station is selected as a prioritized load in order to maintain the quality of service as high as possible for the fast-charging customers. This selection is done because the use of fast charging stations has usually a higher price than charging stations with lower nominal charging power. Thus, the fast-charging station is not controlled by the CCE algorithm. In this step, also the actual 3-phase charging currents of each charging station are read.

Step 3: A set of performance metrics is calculated. The metrics include, for example, the error between the predicted and the actual charging current of each vehicle as well as the total error consisting of the sums of the errors for each time step. Also, the charged energies and the capacity usage rates of each charging station are calculated. Finally, the metrics are saved for
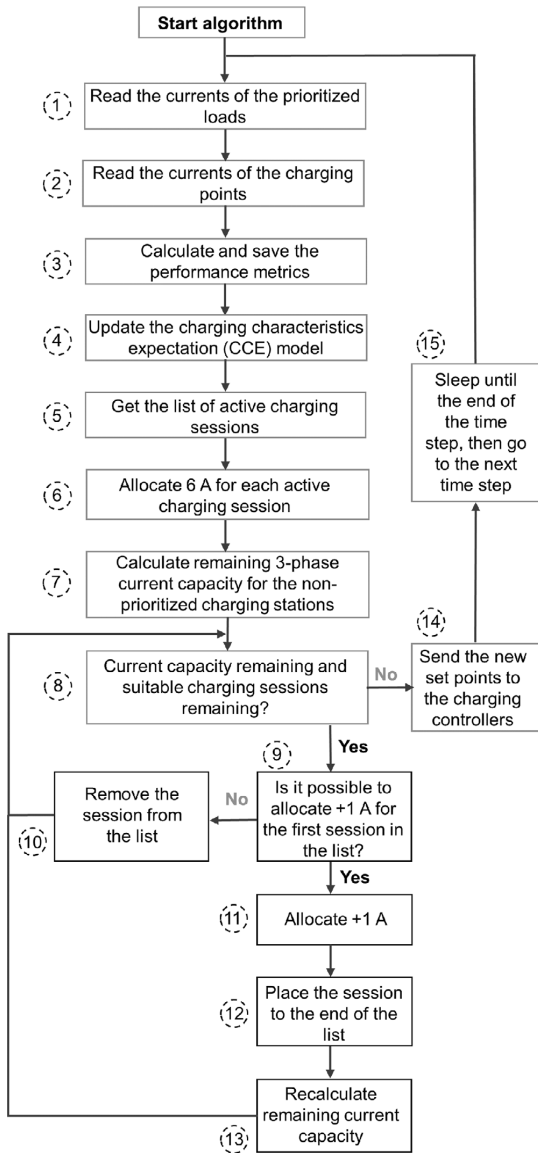
FIGURE 1 A flowchart of the proposed charging algorithm

Step 5: A list of active charging sessions is formed. An active charging session refers to a charging session where an EV is connected to the charging station and is ready to be charged (status B in IEC 61851) or charging (status C or D).

Step 6: 6 A for each active charging session is allocated. This is the minimum non-zero charging current according to IEC 61851. The idea is that each EV can always be charged with at least 6 A, which is important from the user experience point-of-view.

Step 7–8: Once 6 A for each active charging session is allocated, the remaining current capacity is calculated for each phase. The remaining charging capacities are calculated based on the CCE models. If there is still available charging capacity in the network to be allocated, the algorithm continues the inner loop to Step 9. Otherwise, it moves to Step 14.

Step 9: From Step 8, a secondary loop is started. The idea of this loop is to increase the charging current of each EV by 1 A until the whole charging capacity is used or there are no more EVs that can increase their charging current without causing an overload. It is important to notice that the current set points are not sent to the charging stations yet, but only in Step 14. In this step, the possibility to allocate +1 A without causing overloading is estimated using the CCE model. Additionally, the algorithm considers the maximum current limit of the charging point. If it is not possible to allocate +1 A for the first EV in the list, the algorithm moves to Step 10. Otherwise, the algorithm moves to Step 11.

Step 10: If the charging session is unsuitable for further capacity allocation, it is removed from the list of active charging sessions and the algorithm returns to Step 8.

Step 11–13: If possible, +1 A is allocated to the EV and the EV is placed at the end of the list. This ensures even capacity allocation among the active charging sessions. Afterwards, the remaining current capacity is recalculated.

Step 14–15: A physical signal of the current set point is sent from the computer that runs the algorithm to each charging station with an active charging session (including the ones removed from the list). Once the set points are sent, the algorithm waits until the end of the 10 s time step before starting a new time step.

It is important to point out that always, when the remaining current capacity is calculated, it is done so that the current capacity is not exceeded in any of the three phases. So, the current in phases A, B and C must stay below the maximum current limit. The algorithm is developed in Python.

2.1 | Charging characteristics expectation

The CCE model is a way to memorize the charging currents of each EV. The CCE is a crucial component to improve the performance of the algorithm. It is computationally light, which enables fast computation and high scalability.

A CCE model is essentially a matrix that includes the phase currents of an EV at all current set points. The use of CCE allows an accurate prediction of the charging currents of an EV, before the current set point is sent to the charging station (Step

later analysis. In operational use, such detailed data for each time step may not be necessary and the number of metrics can be reduced.

Step 4: The CCE model is updated for each charging session based on current measurements in Step 2. In short, the CCE model enables the algorithm to estimate the upcoming charging currents before applying the current set point. A CCE model is a matrix where the charging current of each phase at each current set point is memorized. The details of the CCE model are described in Section 2.1.

14 in Figure 1). Each CCE model is updated in every iteration of the algorithm with new measurements values of the phase currents of the corresponding charging session. Thus, each CCE model corrects itself during a charging session, which is a way to include non-ideal or non-linear characteristics in the charging algorithm.

When an EV arrives at the charging station, the CCE model supposes that the EV charges exactly according to the current set point and is able to use the maximum current of the charging station. Thus, the initial CCE matrix is

$$
\begin{bmatrix}
 & \begin{matrix} I_{sp} & I_A & I_B & I_C & Meas \end{matrix} \\
\begin{matrix} I_{cs,max} \\ 32.0, \end{matrix} & \begin{bmatrix} 6 & 6.0 & 6.0 & 6.0 & \textit{False} \\ 7 & 7.0 & 7.0 & 7.0 & \textit{False} \\ 8 & 8.0 & 8.0 & 8.0 & \textit{False} \\ \vdots & \vdots & \vdots & \vdots & \vdots \\ 32 & 32.0 & 32.0 & 32.0 & \textit{False} \end{bmatrix}
\end{bmatrix}, \quad (1)
$$

where $I_{cs,max}$ is the maximum current of the charging session. This is typically either 3×16 A or 3×32 A (11 kW or 22 kW) in Europe. I_{sp} is the current set point at the charging station controller. I_A, I_B and I_C are the measured phase currents at the given current set point I_{sp}. The matrix is updated at each iteration loop. At the beginning, the values are set according to the set point values (as in (1)). This is an initial assumption as there is no preliminary knowledge of the charging sessions. *Meas* is a Boolean variable to indicate whether the values of I_A, I_B and I_C are measured values (*True*) or initial values (*False*). For example, after the first loop, if the CCE of a charging station receives measurement at current set point 6 A: $I_A = 6.2\ A$, $I_B = 5.7\ A$ and $I_C = 5.4\ A$, the CCE is updated as

$$
\begin{bmatrix}
 & \begin{matrix} I_{sp} & I_A & I_B & I_C & Meas \end{matrix} \\
\begin{matrix} I_{cs,max} \\ 32.0, \end{matrix} & \begin{bmatrix} 6 & 6.2 & 5.7 & 5.4 & \textit{True} \\ 7 & 7.0 & 7.0 & 7.0 & \textit{False} \\ 8 & 8.0 & 8.0 & 8.0 & \textit{False} \\ \vdots & \vdots & \vdots & \vdots & \vdots \\ 32 & 32.0 & 32.0 & 32.0 & \textit{False} \end{bmatrix}
\end{bmatrix}. \quad (2)
$$

As seen in (2), the updated values are bolded in purple. In this way, the CCE model learns a part of the charging characteristics of the EV, and thus, the accuracy of the CCE model to estimate the upcoming charging currents increases. In order to accelerate the operation of the charging algorithm, CCE includes three auxiliary functions.

The first function detects the charging phases of an EV. When the EV has charged during few seconds and if current at one or two phases are obviously above 0 A and one or two phases are close to 0 A, the corresponding columns (I_A, I_B and I_C) of the latter one(s) will be set to 0.0 A.

The second function verifies the highest charging current of an EV. The function calculates the difference between the current set point and the realized charging current. If the difference

is more than a couple of amperes, the realized current is set as the maximum charging current of the charging session ($I_{cs,max}$).

The third function interpolates values of I_A, I_B and I_C that are not yet measured (*Meas = False*), but lay between two measured values (*Meas = True*). The measured values provide the upper and the lower boundary for the estimation. The interpolated value is placed linearly between the measured values.

When measuring the charging currents to update the CCE model, it is important to consider that each EV has a different reaction time to the input signals. When a new current set point is set, it may take up to even 10 s before the EV starts reacting to the new current set point. Another point is the noise in the measurement devices that should not be confused with charging current.

2.2 | Reference algorithm

The same hardware-in-the-loop simulations are carried out with the CCE algorithm as well as with a reference algorithm. The reference algorithm is a fair sharing algorithm that divides the available charging capacity equally among the charging vehicles as

$$
P_{cs,t} = \frac{P_{available,\ t}}{n_{active,\ t}}, \quad (3)
$$

where $P_{cs,t}$ is the energy that each vehicle receives [10] at a given time step t. $P_{available,\ t}$ is the available charging capacity to be divided between all vehicles at time step t. $n_{active,t}$ is the number of active charging sessions. In addition to [10], the algorithm is used in [9] as well as by several commercial charging operators and charging point manufacturers [25–27]. In [5], the fair sharing algorithm is used as a reference algorithm, like in this paper. Thus, the algorithm can be considered as a benchmark and is referred to as the 'reference' algorithm throughout this paper.

3 | USED DATA, MODELLING AND LABORATORY SETUP

In this section, the used data and how it is used in hardware-in-the-loop simulations are described. Also, general descriptions of the studied cases are provided.

3.1 | Case description

The charging site modelled in the hardware-in-the-loop simulations is located in the district of Kreuzviertel, in the city of Dortmund, Germany. There are plans to install 40 new charging stations in Kreuzviertel in 2021. The charging stations are manufactured by Wirelane and provide three-phase AC charging up to 22 kW via a Type 2 connector. The charging stations are operated by a local energy company. High and irregular variations in load make the EV charging loads at different sites very difficult, or nearly impossible [18], to be predicted with sufficient

accuracy. In addition, a significant rotation of short-time customers will intensify the use of the charging stations. In spite of the demanding charging environment and limited network capacity, a high quality of charging service will be offered. This makes Kreuzviertel a feasible location for an adaptive and capacity-efficient charging algorithm. Furthermore, more AC charging points or DC charging stations might be installed in the area in the future.

3.2 | Used charging data and modelling

As suggested in [28] and in [29], creating synthetic load curves from mobility data involves several possibilities for pitfalls. That is why real charging data is used in this work. The data is measured at a commercial charging site at Dortmund city centre, located close to the planned charging site, and is expected to possess similar user behaviour as the charging site under this case study. The power of these two charging stations is limited to 22 kW and any further smart charging strategies are not employed, so the EVs are charged with their respective maximum charging powers. They are in commercial use and equipped with Type 2 sockets.

The measured average parking time at the site where the charging data is measured is 3 h 53 min and the average charged energy is 11.3 kWh, which is much higher in comparison with other studies, such as [30–34]. From the data set, it is not possible to see when the charging is finished, which means that exact average charging powers cannot be directly concluded.

In this study, four different EV models consisting of six different charging characteristics are used. The EV models are Nissan Leaf ZE0 2012 (1 × 16 A), Nissan Leaf 2019 (1 × 32 A), BMW i3 1Z61 2016 (3 × 16 A) and Smart EQ forfour 2020 (3 × 32 A). The reason behind the selection of these EV models in the study is that they cover the most of the common combinations of phases and maximum AC charging currents on the market:

- 3.7 kW (1 × 16 A),
- 6.6 kW (1 × 32 A),
- 11 kW (3 × 16 A) and
- 22 kW (3 × 32 A).

These EV models are also common in the European market. More details of the EVs used in this study are included in Section 3.3.

From the measured charging data, the used energy is divided by the parking time of the charging session in order to have an estimated average charging power. Then, the EV model of each charging session is concluded as follows:

1. all charging sessions with an estimated average power of > 15 kW are modelled as Smart forfour,
2. all charging sessions with parking time < 2 h and estimated average charging power between 8 kW and 15 kW are modelled as BMW i3,

3. all charging sessions with parking time < 2 h and estimated average charging power between 4 kW and 8 kW are modelled as Nissan Leaf 2019,
4. all charging sessions with parking time < 2 h and estimated average charging power between 0 kW and 4 kW are modelled as Nissan Leaf 2012 and,
5. the EV model for the rest of the charging sessions is selected arbitrarily.

The idea is that each charging session is linked to one of the abovementioned EV models. By far, most charging sessions fall in categories (1) to (4), so the estimate is relatively accurate. The reason why 2 h is selected in categories (2) to (4) is that the shorter the charging session, the more likely it is that the estimated average charging power is close to the real maximum charging power. In other words, the shorter the charging session, the more likely it is to be inflexible [30]. The mode of the BMW i3 ('low', 'reduced' or 'maximum' mode) is selected randomly. More information about the charging modes of BMW i3 can be found in [35] and related measurements are presented in [3].

The charging data from the two charging points are combined to cover eight charging points. This is done so that the different days of the week are not mixed. Three weekdays are selected for this study: Tuesday, Wednesday and Friday. For example, data from several Tuesdays at two charging stations are assembled so that representative data for a Tuesday of eight charging points are obtained. The same is repeated to gather charging sessions for Wednesday and Friday. As a result, the charging schedules of one typical Tuesday, one typical Wednesday and one typical Saturday consisting of real charging sessions are formed. The charging behaviour at a charging site varies typically according to the weekday. In order to form as realistic charging schedules as possible, it is important that charging sessions from different weekdays are not mixed with each other.

The charging data for the fast-charging station is obtained from the same dataset as used in [32]. The charging data is from the urban area of Oslo, which is expected to have similar charging behaviour as a fast-charging site in Dortmund would have. Also, the same weekdays, Tuesday, Wednesday and Friday, are respected when selecting the data from the fast-charging station. The currents of the fast-charging station used in the study for each day are illustrated in Figure 2.

The main intention of the work is to assess the performance of the proposed charging algorithm during a typical day, not in a worst-case scenario. That is why any special circumstances are avoided when selecting the days for the simulations. In this way, it is proven that the algorithm brings benefits to daily operation, instead of only during extreme cases.

In reality, more than four different EV models are used at the real charging site, however, using four categories (e.g. EV models) allows us to construct a rather comprehensive and realistic simulation model for virtual EVs. The load curves of the EVs are modelled very accurately based on real measurements carried out on the same EVs models presented previously. Every possible charging curve within the possibilities of the IEC 61851 charging standard and commercial charging controllers is
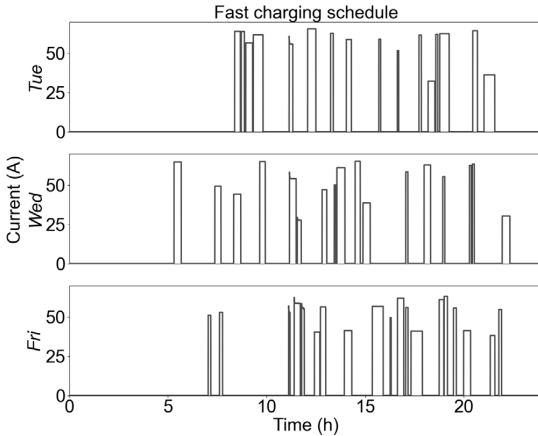
FIGURE 2   The currents of the fast charging for the experiments in different days

considered. This means that the load curves are measured at every current set point with a resolution of 1 second:

- Nissan Leaf 2012 and BMW i3: 6, 7, 8, 9, 10, 11, 12, 13, 14, 15 and 16A, and
- Nissan Leaf 2019 and Smart forfour: 6, 7, 8, 9, 10, 11, 12, 13, 14, 15, 16, 17, 18, 19, 20, 21, 22, 23, 24, 25, 26, 27, 28, 29, 30, 31 and 32 A.

These measurements are used as a model to simulate virtual EVs. More information about the modelling of the virtual EVs used in the HIL-simulation is found in [4].

3.3 | Laboratory setup

The algorithms are tested through hardware-in-the-loop simulations carried out at TU Dortmund University [36]. The laboratory setup resembles a public parking and charging site with eight AC charging stations (22 kW, 32 A each) and one fast charging station (45 kW, 65 A), that are connected to the same 400 V 3-phase feeder. Figure 3 illustrates a simplified scheme of the laboratory setup.

It is important to notice that according to IEC 61851 charging standard, the minimum possible charging current set point is 6 A. Any set points between 6 A and 0 A are not allowed according to the standard. In this case, the total current limit is set high enough that the power of the fast-charging station does not need to be reduced. This is to guarantee a maximum quality of service to the fast-charging station, which is typically more costly to the users than an AC charging station.

A limit of 115 A per phase is set as the maximum current of the whole charging site (I_{max}). The idea behind setting I_{max} to 115 A is that all AC charging stations are able to operate at least with the minimum charging current and the fast-charging station with the nominal one, simultaneously. The
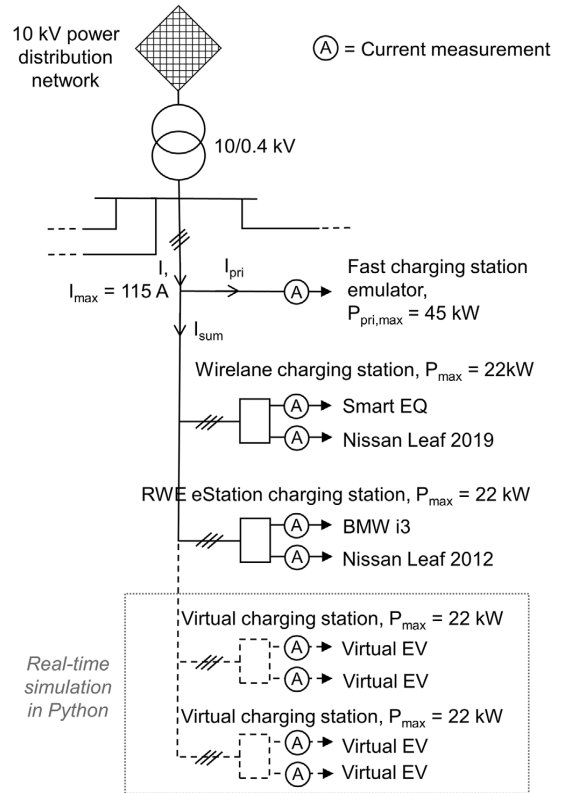
FIGURE 3   Laboratory setup for the Hardware-in-the-Loop simulations to evaluate the algorithms

fast-charging station draws a maximum power of 45 kW that is about 64.95 A per phase. If, at the same moment, all AC charging stations operate at the minimum capacity, that is 6 A, then $64.95 A + 6 \times 8 A \approx 113 A$. Thus 115 A is slightly above 113 A and guarantees the intended operation. This is a trade-off between the flexibility of the charging site, quality of the charging service and customer experience.

The hardware-in-the-loop simulation consists of a hardware and a real-time simulation that are linked to each other via Modbus TCP communication. Four commercial electric vehicles; Nissan Leaf 2012, Nissan Leaf 2019, BMW i3 and Smart forfour EQ, are used. The EVs are connected to two commercial charging stations (each charging station has two charging sockets): Wirelane Doppelstele and RWE eStation. At the RWE charging station, currents from phases A, B and C are measured by using a KoCoS EPPE PX power quality analyser. Wirelane charging station already includes a current measurement off the shelf. The charging stations are connected to the 400 V 3-phase power network of the laboratory. In parallel with the charging stations, a programmable load is connected and used as a fast charging station emulator. The load is controlled according to the fast-charging schedules illustrated in Figure 2. Thus, it has the same electrical characteristics as a fast charging station.
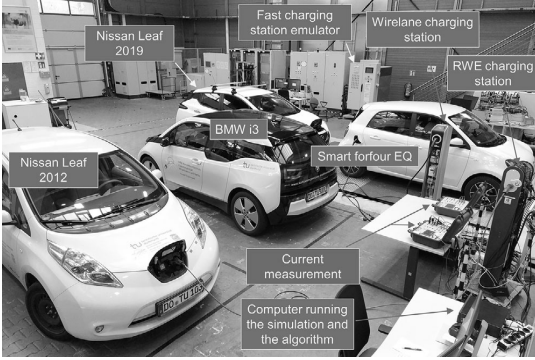
FIGURE 4   Laboratory setup

With the real EVs, the driven distances are calculated based on the energy consumption in the real charging data for each simulated day. When assessing the different algorithms, exactly the same routes are driven, and the same SoCs are obtained, in each case. In this way, the results can be compared with high accuracy.

The real-time simulation is written in Python and runs on a computer in the laboratory. The simulation includes four virtual charging points that are virtually connected to the same feeder as the real charging points. The virtual EV models are selected according to the procedure clarified in Section 3.2. During one day, one charging station can host several virtual charging sessions. In addition, the charging curves of the virtual EVs are based on measurements with an accuracy of 1 s, as explained in Section 3.2. Figure 4 shows a photo of the laboratory during the experiments.

4 | RESULTS

In this section, the results of the hardware-in-the-loop simulations are presented. Each illustration from Figure 5 to Figure 10, shows the results of the CCE algorithm in the upper half and the results of the reference algorithm are in the lower half. The summed charging currents of phases A, B and C as well as the current limit $I_{sum,max}$ are presented from Figure 5 to Figure 10. The current limit $I_{sum,max}$ is the maximum available current capacity that can be shared between all non-prioritized EVs, which means all charging stations, except the fast charging station. Each phase has an own maximum current limit. But since the fast-charging load causes very balanced three-phase loading from the grid point-of-view, the current limit of each phase is almost the same. Thus, only one current limit is shown in the results. The current limits are calculated according to

$$\begin{cases} I_{sum,max,a} = I_{max} - I_{pri,a} \\ I_{sum,max,b} = I_{max} - I_{pri,b} \, , \\ I_{sum,max,c} = I_{max} - I_{pri,c} \end{cases} \tag{7}$$
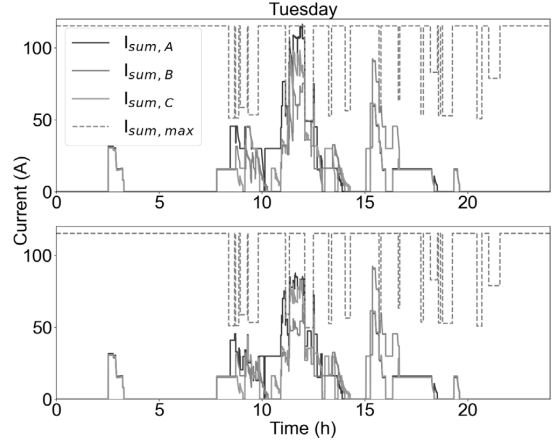
FIGURE 5   The phase currents and the available capacity limit on Tuesday: the CCE algorithm (above) and the reference algorithm (below)
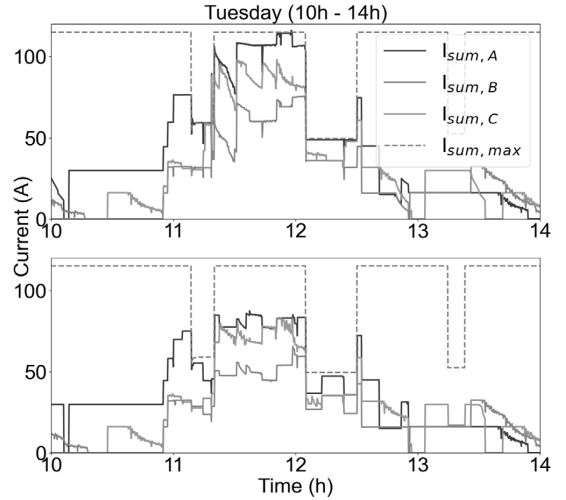
FIGURE 6   The currents of Tuesday from 10 h to 14 h: the CCE algorithm (above) and the reference algorithm (below)

where I_{pri} is the current of the prioritized fast charging point and a–c denotes each phase. When the fast charging station is idle ($I_{pri} = 0$), the current limit I_{max} is 115 A, as presented in (7). When the fast charging station operates, the current limit (I_{sum}) for the AC charging stations is decreased. For the sake of clarity, the results are shown during the whole period (24 h) as well as during the peak hours (10–14 h). The results of Tuesday are presented in Figure 5 and in Figure 6.

In both, Figure 5 and in Figure 6, it can be seen that the charging stations operate closer to their limits when the CCE algorithm is used (upper halves of the figures) as opposed to the reference algorithm (lower halves). This is evident, especially between 11 h 20 min and 12 h 5 min, where the average value
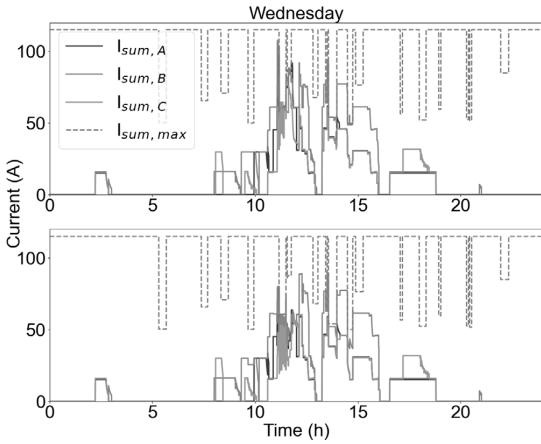
FIGURE 7 The phase currents and the available capacity limit on Wednesday: the CCE algorithm (above) and the reference algorithm (below)
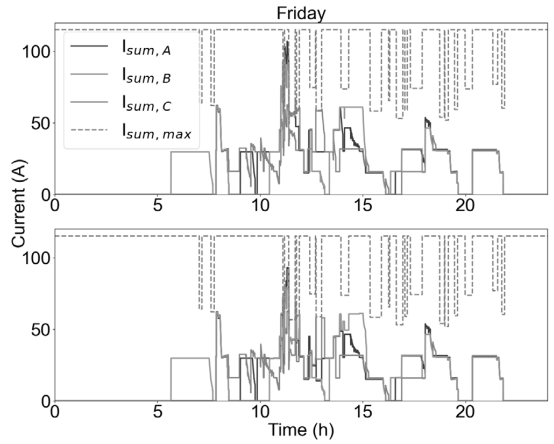

FIGURE 9 The phase currents and the available capacity limit on Friday: the CCE algorithm (above) and the compared algorithm (below)
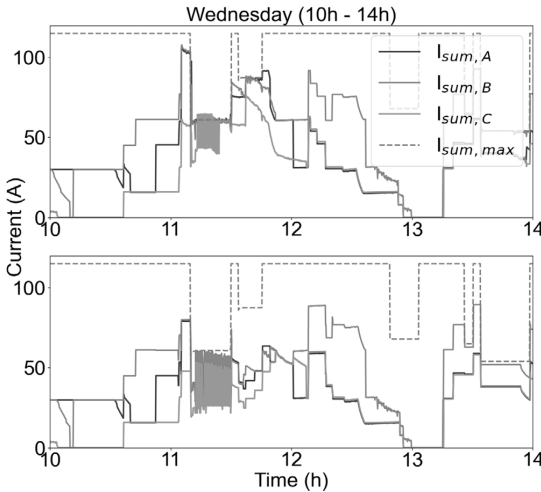

FIGURE 8 The currents of Wednesday from 10 h to 14 h: the CCE algorithm (above) and the reference algorithm (below)
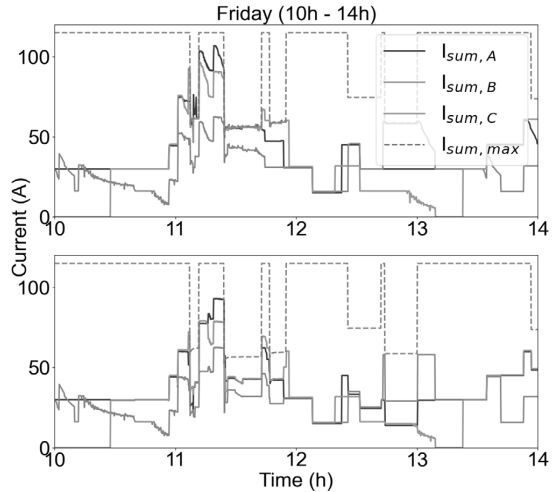

FIGURE 10 The currents of Wednesday from 10 h to 14 h: the CCE algorithm (above) and the compared algorithm (below)

of current on phase A is 104.3 A with the CCE algorithm and 72.9 A with the reference algorithm. This means that during the time the reference algorithm operates at 69.9% of the capacity of the CCE algorithm. This means that at least some of the EVs are able to charge faster with the CCE algorithm than with the reference algorithm. The results of Wednesday are presented in Figure 7 and in Figure 8.

The results of Wednesday are similar to the results of Tuesday; the summed charging currents are often higher, or at least not lower, with the CCE algorithm than with the reference algorithm. A major difference is between 11 h 30 min and 12 h 30 min, when the average current on phase B is 72.2 A with the CCE algorithm and 53.4 A with the reference algorithm. During this time period, the reference algorithm charges 73.9%

of the current on phase B compared with the CCE algorithm. The results of Friday are illustrated in Figure 9 and in Figure 10. Again it is seen that, especially between 11 h and 12 h, the charging current with the CCE algorithm are closer to the current limit ($I_{sum,max}$) when using the CCE algorithm than with the reference algorithm.

Due to the fact that not all EVs are charged fully during the charging sessions, higher charging current means that they charge more energy during the same amount of time when the CCE algorithm is used. If a charging operator charges its customer based on the amount of charged energy, the operator achieves higher earnings with the CCE than with the reference algorithm. Because of the higher charging currents on average, the CCE algorithm causes a slightly higher

TABLE 2 Summarized results when comparing the reference algorithm with the CCE algorithm

	Tuesday (reference)	Tuesday (proposed)	Wednesday (reference)	Wednesday (proposed)	Friday (reference)	Friday (proposed)
Charged energy (kWh)	178.33	194.01	202.19	212.44	261.02	270.69
Gross profit (€)	53.50	58.20	60.66	63.73	78.31	81.21
Capacity utilization rate (%)	18.03	18.84	18.74	19.29	22.20	22.71
Prediction error (A)	48.79	0.42	47.85	0.42	68.80	0.39
Prediction error (%)	130.49	0.85	108.80	0.82	130.34	0.61

TABLE 3 Changes in the performance of the charging site when comparing the reference and the CCE algorithm

	Tuesday	Wednesday	Friday
Charged energy	+15.65 kWh (8.79%)	+10.25 kWh (5.07%)	+9.67 kWh (3.71%)
Gross profit	+4.7 € (8.79%)	+3.07 € (5.07%)	+2.9 € (3.63%)
Capacity utilization rate	+4.30%	+2.85%	+2.25%
Prediction error	−99.14%	−99.12%	−99.43%

capacity utilization rate than the reference algorithm. As the result of the learning mechanism in the CCE algorithm, it can predict the charging currents more accurately than the reference algorithm, which increases the adaptability of the algorithm in general. Table 2 presents the charged energies, gross profits, capacity utilization rates and prediction errors each day with the proposed as well as with the reference algorithm. The gross profit is calculated based on the energy price of 0.3 €/kWh that is a common rate of commercial charging operators at public AC charging sites across Germany [37]. In Table 3, the performance of the CCE algorithm is compared with the reference algorithm.

Table 3 shows the CCE algorithm improves the performance of the charging site in all analysed aspects. On average, daily charged energy increases by 11.86 kWh. The average gross profit increases by 3.56 € per day that is 5.8%. The capacity utilization rate increases by 3.13% and the prediction error decreases by 99.23% per day on average. In the worst day, that is on Friday, the CCE algorithm increases the charged energy of the site by nearly 10 kWh, resulting in almost 3 € higher gross profits than the reference algorithm, which is 8.8%. Consequently, the capacity utilization rate increases by more than 2% and the prediction error decreases by more than 99%. It should be taken into account that the studied charging site is small, consists of only eight charging stations. The benefits of the CCE algorithm are much higher at larger sites, for example, shopping centres, with tens, or even hundreds, of charging stations.

Since the number of EVs increases rapidly and the charging powers are increasing, the EV charging sites are expected to operate closer to their limits in the near future. That is why it is valuable to analyse the difference between the CCE algorithm and the reference algorithm during a peak hour with many simultaneous charging sessions. Table 4 shows the differences in charged energies and gross profit in the time frame from 11 h to 12 h.

Table 4 shows even more drastic differences between the two algorithms. A remarkable difference is that on average, about 24.5% more energy is charged during the peak hour with the CCE algorithm. When comparing Table 3 with Table 4 it can be seen that most of the advantages of the CCE algorithm are gained during the peak time.

5 | DISCUSSION

It is demonstrated that the current state-of-the-art adaptive charging algorithm does not provide as high utilization of available charging capacity as possible. An alternative adaptive charging algorithm is presented and compared against the previous benchmark algorithm. The key factor why the CCE algorithm performs better than the compared benchmark algorithm is that it uses real charging currents as an input to the algorithm. In other words, the algorithm efficiently divides the available charging capacity amongst the active charging sessions while considering their real charging currents. Simply, without current measurements, it is not possible to know how much current the EVs draw and the real-time charging management cannot be organized that accurately. The accuracy of the charging algorithm is further enhanced with a simple learning mechanism, CCE that makes the algorithm capable of memorizing and forecasting the real charging current of each connected EV with a given current set point. It is demonstrated that the CCE algorithm gives a great advantage over the reference algorithm especially during the hours when the charging site operates close to its capacity limits.

For many demand response applications, it is crucial that the charging algorithm recognizes the charging currents of the EVs.

TABLE 4   Changes in the performance of the charging site when comparing the reference and the CCE algorithm between 11 h and 12 h

	Tuesday	Wednesday	Friday
Charged energy	+8.45 kWh (20.56%)	+11.54 kWh (34.43%)	+6.12 kWh (18.42%)
Gross profit	+2.54 €	+3.46 €	+1.84 €

As an example, if a BMW i3 charges at a 22 kW charging point that allows the maximum charging capacity (22 kW, 3 × 32 A, 230 V), consequently the BMW charges at its maximum capacity (11 kW, 3 × 16 A, 230 V). The energy management system of the charging site wishes to set a new current set point to the BMW so that the charging power of the BMW is reduced by 5.5 kW. By using the reference algorithm. The energy management system would reduce the charging power from 22 kW to 16.5 kW (22 kW − 5.5 kW = 16.5 kW). This means that the BMW would still continue charging with its maximum capacity (11 kW, 3 × 16 A, 230 V) and finally, the real charging current is not reduced at all. Without a reasonable measurement and anticipation of charging currents, it may be difficult to obtain the expected load value for a given charging site in a short amount of time. That is why the applicability of the reference algorithm in demand response applications, such as in peak shaving or frequency regulation, is questionable. On the contrary, the CCE algorithm enables an accurate way to set the power consumption of the charging site to a wished value, as demonstrated by the results.

The benefits to be obtained from the use of the CCE algorithm are highly dependent on the number and the type of the charging stations, the maximum allowed charging current and the charging behaviour of the customers (charging durations and simultaneity). The results show meaningful benefits over the reference algorithm even on average days and circumstances. On one hand, the algorithm can be guaranteed that the available charging capacity is used efficiently, which decreases the charging times, improves the customer experience and increases the economic gains of the charging operator. On the other hand, the algorithm can be used to prevent overloads in the feeding distribution network. After all, the algorithm leads to increased utilization of network capacity, which can lead to savings in the network investment costs.

From the power system-viewpoint, the constant-voltage phase of the charging curve is where a notable share of the charging capacity may be lost, if the decreasing charging current is not recognized by the algorithm Due to the fact that the EVs with 32 A charging current may have a longer constant-voltage phase, the difference between the charging current and the current set point is significant during longer time than with 16 A EVs. For example, for Nissan Leaf 2012, the constant-voltage phase takes about 25 minutes, and for Nissan Leaf 2019, it takes about 1 h 28 min, under the nominal charging currents, 16 A and 32 A, respectively. An example of the lost network capacity and the effectiveness of the CCE algorithm is illustrated in Figure 11.

In Figure 11, the grey dotted line shows the current set point. When the reference algorithm is used, the control system
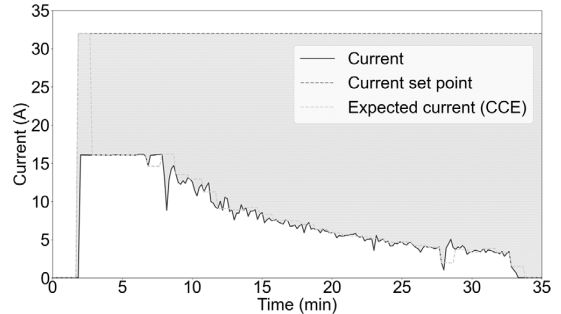
FIGURE 11   Idle charging capacity that can be allocated to other electric vehicles (grey area) during the constant-voltage charging phase. The purple line is the measured charging current (Phase A) of Nissan Leaf 2012. The grey dotted line is the current set point. The yellow line is the expected charging current of the CCE algorithm

practically assumes that the realized loading follows the set point. On the contrary, the yellow dotted line illustrates the expected charging current, when the CCE algorithm is applied. When the reference algorithm is used and the current drawn by the EV is supposed to be the same as the nominal current of the charging station, the unused capacity in the network is the difference between the realized charging current and the current set point (the grey area in Figure 11). When the algorithm is used, this capacity is estimated and allocated to other vehicles if there are no additional network constraints. Due to small and sudden fluctuations of the charging currents in practice, sometimes the CCE algorithm forecasts the expected charging current marginally lower than it is. In such a situation, the algorithm can allocate more charging capacity to the charging site than it has. In reality, such errors are relatively rare and are likely to be evened with the simultaneous charging of several vehicles.

Some commercial EVs turn to a 'waiting' mode, when the charging cable is connected to the EV if the charging station does not instantly allow charging. The EV remains in this mode until the charging starts. However, some EV models stay in the 'waiting' mode for some minutes. If the charging process does not start, let's say, within 1–2 min, the EV goes to a "stand by" mode. During the 'stand by' mode, the charging process cannot be started without disconnecting and connecting the charging cable physically from the EV. Such behaviour is observed for BMW i3, for example [35].

In the future, peak-power based electricity tariffs are likely to become more common as they improve the cost-reflectivity of the electricity pricing [38]. As a consequence. there may be situations where it is economically feasible to limit the peak loading

at the charging site below the capacity that would normally be available. This further emphasizes the need to effectively utilize the available charging capacity.

Although the algorithm presented in this paper is intended for a charging site where all charging stations are connected in a star-configuration, the CCE feature of the algorithm is topology-independent and can be applied to more complex network configurations, including several series and parallel connections. In this case, the rest of the algorithm, excluding CCE, should be adapted to such network configuration.

5.1 | Deployment of the proposed charging algorithm in practice

When a charging point operator plans to use the CCE algorithm in the daily operation of its charging sites, it does not entail significant additional equipment of operational costs compared with the already existing solution. Most importantly, each charging station must be equipped with a controller that is able to control the charging current according to the local standard, such as IEC 61851, in Europe. In addition, the charging station should have a current measurement, this can be embedded in the energy meter or can be a separate device. Generally, energy meters with the capability to deliver a current measurement are common in modern charging stations. A usual industrial solution is that an energy meter is physically connected to the charging controller, via a master-slave structure, where the charging controller is the master and the energy meter is the slave. When a current measurement is asked by, for example, the server where the CCE algorithm is running, the server sends a message to the controller that further reads the measurement value from the energy meter and sends the measurement value to the server.

The crucial technical requirements to be able to operate the CCE algorithm in a real case are:

- a charging controller,
- a current measurement device,
- communication media, such as LTE, 4G or Ethernet, and
- a backend server, where the algorithm is running.

In practice, all requirements are already fulfilled by a typical European charging point operator. Thus, it can be said that deploying the CCE algorithm does not entail significant additional equipment or operational costs compared with most solutions of today. There may be regulations considering data privacy and communication media that vary from country to country, which must be taken into account.

6 | CONCLUSION AND FUTURE WORK

The adaptive charging algorithms of today overlook the non-ideal charging characteristics of EVs. As a consequence, they are likely to operate in a non-optimal way, leading to wasted charging capacity and increased charging times. To contribute to this problem, a new charging algorithm that shows an evident advantage over the benchmark charging algorithm is proposed. The performance of the charging algorithm is proved under realistic circumstances and tested with real EVs. In a site of eight charging stations, the proposed CCE algorithm increases the capacity utilization rate by 3.13% and the charging capacity by 11.9 kWh per day on average. This means that the algorithm brings an additional gross profit of about 3.6 € per day for eight charging points, so about 0.6 € per charging point, to the charging operator. This means an increment of 5.8% in the average gross profit. During the peak hour, the CCE algorithm can deliver 24.4% more energy to the EVs than the reference algorithm, which shows that the benefits of the algorithm are likely to increase in the near future when charging sites will be used more than they are used today.

The algorithm is compatible with the IEC 61851 charging standard and can be applied as presented in this paper. Besides, no information, such as the state-of-charge of the battery or leaving time, from the user is necessary. The algorithm can be applied to modern charging stations without the need for specialized additional hardware.

Future work focuses on testing the algorithm in commercial operation, altogether in about 40 charging stations in Dortmund, Germany. To gain more insights from the pilot test, additional metrics that help to design following versions of the algorithm are developed. Additionally, it will be studied, how much CCE can improve the performance of other charging algorithms found in the research literature. Also, the use of the proposed algorithm in the case of complex configurations (several parallel and series connections) of the power network within a charging site will be studied.

CONFLICT OF INTEREST
The authors declare no conflict of interest.

DATA AVAILABILITY STATEMENT
The data that support the findings of this study are available from the corresponding author upon reasonable request.

ORCID
Kalle Rauma https://orcid.org/0000-0002-5553-8751
Toni Simolin https://orcid.org/0000-0002-0254-1113

REFERENCES

1. Melliger, A., van Vliet, O., Liimatainen, H.: Anxiety vs reality sufficiency of battery electric vehicle range in Switzerland and Finland. Transp. Res. Part D 65, 101–115 (2018)
2. Brinkel, N., Schram, W., AlSkaif, T., Lampropoulos, I., van Sark, W.: Should we reinforce the grid? Cost and emission optimization of electric vehicle charging under different transformer limits. Appl. Energy 276 (2020)
3. Rauma, K., Simolin, A., Rautiainen, A., Järventausta, P. & Rehtanz, C.: Overcoming non-idealities in electric vehicle charging management. IET Electrical Systems in Transportation. (2021). http://doi.org/10.1049/els2.12025
4. Simolin, T., Rauma, K., Rautiainen, A., Järventausta, P. & Rehtanz, C.: Foundation for adaptive charging solutions: Optimised use of electric vehicle charging capacity. IET Smart Grid. (2021). http://doi.org/10.1049/stg2.12043
5. Frendo, O., Graf, J., Gaertner, N., Stuckenschmidt, H.: Data-driven smart charging for heterogeneous electric vehicle fleets. Energy and AI 1, (2020)
6. Sun, C., Li, T., Low, S., Li, V.: Classification of electric vehicle charging time series with selective clustering. Electr. Power Syst. Res. 189, (2020)
7. Wang, Y., Yao, E., Pan, L.: Electric vehicle drivers' charging behavior analysis considering heterogeneity and satisfaction. J. Cleaner Prod. 286, (2020)
8. Shepero, M., Munkhammar, J.: Spatial Markov chain model for electric vehicle charging in cities using geographical information system (GIS) data. Appl. Energy 231, 1089–1099 (2018)
9. Heredia, W.B., Chaudhari, K., Meintz, A., Jun, M., Pless, S.: Evaluation of smart charging for electric vehicle-to-building integration: A case study. Appl. Energy 266, (2020)
10. Zhang, T., Pota, H., Chu, C., Gadh, R.: Real-time renewable energy incentive system for electric vehicles using prioritization and cryptocurrency. Appl. Energy 226, 582–594 (2018)
11. García Veloso, C., Rauma, K., Fernández Orjuela, J., Rehtanz, C.: Real-time agent-based control of plug-in electric vehicles for voltage and thermal management of LV networks: Formulation and HIL validation. IET Gener. Transm. Distrib. 14(11), 2169–2180 (2020),
12. Boglou, V., Karavas, C., Arvanitis, K., Karlis, A.: A fuzzy energy management strategy for the coordination of electric vehicle charging in low voltage distribution grids. Energies 13, 3709 (2020)
13. Da Silva, F.L., Nishida, C.E.H., Roijers, D.M., Reali Costa, A.H.: Coordination of electric vehicle charging through multiagent reinforcement learning. IEEE Trans. Smart Grid 11(3), 2347–2356 (2020)
14. Khaki, B., Chu, C., Gadh, R.: Hierarchical distributed framework for EV charging scheduling using exchange problem. Appl. Energy 241, 461–471 (2019)
15. Liu, J., Lin, G., Huang, S., Zhou, Y., Li, Y., Rehtanz, C.: Optimal logistics EV charging scheduling by considering the limited number of chargers. IEEE Trans. Transp. Electrif. 7(3), 1112–1122 (2020)
16. Godina, R., Rodrigues, E., Matias, J., Catalão, J.: Smart electric vehicle charging scheduler for overloading prevention of an industry client power distribution transformer. Appl. Energy 178, 29–42 (2016)
17. Graber, G., Calderaro, V., Mancarella, P., Galdi, V.: Two-stage stochastic sizing and packetized energy scheduling of BEV charging stations with quality of service constraints. Appl. Energy 260, (2020)
18. Zheng, Y., Shang, Y., Shao, Z., Jian, L.: A novel real-time scheduling strategy with near-linear complexity for integrating large-scale electric vehicles into smart grid. Appl. Energy 217, 1–13 (2018)
19. Seddig, K., Jochem, P., Fichtner, W.: Two-stage stochastic optimization for cost-minimal charging of electric vehicles at public charging stations with photovoltaics. Appl. Energy 242, 769–781 (2019)
20. Shang, Y., Liu, M., Shao, Z., Jian, L.: Internet of smart charging points with photovoltaic Integration: A high-efficiency scheme enabling optimal dispatching between electric vehicles and power grids. Appl. Energy 278, (2020)
21. Wang, R., Wang, P., Xiao, G.: Two-Stage Mechanism for Massive Electric Vehicle Charging Involving Renewable Energy. IEEE Trans. Veh. Technol. 65(6), 4159–4171 (2016)
22. Xydas, E., Marmaras, C., Cipcigan, L.: A multi-agent based scheduling algorithm for adaptive electric vehicles charging. Appl. Energy 177, 354–365 (2016)
23. Mobarak, M.H., Bauman, J.: Vehicle-Directed Smart Charging Strategiesto Mitigate the Effect of Long-Range EV Charging on Distribution Transformer Aging. IEEE Trans. Transp. Electrif. 5(4), 1097–1111 (2019)
24. Yang, Y., Zhang, Y., Meng, X.: A Data-Driven Approach for Optimizing the EV Charging Stations Network. IEEE Access 118592–118592 (2020)
25. Liikennevirta Oy: Virta Platform Overview. www.virta.global, accessed on the 8th January 2021
26. EVling Charging Stations Commissioning Guide. www.schneider-electric.com (2019), accessed on the 8th January 2021
27. The Mobility House GmbH: ChargePilot–The Charging and Energy Management by The Mobility Houser. www.mobilityhouse.com/int_en/charging-and-energy-management, accessed on the 8th January 2021
28. Pareschi, G., Küng, L., Georges, G., Boulouchos, K.: Are travel surveys a good basis for EV models? Validation of simulated charging profiles against empirical data. Appl. Energy 275, (2020)
29. Zhang, J., Yan, J., Liu, Y., Zhang, H., Lv, G.: Daily electric vehicle charging load profiles considering demographics of vehicle users. Appl. Energy 274, (2020)
30. Fenner, P., Rauma, K., Rautiainen, A., Supponen, A., Rehtanz, C., Järventausta, P.: Quantification of peak shaving capacity in electric vehicle charging–Findings from case studies in Helsinki Region. IET Smart Grid 3(6), 777–785 (2020)
31. Fernández, J., Herrera, O., Mérida, W.: Impact of an electrified parkade on the built environment: An unsupervised learning approach. Transp. Res. Part D 78, (2020)
32. Rautiainen, A., Rauma, K., Rohde, L., Supponen, A., Raulf, F., Rehtanz, C., Järventausta, P.: Anatomy of electric vehicle fast charging: Peak shaving through a battery energy storage–A case study from Oslo. IET Electr. Syst. Transp. 1–12 (2020)
33. Pareschi, G., Küng, L., Georges, G., Boulouchos, K.: Are travel surveys a good basis for EV models? Validation of simulated charging profiles against empirical data. Appl. Energy 275 (2020)
34. Flammini, M., Prettico, G., Julea, A., Fulli, G., Mazza, A., Chicco, G.: Statistical characterisation of the real transaction data gathered from electric vehicle charging stations. Electr. Power Syst. Res. 166, 136–150 (2019)
35. Bayerische Motoren Werke AG: The BMW i3. Owners Manual. BMW AG, München, pp. 183 (2016)
36. Spina, A., Rauma, K., Aldejohann, C., Holt, M., Maasmann, J., Berg, P., Häger, U., Rettberg, F., Rehtanz, C.: Smart Grid Technology Lab– A full-scale low voltage research facility at TU Dortmund University. AEIT International Annual Conference, Bari, Italy, 3–5 October (2018)
37. A.llgemeiner Deutscher Automobil-Club e.V. (ADAC), 'Ladestationen für Elektroautos: Das kostet der Strom', 6.10.2020. https://www.adac.de/rund-ums-fahrzeug/elektromobilitaet/laden/elektroauto-ladesaeulen-strompreise/
38. Öhrlund, I., Schultzberg, M., Bartusch, C.: Identifying and estimating the effects of a mandatory billing demand charge. Appl. Energy 237, 885–895 (2019)

PUBLICATION
11

Assessing the influence of the temporal resolution on the electric vehicle charging load modeling accuracy

T. Simolin, K. Rauma, A. Rautiainen, P. Järventausta, C. Rehtanz

Assessing the influence of the temporal resolution on the electric vehicle charging load modeling accuracy

Toni Simolin [a],[*], Kalle Rauma [b], Antti Rautiainen [a], Pertti Järventausta [a], Christian Rehtanz [b]

[a] *Unit of Electrical Engineering, Tampere University, Korkeakoulunkatu 7, 33720 Tampere, Finland*
[b] *Institute of Energy Systems, Energy Efficiency and Energy Economics, TU Dortmund University, Emil-Figge-Str. 76, 44227 Dortmund, Germany*

A B S T R A C T

In the scientific literature, various temporal resolutions have been used to model electric vehicle charging loads. However, in most studies, the used temporal resolution lacks a proper justification. To provide a strengthened theoretical background for all future studies related to electric vehicle charging load modeling, this paper investigates the influence of temporal resolution in different scenarios. To ensure reliable baselines for the comparisons, hardware-in-the-loop simulations with different commercial electric vehicles are carried out. The conducted hardware-in-the-loop simulations consists of 134 real charging sessions in total. In order to compare the influence of different temporal resolutions, a simulation model is developed. The simulation model utilizes comprehensive preliminary measurement-based charging profiles that can be used to model controlled charging in fine detail. The simulation results demonstrate that the simulation model provides sufficiently accurate results in most cases with a temporal resolution of one second. Conversely, a temporal resolution of 3600 s may lead to a modeling error of 50% or even higher. Additionally, the paper shows that the necessary resolution to achieve a modeling error of 5% or less vary between 1 and 900 s depending on the scenario. However, in most cases, resolution of 60 s is reasonably accurate.

1. Introduction

In the scientific literature, it has been a common practice to model electric vehicle (EV) charging loads by using a temporal resolution of 15–60 min. However, the accuracies of different temporal resolutions are not properly analyzed. Therefore, the inaccuracies of the modeling results remain currently unknown.

When using a temporal resolution of, e.g., 60 min, the model rounds up the arrival and departure times to full hours. Additionally, only an average load of each time step can be modeled. Naturally, the coarser the resolution, the more significant the inaccuracies are likely to be. Furthermore, in case a charging control algorithm is used, the used temporal resolution of the simulation model also has an influence on the control signal. This may be a crucial factor from two points of view. Firstly, according to the charging standard IEC 61851, the minimum allowed current limit to be set by the EV supply equipment (EVSE) is 6 A which equals to 1.38 kW (230 V) in a single-phase charging point. Thus, the EVSE cannot force an EV to charge with a power of, e.g., 1 kW. Secondly, as shown in [1], EVs may not be able to use all charging currents between the minimum current limit of the EVSE (6 A) and the

maximum supported charging current of the on-board charger (OBC) of the EV. By overlooking these factors, the charging load modeling may be inaccurate especially in case of controlled charging.

1.1. Related studies

The influence of temporal resolution have been assessed e.g. from a PV self-consumption point-of-view [2,3]. In [2], it is shown that the temporal resolution of the load profiles is more critical for the accuracy of the determination of self-consumption rates than the resolution of the PV generation. In [3], it is demonstrated that the error in yearly self-consumption is around 3.6%, 6.1%, 9.3%, and 12.5% when the temporal resolution is 5, 15, 30, and 60 min, respectively. According to these studies, a temporal resolution of 15 min is reasonably accurate to assess self-consumption of the PV generations. Conversely, for the optimal sizing of a battery inverter power of an energy storage system, a temporal resolution of 5 min or finer is necessary [2]. In case of modeling an uncontrolled EV charging load, these results could potentially be used as guidelines as there are no charging control signals to be considered. However, as mentioned earlier, there are two especially

Table 1.

Recent studies related to EV charging load modeling.

Refs.	T	The main objective of the study
[5]	2 h	Define Markov decision process formulation in reinforcement learning framework
[6]	1 h	Minimize charging costs and negative impacts of volatile renewable energy resource output
[7]	1 h	Voltage control through a charging pricing strategy of fast charging stations
[8]	1 h	Develop a multi-agent system to simulate energy hub with various EV penetrations
[9]	1 h	Optimize the quality of the charging service through a pricing scheme
[10]	1 h	Determine optimal EV charging stations and distributed generation units to minimize costs
[11]	1 h	Determine optimal charging stations in case of increasing EV penetration
[12]	1 h	Frequency regulation through vehicle-to-grid control while considering several uncertainties
[13]	1 h	Reduce power system generation costs through a flexible EV charge/travel schedule
[14]	30 min	Minimize EV charging costs through scheduling models
[15]	30 min	Reduce peak demand in the grid through charging scheduling
[16]	30 min	Minimize load variance and charging costs through charging behavior prediction
[17]	30 min	Propose a probabilistic approach to evaluate the impact of EVs on distribution system
[18]	15 min	Propose a spatial-temporal method to model EV charging loads in distribution network
[19]	15 min	Manage the power imbalance among feeders through tie-line voltage-source converters
[20]	15 min	Minimize peak-valley load difference through coordinated charging scheduling
[21]	15 min	Minimize charging costs and emissions with and without grid reinforcement
[22]	15 min	Reduce EV charging costs in a workplace through vehicle-to-grid control
[23]	10 min	Analyze the impacts of the EV charging load on the grid using Markov Chain simulation
[24]	5 min	Propose a data-driven approach for load modeling to guide infrastructure planning
[25]	1 min	Maximize self-consumption of photovoltaic generation via charging coordination
[26]	1 min	Present a spatial-temporal EV charging load simulation model that considers e.g. traffic
[27]	1 min	Minimize charging costs while ensuring quality of charging service
[28]	15 s	Provide centralized frequency regulation with reduced communication requirements
[29]	10 s	Coordinate EV charging loads to increase photovoltaic self-consumption

notable factors in controlled charging which may require a finer temporal resolution in order to preserve reasonable modeling accuracy.

In [4], the impact of different temporal resolutions on the peak of the normalized power (PNP) of uncontrolled EV charging is assessed. The results show that the PNP can be relatively accurately evaluated even with a resolution of 60 min when considering charging powers of 3.7 kW. When considering 22 kW charging powers, a resolution of 1 min is notably more accurate than 5 min. However, no further analyses of the impacts of the temporal resolution are conducted, and finer temporal resolutions are not considered. According to the authors' knowledge, no other studies regarding the assessment of the influence of the temporal resolution on EV charging load modeling are yet carried out.

To give an outlook of the research related to EV charging load modeling, Table 1 lists 25 recent studies. For each study, the temporal resolution (T) of the modeling is presented. Additionally, a short description of the objective of the study is shown.

As shown in Table 1, a wide range of temporal resolutions is used to model EV charging loads. In all aforementioned studies, modeling of multiple EVs were considered. Additionally, controlled charging was considered in each study except in [17–19,23,26]. However, very little

effort is made to justify the selected resolutions or to assess the potential inaccuracies of the results. In [5] and [22], it is acknowledged that the temporal resolution affects the accuracy of the results. However, a further investigation is left out of the papers.

1.2. Contributions and structure

Based on the literature review, it seems necessary to assess the impacts of the temporal resolution of the EV charging load modeling. To fill the gaps in the literature, four research questions are formed:

1 *What is the impact of the temporal resolution when modeling home charging or a small charging site?* To address this question, multiple hardware-in-the-loop (HIL) simulations are carried out using 1–4 commercial EVs. The results are then compared with simulation results obtained by using different temporal resolutions (Sections 3.1 and 3.2).

2 *What is the impact of the temporal resolution when modeling a large charging site?* This question is addressed by simulating a three-month period using different temporal resolutions (Section 3.3). In this scenario, the EV charging behavior is based on real-world charging data of a commercial charging site.

3 *How accurately the EV charging loads can be modeled using the developed simulation model?* To address this question, the results of the HIL simulations are compared with the simulations results obtained by using one second temporal resolution (Section 3.5).

4 *Which temporal resolutions are necessary in different situations to ensure reasonably accurate modeling?* To address this question, the coarsest temporal resolutions that achieve a modeling error of less than 5% are presented separately for each scenario (Section 3.6).

The contribution of this paper is to carry out a thorough analysis that fills the related gap in the scientific literature and provides justified answers for the research questions. Furthermore, the goal is to provide useful guidelines and a strengthened scientific background for future studies regarding the EV charging load modeling.

The rest of the paper is as follows. Section 2 describes the assessment method. Section 3 analyses the results of each scenario. Additionally, the results are analyzed from the perspective of the overall accuracy of the simulation model, and the necessary resolutions to achieve reasonably accurate results in different scenarios are presented. The paper is finalized with conclusions in Section 4 where the research questions are addressed separately.

2. Assessment method

This section describes the used data, the key values of interest, the examined scenarios, the used control method, the experimental setup of the HIL simulations, and the used simulation model. Each part forms its own subsection.

2.1. Used data

To evaluate home charging, household electricity consumption data of a five-day period is used. The data was measured in December 2018 in one-second resolution at a detached house located in Pirkanmaa, Finland. The building is built in 2010 and its floor area is 158 m^2. A geothermal heat pump is used as the main heating system. This represents a typical new Finnish detached house. The daily energy consumption and the daily peak load varies between 34.4–59.0 kWh and 5.9–7.9 kW, respectively.

In order to evaluate a large charging site in a realistic manner, charging session data of REDI is used. REDI is a shopping center located in Helsinki, Finland, and has over 200 charging points that support 22 kW charging [30]. The data is gathered over a three-month period in 2020 (January–March) and contains 3801 charging sessions which
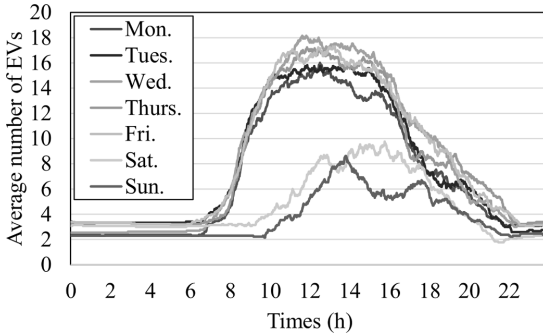
Fig. 1. The average number of EVs plugged in at REDI.

Table 2.
The used electric vehicles.

EV	Max charging power
Nissan Leaf 2012	3.7 kW (1 × 16 A)
Nissan Leaf 2019	7.4 kW (1 × 32 A)
BMW i3 2016	11.0 kW (3 × 16 A)
Smart EQ forfour 2020	22.1 kW (3 × 32 A)

Table 3
Examined scenarios.

	Site	N_{max}	N_e	Control method
S1	A household with one EV	1	45	PLM
S2	A small charging site	4	25	PLM
S3	A large charging site	21	89 [a]	Unc. / PLM

N_{max} is the maximum number of simultaneous charging sessions.
N_e is the number of different events.
[a] Scenario 3 is examined using pure simulations over an 89-day period.

results in 42.7 charging sessions per day. The data includes arrival and departure times in one second temporal resolution, charged energy, and charging peak power. According to the data, EVs have on average a stay duration of 236 min, an active charging time of 101 min, and a charged energy of 7.4 kWh. It is also seen that in 59.3% of the charging sessions the stay duration is less than 5 min longer than the active charging time. This means that the stay duration often acts as a bottleneck, and consequently, most EVs are not fully charged before departure. The average daily number of EVs plugged in at REDI is illustrated in Fig. 1.

2.2. Key values of interest

This paper aims to assess the impacts of temporal resolution in various scenarios. In order to assess the influence, three key values are examined. The key values are:

- The highest momentary peak load (P)
- The highest hourly peak load (P_h)
- The charged energy (E)

The highest momentary peak load simply refers to the highest peak load value of a single time step in a single day. The highest hourly peak load refers to the highest average loading during a one-hour long period in a single day. This is an interesting value as it can be the basis for a power-based distribution tariff component as in [31–33]. In Scenario 1, the peak loads include both the EV charging load and the household's electricity consumption. The charged energy refers to the energy that is charged during each one-hour time slot (i.e., 0:00–1:00, 1:00–2:00 etc.).

This definition is made due to the selection that one hour is the coarsest temporal resolution. Furthermore, the temporal resolution in electricity pricing is often one hour and thus a modeling error in the hourly energy consumptions may affect certain cost or benefit analysis.

2.3. Examined scenarios

The simulations focus on three scenarios: (S1) a household with one EV, (S2) a small charging station with four charging points, and (S3) a large charging site with up to 21 simultaneous charging sessions. The first scenario (S1) is carried out using three EVs: Nissan Leaf 2012, Nissan Leaf 2019, and BMW i3. The home charging sessions are assumed to begin at evening. However, to generate more different circumstances, the HIL experiments are carried out using three different starting times for the charging sessions: 17:00, 19:00, and 21:00 h. A single simulated circumstance that has certain arrival time(s) and energy requirement(s) is referred to as an event. In Scenario 1, there are 45 (5 days × 3 starting times × 3 EVs) different events. To ensure more straightforward comparability, the driving distances of the EVs are kept constant at 24 km, which equals to the average daily driving distance in Finland [34]. Depending on the charging and driving efficiencies of the EVs, the energy drawn from the grid (the charging losses are included) varies between 3.5 and 6.0 kWh.

The second scenario (S2) is carried out in 25 different events. In each event, 3 or 4 of the EVs shown in Table 2 are used which results in 89 HIL charging sessions in total. For each event, the arrival times, the departure times, and the driving distances are randomly selected. In this scenario, the average driving distance is 19.1 km (distances vary between 4.3 and 65.0 km). This results in an average energy requirement of 3.8 kWh (energies vary between 0.8 and 11.6 kWh) from the grid point of view. The arrival times of the EVs varies between 16 h and 22 h and thus create circumstances where 1–4 EVs are simultaneously requesting charging. Sojourn times were assumed to be long enough so that the EVs can be fully charged.

The third scenario (S3) is formed using the charging session data of REDI. For the modeling purposes, the recorded charging peak powers are used to determine the type of the EV according to Eq. (1), where P_p is charging peak power. The third scenario is divided into three sub-scenarios based on the used control method: an uncontrolled charging, a peak load management (PLM) with a total charging current limit of 3 × 160 A, or a PLM with a total charging current limit of 3 × 126 A. In the case of uncontrolled charging, the highest peak current was 191 A according to the simulations. These subscenarios are used to determine the impact of the temporal resolution together with the use of charging control to the modeling accuracy in a large charging site. The control method is presented in the next subsection.

The EVs and the key parameters of the scenarios are presented in Tables 2 and 3, respectively. According to an ablation study [35], the actual EV model is not necessary attribute to model charging profiles accurately. Instead, the number of used phases and the maximum current drawn are more crucial. Therefore, as the four EVs considered in this paper have different combinations of the number of used phases and the maximum current drawn, they can be used to represent different EV fleets quite well.

$$\begin{cases} EV_{type} = Nissan\ Leaf\ 2012, & if\ 0\ kW < P_p \le 4.5\ kW \\ EV_{type} = Nissan\ Leaf\ 2019, & if\ 4.5\ kW < P_p \le 10\ kW \\ EV_{type} = BMW\ i3\ 2016, & if\ 10\ kW < P_p \le 15\ kW \\ EV_{type} = Smart\ EQ\ 2020, & if\ 15\ kW < P_p \le 25\ kW \end{cases} \quad (1)$$

It is worth mentioning that the charging data of REDI cannot be used to accurately determine the initial missing energy from the EVs. As around 60% of the EVs depart before the charging is finished, the charged energies essentially pose a lower bound for the initially missing energies of the EVs. In this paper, the charged energy in the data is assumed to be the exact energy that is initially missing from the EV when it is plugged in. This simplification means that the total charging
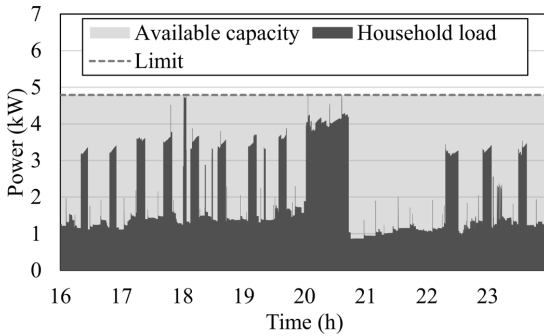
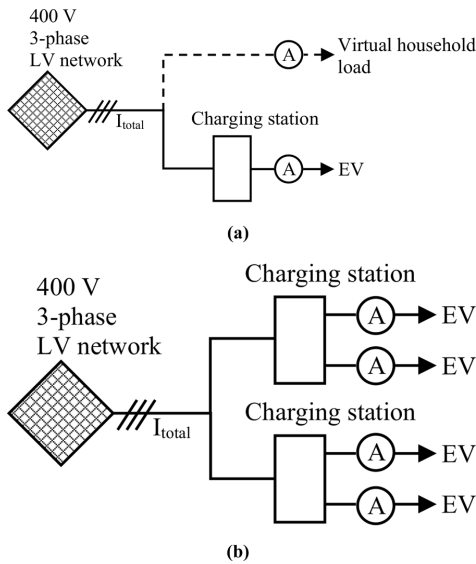**Fig. 2.** Household electricity consumption and available charging capacity.

(a)

(b)

Fig. 3. The experimental setup for (a) Scenario 1 and for (b) Scenario 2.

Fig. 4. The laboratory setup.

energies in the simulations are likely lower than in reality. However, the same assumption is applied for the simulations of each temporal resolution and thus the results are comparable with each other.

To form a baseline, each event in Scenarios 1 and 2 is carried out as a HIL simulation with commercial EVs. After that, the events are simulated with seven different temporal resolutions (1, 10, 30, 60, 300, 900, and 3600 s). These simulations are carried out without any HIL component. Scenario 3 is only simulated with the different temporal resolutions, and the results obtained using the temporal resolution of one second is chosen to be the baseline for this scenario. Further explanation of the experimental HIL simulation setup and the simulation model is given in Sections 2.5 and 2.6, respectively.

2.4. Control method

It is worth emphasizing that the following control method in itself is not the focus of this paper. Instead, the idea is simply to create situations where the charging currents are limited by the control system in contrast to the uncontrolled charging where the charging currents are only limited by the OBCs of the EVs. The aim of the control method is to limit peak loading. In Scenario 1, the daily load peak of the household is assumed to be known in advance and the charging power is limited so that the total load of the real estate and EV charging does not cause a higher daily load peak. An illustration of the loading of the household and the peak load limit is given in Fig. 2. In the figure, the green area between the peak load limit (gray dotted line) and the electricity consumption of the household (purple area) represents the capacity that is available for EV charging. The charging capacity for the EV can be calculated according to Eq. (2), where t is a time step, P_{max} is the highest daily peak load of the household, and $P_{household}$ is the power consumption of the household.

$$P_{EV}(t) = P_{max} - P_{household}(t). \tag{2}$$

In Scenario 2, the total loading of the charging station is limited to 3 × 32 A which allows all four charging sessions to be simultaneously active, yet a dynamic load management is required if more than one EV is charging simultaneously. In this paper, fair sharing algorithm presented in [36] is used which divides the available charging capacity evenly among the EVs. The capacity allocation is illustrated in Eq. (3) [36], where P_{EV} is the allocated power for each EV, $P_{capacity}$ is the available total charging capacity, and N is the number of active EVs requesting to be charged. Scenario 3 is essentially the same than Scenario 2 except that depending on the subscenario the total loading is either: not limited, limited to 3 × 160 A, or limited to 3 × 126 A.

$$P_{EV}(t) = \frac{P_{capacity}}{N(t)}. \tag{3}$$

As stated in the charging standard IEC 61851, an EVSE cannot set a new charging current limit for an EV more frequently than once every 5 s. Therefore, in case of HIL simulation or simulation with one-second resolution, the control algorithm is run every 5 s. In case of other resolutions, the control algorithm is run every time step.

2.5. Experimental setup

The idea of the experimental setup is to form the baselines for Scenarios 1 and 2 by measuring the real charging events. Then, the baselines are compared with the simulations. The experiments are carried out as HIL simulations at the Smart Grid Technology Lab [37] at TU Dortmund University. The hardware components include the four EVs (shown in Table 2) and two charging stations (Wirelane Doppelstele and RWE eStation). Both charging stations include two 22 kW (230 V, 3 × 32 A) sockets. The charging currents at RWE charging station are measured by using KoCoS EPPE PX power quality analyzers whereas Wirelane charging station includes built-in current measurement devices for both sockets.

The control algorithm is implemented using Python programming language. The algorithm is run on a computer that is connected to the same local network with the charging points so that the system is able to adjust the charging current limits of the EVSE and read measurements of
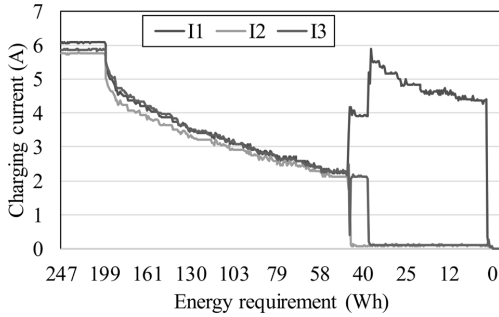
Fig. 5. Lookup table illustration of the charging of BMW i3 2016 with a current limit of 6 A, where I1–I3 represents phase currents.
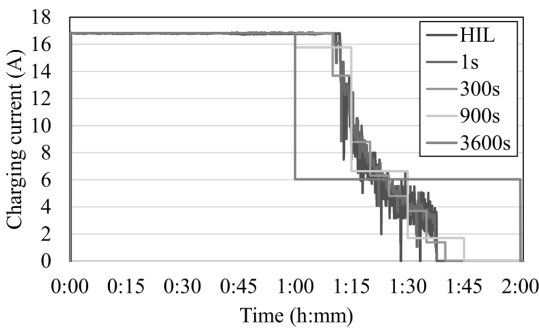

Fig. 6. Block diagram of the simulation model.

the realized charging currents in real-time. A pre-recorded household electricity consumption data (described in Section 2.1) is read from an Excel file to simulate the household electricity consumption. The experimental setups for Scenarios 1 and 2 are shown in Fig. 3. Due to the limitations of the laboratory equipment, Scenario 3 with up to 21 simultaneous charging sessions can only be simulated. The simulated setup for Scenario 3 is similar than the setup shown in Fig. 3(b) but there are 21 virtual charging points instead of the 4 physical charging points. A picture of the laboratory setup is shown in Fig. 4.

2.6. Simulation model

The idea of the simulation model is to allow the baselines of each scenario to be replicated with different temporal resolutions. These must be done as pure simulations without any HIL components. To model the EVs as accurately as possible, the modeling of the EVs is based on actual preliminary measurements of the EVs. The charging profile is measured in 1 s resolution for each EV for each possible charging current limit (integer) set by the EVSE. Only the current limit integers (6, 7, 8, … 32 A) are considered as the charging stations does not allow floating point numbers as current limits.

The preliminary measurements are used to calculate the missing energy from the batteries in each time step. The calculation begins from the end of the measurement where the missing energy is zero (i.e., the EV is fully charged). Then, a lookup table is formed to link a missing energy (Wh) to a charging current vector representing each phase current (A). The process and a formed lookup table is illustrated in Fig. 5. In the figure, the EV model is BMW i3 2016 and the current limit set by the EVSE is 6 A. A separate lookup table is formed for each EV and for each possible current limit. The lookup table is formed only for the part where
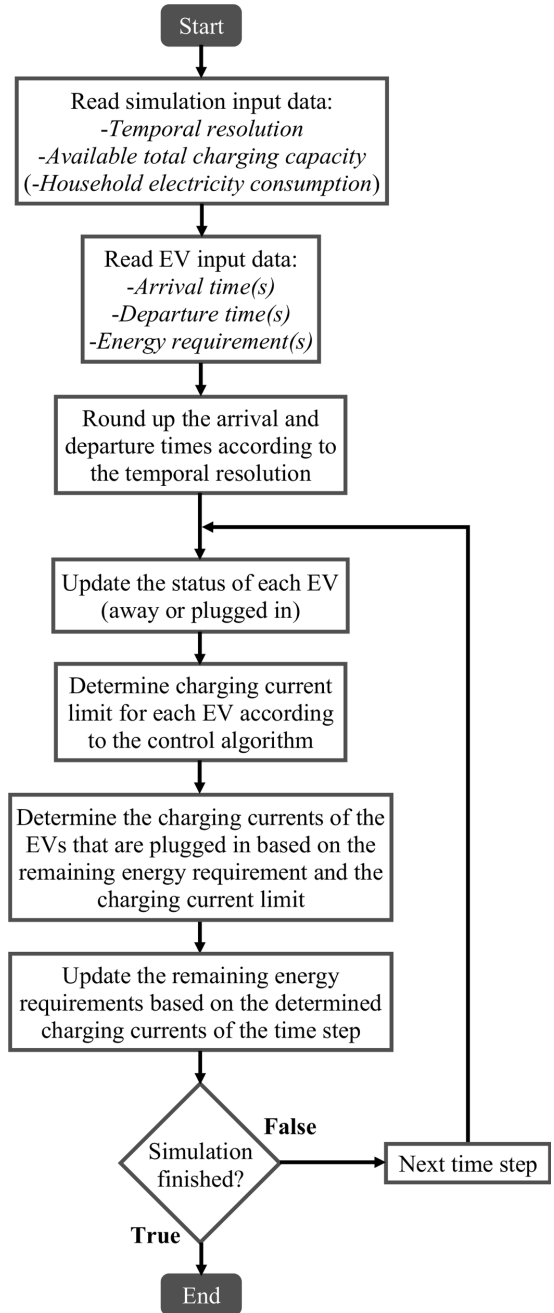

Fig. 7. Illustration of Nissan Leaf 2012 charging profile.

the charging current is decreasing. For the constant power part (e.g., energy requirement of ≥ 199 Wh in Fig. 5), the model assumes constant currents. The process and the received charging profile models are essentially the same than the ones mentioned in [38]. However, in this paper, different current limits are considered and thus the model can be
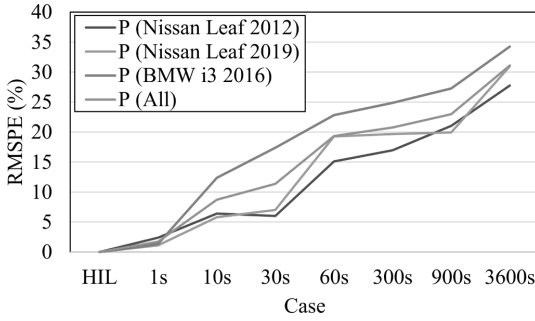
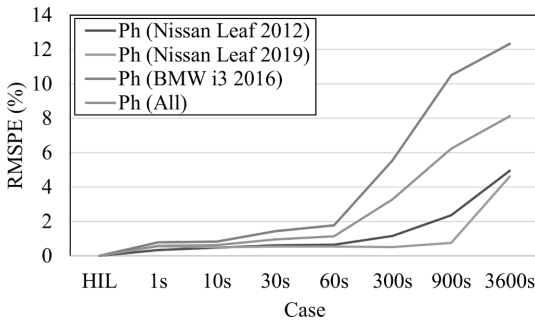**Fig. 8.** RMSPE in the highest momentary peak loads in Scenario 1.

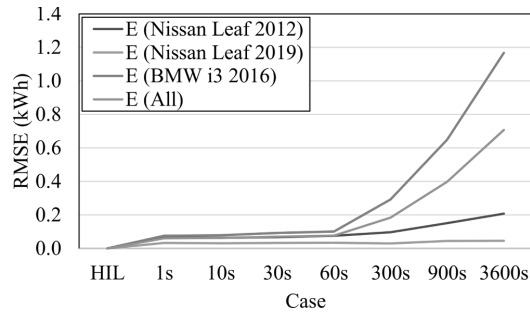**Fig. 9.** RMSPE in the highest hourly peak loads in Scenario 1.

Fig. 10. RMSE in the charged energies in Scenario 1.

used to simulate controlled charging instead of only uncontrolled charging. In this paper, the energy that is missing from the battery of an EV is referred to as energy requirement.

As opposed to [38], the simulation model is modified to consider different time resolutions. Coarser time resolutions are obtained by averaging the values of the considered time period. In Fig. 6, an uncontrolled charging session of Nissan Leaf 2012 (i.e., the current limit set by the EVSE is $\geq$ 16 A) is illustrated in different cases. In the figure, "HIL" represents actual laboratory measurements whereas the rest represent simulation results with different temporal resolutions. In each of these cases, the EV draws 5.2 kWh from the grid. However, it can be clearly seen that a coarser time resolution results in a higher deviation between the measured charging profile and the simulated charging profile.

The operation of the simulation model is illustrated in Fig. 7. At the

beginning, the model reads general input data and EV related input data. Since the arrivals and departures may not necessarily occur at an exact time step in all temporal resolutions, they are rounded to the closest time step. For example, an arrival time of 12:33:21 would be rounded to 12:30:00 or 13:00:00 in case of 15 min or 1 h resolutions, respectively.

After determining the initial values, the model simulates the EV charging until all EVs are fully charged or departed. In each time step, the model determines the status of each EV (away of plugged in). For the EVs that are plugged in, the charging control algorithm determines the charging current limits according to Eq. (2) or (3) depending on the scenario. After that, the charging currents are determined according to the charging profile models (lookup tables) where the realized charging currents depends on the current limits and the energy requirements. Finally, at the end of each time step, the remaining energy requirements of the EVs are updated based on the determined charging currents (assuming 230 V).

In the home charging scenario, the real-time power consumption of the household acts as a control signal for the EV charging according to Eq. (2). Even though the control is in real-time, it includes a small delay as the power consumption must be measured first before it can be used as a control signal. In the simulations, the delay is considered in case of temporal resolutions of 1–30 s. For example, in case of 30 s temporal resolution, this means that an average household power consumption of the previous 30 s period is used to determine the EV charging current limit for the next 30 s period. In case of resolutions of 60–3600 s, the delay of the real-time control is neglected as it yields more accurate results than using a delay of 60–3600 s. Therefore, for temporal resolutions of 60–3600 s, the average power consumption of a single time step is used to determine the EV charging current limit for the very same time step.

It is worth noting that minor deviation between the HIL measurements and the simulation results are expected as the simulation model does not consider factors such as battery temperatures in the modeling. It is commonly known that the battery temperature plays an important role in the EV charging and it must be considered by the battery management system to prevent dangerous situations and to maximize the performance and cycle life of battery [39]. From the power grid point of view, this can be seen, e.g., as a reduced charging current if the OBC tries to protect the battery from overheating [40]. However, due to the increased complexity of the modeling and the data requirements to form the model, the temperature factor is excluded from the simulation model.

3. Results

In this section, the results of each scenario are presented in separate subsections. In Scenarios 1–3, the results related to powers are presented as root mean square percentage errors (RMSPEs) calculated according to Eq. (4), where $\widehat{p}$ represents the baseline, p represents the compared case (i.e., simulation results obtained with different temporal resolutions), and t is a charging event (or a day in Scenario 3). As mentioned earlier, HIL measurements form the baselines in Scenario 1 and 2. Since there are not enough EVs to carry out the Scenario 3 in a similar fashion than Scenarios 1 and 2, the simulation results of the most accurate temporal resolution (1 s) are chosen to form the baseline for Scenario 3. The results related to charged energy are presented as root mean square errors (RMSEs). Percentual error related to the charged energy is assessed later in Section 3.4. Additionally, the general accuracy of the simulation model and the recommended temporal resolutions are investigated separately in Sections 3.5 and 3.6, respectively.

$$p_{RMSPE} = \sqrt{\frac{\sum_{t=1}^{T} \left(\frac{\widehat{p}_t - p_t}{\widehat{p}_t} \right)^2}{T}} \times 100\%. \qquad (4)$$

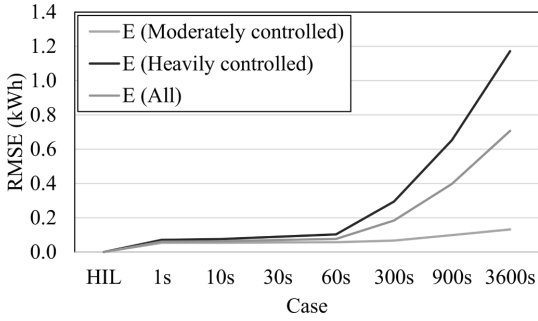To provide further values that may help future studies to select the

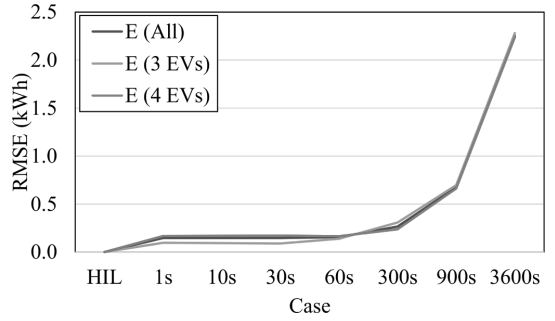**Fig. 11.** RMSPE in the highest momentary peak loads in Scenario 2.

Fig. 14. RMSPE in the highest hourly peak loads in Scenario 2.

Table 4
RMSPE and RMSE for all charging events in Scenario 1.

Case	P (%)	P_h (%)	E	E^a	E^b
HIL	0.0	0.0	0 Wh	0 Wh	0 Wh
1s	1.7	0.6	60 Wh	53 Wh	71 Wh
10s	8.7	0.6	62 Wh	54 Wh	75 Wh
30s	19.2	0.9	69 Wh	56 Wh	89 Wh
60s	19.3	1.1	77 Wh	57 Wh	103 Wh
300s	20.8	3.3	184 Wh	66 Wh	295 Wh
900s	23.0	6.2	398 Wh	98 Wh	654 Wh
3600s	31.1	8.1	707 Wh	132 Wh	1172 Wh

[a] includes only the charging sessions that are moderately controlled.
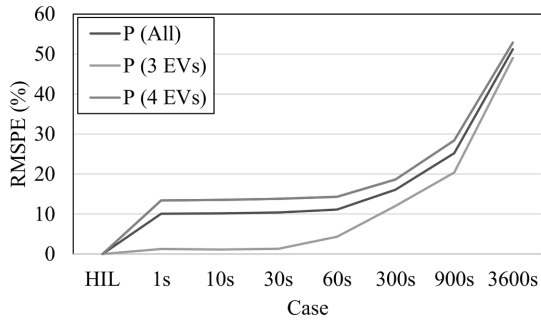[b] includes only the charging sessions that are heavily controlled.

Table 5
RMSPE and RMSE for all charging events in Scenario 2.

Case	P	P_h	E
HIL	0.0%	0.0%	0 Wh
1s	10.1%	1.9%	145 Wh
10s	10.2%	1.9%	145 Wh
30s	10.4%	1.9%	146 Wh
60s	11.1%	1.9%	155 Wh
300s	16.1%	2.8%	265 Wh
900s	25.2%	7.5%	676 Wh
3600s	51.2%	27.1%	2254 Wh

Fig. 12. RMSE in the charged energies for moderately controlled and heavily controlled charging sessions in Scenario 1.

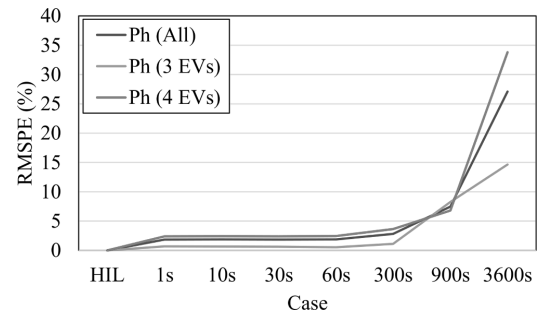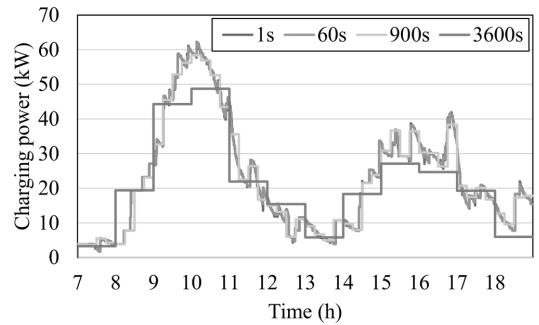**Fig. 15.** Modeled charging load on 25 February 2020 in different temporal resolutions.

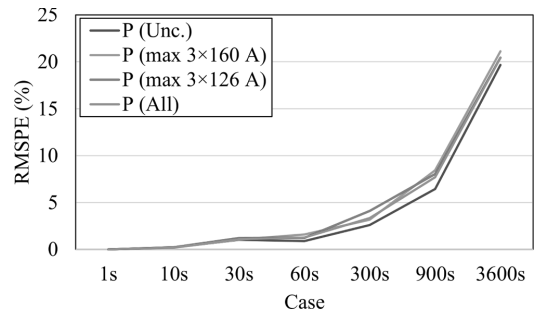**Fig. 13.** RMSE in the charged energies in Scenario 2.

Fig. 16. RMSPE in the highest momentary peak loads in Scenario 3.

appropriate temporal resolution, mean absolute errors (MAEs) are also
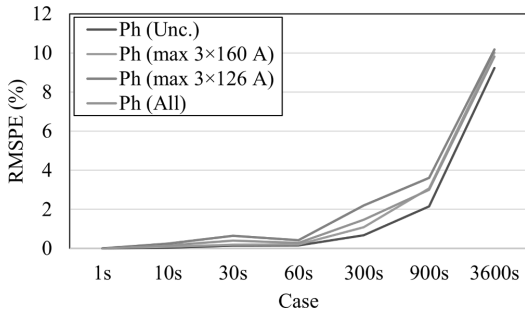
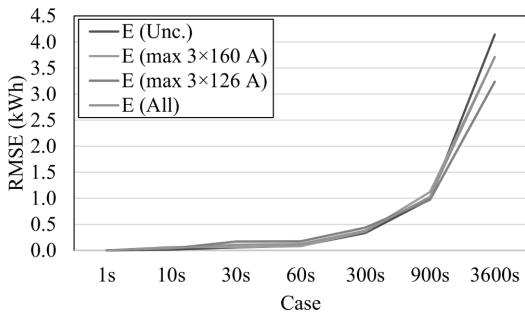**Fig. 17.** RMSPE in the highest hourly peak loads in Scenario 3.

Fig. 18. RMSE in charged energies in Scenario 3.

Table 6
RMSE for all charging events in Scenario 3.

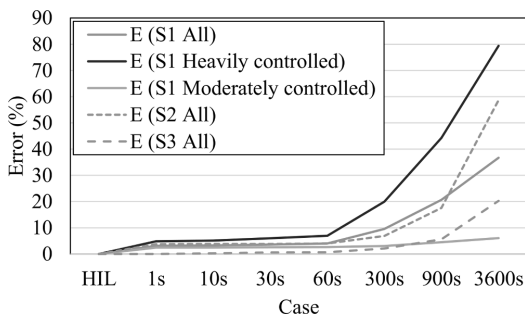| Case	P (%)	P$_h$ (%)	E
1s	0.0	0.0	0 Wh
10s	0.2	0.2	44 Wh
30s	1.1	0.4	110 Wh
60s	1.3	0.3	121 Wh
300s	3.3	1.5	380 Wh
900s	7.7	3.0	1026 Wh
3600s	20.4	9.8	3713 Wh

Fig. 19. Percentual error for charged energy in all scenarios.

calculated. However, to retain the flow of the paper, the MAEs are presented in the Appendix. The MAEs for Scenarios 1–3 are presented in Tables A1–A3, respectively.

Table 7
RMSE for Scenarios 1 and 2 with 1 s temporal resolution.

Scenario	P (%)	P$_h$ (%)	E (%)
S1 (Nissan Leaf 2012)	2.4	0.3	2.8
S1 (Nissan Leaf 2019)	1.1	0.6	1.6
S1 (BMW i3 2016)	1.4	0.8	4.8
S1 (All)	1.7	0.6	3.1
S2 (3 EVs)	1.3	0.7	2.3
S2 (4 EVs)	13.4	2.4	4.3
S2 (All)	10.1	1.9	3.8

Table 8
Recommended temporal resolutions depending on the type of scenario and the considered values.

Scenario	P	P$_h$	E
Home charging, uncontrolled	1 s	300 s	900 s
Home charging, controlled	1 s	300 s	1 s
A small charging site, controlled	60 s [a]	300 s	60 s
A large charging site, uncontrolled	300 s [b, c]	900 s [b]	300 s [b]
A large charging site, controlled	300 s [b, c]	900 s [b]	300 s [b]

[a] In a few simulations, even a temporal resolution of 1 s resulted in an error of >10%. However, in such events, the temporal resolution of 60 s yielded results as good as the 1 s resolution. Therefore, the 60 s resolution is seen sufficient.
[b] Baseline (i.e. reference point) is the simulation result with 1 s temporal resolution instead of hardware-in-the-loop simulation.
[c] The evaluation of the simulation model indicates that the modeling of the highest momentary peak load is subject to a notable error and thus the presented temporal resolution may not be accurate.

3.1. Scenario 1: a household with one EV

In Scenario 1, the households electricity consumption acts as a control signal for the EV charging according to Eq. (2) as mentioned earlier. The results for the scenario are illustrated in Figs. 8–11. In Fig. 8, the RMSPEs in the highest momentary peak loads are presented. In the figure, it can be seen that the error is notable (5.8–12.4%) with even a temporal resolution of 10 s. For temporal resolution of 1 s and 60 s the error varies between 1.1–2.4% and 15.1–22.8%, respectively. These results were expected due to the volatile nature of the electricity consumption in households where the highest momentary peak load often lasts only for a short duration. In case of one-hour temporal resolution, the RMSPE is 27.8–34.3%. The relative errors in the highest hourly peak loads are presented for Scenario 1 in Fig. 9. When comparing Figs. 8 and 9, it can be seen that in all cases the error in the highest hourly peak loads is lower than the error in the highest momentary peak loads. Even in case of one-hour temporal resolution the error is less than 12.4%. For temporal resolutions of 60 s and 300 s the error varies between 0.5–1.8% and 0.5–5.6%, respectively.

The RMSEs in the charged energies are presented in Fig. 10. As seen in the figure, the relative error is very small (34–101 Wh) when the temporal resolution is 60 s. However, coarser resolutions tend to result in notably higher errors. In one-hour resolution, the error of all EVs is 707 Wh. By considering the fact that the average charging load of all hourly time slots in Scenario 1 where an EV is charging is 1927 Wh, the RMSE is seen considerable. A closer examination regarding the charged energy reveals a clear correlation between the magnitude of the error and the charging control. As mentioned earlier, an EVSE can adjust the charging current limit only between 6 and 80 A in charging mode 3 according to the IEC 61851 charging standard. If the available charging capacity is below 6 A, the charging must be paused until there is enough capacity available. In case of coarser temporal resolutions, more details of the household's electricity consumption are lost. And, since the household's electricity consumption is a key factor for the EV charging control in Scenario 1, coarser temporal resolutions may have notable impacts on the error of the charged energy.

In Fig. 11, the errors in the charged energies are presented separately for the charging sessions that are moderately controlled and heavily controlled. The term "moderately controlled" refers to charging sessions where the charging of the baseline did not have to be paused due to a lack of available capacity whereas the term "heavily controlled" refers to charging sessions where the charging of the baseline was paused. As seen in the figure, a finer resolution is much more important if the algorithm has to temporarily disable the charging. It is also worth noting that the IEC 61851 charging standard does not allow each phase to be controlled separately. Therefore, a three-phase charging session requires a higher minimum capacity than a single-phase charging session. This explains why the error for BMW in Fig. 10 is more heavily dependent on the temporal resolution compared to the two other EVs. The results for Scenario 1 are presented in Table 4.

It is reasonable to note that in Scenario 1, the plug-in times for the EVs were at 17:00:00, 19:00:00, or 21:00:00 and thus they were not affected by the change of the temporal resolution. Therefore, the errors seen in the results presents the influence of the temporal resolution of the control signal for a single EV. However, when modeling real-life situations, the temporal resolution is likely to affect the modeling accuracy also if the plug-in and plug-out times are rounded up by the model.

3.2. Scenario 2: a small charging site

The results of Scenario 2 are illustrated in Figs. 12–14. In Fig. 12, it can be seen that the highest momentary peak loads cannot always be accurately modeled by the simulation model even with the 1 s resolution. This means that the other assumptions and simplifications in the simulation model, such as the exclusion of considering battery temperatures, can have notable impacts to the modeling accuracy. According to a closer investigation, the simulation model was not always able to model the charging currents in the decreasing current stage correctly. This caused some charging sessions in the simulation model to finish a few minutes earlier or later than in HIL measurements. And, since the available charging capacity is divided evenly among the EVs that are requesting to be charged according to Eq. (3), a modeling error in one charging sessions can influence the charging capacity distribution if there is a charging control algorithm in use as in this scenario. As the status of the EVs are modeled wrong for only a few minutes, it does not affect the hourly peak powers or charged energies very much as it can affect the momentary peak loads as seen in Figs. 12–14. It is also worth mentioning that the issue is especially significant due to the fact that there are only a few EVs. In case of multiple EVs (as in Scenario 3), it is less impactful if, e.g., the status of one EV (requesting charging or not) is modeled wrong as it does not have relatively high influence on the total load. Conversely, if there is only one EV (as in Scenario 1), the same issue is not possible.

The above-mentioned issue occurs only in the events with four EVs, and thus, the events with three EVs are modeled more accurately especially in case of 1–60 s resolutions. For coarser resolutions (≥ 300 s), the error becomes increasingly more notable and the difference between the events that have three or four EVs diminish. This is assumed to be due to the errors caused by coarse temporal resolutions become much more significant than the error caused by the other assumptions and simplifications in the simulation model excluding the temporal resolution.

The errors in the highest hourly peak loads are presented in Fig. 13. The errors seem to be relatively consistent, between 0.5–3.6%, for resolutions of 1–300 s. For resolutions of 900 s and 3600 s, the error increases to 6.8–8.3% and 14.7–33.8%, respectively. The errors in the charged energies are presented for Scenario 2 in Fig. 14. The errors for all charging events are between 145 and 155 Wh in case of temporal resolutions of 1–60 s. For coarser resolutions of 300, 900, and 3600 s, the error increases exponentially to 265, 676, and 2254 Wh, respectively. The results for Scenario 2 are presented in Table 5.

3.3. Scenario 3: a large charging site

To demonstrate the influence of different temporal resolutions in a commercial charging site, an illustration of Scenario 3 is given in Fig. 15. The day selected for the figure represents an average day in terms of daily charged energy. As seen in the figure, one-hour temporal resolution clearly results in a lower total charging power compared to other resolution. This is due to the fact that in 13.3% of the 3801 charging sessions the arrival and departure times round up to the same hour, i.e., the charging session do not essentially happen in case of one-hour resolution. In case of 900 s resolution, the arrival and departure times round up to the same moment in 3.1% of the charging sessions. In terms of energy, these charging sessions represents 3.0% (3600 s resolution) and 0.04% (900 s resolution) of the total charged energy according to the charging data.

The errors in the highest momentary peak loads in Scenario 3 is presented in Fig. 16. The figure shows that the error is relatively small ($\leq 1.6\%$) when the resolution is ≤ 60 s. For coarser resolutions, the error begins to increase notably. For the highest hourly peak loads, the results are similar but around half of the magnitude. The relative errors in the highest hourly peak loads are illustrated in Fig. 17. The errors in the charged energies in Scenario 3 are presented in Fig. 18. For each sub-scenario, the errors are ≤ 174 Wh for resolutions of ≤ 60 s. For coarser resolutions of 300, 900, and 3600 s, the errors increase exponentially to 334–436, 971–1122, and 3236–4142 kWh, respectively. The results for Scenario 3 are presented in Table 6.

3.4. Comparison of the absolute errors of the charged energies

Due to the fact that the temporal resolution affects the charged energies in each hourly time slot and may cause it to be zero in some hourly slots, the RMSPE for the charged energies were not possible to be calculated in a similar fashion than the peak loads. The RMSE in the charged energy is converted into percentual RMSE using Eq. (5), where the E_{RMSE} is the absolute RMSE (kWh) and E_{Avg} is the average hourly load of all one-hour time slots where at least one EV is charging. The results are presented in Fig. 19, where S1–S3 represents different scenarios. It can be seen that the relative error is moderately low (0.7–7.0%) in all scenarios in case of 60 s temporal resolution. In case of coarser resolutions, the error increases, but the increment is substantially dependent on the scenario.

$$E_{RMSE,\%} = \frac{E_{RMSE}}{E_{Avg}}. \tag{5}$$

3.5. Evaluating the simulation model

According to the simulation results of Scenarios 1 and 2, the simulation model successfully models the key values accurately with one second temporal resolution. The simulation results of the one-second temporal resolution are presented in Table 7. In most scenarios, the relative error in the highest momentary peak load is around 1–2%. However, the error in Scenario 2 with charging events of four EVs or all events is over 10%. As mentioned earlier, this exceptionally high error originates from the other assumptions and simplifications in the simulation model, such as the exclusion of considering battery temperatures in the modeling. Similar effect is seen also in the errors of the highest hourly peak loads. However, in all scenarios, the error in the highest hourly peak loads is much smaller compared to the errors of the highest momentary peak loads. The errors of the charged energies vary between 1.6 and 4.8% and there do not seem to be a clear trend between the scenarios and the magnitude of the error. Overall, the results indicate that the simulation model is sufficiently accurate to model the key values of the EV charging in most scenarios even though the battery temperatures are not considered in the model.

As mentioned earlier, the simulation model does not consider all

factors that influence the charging load modeling. Therefore, the simulations with different temporal resolutions include two types of modeling inaccuracies: temporal resolution-based modeling error and the errors cause by all other factors, such as the exclusion of battery temperature in the modeling. In case of a fine temporal resolution, the other factors are the dominant cause for the modeling errors whereas, in case of a coarse resolution, the temporal resolution-based inaccuracies are dominant. In Scenarios 1 and 2, the temporal resolution-based error seems to become the dominant cause of modeling errors after the temporal resolution of 60 s. This explains why the error is relatively steady for resolutions of 1–60 s and increases rapidly after resolution of 60 s in, e.g., Figs. 9–14. Additionally, as the baseline for the comparisons in Scenario 3 is the simulation results with 1 s temporal resolution instead of HIL measurements, the results include only the temporal resolution-based errors. Therefore, a more consistent correlation between the modeling errors and the temporal resolution is seen in Scenario 3 than in Scenarios 1 and 2.

3.6. Recommended temporal resolutions

As seen in the results, simplified simulations with excessively coarse temporal resolutions may lead to significant modeling inaccuracies. For example, when using one-hour temporal resolution, the error may be over 50% in the highest momentary peak loads (as seen in Fig. 12), over 30% in the highest hourly peak loads (as seen in Fig. 13), or almost 80% in the charged energies (as seen in Fig. 19). Therefore, it is clear that the use of a justified temporal resolution in simulations is vital to ensure a reasonable modeling accuracy.

In Table 8, the necessary temporal resolution to achieve a relative error of less than 5% is shown separately for each key value and for each different type of scenario. Since Scenario 3 could not be carried out as HIL simulation, the baseline is the simulation results with 1 s temporal resolution. To summarize Table 8, it can be said that to model the highest momentary peak load accurately, a fine temporal resolution of 1–60 s is necessary. To model the highest hourly peak load, a temporal resolution of 300–900 s is reasonable.

In order to model the charged energies accurately, the necessary temporal resolution vary more notable depending on the situation. If there is a volatile control signal (e.g., household's energy consumption-based control) and the charging session may be required to be temporally stopped, a very fine temporal resolution of even 1 s may be necessary. Conversely, to model the charged energy of a single EV without a complex control mechanism, a temporal resolution of 300–900 s should be sufficiently accurate. In a scenario that is between the two extremes, a temporal resolution of 60 s is likely to be reasonably accurate.

It is worth noting that this paper considers measurement-based charging load profiles in the modeling which often leads to quite accurate results as shown in Section 3.5. In case of more simplified charging load modeling approaches, the charging load modeling may contain some inaccuracies that are not related to the temporal resolution. Thus, even the use of temporal resolution of 1 s may not lead to accurate results in that case. However, by using the recommended temporal resolutions of Table 8, it is reasonable to assume that the EV charging load modeling will not include any significant temporal resolution related errors.

3.7. Discussion

The simulations of this paper consider only uncontrolled charging and controlled charging with a peak load management. It is expected that different scenarios using different control algorithms may require

different temporal resolutions to be sufficiently accurate. However, all control algorithms presented in the scientific literature cannot be tested using HIL simulations with commercial EV, which sets some limitations to this kind of study. For example, the considered EVs do not support vehicle-to-grid operation and are not able to transfer information, such as battery-status, to the control system.

However, the results of this paper can also be used as guidelines for different scenarios that use other charging control algorithms. To determine the reasonably accurate temporal resolutions in case of other control algorithms, the focus should be put on the control signal and how it is affected by the change of the temporal resolution. For example, if charging is controlled based on hourly electricity prices, the control signal's resolution is an hour. Therefore, the use of one-hour resolution or finer does not negatively influence on the accuracy of the control signal. This means that charging control based solely on hourly electricity prices could be simulated with a similar accuracy as uncontrolled charging, and sufficiently accurately results could be obtained using 300–900 s resolution (see Table 8.). Furthermore, if a control algorithm combines a peak load management with a volumetric electricity price (€/kWh) optimization, the price optimization is not assumed to have an influence on the recommended temporal resolution, and thus the recommended temporal resolution is 1–300 s depending on the situation (see Table 8).

Other benchmark algorithms, such as earliest deadline first and least laxity first, may depend on the mobility requirements of the EVs including departure time or energy requirements. However, these algorithms are not expected to be notably dependent on the used temporal resolution. This is because the change of temporal resolution does not influence on the energy requirement. Additionally, the simulation model already has to consider the departure time even in the case of uncontrolled charging to determine when charging is allowed or not. A similar reasoning can potentially be used in case of other control algorithms to determine a reasonably accurate temporal resolution.

4. Conclusions

In this paper, the influence of the temporal resolution on the electric vehicle charging load modeling is assessed. To form realistic baselines for the simulations, laboratory experiments with up to four commercial electric vehicles are carried out. In addition, to evaluate electric vehicle charging at home or at a large charging site, detailed household's electricity consumption data and charging session data of REDI shopping center was used. Furthermore, a laboratory measurement–based electric vehicle charging simulation model is developed.

The investigated research questions and the findings of the study are as follows:

1 *What is the impact of the temporal resolution when modeling home charging or a small charging site?* In most cases, the modeling error is relatively modest with temporal resolutions of ≤ 60 s but increases exponentially with higher temporal resolutions. However, for home charging in which the peak load is the sum of the charging load and the household's electricity consumption, the modeling error is notable ($\geq 8.7\%$ on average) already with temporal resolutions of ≥ 10 s.

2 *What is the impact of the temporal resolution when modeling a large charging site?* According to the results, a temporal resolution of 300–900 s may be sufficient to model the total load of a large charging site in case of uncontrolled charging or a relatively simple control method. However, it is noted that in commercial charging sites, the parking duration may not always be very long. Therefore,

exceedingly coarse resolution (e.g. one-hour) may lead to a situation where some of the charging sessions are excluded from the modeling.

3 *How accurately the electric vehicle charging loads can be modeled using the developed simulation model?* The simulation results indicate that the developed simulation model is sufficiently accurate (error less than 5%) in most cases even though the battery temperatures are not included in the model. However, the results also show that due to this simplification, there may be notable inaccuracies mostly in the highest momentary peak loads.

4 *Which temporal resolutions are necessary in different situations to ensure reasonably accurate modeling?* To model the highest hourly peak loads, a temporal resolution of 300 s is seen sufficiently accurate regardless of the size of the charging site and the use of control algorithm. To model the highest momentary peak loads in a charging site, a temporal resolution of 60–300 s is reasonably accurate. However, if the peak load is also dependent on an external load, such as a volatile household's electricity consumption, a very fine resolution of 1 s may be necessary. To model the charged energy in each hourly time slot accurately, the necessary temporal resolution varies significantly depending on the scenario. In case of uncontrolled charging of a single electric vehicle, a resolution of up to 900 s may be sufficient. However, if the charging is controlled and there is a chance that the charging must be temporally stopped (e.g. to avoid load peaks), a very fine temporal resolution of 1 s may be necessary. In other cases, a temporal resolution of 60 s is likely to be sufficiently accurate to model the charge energy.

As shown in this paper, the influence of the temporal resolution is of great importance and the use of a justified resolution should not be overlooked. To strengthen the theoretical background of all future electric vehicle charging related simulations, this paper provides guidance in terms of the necessary temporal resolution of the electric vehicle charging load modeling. Since the modeling methods and parameters play an important role in the simulations, future work should consider different EVs and investigate how different modeling methods influence on the modeling accuracy.

CRediT authorship contribution statement

Toni Simolin: Conceptualization, Software, Data curation, Formal analysis, Methodology, Validation, Visualization, Writing – original draft, Writing – review & editing. **Kalle Rauma:** Conceptualization, Data curation, Investigation, Resources, Validation, Writing – original draft, Writing – review & editing. **Antti Rautiainen:** Writing – review & editing. **Pertti Järventausta:** Writing – review & editing. **Christian Rehtanz:** Funding acquisition.

Declaration of Competing Interest

The authors declare that they have no known competing financial interests or personal relationships that could have appeared to influence the work reported in this paper.

Appendix

Tables A1–A3.

Table A1
MAEs for Scenario 1.

Case	P	P_h	E	E^a	E^b
HIL	0 W	0 W	0 Wh	0 Wh	0 Wh
1s	57 W	23 W	29 Wh	30 Wh	27 Wh
10s	572 W	25 W	31 Wh	29 Wh	35 Wh
30s	694 W	36 W	41 Wh	32 Wh	57 Wh
60s	1513 W	39 W	47 Wh	38 Wh	63 Wh
300s	1660 W	86 W	106 Wh	46 Wh	210 Wh
900s	1883 W	165 W	203 Wh	66 Wh	443 Wh
3600s	2613 W	252 W	332 Wh	77 Wh	777 Wh

[a] includes only the charging sessions that are moderately controlled.
[b] includes only the charging sessions that are heavily controlled.

Table A2
MAEs for Scenario 2.

Case	P	P_h	E
HIL	0 W	0 W	0 Wh
1s	822 W	100 W	85 Wh
10s	820 W	100 W	87 Wh
30s	857 W	98 W	92 Wh
60s	975 W	97 W	103 Wh
300s	1615 W	172 W	194 Wh
900s	3371 W	462 W	506 Wh
3600s	7908 W	1323 W	1707 Wh

Table A3
MAEs for Scenario 3.

Case	P	P_h	E
1s	0 W	0 W	0 Wh
10s	41 W	19 W	11 Wh
30s	181 W	63 W	43 Wh
60s	280 W	67 W	59 Wh
300s	964 W	339 W	238 Wh
900s	2517 W	929 W	685 Wh
3600s	8891 W	3375 W	2577 Wh

References

[1] K. Rauma, T. Simolin, A. Rautiainen, P. Järventausta, C. Rehtanz, Overcoming non-idealities in electric vehicle charging management, IET Electr. Syst. Transp. (2021), https://doi.org/10.1049/els2.12025 in pressaccepted in 13 April.

[2] T. Beck, H. Kondziella, G. Huard, T. Bruckner, Assessing the influence of the temporal resolution of electrical load and PV generation profiles on self-consumption and sizing of PV-battery systems, Appl. Energy 173 (2016) 331–342, https://doi.org/10.1016/j.apenergy.2016.04.050.

[3] M. Jaszczur, Q. Hassan, A.M. Abdulateef, J. Abdulateef, Assessing the temporal load resolution effect on the photovoltaic energy flows and self-consumption, Renew. Energy 169 (2021) 1077–1090, https://doi.org/10.1016/j.renene.2021.01.076.

[4] M. Shepero, J. Munkhammar, Spatial Markov chain model for electric vehicle charging in cities using geographical information system (GIS) data, Appl. Energy 231 (2018) 1089–1099, https://doi.org/10.1016/j.apenergy.2018.09.175.

[5] N. Sadeghianpourhamami, J. Deleu, C. Develder, Definition and evaluation of model-free coordination of electrical vehicle charging with reinforcement learning, IEEE Trans. Smart Grid 11 (1) (2020) 203–214, https://doi.org/10.1109/TSG.2019.2920320.

[6] L. Gong, W. Cao, K. Liu, Y. Yu, J. Zhao, Demand responsive charging strategy of electric vehicles to mitigate the volatility of renewable energy sources, Renew. Energy 156 (2020) 665–676, https://doi.org/10.1016/j.renene.2020.04.061.

[7] X. Dong, Y. Mu, X. Xu, H. Jia, J. Wu, X. Yu, et al., A charging pricing strategy of electric vehicle fast charging stations for the voltage control of electricity distribution networks, Appl. Energy 225 (2018) 857–868, https://doi.org/10.1016/j.apenergy.2018.05.042.

[8] H. Lin, Y. Liu, Q. Sun, R. Xiong, H. Li, R. Wennersten, The impact of electric vehicle penetration and charging patterns on the management of energy hub – a multi-

agent system simulation, Appl. Energy 230 (2018) 189–206, https://doi.org/10.1016/j.apenergy.2018.08.083.

[9] Y. Zhang, P. You, L. Cai, Optimal charging scheduling by pricing for EV charging station with dual charging modes, IEEE Trans. Intell. Transp. Syst. 20 (9) (2019) 3386–3396, https://doi.org/10.1109/TITS.2018.2876287.

[10] M.F. Shaaban, S. Mohamed, M. Ismail, K.A. Qaraqe, E. Serpedin, Joint planning of smart EV charging stations and DGs in eco-friendly remote hybrid microgrids, IEEE Trans. Smart Grid 10 (5) (2019) 5819–5830, https://doi.org/10.1109/tsg.2019.2891900.

[11] Y. Zhang, J. Chen, L. Cai, J. Pan, Expanding EV charging networks considering transportation pattern and power supply limit, IEEE Trans. Smart Grid 10 (6) (2019) 6332–6342, https://doi.org/10.1109/TSG.2019.2902370.

[12] H. Liu, J. Qi, J. Wang, P. Li, C. Li, H. Wei, EV dispatch control for supplementary frequency regulation considering the expectation of EV owners, IEEE Trans. Smart Grid 9 (4) (2018) 3763–3772, https://doi.org/10.1109/TSG.2016.2641481.

[13] Y. Sun, Z. Chen, Z. Li, W. Tian, M. Shahidehpour, EV charging schedule in coupled constrained networks of transportation and power system, IEEE Trans. Smart Grid 10 (5) (2018) 4706–4716, https://doi.org/10.1109/TSG.2018.2864258.

[14] K. Zhou, L. Cheng, X. Lu, L. Wen, Scheduling model of electric vehicles charging considering inconvenience and dynamic electricity prices, Appl. Energy 276 (2020), 115455, https://doi.org/10.1016/j.apenergy.2020.115455.

[15] B. Khaki, C. Chu, R. Gadh, Hierarchical distributed framework for EV charging scheduling using exchange problem, Appl. Energy 241 (2019) 461–471, https://doi.org/10.1016/j.apenergy.2019.03.008.

[16] Y.W. Chung, B. Khaki, T. Li, C. Chu, R. Gadh, Ensemble machine learning-based algorithm for electric vehicle user behavior prediction, Appl. Energy 254 (2019), 113732, https://doi.org/10.1016/j.apenergy.2019.113732.

[17] M.P. Anand, B. Bagen, A. Rajapakse, Probabilistic reliability evaluation of distribution systems considering the spatial and temporal distribution of electric vehicles, Int. J. Electr. Power Energy Syst. 117 (2020), 105609, https://doi.org/10.1016/j.ijepes.2019.105609.

[18] Y. Xiang, Z. Jiang, C. Gu, F. Teng, X. Wei, Y. Wang, Electric vehicle charging in smart grid: a spatial-temporal simulation method, Energy 189 (2019), 116221, https://doi.org/10.1016/j.energy.2019.116221.

[19] J. Su, T.T. Lie, R. Zamora, Integration of electric vehicles in distribution network considering dynamic power imbalance issue, IEEE Trans. Ind. Appl. 56 (5) (2020) 5913–5923, https://doi.org/10.1109/TIA.2020.2990106.

[20] K. Zhou, L. Cheng, L. Wen, X. Lu, T. Ding, A coordinated charging scheduling method for electric vehicles considering different charging demands, Energy 213 (2020), 118882, https://doi.org/10.1016/j.energy.2020.118882.

[21] N.B.G. Brinkel, W.L. Schram, T.A. AlSkaif, I. Lampropoulos, W.G.J.H.M. van Sark, Should we reinforce the grid? Cost and emission optimization of electric vehicle charging under different transformer limits, Appl. Energy 276 (2020), 115285, https://doi.org/10.1016/j.apenergy.2020.115285.

[22] G.R.C. Mouli, M. Kefayati, R. Baldick, P. Bauer, Integrated PV charging of EV fleet based on energy prices, V2G, and offer of reserves, IEEE Trans. Smart Grid 10 (2) (2019) 1313–1325, https://doi.org/10.1109/TSG.2017.2763683.

[23] Y. Wang, D. Infield, Markov chain Monte Carlo simulation of electric vehicle use for network integration studies, Int. J. Electr. Power Energy Syst. 99 (2018) 85–94, https://doi.org/10.1016/j.ijepes.2018.01.008.

[24] B. Wang, D. Zhao, P. Dehghanian, Y. Tian, T. Hong, Aggregated electric vehicle load modeling in large-scale electric power systems, IEEE Trans. Ind. Appl. 56 (5) (2020) 5796–5810, https://doi.org/10.1109/TIA.2020.2988019.

[25] U. Fretzen, M. Ansarin, T. Brandt, Temporal city-scale matching of solar photovoltaic generation and electric vehicle charging, Appl. Energy 282 (2021), 116160, https://doi.org/10.1016/j.apenergy.2020.116160.

[26] J. Yan, J. Zhang, Y. Liu, G. Lv, S. Han, I.E.G. Alfonzo, EV charging load simulation and forecasting considering traffic jam and weather to support the integration of renewables and EVs, Renew. Energy 159 (2020) 623–641, https://doi.org/10.1016/j.renene.2020.03.175.

[27] Z. Wei, Y. Li, Y. Zhang, L. Cai, Intelligent parking garage EV charging scheduling considering battery charging characteristic, IEEE Trans. Ind. Electron. 65 (3) (2018) 2806–2816, https://doi.org/10.1109/TIE.2017.2740834.

[28] M. Wang, Y. Mu, Q. Shi, H. Jia, F. Li, Electric vehicle aggregator modeling and control for frequency regulation considering progressive state recovery, IEEE Trans. Smart Grid 11 (5) (2020) 4176–4189, https://doi.org/10.1109/TSG.2020.2981843.

[29] H. Kikusato, Y. Fujimoto, S. Hanada, D. Isogawa, S. Yoshizawa, H. Ohashi, et al., Electric vehicle charging management using auction mechanism for reducing PV curtailment in distribution systems, IEEE Trans. Sustain. Energy 11 (3) (2020) 1394–1403, https://doi.org/10.1109/TSTE.2019.2926998.

[30] REDI, "Parking", 2022, https://www.redi.fi/parking/?lang=en (accessed Sep. 1, 2021).

[31] Helen Electricity Network LTD, "Electricity distribution tariffs", 2022, https://www.helensahkoverkko.fi/globalassets/hinnastot-ja-sopimusehdot/hsv—en kku/distribution_tariffs.pdf (accessed Sep. 1, 2021).

[32] Kuopion Sähköverkko Oy, "Sähkönsiirto hinnasto - Electricity distribution tariffs", 2022, https://www.kuopionenergia.fi/wp-content/uploads/2020/07/Sähkönsii rtohinnasto-01012020.pdf (accessed Sep. 1, 2021).

[33] LE-Sähköverkko Oy, "Verkkopalveluhinnasto - Electricity service price list", 2022, https://www.lahtienergia.fi/wp-content/uploads/2021/06/verkkopalveluhi nnasto_01082019.pdf (accessed Sep. 1, 2021).

[34] Finnish Transport and Communications Agency Traficom, "Henkilöliikennetutkimus - National passenger traffic survey 2016", 2018, https://julkaisut.vayla.fi/pdf8/lti_2018-01_henkiloliikennetutkimus_2016_web.pdf (accessed Sep. 1, 2021).

[35] O. Frendo, J. Graf, N. Gaertner, H. Stuckenschmidt, Data-driven smart charging for heterogeneous electric vehicle fleets, Energy AI 1 (2020), 100007, https://doi.org/10.1016/j.egyai.2020.100007.

[36] T. Zhang, H. Pota, C.C. Chu, R. Gadh, Real-time renewable energy incentive system for electric vehicles using prioritization and cryptocurrency, Appl. Energy 226 (2018) 582–594, https://doi.org/10.1016/j.apenergy.2018.06.025.

[37] A. Spina, K. Rauma, C. Aldejohann, M. Holt, J. Maasmann, P. Berg, et al., Smart grid technology lab - a full-scale low voltage research facility at TU dortmund university, in: Proceedings of the 110th AEIT International Annual Conference, 2018, pp. 1–6, https://doi.org/10.23919/AEIT.2018.8577378. Oct.

[38] T. Simolin, K. Rauma, R. Viri, J. Mäkinen, A. Rautiainen, P. Järventausta, Charging powers of the electric vehicle fleet: evolution and implications at commercial charging sites, Appl. Energy 303 (2021) 117651, https://doi.org/10.1016/j.apenergy.2021.117651.

[39] L.H.J. Raijmakers, D.L. Danilov, R.A. Eichel, P.H.L. Notten, A review on various temperature-indication methods for Li-ion batteries, Appl. Energy 240 (2019) 918–945, https://doi.org/10.1016/j.apenergy.2019.02.078.

[40] Z.J. Lee, D. Chang, C. Jin, G.S. Lee, R. Lee, T. Lee, et al., Large-scale adaptive electric vehicle charging, in: Proceedings of the IEEE International Conference On Communications, Control, and Computing Technologies For Smart Grids (SmartGridComm), 2018, pp. 1–7, https://doi.org/10.1109/SmartGridComm.2018.8587550. Oct.

PUBLICATION
12

Assessing the influence of electric vehicle charging profile modelling methods

T. Simolin, K. Rauma, A. Rautiainen, P. Järventausta, C. Rehtanz

IET Generation, Transmission & Distribution

IET The Institution of Engineering and Technology WILEY

Assessing the influence of electric vehicle charging profile modelling methods

Toni Simolin[1] | **Antti Rautiainen**[1] | **Pertti Järventausta**[1] | **Kalle Rauma**[2,3] | **Christian Rehtanz**[2]

[1]Unit of Electrical Engineering, Tampere University, Tampere, Finland

[2]Institute of Energy Systems, Energy Efficiency and Energy Economics, TU Dortmund University, Dortmund, Germany

[3]VTT Technical Research Centre of Finland, Espoo, Finland

Correspondence

Toni Simolin, Unit of Electrical Engineering, Tampere University, Raamikatu 2 A 70, 33400 Tampere, Finland.
Email: toni.simolin@tuni.fi

Abstract

In the scientific literature, it has been a common assumption that electric vehicles (EVs) draw a constant current during the whole charging session. In reality, EV charging profiles are not linear, and the non-linearities have recently gained more attention. However, a thorough analysis of the influences of different charging profile modelling methods is not yet carried out. This paper aims to fill this gap by comparing experimental measurements of four commercial EVs and results of a developed simulation model that considers different charging profile modelling methods. According to the results, the use of linear charging profiles may lead to notable modelling inaccuracies (error > 30%) whereas the use of measurement-based non-linear charging profile models yields relatively accurate results (error mostly ≤ 3.5%). The results also demonstrate that the use of a simple, but justified, bilinear charging profile model is likely to be sufficiently accurate in most scenarios.

1 | INTRODUCTION

Over the past few years, a lot of work has been done to improve the electric vehicle (EV) charging load modelling methods. This work is necessary in order to accurately predict EV charging loads which further enables safe and efficient operation of the power grid [1]. However, at the present, there remains a gap in the scientific literature regarding the modelling accuracies.

1.1 | Literature review

To give an outlook of the EV charging load modelling related research found in the scientific literature, 25 recent studies are listed in Table 1. For each study, the modelling method of the EV charging profiles is presented. In this paper, a charging profile refers to the charging current behaviour over the charging session.

As seen in the Table 1, most of these recent studies consider a linear charging profile (i.e. the simplest method where the current stays constant over the whole charging session) to model the EV charging. In [24–26], it is acknowledged that the charging power is non-linearly dependent on the state of charge (SoC). To overcome the issue, only SoCs between 5% and 95% are considered in [24]. In [25] and [26], bilinear charging profiles are used. However, very little effort is made to justify the modelling method or to assess its influence on the modelling accuracy.

To classify different charging profiles, an iterative clustering framework is developed in [27]. The results show that even though the number of different charging profiles is significant, they can be classified into a small number of types (in the study, 304 different charging profiles are successfully classified into six types). These types can then be used to model charging behaviour with a reasonable accuracy. In [28], machine learning is used to form charging profile models and predict charging currents. The simulation results show that the XGBoost machine learning model yields the most accurate results with a mean absolute error of 126 W. Additionally, an ablation study is conducted to demonstrate that the exact EV model is not necessary to attribute to accurately model charging profiles. Instead, the necessary information includes charging features such as the number of phases and the maximum current used for charging.

TABLE 1 Recent studies

Ref.	Charging profile modelling method
[1–24]	Linear
[25]	Bilinear: charging power decrease linearly to zero after 60% SoC
[26]	Bilinear: charging power decrease linearly to zero after 80% SoC

Based on [27] and [28], it seems that there is no need to have a separate charging profile model for each different EV model. However, these studies do not assess the influence of the use of simplified charging profiles on the modelling accuracy. Therefore, the need to consider more accurate charging profile models remains currently unknown.

1.2 | Contribution and structure

Based on the literature review, it seems necessary to assess the influence of the EV charging profile modelling methods on the charging load modelling. To fill the gap in the literature, experimental measurements of a small charging site are compared with simulation results obtained by using different charging profile models. Similar simulations are also carried out for a large charging site using real charging data. The goal is to analyze the impact of different charging profile modelling methods on the charging load modelling accuracy in different situations. The results provide guidance and strengthen the scientific background for future studies related to EV charging load modelling. It is worth emphasizing that this paper focuses on the charging loads seen from the charging site point-of-view. The contributions of this paper are listed below.

- Assessing the accuracy of the linear charging profile modelling method that is widely used in the scientific literature.
- Assessing the accuracy of a measurement-based non-linear charging profile modelling method, in which the charging profiles are formulated based on experimental measurements of the considered EVs.
- Formulating bilinear charging profiles based on the experimental measurements and assessing the modelling accuracies of these charging profile models. Two bilinear charging profile modelling methods are considered. The first utilizes a separate charging profile for each EV and for each current limit, and the second utilizes a single bilinear charging profile that is applied for all EVs and for all current limits.
- Evaluating the influence of using charging control together with different charging profile modelling methods on the modelling accuracy.

The rest of the paper is as follows. Section 2 describes the assessment method including the simulation model and the experimental hardware-in-the-loop (HIL) measurements. Section 3 presents and analyses the results. The paper is finalized with conclusions in Section 4.

2 | ASSESSMENT METHOD

This section describes the key values of interest, the different charging profile modelling methods, the used charging data, the two examined scenarios, the used control method, the experimental HIL laboratory setup, and the used simulation model. Each topic forms its own subsection.

2.1 | Key values of interest

This paper assesses the influence of different charging profile modelling methods on the modelling accuracy in two different scenarios. To achieve this, three key values are examined: the highest peak power (P), the highest hourly peak power (Ph), and the charged energy (E). These values are often needed to determine, for example, the charging costs of an EV user, the costs and profits of a charging site operator, and the EV user satisfaction. Consequently, if these values are incorrect, the economical assessment of the charging site will also be unreliable. These values can also be used to estimate the optimal sizing of the charging infrastructure, and thus, inaccurately modelling the values could lead to over sizing or under sizing. Therefore, these values should be modelled accurately, and thus, they are considered as the key values in the assessment.

The highest peak power simply refers to the highest peak power measurement value of a single time step (10 s) in a day, whereas the highest hourly peak power refers to the highest average loading during a 1-h-long period in a day. The highest hourly peak power is an interesting value because it can be the basis for a power-based distribution tariff component as in [29]. The charged energy refers to the energy that is charged during each 1-h time slot (i.e. 0:00–1:00, 1:00–2:00 etc.). This definition is made because the temporal resolution in electricity pricing is often 1 h, and thus, a modelling error in the hourly level may affect certain cost or benefit analysis.

For each key value, a percentual root mean square error (RMSE) is calculated by comparing the simulation results to the results of the selected baseline (described in Section 2.4). The percentual RMSE for the highest peak power and the highest hourly peak power is calculated using (1), where $Value$ is either P or Ph, N_d is the number of cases or days (25 cases for Scenario 1 and 89 days for Scenario 2, described in Section 2.4), subscript b represents baseline, and subscript c represents the compared value. Since an hourly charged energy can be zero, the percentual RMSE for the charged energy is calculated using (2) and (3), where $E_{RMSE,abs}$ is the absolute RMSE (in kWh) and E_{avg} is the average hourly charging load (in kWh).

$$Value_{RMSE,\%} = \sqrt{\frac{1}{N_d} \times \sum_{n=1}^{N_d} \left(\frac{Value_{b,n} - Value_{c,n}}{Value_b} \right)^2} \times 100\%. \tag{1}$$

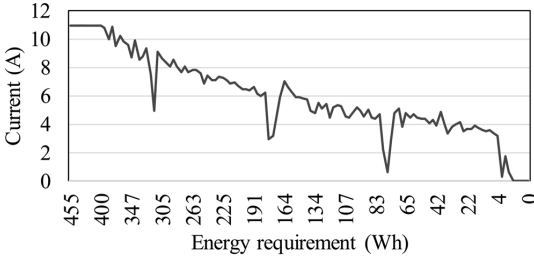$$E_{RMSE,abs} = \sqrt{\frac{1}{N_d \times 24} \times \sum_{h=1}^{N_d \times 24} \left(E_{b,h} - E_{c,h} \right)^2}. \tag{2}$$

FIGURE 1 Charging profile lookup table for Nissan Leaf 2012 with 11 A current limit

TABLE 2 The used electric vehicles

EV	Charging power
Nissan Leaf 2012	3.7 kW (1 × 16 A)
Nissan Leaf 2019	7.4 kW (1 × 32 A)
BMW i3 2016	11.0 kW (3 × 16 A)
Smart EQ for four 2020	22.1 kW (3 × 32 A)

$$E_{\mathrm{RMSE},\%} = \frac{E_{\mathrm{RMSE,\ abs}}}{EE}. \tag{3}$$

2.2 | Different charging profile models

In this study, five different charging profiles are compared: real HIL measurement, measurement-based non-linear (NL) model, bilinear (BL) model made separately for each EV and for each current limit set by the EV supply equipment (EVSE), unified bilinear (UBL) model which is used for each EV and for each current limit set by the EVSE, and linear (L) model.

The NL charging profiles are obtained by measuring the current drawn from the grid of each EV with all possible current limits (integers) set by the EVSE in 10-s resolution. Only current limit integers are considered as the used charging points (described in Section 2.6) do not support floating point current limits. The measurements are used to calculate the missing energy from the batteries in each time step. The calculation begins from the end of the charging session where the missing energy, referred to as energy requirement, is zero (i.e. the EV is fully charged). The process is illustrated in Figure 1 for the charging of Nissan Leaf 2012 with a current limit of 11 A set by the EVSE. In this case (Figure 1), the energy requirement (E_{R}) of 400 Wh separates the constant power (CP) and the constant voltage (CV) stages. After calculating the energies, a lookup table is formed to link the calculated energy requirements to the measured charging currents.

The lookup table is formed only for the CV stage of the charging profile. The charging current is assumed to be constant over the whole CP stage in the modelling methods. This is seen reasonably accurate because the charging current is shown to be very steady (variation of less than 0.5 A) during the CP stage [30]. After forming the lookup tables for all current limits, a three-dimensional lookup table is formed which links the current limit set by the EVSE (in amperes) and the missing energy of the EV (in Wh) to the charging currents (each phase current in amperes). A separate three-dimensional lookup table is formed for each EV. The process and the received charging profile models are similar than the ones mentioned in [30] and [31]. However, in this paper, other charging profile modelling methods (BL, UBL, and L) are also considered and compared.
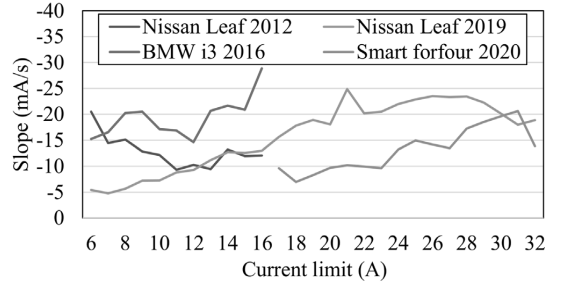

FIGURE 2 Slope of charging current in CV stage

The BL charging profile model utilizes the previously mentioned measurements to determine the energy requirement (E_{R} in Wh) at which point the charging currents begin to decrease (i.e. the point separating CP and CV stages). Then, Equation (4) is used to calculate the slope α that leads to the same energy (E_{R}) being charged in the CV stage, where L denotes current limit set by the EVSE, M denotes EV model, I_{CP} denotes the current in the CP stage, U denotes phase voltage (230 V). For the three-phase EVs (namely BMW and smart, as shown later in Table 2), separate slope for each phase is calculated. In the BL charging profile model, the slope is calculated separately for each EV and for each current limit set by the EVSE. The slopes are illustrated in Figure 2. For current limits 6–16 A, the charging of smart stop without a clear CV stage. This results in a very small E_{R} and thus a very high α. These slopes are considered to be outliers, and thus, they are excluded from the consideration and from the figure. Additionally, only the average slope of the three phases is presented for BMW and smart in the figure.

$$\alpha\,(L, M) \;=\; -\,\frac{(I_{\mathrm{CP}}\,(L, M))^2 \times U}{2 \times E_{\mathrm{R}}\,(L, M)}. \tag{4}$$

The UBL charging profiles are formed using the same average slope for all EVs and all current limits set by the EVSE. The slope is the result of first calculating an average slope of each EV (Nissan Leaf 2012—12.8 mA/s, Nissan Leaf 2019—15.9 mA/s, BMW i3 2016—19.4 mA/s, Smart for four 2020—13.1 mA/s), and then calculating the average of all EVs which is −15.3 mA/s. The same average slope is assumed to affect each phase current, and thus, the charging powers of the three-phase EVs are decreasing three times as fast as the powers of the single-phase EVs.
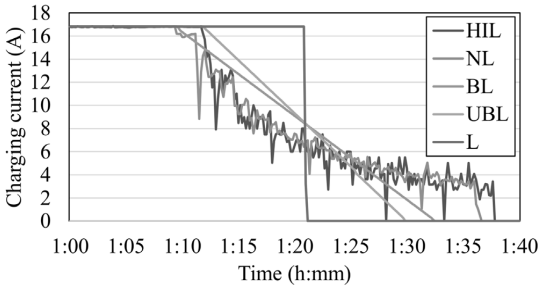
FIGURE 3 Illustration of Nissan Leaf 2012 charging profile

The L charging profile model assumes that the charging currents do not decrease when the EV is becoming fully charged. The charging profiles are illustrated in Figure 3 for Nissan Leaf 2012. In the figure, the charging is uncontrolled (i.e. current limit is $\geq$16 A) and the initial energy requirement is 5.2 kWh. Regardless of the modelling method, the EV draws 5.2 kWh from the grid. However, it can be clearly seen that different modelling methods result in different currents in the CV stage.

It is worth noting that some deviations between the HIL measurements and the simulation results are expected because the simulation model does not consider battery temperatures in the modelling. It is commonly known that a battery temperature plays an important role in the charging management of an EV, and thus, it should be considered the battery management system of the EV. However, due to the increased complexity of the modelling and the data requirements to form the model, the temperature factor is excluded from the charging load simulation model.

Additionally, this paper does not consider either percentual SoCs or charging efficiencies. Since the HIL charging current measurements were not able to record the SoCs of the EVs during the charging and the considered charging session data (described in Section 2.3) also measured charged energies in kWh, it is more convenient to consider energy requirements in kWh instead of utilizing SoC in this paper. Because this paper only deals with charging energies and currents seen from the grid point-of-view, the charging losses are being included. Therefore, the impact of not considering charging efficiencies explicitly is not expected to have a notable influence on the results.

2.3 | Used data

To evaluate a large charging site in a realistic manner, charging session data of REDI is used. REDI is a shopping centre located in Helsinki, Finland, which has over 200 charging points that support 22-kW charging [32]. The data is gathered over 89 days in 2020 (January–March) and contains 3801 charging sessions which results in 42.7 charging sessions per day. The data includes arrival and departure time, active charging time, charged energy, and charging peak power. All charging sessions are uncontrolled.

TABLE 3 Examined scenarios

	Site	N_{max} [a]	Control method	N_d [b]
1.	A small charging site	4	PLM	25
2.	A large charging site	21	Unc. / PLM	89

[a] N_{max} is the highest number of EVs simultaneously charging.
[b] N_d is the number of investigated cases or days.

According to the data, the EVs have an average stay duration of 236 min, an average active charging time of 101 min, and an average charged energy of 7.4 kWh. It is also seen that in 59.3% of the charging sessions the stay duration is less than 5 min longer than the active charging time. This indicates that the stay duration often acts as a bottleneck, and consequently, most EVs are not fully charged before departure. It is worth noting that a further analysis of the EV usage-related behaviour (parking time and driving requirements) is excluded from the paper. Instead, the focus is on the charging profiles (i.e. charging current drawn over the charging session) and the modelling accuracies of the different charging profile models.

2.4 | Examined scenarios

The simulations focus on two scenarios: a small charging station with four charging points and a large charging site with up to 21 simultaneous charging sessions. Scenario 1 is carried out in 25 different cases. In each case, three or four of the EVs shown in Table 2 are charged which results in 89 HIL charging sessions in total. For each event, the arrival times, the departure times, and the driving distances are randomly selected. In this scenario, the average driving distance is 19.1 km (min 4.3 km and max 65.0 km). This leads to an average energy requirement of 3.8 kWh (min 0.8 kWh and max 11.6 kWh) from the grid point-of-view (i.e. the charging losses are included). The arrival times of the EVs vary between 16 and 22 h and thus create circumstances where 1–4 EVs are simultaneously requesting charging. Sojourn times are assumed to be long enough so that the EVs can be fully charged. In each event, a peak load management (PLM) with a total charging current limit of 3×32 A is used. The used PLM is described in Section 2.5.

Scenario 2 is formed using the charging session data of the 89 days of REDI. For the modelling purposes, the recorded charging peak powers are used to determine the type of the EV according to (5), where P_p is the charging peak power. The second scenario is divided into three subscenarios based on the used control method: an uncontrolled charging (Unc.), PLM with a total charging current limit of 3×160 A, or PLM with a total charging current limit of 3×126 A. These limits are chosen based on preliminary simulation results that show that the highest peak current is 191 A in case of uncontrolled charging. The subscenarios are used to determine the impact of the modelling method together with the use of charging control to the modelling accuracy in a large charging site. The EVs and the key parameters of the scenarios are presented in Tables 2 and 3, respectively. The control method is presented in the next

subsection.

$$
\begin{cases}
EV_{\text{type}} = \text{ Nissan Leaf 2012, if } 0 \text{ kW} < P_{\text{p}} \leq 4.5 \text{ kW} \\
EV_{\text{type}} = \text{ Nissan Leaf 2019, if } 4.5 \text{ kW} < P_{\text{p}} \leq 10 \text{ kW} \\
EV_{\text{type}} = \text{ BMW } i3 \text{ 2016, if } 10 \text{ kW } < P_{\text{p}} \leq 15 \text{ kW} \\
EV_{\text{type}} = \text{ Smart EQ fourfour 2020, if } 15 \text{ kW } < P_{\text{p}} \leq 25 \text{ kW}
\end{cases}
$$

$$(5)$$

In Scenario 1, HIL measurements are used to set realistic baselines for the comparisons. Due to the limited number of available EVs, Scenario 2 with up to 21 simultaneous charging sessions can only be simulated. In that scenario, the measurement-based NL charging profile models are used to form the baselines because they are the most accurate in Scenario 1 according to the results seen in Section 3.1.

2.5 | Charging control method

In this paper, a benchmark control algorithm, fair sharing, presented in [33] is used. The algorithm divides the available charging capacity evenly among the EVs. The capacity allocation is illustrated in (6), where I_{EV} is the allocated current for each EV, I_{total} is the available total charging capacity, and N is the number of active EVs requesting to be charged. The current limit is then sent to the EV through the corresponding EVSE according to IEC 61,851 charging mode 3.

$$
I_{\text{EV}}\ (t) = \frac{I_{\text{total}}}{N\ (t)} \tag{6}
$$

It should be noted that the following control method in itself is not the focus of this paper. Instead, the goal is to create a situation that is the opposite of uncontrolled charging: the charging capacity is very limited and the state of a single EV (charging or not charging) influences on the available charging capacity of all EVs that are charging at the moment. In Scenario 1, the maximum total loading of the charging station (3 × 32 A) allows all four charging sessions to be simultaneously active. However, a dynamic PLM is required if more than one EV is simultaneously charging. The subscenarios of Scenario 2 are effectively the same than Scenario 1 except that the total loading is either not limited, limited to 3 × 160 A, or limited to 3 × 126 A.

2.6 | Experimental setup

The idea of the experimental setup is to form the baselines for Scenario 1 by measuring the real charging events. The experiments are carried out as HIL simulations at TU Dortmund University [34]. The hardware components include the four EVs mentioned in Table 2 and two charging stations (Wirelane Doppelstele and RWE eStation). Both charging stations include two 22 kW (230 V, 3 × 32 A) sockets. The charging currents at the
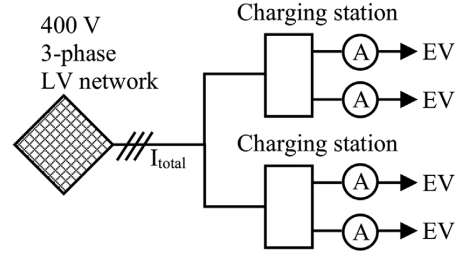

FIGURE 4 The experimental setup for Scenario 1

FIGURE 5 The laboratory setup

RWE charging station are measured by using KoCoS EPPE PX power quality analysers, whereas Wirelane charging station includes built-in current measurement devices for both sockets.

PLM is implemented using Python programming language. The algorithm is run on a computer that is connected to the same local network with the charging points so that the system is able to adjust the charging current limits of the EVSE and read the measurements of the realized charging currents in real time. The experimental setup for Scenario 1 is shown in Figure 4. The simulated setup for Scenario 2 is similar than the setup shown in Figure 4, but there are 21 virtual charging points instead of the four physical charging points. A picture of the laboratory setup is shown in Figure 5.

2.7 | Simulation model

The idea of the simulation model is to allow the real charging sessions to be replicated with different charging profile modelling methods. These must be done as pure simulations without any HIL components. A similar simulation model is used previously in [30] and [31]. However, in these studies, only a single charging profile modelling method (NL) was considered, and thus, the influence of different modelling methods could not be assessed.

The operation of the simulation model is illustrated in Figure 6. At the beginning, the model reads general input data and EV related input data. After the initialization, the model simulates the EV charging until all EVs have either been fully charged or been departed. In each time step, the model
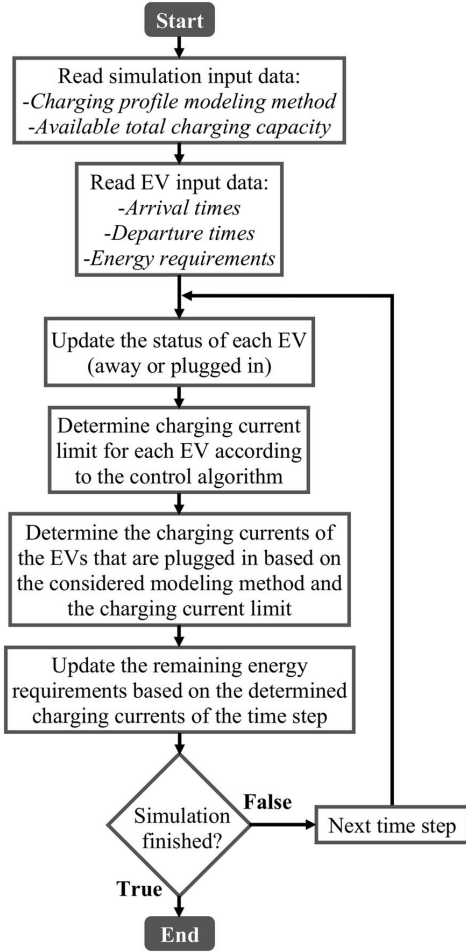
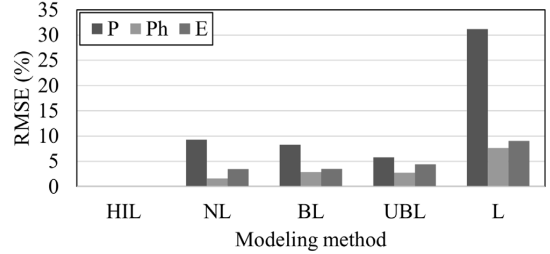**FIGURE 6** Block diagram of the simulation model

FIGURE 7 Results of scenario 1

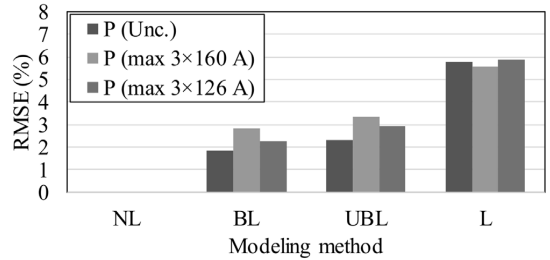**FIGURE 8** RMSE of the highest peak powers in Scenario 2
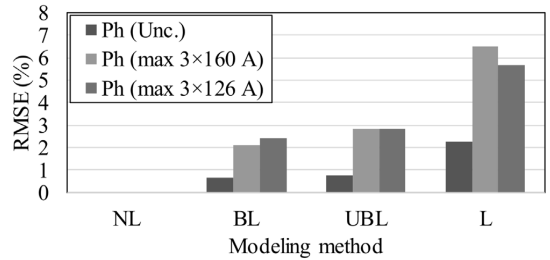
FIGURE 9 RMSE of the highest hourly peak powers in Scenario 2

determines the status of each EV (away or plugged in). For the EVs that are plugged in, the charging control algorithm determines the charging current limits according to (6). After that, the charging currents are determined according to the considered charging profile models and the determined current limits. Finally, at the end of each time step, the remaining energy requirements of the EVs are updated based on the determined charging currents. The simulation model uses a temporal resolution of 10 s.

3 | RESULTS

3.1 | Scenario 1: A small charging site

The results of Scenario 1 are presented in Figure 7. It can be seen that the highest hourly peak power and the charged energy can be modelled most accurately using the NL charging profiles

(RMSE of 1.62% and 3.45%, respectively). The use of separate BL charging profiles or the UBL charging profile yields smaller RMSEs in terms of the highest peak power (8.30% and 5.80%, respectively) and slightly higher RMSEs in terms of the highest hourly peak power (2.88% and 2.72%, respectively) and the charged energy (3.49% and 4.39%, respectively). Most significantly, the results show that the use of L charging profile leads to notable modelling errors (31.21% for the highest peak load, 7.62% for the highest hourly peak power, and 9.05% for the charged energy).

3.2 | Scenario 2: A large charging site

The modelling RMSEs of each key value of Scenario 2 are presented separately in Figures 8–10. Again, the results clearly indicate that the use of L charging profiles yields the highest RMSEs (5.59%–5.86% for the highest peak power, 2.29%–6.52% for
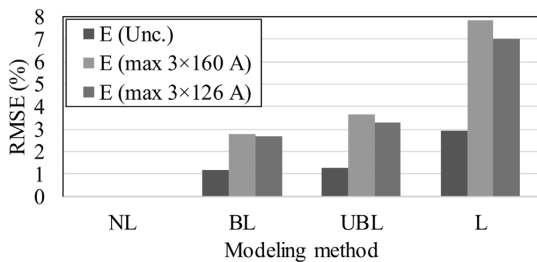
FIGURE 10 RMSE of the charged energy in Scenario 2

the highest hourly peak power, and 2.95%–7.84% for the charge energy). Compared to each other, the use of BL or UBL charging profiles yields similar results (1.87%–3.37% for the highest peak power, 0.64%–2.83% for the highest hourly peak power, and 1.19%–3.65% for the charged energy) even though the BL charging profile is slightly more accurate in each scenario.

4 | DISCUSSION

The results of Scenario 1 demonstrate that the use of NL charging profiles can be made to enable a high modelling accuracy for the EV charging load simulations even though the battery temperatures are not taken into account. However, some modelling inaccuracies were expected and seen due to this simplification. According to the results, the highest hourly peak power and the charged energy can be modelled accurately (RMSE of ≤ 3.45%), whereas the highest peak power is more susceptible to modelling errors (RMSE of 9.29%).

In general, the results show that the use of L charging profiles is likely to lead to significant modelling errors (RMSE of 2.29%–31.21%). Conversely, the use of BL or UBL charging profiles seems to be reasonably accurate compared to the HIL measurements and to the results obtained using NL charging profiles (RMSE of 0.64%–4.39% when excluding the highest peak power in Scenario 1). These results indicate that the use of a simple BL charging profile is likely to be sufficiently accurate in most cases as long as the slope of the CV stage is justified. This kind of result was expected because the studies [27] and [28] indicated that an EV model-specific charging profile model (such as the non-linear profile model considered in this paper) may not be needed in order to model charging loads relatively accurately.

The comparison of the three subscenarios of Scenario 2 shows that the uncontrolled charging can be modelled more accurately in terms of the highest hourly peak power (seen in Figure 9) and the charged energy (seen in Figure 10) than the controlled charging. This is assumed to be due to two reasons. Firstly, in case of controlled charging, the capacity allocation is influenced by the number of EVs actively requesting energy. Secondly, compared to the usage of the other modelling methods, the EVs become fully charging faster when using linear charging profile model (seen in Figure 3). This means that the use of linear charging profiles is inaccurate to model the

charging states of the EVs (requesting to be charged or not) which further influences the control algorithm. In general, these results indicate that the more complex the considered control algorithm is, the more complex charging profile modelling methods should be used. In terms of the highest peak power, there does not seem to be a similar correlation to the use of charging control (seen in Figure 8) even though the loads are affected in case of controlled charging by the two reasons just mentioned. This is expected to be due to the fact that the highest peak load only takes into account the single highest value. So, despite the loads being modelled more inaccurately over the course of the simulated periods in case of controlled charging, it seems that the highest momentary power is often achieved with a similar accuracy regardless of the use of charging control. It is also worth noting that the highest peak load seems to be less susceptible to modelling inaccuracies when the number of EVs increases. This can be seen by comparing the results of Scenarios 1 and 2.

5 | CONCLUSIONS

In this paper, the influence of the charging profile modelling method on the EV charging load is assessed. Laboratory experiments with up to four commercial EVs are carried out to form realistic baselines for the comparisons. In addition, to evaluate charging at a large charging site, charging session data of REDI shopping centre is used.

The results show that the use of linear charging profile can lead to significant modelling errors, and thus, it is not recommended to be used especially in case of controlled charging. It is shown that the use of measurement-based non-linear charging profiles is likely to lead to the most accurate modelling. However, the results also demonstrate that the use of a simple, but justified, bilinear charging profile model can also lead to reasonably accurate results.

According to the measurements and calculations of this paper, the charging currents of commercial EVs decrease around 15.3 mA/s per phase on average in the constant voltage stage. Also, the results shown in this paper demonstrate that using this value to model charging profiles leads to reasonable low modelling errors of 0.64%–4.39% for the highest hourly peak power and the charged energy. Therefore, it can be used in future studies, which relates to EV charging load modelling from the charging site point-of-view, to ensure reasonable modelling accuracy with reduced computational requirements. Additionally, the results of this paper show that the battery temperatures do not have a notable influence on the charging loads seen from the charging site point-of-view, and thus, it may not be necessary to consider them in the related studies.

The results of this paper indicate that uncontrolled charging can be modelled more accurately than controlled charging. To investigate the accuracies of different charging profile modelling methods in case of different control algorithms, more work is required. However, this can be a challenging task because the commercially available EVs may have some limitations. For example, some EVs may not support vehicle-to-grid, or they

may not be able to communicate certain information, such as SoC, to the control system. And, if real measurements are not used as a baseline for the comparisons, it may be difficult to assess the accuracies of different modelling methods in different scenarios.

CONFLICT OF INTEREST
The authors declare that they have no known competing financial interests or personal relationships that could have appeared to influence the work reported in this paper.

FUNDING INFORMATION
There is no funding information to be reported.

DATA AVAILABILITY STATEMENT
The data that support the findings of this study are available from the corresponding author upon reasonable request.

REFERENCES

1. Ge X., Shi L., Fu Y., Muyeen S.M., Zhang Z., et al.: Data-driven spatial-temporal prediction of electric vehicle load profile considering charging behavior. Electr. Power Syst. Res. 187, 106469 (2020)
2. Sadeghianpourhamami N., Deleu J., Develder C.: Definition and evaluation of model-free coordination of electrical vehicle charging with reinforcement learning. IEEE Trans. Smart Grid, 11(1), 203–214 (2020)
3. Gong L., Cao W., Liu K., Yu Y., Zhao J.: Demand responsive charging strategy of electric vehicles to mitigate the volatility of renewable energy sources. Renew. Energy, 156, 665–676 (2020)
4. Dong X., Mu Y., Xu X., Jia H., Wu J., et al.: A charging pricing strategy of electric vehicle fast charging stations for the voltage control of electricity distribution networks. Appl. Energy, 225, 857–868 (2018)
5. Lin H., Liu Y., Sun Q., Xiong R., Li H., et al.: The impact of electric vehicle penetration and charging patterns on the management of energy hub – A multi-agent system simulation. Appl. Energy, 230, 189–206 (2018)
6. Zhang Y., You, Cai L.: Optimal charging scheduling by pricing for EV charging station with dual charging modes. IEEE Trans. Intell. Transp. Syst. 20(9), 3386–3396 (2019)
7. Shaaban M.F., Mohamed S., Ismail M., Qaraqe K.A., Serpedin E.: Joint planning of smart EV charging stations and dgs in eco-friendly remote hybrid microgrids. IEEE Trans. Smart Grid, 10(5), 5819–5830 (2019)
8. Zhang Y., Chen J., Cai L., Pan J.: Expanding EV charging networks considering transportation pattern and power supply limit. IEEE Trans. Smart Grid 10(6), 6332–6342 (2019)
9. Liu H., Qi J., Wang J., Li, Li C., et al.: EV dispatch control for supplementary frequency regulation considering the expectation of EV owners. IEEE Trans. Smart Grid 9(4), 3763–3772 (2018)
10. Sun Y., Chen Z., Li Z., Tian W., Shahidehpour M.: EV charging schedule in coupled constrained networks of transportation and power system. IEEE Trans. Smart Grid, 10(5), 4706–4716 (2018)
11. Zhou K., Cheng L., Lu X., Wen L.: Scheduling model of electric vehicles charging considering inconvenience and dynamic electricity prices. Appl. Energy, 276, 115455 (2020)
12. Khaki B., Chu C., Gadh R.: Hierarchical distributed framework for EV charging scheduling using exchange problem. Appl. Energy, 241, 461–471 (2019)
13. Chung Y.W., Khaki B., Li T., Chu C., Gadh R.: Ensemble machine learning-based algorithm for electric vehicle user behavior prediction. Appl. Energy, 254, 113732 (2019)
14. Anand M.P., Bagen B., Rajapakse A.: Probabilistic reliability evaluation of distribution systems considering the spatial and temporal distribution of electric vehicles. Int. J. Electr. Power Energy Syst. 117, 105609 (2020)
15. Xiang Y., Jiang Z., Gu C., Teng F., Wei X., et al.: Electric vehicle charging in smart grid: A spatial-temporal simulation method. Energy, 189, 116221 (2019)
16. Su J., Lie T.T., Zamora R.: Integration of electric vehicles in distribution network considering dynamic power imbalance issue. IEEE Trans. Ind. Appl. 56(5), 5913–5923 (2020)
17. Zhou K., Cheng L., Wen L., Lu X., Ding T.: A coordinated charging scheduling method for electric vehicles considering different charging demands. Energy, 213, 118882 (2020)
18. Brinkel N.B.G., Schram W.L., AlSkaif T.A., Lampropoulos I., van Sark W.G.J.H.M.: Should we reinforce the grid? Cost and emission optimization of electric vehicle charging under different transformer limits. Appl. Energy, 276, 115285 (2020)
19. Wang Y., Infield D.: Markov Chain Monte Carlo simulation of electric vehicle use for network integration studies. Int. J. Electr. Power Energy Syst. 99, 85–94 (2018)
20. Fretzen U., Ansarin M., Brandt T.: Temporal city-scale matching of solar photovoltaic generation and electric vehicle charging. Appl. Energy 282, 116160 (2021)
21. Yan J., Zhang J., Liu Y., Lv G., Han S., et al.: EV charging load simulation and forecasting considering traffic jam and weather to support the integration of renewables and EVs. Renew. Energy 159, 623–641 (2020)
22. Wang M., Mu Y., Shi Q., Jia H., Li F.: Electric vehicle aggregator modeling and control for frequency regulation considering progressive state recovery. IEEE Trans. Smart Grid 11(5), 4176–4189 (2020)
23. Kikusato H., Fujimoto Y., Hanada S., Isogawa D., Yoshizawa S., et al.: Electric vehicle charging management using auction mechanism for reducing PV curtailment in distribution systems. IEEE Trans. Sustain. Energy 11(3), 1394–1403 (2020)
24. Wang B., Zhao D., Dehghanian, Tian Y., Hong T.: Aggregated electric vehicle load modeling in large-scale electric power systems. IEEE Trans. Ind. Appl. 56(5), 5796–5810 (2020)
25. Wei Z., Li Y., Zhang Y., Cai L.: Intelligent parking garage EV charging scheduling considering battery charging characteristic. IEEE Trans. Ind. Electron. 65(3), 2806–2816 (2018)
26. Mouli G.R.C., Kefayati M., Baldick R., Bauer P.: Integrated PV charging of EV fleet based on energy prices, V2G, and offer of reserves. IEEE Trans. Smart Grid 10(2), 1313–1325 (2019)
27. Sun C., Li T., Low S.H., Li V.O.K.: Classification of electric vehicle charging time series with selective clustering. Electr. Power Syst. Res. 189, 106695 (2020)
28. Frendo O., Graf J., Gaertner N., Stuckenschmidt H.: Data-driven smart charging for heterogeneous electric vehicle fleets. Energy AI 1, 100007 (2020)
29. Helen Electricity Network LTD: Electricity distribution tariffs. [Online]. Available: https://www.helensahkoverkko.fi/globalassets/hinnastot-ja-sopimusehdot/hsv---enkku/distribution_tariffs.pdf
30. Simolin T., Rauma K., Rautiainen A., Järventausta, Rehtanz C., Foundation for adaptive charging solutions: optimized use of EV charging

capacity. IET Smart Grid, Early view. (021), https://doi.org/10.1049/stg2.12043

31. Simolin T., Rauma K., Viri R., Mäkinen J., Rautiainen A., et al.: Charging powers of the electric vehicle fleet: Evolution and implications at commercial charging sites. Appl. Energy 303, 117651 (2021)

32. REDI: Parking - REDI. [Online]. Available: www.redi.fi/parking/?lang=en

33. Zhang T., Pota H., Chu C.C., Gadh R.: Real-time renewable energy incentive system for electric vehicles using prioritization and cryptocurrency. Appl. Energy 226, 582–594 (2018)

34. Spina A., Rauma K., Aldejohann C., Holt M., Maasmann J., et al.: Smart grid technology lab – A full-scale low voltage research facility at. TU Dortmund University. In: 2018 110th AEIT International Annual Conference, pp. 1–6 (2018)